ANL-76-96

ANL-76-96

MASTER

PHYSICS DIVISION
ANNUAL REVIEW
1 April 1975–31 March 1976

U of C-AUA-USERDA

ARGONNE NATIONAL LABORATORY, ARGONNE, ILLINOIS

repared for the U. S. ENERGY RESEARCH
AND DEVELOPMENT ADMINISTRATION
under Contract W-31-109-Eng-38

DISCLAIMER

Printed in the United States of America
Available from
National Technical Information Service
U. S. Department of Commerce
5285 Port Royal Road
Springfield, Virginia 22161
Price: Printed Copy $9.25; Microfiche $3.00

Distribution Category:
Physics-General (UC-34)

ANL-76-96

ARGONNE NATIONAL LABORATORY
9700 South Cass Avenue
Argonne, Illinois 60439

PHYSICS DIVISION ANNUAL REVIEW
1 APRIL 1975–31 MARCH 1976

Gerald T. Garvey, Division Director

Preceding Annual Reviews:

ANL-7971, Annual Review 1971—1972
ANL-8035, Annual Review 1972—1973
ANL-75-75, Annual Review 1974—1975

FOREWORD

The Physics Division Annual Review presents a broad but necessarily incomplete view of the research activity within the Division for the year ending in April 1976.

At the back of this report a complete list of publications along with the Divisional roster can be found.

TABLE OF CONTENTS

THIS PAGE

WAS INTENTIONALLY

LEFT BLANK

NUCLEAR PHYSICS RESEARCH

INTRODUCTION

The program in nuclear research within the Physics Division is very broadly based touching upon most areas of importance. The range of activities employs both strong and electromagnetic probes of nuclear structure at energies ranging from thermal neutrons to energetic pions produced at the ZGS and LAMPF. A strong nuclear theory group works on fundamental issues in nuclear matter as well, producing "state of the art" shell-model wave function and direct reaction calculations essential to any phenomenological understanding of nuclear structure. Furthermore, realizing that the health of a physical science depends on developing even better research tools, a sizable project to develop and construct an energy booster for heavy ions from our tandem electrostatic accelerator is also well under way.

THIS PAGE

WAS INTENTIONALLY

LEFT BLANK

I. HEAVY-ION ENERGY BOOSTER

L. M. Bollinger, R. Benaroya,* B. E. Clifft,* A. H. Jaffey,* K. W. Johnson,* T. K. Khoe,† M. C. Olesen, C. H. Scheibelhut,‡ K. W. Shepard, T. P. Wangler, and W. A. Wesolowski*

INTRODUCTION

This project, which started in July 1975, is concerned with the design, construction, installation, and testing of a small superconducting linear accelerator,[1] which will serve as an energy booster for heavy-ion beams from the FN tandem accelerator. The principal justification for the work is the opportunity it affords to advance the development of superconducting rf-accelerator technology. However, the project is also expected to result in a useful accelerator system. The project is closely related to the following activities described elsewhere in this document: (1) the general Superconducting Linac Development program, (2) the development of the technology for heavy-ion bunching, and (3) the upgrading of the FN tandem.

The main goals of the project are to produce a superconducting linac that (1) provides at least 13.5 MV of acceleration and that (2) has an output beam with very good quality. In order to achieve the second objective, we intend to use an accelerating structure with a relatively low (about 100 MHz) rf frequency. The linac will consist of independently-phased resonators so as to make it useful for a wide range of projectiles. The system will be formed of modular components and will be designed to be as simple and flexible as possible so that it will be feasible to make use of future improvements in a rapidly developing technology.

A schematic of the planned tandem-linac facility is given in Fig. 1. The existing FN-model tandem Van de Graaff, the injector of

---

*Chemistry Division, ANL.

†Accelerator Research Facilities Division, ANL.

‡Engineering Division, ANL.

[1] L. M. Bollinger et al., in Proceedings of the 1976 Proton Linear Accelerator Conference, Chalk River, Canada, September 14-17, 1976 (to be published).

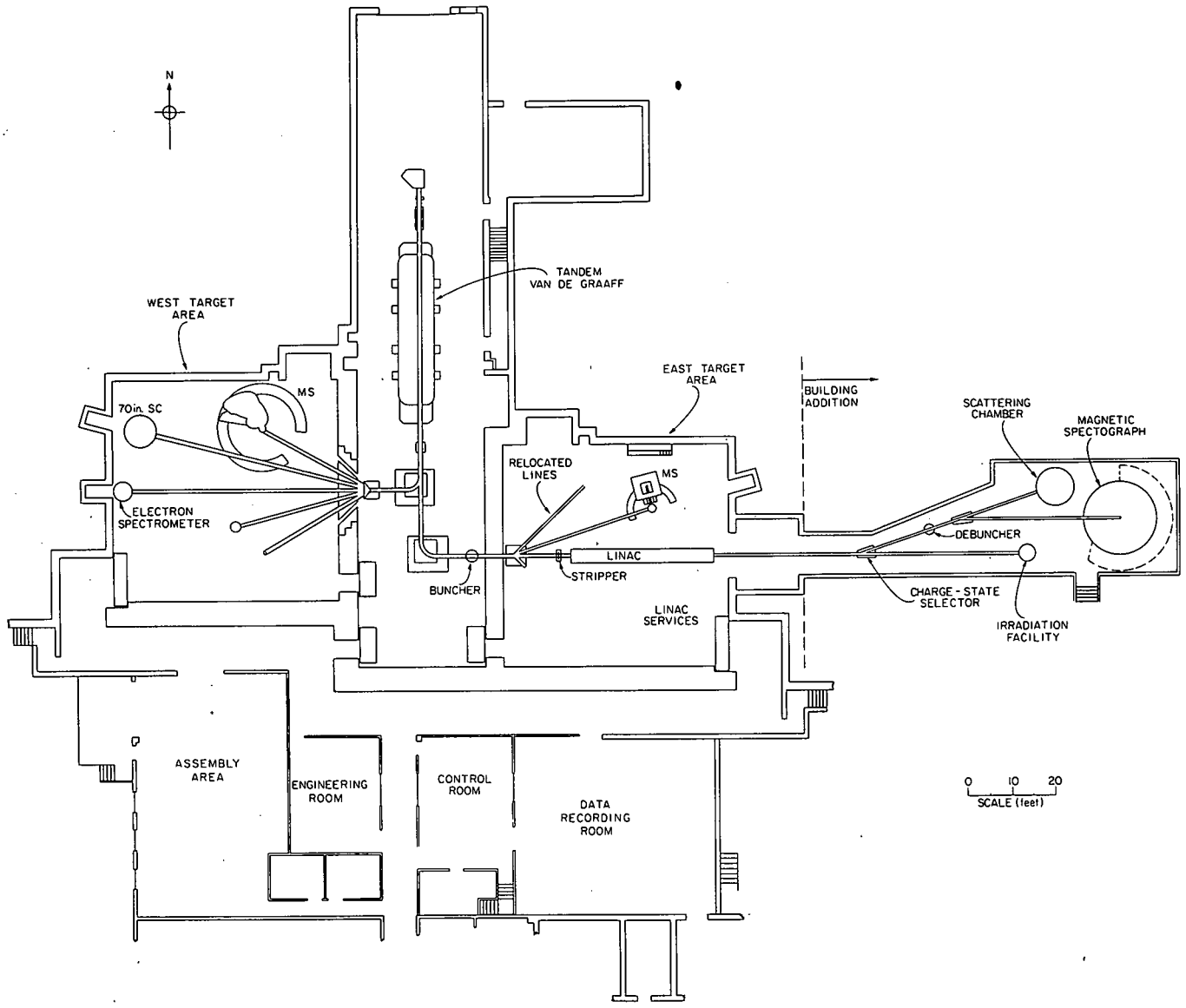

Fig. 1. Overall layout of the planned tandem-linac facility.

the system, will remain in its present location but be upgraded in the way described in Sec. V.A.

The first year of the project is being devoted to design and to other preparations for fabrication of the linac. Major parts of this initial effort are (1) the design, construction, and testing of prototype resonators, (2) design of the mechanical and cryogenic system as a whole, (3) the ordering of materials, (4) the development of specifications for a refrigerator, and (5) design of the rf system. The fabrication of major components is scheduled to start in October 1976.

A. LINAC DEVELOPMENT

(i) Main Features of the Design. The linac will consist of an array of independently-phased accelerating structures within a vacuum-cryogenic system about 10 meters long. The accelerating structures will be of the split-ring type[2] operating at an rf frequency of about 100 MHz and at a temperature of $\sim 4.2^{\circ}$K. The vacuum-cryostat system will be planned to have space for 18 such resonators, but at the present level of funding it will be possible to build only about three-quarters of them. About half of the resonators will be optimized for a velocity $\beta \approx 0.11$ and the remainder for $\beta \approx 0.07$. The beam will be confined radially by a superconducting solenoid after each second resonator. Tentatively, it is planned to build the resonators in several successive batches so as to be able to modify the design, if desirable, during the course of the project.

For ease of construction and assembly, there will be no vacuum wall between the interiors of the resonators and the insulation vacuum. Cryogenic pumping on the cold outer surfaces of the resonator will prevent gas from the warm vacuum wall from reaching the resonator interiors. The resonator will be cooled by locally cooling the resonator housing rather than by means of a helium bath.

The configuration of the cryostat-vacuum system has not yet been fully established. From the point of view of beam optics and perhaps cost, it is desirable to have all resonators within a single vacuum tank. However, from the point of view of flexibility in servicing the linac, it is highly desirable to have relatively small independent vacuum systems. The concept that is being pursued as a working model is one in which each vacuum tank will contain six independently-phased resonators. This arrangement appears to be close to the optimum compromise for the several conflicting requirements.

---

[2] K. W. Shepard et al., IEEE Trans. Nucl. Sci. NS-22, 1179 (1975).

The ion beam injected into the linac will be formed into very narrow pulses by a bunching system consisting of a pretandem room-temperature buncher followed by a post-tandem superconducting buncher located about 6 meters from the linac. A foil stripper will be located immediately in front of the linac.

The layout of the accelerator system is planned so that at a later time a debunching resonator can easily be added to manipulate the phase ellipse of the ion beam after acceleration through the linac.

The rf system will initially have manual control with computer assistance to the operator.

(ii) Resonator Prototype. A prototype of a split-ring resonator[3] made of niobium has been constructed and tested. A photograph of the interior components of the resonator is shown in Fig. 2. The resonator housing is 16 in. in diameter and 14 in. long, and the system operates at 97 MHz. Acceleration is optimum for a particle with a velocity $\beta \approx 0.11$.

Measurements on the full-scale niobium resonator and on full-scale copper models of it have led to a good understanding of field distributions, mode mixing, and sensitivity to geometrical parameters. Such investigations were essential because our design is rather different from that developed originally at Cal Tech.[2]

The superconducting split-ring resonator has been operated several times and the following results were obtained.

(1) The device is very stable mechanically, and hence vibration-induced rf-frequency variations are small. In a working accelerator environment, the frequency variations are only ±60 Hz, small enough that the resulting rf-phase variations can be controlled with established techniques.

---

[3] K. W. Shepard et al., in Proceedings of the 1976 Applied Superconductivity Conference, Stanford University, August 17-20, 1976 (to be published).

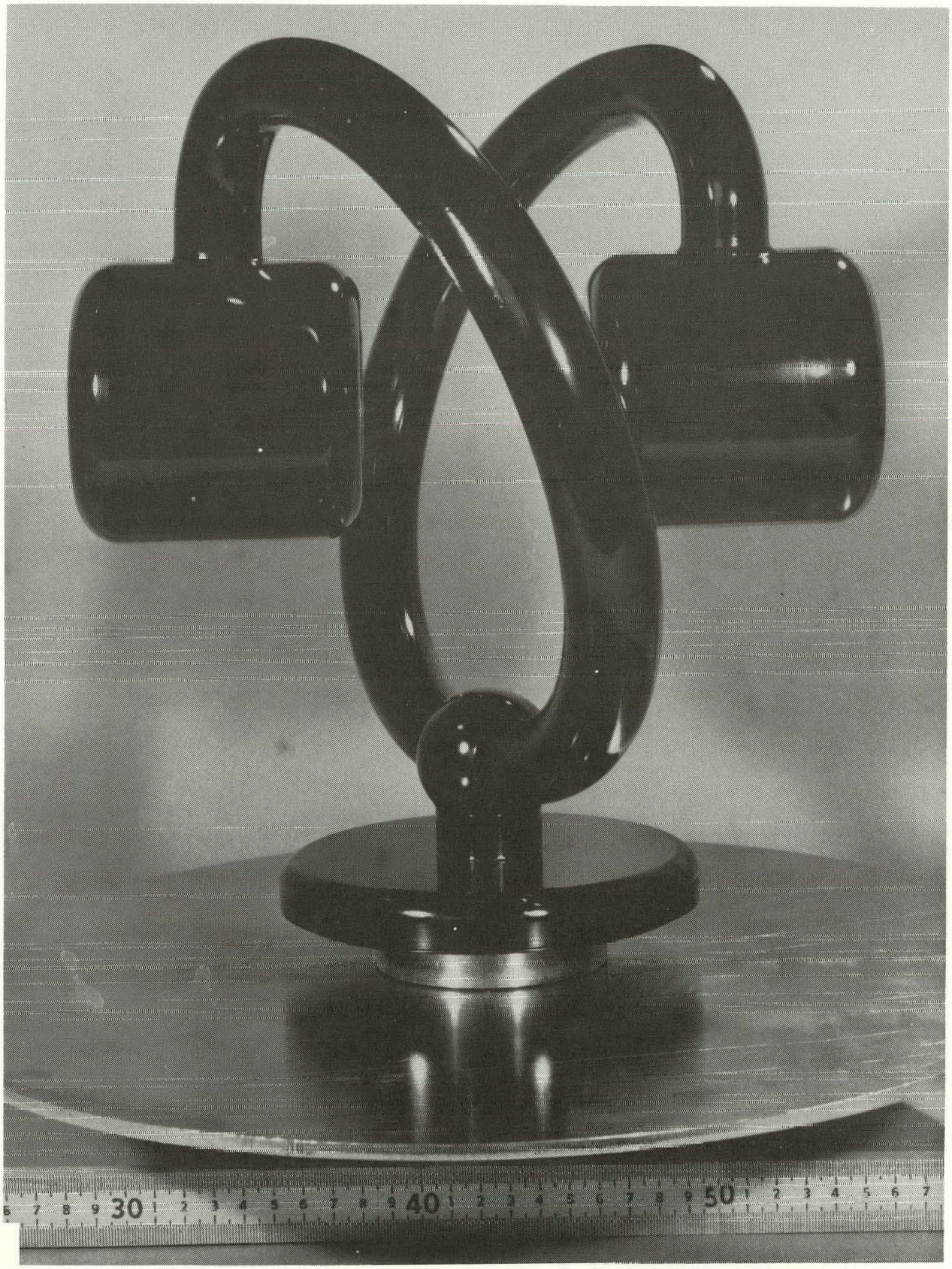

Fig. 2. The drift-tube assembly of a superconducting split-ring resonator.

(2) The static frequency shift induced by radiation pressure is about 400 times smaller than for the helix structures studied earlier. This characteristic is highly advantageous because it essentially eliminates instability caused by electromechanical coupling.

(3) The structure has been operated with a maximum accelerating field of 3.6 MV/m with 10 W of input rf power. This accelerating field corresponds to a voltage gain of 1.3 MV, which would give a maximum energy gain of $\sim$25 MeV for Ni^{20+}, for example. The maximum accelerating field of the structure appears to be limited by field emission of electrons from the ends of the drift tubes, where the surface electric field is highest. Since all of the helix resonators studied earlier[4—6] were made to operate well with surface electric fields greater than 20 MV/m, it is reasonable to expect such performance from the split ring also. If so, the accelerating field will be $\geq$4.25 MV/m. On the basis of our investigations of helix resonators, the surface magnetic field is not expected to be a limitation unless the accelerating field is ultimately pushed up much higher.

(4) The resonator performs well at 4.2°K. This is important because a 4.2° refrigerator costs only about 40% as much as a 1.8° refrigerator.

(5) Multipacting losses appear not to be serious. Low-field multipacting barriers are overcome with relative ease, and barriers are not apparent at higher fields.

(iii) Demountable RF Joint. In the initial fabrication of our niobium split-ring resonator, the inner components were joined to the outer housing by means of a demountable joint that carried rf current. Tests on the split-ring resonator and on another test unit recently put into operation have established that this kind of contact involving niobium surfaces

---

[4] J. Aron et al., IEEE Trans. Nucl. Sci. NS-20, 76 (1973).

[5] J. Aron et al., Proceedings of the 9th International Conference on High Energy Accelerators, SLAC, Stanford University, 2-7 May 1974 (USAEC 1974), CONF-740522, p. 159

[6] R. Benaroya et al., IEEE Trans. Magn. MAG-11, 413 (1975).

results in unacceptable losses in rf power. Therefore, the support contact has been welded, which solved the problem, although at the cost of some inconvenience in the procedures used to treat the interior surfaces of the resonator.

The end plate of the resonator is a second part that involves a demountable rf seal. Here the currents are relatively low, so that our established techniques[3] for making rf contact may be adequate. However, this has not yet been established with certainty.

(iv) Niobium Fabrication Techniques. A great deal of effort has been devoted to the development of effective ways of fabricating niobium structures. For our first resonator, the techniques were entirely successful and cost effective in the fabrication of the inner parts (the ring and drift tubes). However, the initial design of the outer housing proved to be too complex (in unnecessary ways), with the result that its cost is unacceptably high. The design is being greatly simplified.

The initial design of the housing required a large amount of electron-beam welding of preformed components. Two radically different approaches aimed at eliminating such welding are being developed, and both appear to offer excellent solutions to the fabrication problem. In one, the component parts are welded together while they are in the form of flat sheets, and these sheets are then formed into the required double-walled configuration by means of bending and forming techniques. In the second approach, the structural material is niobium that is explosively bonded to copper. The inner niobium sheet provides the superconducting rf path, and the outer copper provides mechanical strength and a heat-conduction path.

The second of the above new methods of fabrication has been selected as the most promising of the two and will have been subjected to extensive tests by the end of 1976. The first split-ring resonator of the new kind is scheduled for completion in September 1976.

(v) Superconducting Solenoids. In the planned linac, small superconducting solenoids[7,8] will be used to control the radial expansion of the beam. A prototype of the solenoid has been designed, constructed, and tested. The unit satisfies design requirements in all respects, including cost. The central field is ~60 000 G.

(vi) Heavy-Ion Bunching. The planned heavy-ion bunching system consists of a room-temperature buncher at the input to the tandem, a superconducting buncher after the tandem, and an ion-bunch phase detector to tie the two bunchers together electrically. The pretandem buncher and the bunch-phase detector are part of an accelerator improvement project described in Sec. V.A of this document.

The feasibility of using superconducting accelerating structures to bunch tandem beams into ultrashort pulses was demonstrated[9] experimentally in early 1975. Now effort is being devoted to the design and fabrication of a practical bunching system suitable for routine use. The design of the post-tandem buncher assembly has been completed, and fabrication will be finished in late 1976. The bunching resonator will consist of an existing superconducting $\lambda/2$ helix, which will bunch beams of any ion in the mass range $10 < A < 110$. Beam pulses less than 50 psec wide are expected.

This bunching system will be used initially for ion beams that are accelerated only by the tandem.

(vii) Cryostat. During 1974 and 1975 a large cryostat was built to house a $5\lambda/2$ helix resonator. During the past year this system was extensively modified so as to make it suitable for use with the

---

[7] A. H. Jaffey and T. Khoe, Nucl. Instrum. Methods 121, 413 (1974).

[8] R. Benaroya et al., in Proceedings of the 1976 Proton Linear Accelerator Conference, Chalk River, Canada, September 14-17, 1976 (to be published).

[9] L. M. Bollinger et al., IEEE Trans. Nucl. Sci. NS-22, 1148 (1975).

split-ring resonator or possibly other large accelerating structures. Many control features that are similar to what would be required for a cryogenic accelerator have been incorporated into the modified cryostat.

The modified cryostat has been used successfully in the study of the split-ring resonator. This experience with a large, complex cryogenic system is helping to provide the insights needed for the design (now in progress) of the cryogenic system for the linac.

(viii) Building Addition. The design of the small new target room required for use of the beam from the linac has been completed and construction has been started. When completed (in late 1976), the room will be used initially as an assembly area for work on the linac.

Schedule. The period July-September 1976 will be one of final preparations for the start of construction of the linac. Emphasis will be on the system design. Major quantities of niobium metal required for the resonators will be ordered. Work on specifications for the helium refrigerator and for the rf-control system will proceed.

The fabrication of major components of the linac is scheduled to start in October 1976 and extend throughout 1977. Fabrication of the vacuum-cryostat system and of the rf-control system will be carried out during the same period. Because of the special skills and equipment required, the main operations involved in the construction of the niobium resonators will be carried out at Argonne.

The helium refrigerator will be installed in late 1977.

The design of the superconducting linac has now progressed far enough that it is meaningful to project that the first useful beam will be accelerated* in April 1978. In view of the developmental nature of the work, it is probable that there will be a relatively long period of testing and debugging before the machine is routinely available to users.

---

*It should be noted that test ion beams were first accelerated[4,5] hrough superconducting resonators in early 1973.

B. PERFORMANCE OF THE TANDEM-LINAC SYSTEM

(i) Output Energy. Two projections of the maximum energies of ion beams from the planned tandem-linac system are summarized in Fig. 3. There is uncertainty in these projections, both because of uncertainty in the maximum accelerating field that will be achieved and because of uncertainty in the number of resonators that can be built at the present level of funding.

Curve A is the performance that was projected in our original proposal to build a small superconducting energy booster. This is our minimum objective and appears to be readily achievable.

Curve B is the performance expected for a linac consisting of 18 resonators operating at a field of 4.25 MV/m, which corresponds to the maximum surface field of 20 MV/m achieved for many helix resonators. It is probable that this level of performance will not be achieved initially because we will not be able to complete all 18 resonators. However, our objective is to reach this size and level of performance as soon as possible.

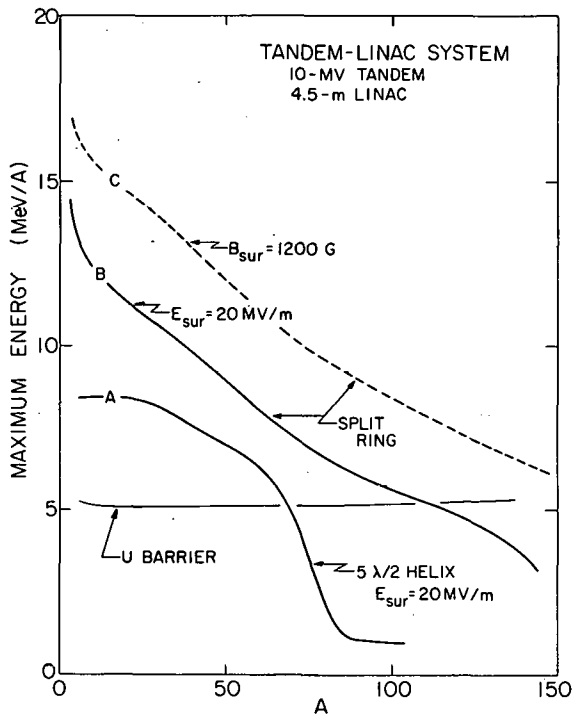

Fig. 3. Performance characteristics of a tandem-linac accelerator system under several sets of assumptions. Curve A was calculated for a linac consisting of 6 helix resonators, each of which is 5 half-wavelengths long. The sharp cut-off at $A \approx 75$ is a beam transit-time effect that results from the considerable length of these resonators. Curves B and C were calculated for 18 split-ring resonators, for which transit-time effects play only a minor role for $A > 100$ under the assumptions listed in the text. For curve C, a surface magnetic field $B_{sur} = 1200$ G corresponds to a surface electric field $E_{sur} = 33$ MV/m, which is less than has been achieved in helix resonators.[6]

Curve C gives the energies that would be provided by an 18-resonator system if all units operate at the highest surface fields that have been measured in a helix resonator.[6] Performance at this level is not likely to be achieved soon, but it is a reasonable long-term goal, since it is consistent with the demonstrated properties of niobium.

(ii) Beam Quality. For several years a major design objective of this project has been to obtain output beams of good quality by minimizing all nonlinear effects in the accelerating process. Among other things, this requires that the input beam should be formed into very narrow pulses and that the radial dimensions of the beam should be kept small by the use of focussing elements at frequent intervals. Since our design incorporates these and other needed features, it is expected that the output-beam quality will be determined largely by the quality of the beam from the tandem. The design objectives are an output beam with $\Delta E/E \leq 10^{-3}$ and $\Delta t \leq 50$ psec. A debunching resonator located about 10 meters downstream from the linac will allow the energy spread of the beam delivered to the user to be made about five times smaller, if desirable.

(iii) Energy Variability. The output energy of the linac can be varied in several ways. The easiest approach is to keep fixed the parameters of all components prior to the last resonator in use and to vary the phase of this last unit over the linear range of its accelerating force. In this way the output energy can be varied continuously over a range that is typically 30 MeV. If this range is not enough, the last resonator is turned off and the phase of the second last resonator is varied in the same way. Thus, the energy can be varied easily and rapidly, a feature that is expected to be extremely useful for nuclear-structure investigations.

(iv) Beam Intensity. For all except rather light ions, it ll be necessary to use two strippers during the acceleration process,

one in the tandem terminal and another between the tandem and linac. Thus, even though the linac is expected to accelerate most of the incident beam, the beam of projectiles issuing from the linac will be only about 2% as intense as the beam injected into the tandem. Typically, then, the beam current is expected to be ~20 pnA for favorable ions and lower for others. In view of the good quality of the beam, this is enough for most nuclear-structure experiments.

II. MEDIUM-ENERGY PHYSICS

INTRODUCTION

The medium-energy research program is conceived as part of the overall study of nuclear phenomena. The physicists who work in the medium-energy program are the same people who also work in other parts of the nuclear research program, and the scientific bases of the problems and the techniques used to solve them also overlap. The primary effort at present is to study pion-induced nuclear reactions by gamma-ray measurements. Similar work is done to study proton-induced reactions. Pion-channeling experiments are also being pursued, and pion-elastic and inelastic scattering measurements are being planned for the near future. Some effort is being devoted to considering the possible uses of kaon beams.

The technique of measurement of on-line gamma rays has been developed first at the ZGS and then at LAMPF as a means of identifying product nuclides from pion-induced nuclear reactions. The very successful run at LAMPF, late in 1975, has been analyzed and a further experiment planned which is likely to be carried out late in 1976. Experiments of this type are perhaps the only means of getting an overall measure of the distribution of reaction channels from pion-induced reactions on complex nuclei. The distribution of intensities, average number of nucleons removed and the average neutron excess of residual nuclides are valuable clues towards understanding the gross features of this interaction.

The pion-channeling experiment will be carried out after the EPICS channel at LAMPF becomes operational in late 1976. Experiments on elastic and inelastic scattering are also planned for EPICS, possibly in mid-1977.

A trailer has been instrumented at Argonne for use in the various experiments now planned for Los Alamos. This trailer contains a PDP-11 computer system which is virtually identical to the computer system now being used at Argonne for work at the Tandem and Dynamitron accelerators. The trailer will also contain the detector and other auxiliary electronics. When not in use at Los Alamos, this trailer will be available for use at Argonne and, should Argonne groups run experiments at other off-site locations, the trailer would be available.

A. EXPERIMENTS AT THE ZGS

a. Nuclear Reactions Induced by 380-MeV π^-

R. E. Segel, L. R. Greenwood, P. T. Debevec, H. E. Jackson, D. G. Kovar, L. Meyer-Schützmeister, J. E. Monahan, F. J. D. Serduke, T. P. Wangler, W. R. Wharton, and B. Zeidman

Using a Ge(Li) detector, gamma-ray spectra coincident with incident 380-MeV π^- have been measured for targets of S, Ar, Ca, V, ^{60}Ni, and As. The production cross sections for identified gamma rays vary from about 200 mb to about 500 mb, depending on the target, although there is considerable uncertainty in the absolute cross sections. Comparison with data taken at lower energies leads to the conclusion that the spectra do not significantly change with pion energy over the range 100 MeV $\leq T_\pi \leq$ 400 MeV. Formation of nuclei which can be made by removing an integral number of alpha particles, or, in the case of odd targets, a triton plus an integral number of alphas, appears to be usually favored but it is not certain that it is necessary to invoke special clustering effects in order to explain the presently available data. Some clues as to the reaction mechanism can be found in the data.

b. Study of the Feasibility of Obtaining and Utilizing a High Intensity, Low Momentum Kaon Beam

R. E. Segel, J. P. Schiffer, D. G. Kovar, and H. E. Jackson

The work done by the Argonne group with pions and also the work done at other laboratories with kaons makes it abundantly clear that a great deal could be learned about the nucleus by studying kaon-induced nuclear reactions. As a preliminary goal we have tried to see if a kaon beam could be obtained at the ZGS or elsewhere that is roughly comparable to the pion beam that the Argonne group has been using at LAMPF. After considerable discussion with various high-energy physicists and accelerator people at Argonne, it has been concluded that a 2×10^5/sec K^+ beam operating at 750 MeV/c could be built at the ZGS using present techniques. Such a beam would be very useful for nuclear structure studies.

B. EXPERIMENTS AT LAMPF

a. Systematics of Pion and Proton Interactions with Ni Nuclides

H. E. Jackson, D. G. Kovar, L. Meyer-Schützmeister, R. E. Segel, J. P. Schiffer, S. E. Vigdor, T. P. Wangler, R. L. Burman,* D. M. Drake,* P. A. M. Gram,* R. P. Redwine, V. G. Lind,† E. N. Hatch,† O. H. Otteson,† R. E. McAdams,† B. C. Cook,‡ and R. B. Clark§

Gamma-ray spectra have been observed following the interaction of 220-MeV π^+ and π^- and 200-MeV protons with ^{58}Ni and ^{60}Ni and 100-MeV π^+ with ^{58}Ni. Product nuclides that have been identified from characteristic γ-ray lines correspond to total cross sections of ~500 mb. The spectra are found to vary little with pion energy and also to vary little with pion charge. It is concluded that at least for the nuclei far away from the target nucleus the reaction must have been initiated by the pion being absorbed. Proton initiated reactions appear on the average to remove fewer nucleons from the target, again supporting the notion that often the initial pion is absorbed. However, it does not appear to be possible to explain the available data on fast pion initiated reactions by a mechanism in which the pion is initially absorbed on two nucleons followed by understood nuclear processes.

b. Absolute Cross Sections for Production of Prompt Nuclear Gamma Rays by Fast Pions

H. E. Jackson, D. G. Kovar, L. Meyer-Schützmeister, S. E. Vigdor, T. P. Wangler, R. E. Segel, J. P. Schiffer, R. L. Burman,* P. A. M. Gram,* D. M. Drake,* V. G. Lind,† E. N. Hatch,† O. H. Otteson,† R. E. McAdams,† B. C. Cook,‡ and R. B. Clark§

Cross sections have been measured for the production of prompt nuclear γ rays in the pion bombardment of Al, Ca, V, and ^{60}Ni.

*Los Alamos Scientific Laboratory, Los Alamos, New Mexico.

†Utah State University, Logan, Utah.

‡Iowa State University, Ames, Iowa.

§Texas A & M University, College Station, Texas.

Several disagreements with values in the literature are noted. In particula the large cross section previously reported by another group for the alpha removal from calcium-40 was found to be substantially in error. It now appears that nowhere does alpha removal account for more than about 20% of the total reaction cross section. It still remains an open question as to whether the observed alpha-removal cross section can be explained without requiring a preferential interaction of mesons with alpha clusters.

c. Nuclear Reactions Induced by Fast Pions

R. E. Segel, J. P. Schiffer, L. Meyer-Schützmeister, S. E. Vigdor, S. L. Tabor, L. Rutledge,* S. B. Kaufman,† R. L. Burman,‡ R. P. Redwine, and P. A. M. Gram‡

A run is scheduled for June 1976. In this run it is expected that the studies of prompt-gamma-ray spectra will be completed. The data from ^{58}Ni and ^{60}Ni demonstrated that important information can be obtained by studying nearby isotopes. It is therefore planned to extend this work by using targets of the isotopes ^{62}Ni and ^{64}Ni. Another important issue seems to be the dependence of the spectra on the pion energy. It is therefore planned to go down to lower energies. In particular, a run on ^{58}Ni at 50 MeV is planned which is about the lowest pion energy conveniently available from the LEP channel at LAMPF. It is also planned during this run to start looking at some charged-particle spectra. The spectrum of high-energy protons from a pion-induced reaction is particularly important becuase if there is a paucity of such protons, as some evidence indicates, it is implied that the initial reaction is taking place on a cluster of nucleons rather than on just two nucleons. It is therefore planned to use a plastic scintillator—5" NaI telescope to look at the spectra of high-energy protons from a thin Ni target bombarded with 200-MeV pions.

*Northwestern University, Evanston, Illinois.

†Chemistry Division, ANL.

‡Los Alamos Scientific Laboratory, Los Alamos, New Mexico.

III. HEAVY-ION PHYSICS

INTRODUCTION

The program of research in heavy-ion physics at the Argonne FN tandem brings to bear a variety of precision techniques to study heavy-ion-induced reactions in the range of projectile mass and energy available here.

A number of new techniques, particularly ultra-fast time-resolution (0.5×10^{-10} s) time-of-flight telescopes, and very thin ΔE detectors for fusion measurements, as well as the development of a focal-plane detector system for heavy ions have allowed this effort to continue to be extremely productive.

The study of high-resolution spectroscopy has, in the past year, been augmented by systematic measurements to account for the distribution of total reaction strength among the various heavy-ion reaction modes. The refined time-of-flight techniques have allowed clear separation of all reaction products even for channels where no charge transfer is involved. The detailed investigations at Argonne have led to the experimental observation that the sum total of all quasielastic channels exhausts all the available cross section for grazing collisions. This fact has led to serious questions regarding some of the basic assumptions underlying accepted reaction theories. Other difficulties in reaction models have come out of the study of transfer-reaction systematics with high-energy resolution. The range of validity of DWBA calculations appears to be very limited and the difficulties may well have their source in the fact that in heavy-ion reactions the interacting nuclei are strongly coupled.

This year a program of careful measurements of fusion cross sections has been started. The data supplement the information on direct reactions and give, for the first time, a reliable measure of total reaction cross sections. The technique has also been applied in lighter systems, where qualitatively new phenomena have emerged. One of these is a sharp difference in the absolute magnitude of the fusion cross section which seems to depend on the presence of unpaired valence nucleons. The other is the observation of distinct resonances, suggestive of shape resonances, in the fusion cross section for tightly bound systems.

The completion of an advanced beam-bunching system in the coming year will provide an important new capability for time-of-flight studies of heavy-ion reactions, and this capability will be exploited as soon as available. In the longer perspective, the superconducting energy booster will extend the horizons of the whole heavy-ion research program at Argonne.

A. MACROSCOPIC FEATURES OF HEAVY-ION REACTION CROSS SECTIONS

For a proper understanding of the mechanisms of heavy-ion-induced reactions, it is necessary that one obtain adequate data for the distribution of reaction strengths. Such complete data have recently been obtained at Argonne in the ^{16}O + Ca isotope system. The quasielastic (transfer and inelastic scattering) data were obtained using time-of-flight telescopes. Fusion cross sections were obtained with very thin ΔE detectors. The distribution among channels has been studied as a function of target mass through the Ca isotopes and as a function of bombarding energy by using the Berkeley 88-in. cyclotron for the higher bombarding energies. A rather complete picture is beginning to emerge from these data, although the validity of theoretical models is still far from clear.

The study of fusion cross sections as a function of bombarding energy has been pursued in some detail in light systems. Here the theoretical expectation by Mosel is for the fusion cross section to start decreasing at higher bombarding energies. Such an effect is indeed seen in the $^{16}O + ^{12}C$, $^{18}O + ^{12}C$, $^{19}F + ^{12}C$, and $^{12}C + ^{12}C$ systems. But in addition, with the most tightly bound structures ($^{16}O + ^{12}C$) and ($^{12}C + ^{12}C$), resonant structures are observed in the total fusion cross section. Such structures seem to extend to much higher excitation energies than had been previously suspected and their interpretation is far from clear.

a. Study of the Reactions $^{16}O + ^{40,42,44,48}Ca$ at 56 MeV: Individual Transfer

D. G. Kovar, Y. Eisen, W. Henning, B. Zeidman, H. T. Fortune, T. R. Ophel, P. Sperr, and S. E. Vigdor

As part of our broader program to study all reaction channels in the interactions of ^{16}O with $^{40,42,44,48}Ca$ at 56 MeV, we have completed measurements of angular distributions for all inelastic scattering and one-, two-, and multinucleon transfer reactions leading to final states whose strength allowed clear resolution and identification in our ΔE-E (TOF) telescope system.[1] An example of the spectra obtained

[1] B. Zeidman, W. Henning, and D. G. Kovar, Nucl. Instrum. Methods 118, 361 (1974).

in our measurements is shown in Fig. 4 for the reactions $^{42}Ca(^{16}O, ^{13,14,15}N)^{45,44,43}Sc$ at $\theta_L = 16^\circ$. Portions of our data have been reported already[2—5]; however, the motivation of this study is to obtain sufficient data to give an overall picture of the reaction processes. The completeness of our set of data is important for several reasons: (1) the systematic trends observed in the transfer strengths should provide clues to the nature of required modifications to the reaction theories, and (2) the simultaneous measurements of all strong channels provide sufficient data to adequately test the more complex reaction models in which the effects of various direct channels are coupled. In general our results show (1) that levels populated strongly in light-ion-induced reactions are strongly populated

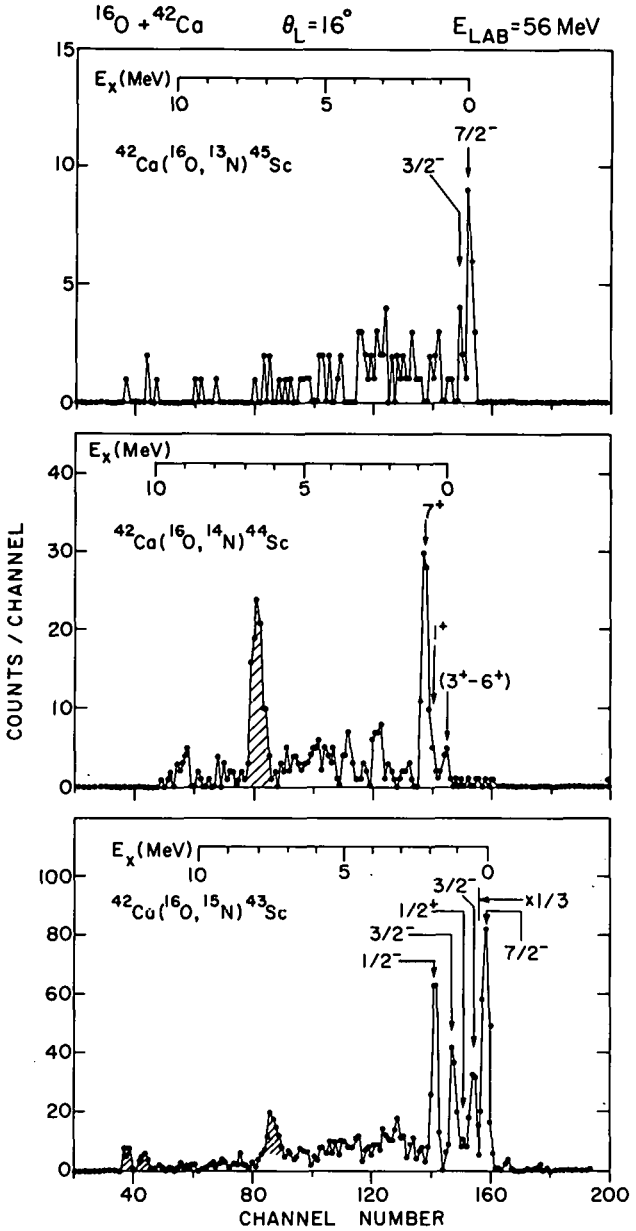

Fig. 4. Energy spectra obtained for $^{42}Ca(^{16}O, 13, 14, 15N)45, 44, 43Sc$ reactions in measurements with the ΔE-E (TOF) system.

[2] W. Henning, D. G. Kovar, B. Zeidman, and J. R. Erskine, Phys. Rev. Lett. 32, 1015 (1974).

[3] D. G. Kovar, W. Henning, B. Zeidman, Y. Eisen, and H. T. Fortune, Phys. Rev. Lett. 33, 1611 (1974).

[4] H. T. Fortune, W. Henning, D. G. Kovar, B. Zeidman, and Y. Eisen, hys. Lett. 57B, 445 (1975).

[5] Y. Eisen, H. T. Fortune, W. Henning, D. G. Kovar, S. Vigdor, and B. Zeidman, Phys. Rev. C 13, 699 (1976).

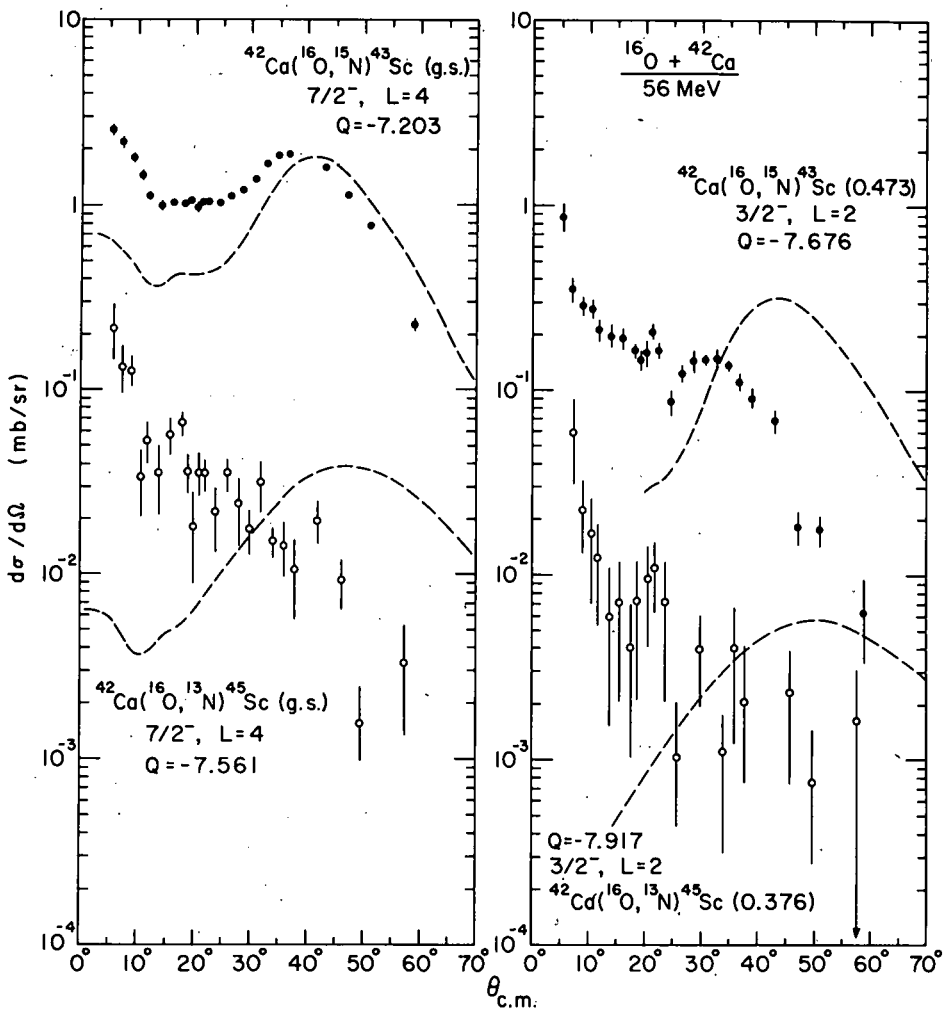

Fig. 5. Angular distributions measured for $^{42}Ca(^{16}O,^{13,15}N)^{45,43}Sc$ transfers. The dashed curves are DWBA calculations performed with the exact finite range code LOLA.

in the corresponding ^{16}O induced reactions and vice versa, (2) that the excited states of the outgoing projectile are almost always observed and in many cases are populated more strongly than the ground states of these projectiles, and (3) that with rare exceptions conventional DWBA calculations are not able to reproduce the observed angular distributions, with some evidence that the degree of discrepancy is correlated with the degree of kinematic mismatch. In Fig. 5 angular distributions for $^{42}Ca(^{16}O,^{15}N)^{43}Sc$ and $^{42}Ca(^{16}O,^{13}N)^{45}Sc$ transfers are shown, togeth with the DWBA predictions to exemplify the kind of discrepancies typically

encountered. At present, we are involved in a collaboration with reaction theorists performing coupled-channels calculations for some of the transitions studied.

b. Study of the Reactions $^{16}O + ^{40,42,44,48}Ca$ at 56 MeV: Properties of Quasielastic Processes

D. G. Kovar, S. E. Vigdor, Y. Eisen, W. Henning, T. R. Ophel, P. Sperr, and B. Zeidman

Measurements[1—3] have been completed on the B-Ne isotopes produced in $^{16}O + ^{40,42,44,48}Ca$ reactions at $E_{lab}(^{16}O) = 56$ MeV using the ΔE-E (TOF) telescope system.[4] The energy resolution and dynamic range of this system made possible the extraction of angular distributions, both for individual transitions and for the total reaction channels. These data are important because they provide a link between those processes which are currently analyzed with microscopic models, such as DWBA or CCBA,[5] and reaction cross sections which are treated in macroscopic-reaction models.[6]

---

[1] D. G. Kovar, S. E. Vigdor, Y. Eisen, P. Sperr, W. Henning, T. Ophel, and B. Zeidman, Bull. Am. Phys. Soc. 20, 1191 (1975).

[2] D. G. Kovar, Y. Eisen, W. Henning, T. R. Ophel, B. Zeidman, J. R. Erskine, H. T. Fortune, P. Sperr, and S. E. Vigdor, in Proceedings of Symposium on Macroscopic Features of Heavy Ion Collisions. Vol. II - Contributed Papers, Argonne National Laboratory, Argonne, Illinois, 1-3 April 1976, Physics Division Report ANL-PHY-76-2 (May 1976), p. 645.

[3] S. E. Vigdor, in Proceedings of Symposium on Macroscopic Features of Heavy Ion Collisions. Vol. I - Invited Papers, Argonne National Laboratory, Argonne, Illinois, 1-3 April 1976, Physics Division Report ANL-PHY-76-2 (May 1976), p. 95.

[4] B. Zeidman, W. Henning, and D. G. Kovar, Nucl. Instrum. Methods 118, 361 (1974).

[5] For example, see Y. Eisen, H. T. Fortune, W. Henning, D. G. Kovar, S. Vigdor, and B. Zeidman, Phys. Rev. C 13, 699 (1976).

[6] For example, see L. G. Moretto and J. S. Sventek, in Proceedings of Symposium on Macroscopic Features of Heavy Ion Collisions. Vol. I - Invited Papers, Argonne National Laboratory, Argonne, Illinois, 1-3 April 1976, Physics Division Report ANL-PHY-76-2 (May 1976), p. 235; J. Wilczynski, ibid, p. 211.

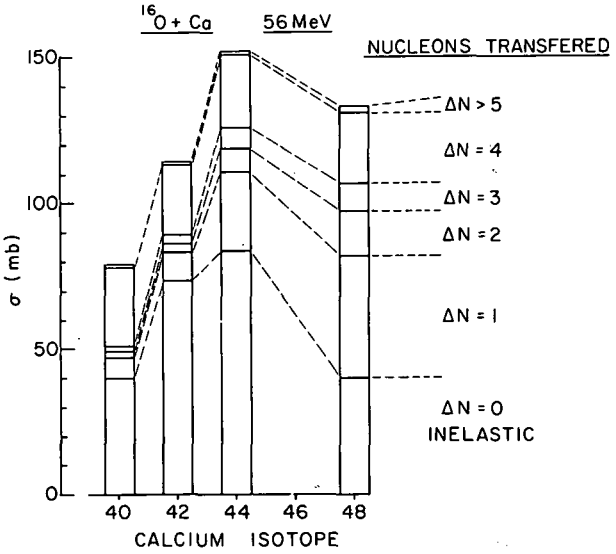

Fig. 6. Distribution of the total ^{16}O + Ca direct-reaction cross section as function of the number of nucleons transferred. Most of the transfer-reaction strength corresponds to the addition of nucleons to the target nucleus.

The gross systematic features observed for the quasielastic cross sections in this study show effects of macroscopic aspects of the heavy-ion interaction (similar to those found for much heavier systems), combined with microscopic nuclear-structure effects. The following general trends are clear: (1) with increasingly negative Q value in any particular channel, and with increasing mass transfer, the angular distributions evolve smoothly from shapes dominated by a grazing peak, as predicted by DWBA, to shapes which are strongly forward peaked and fall monotonically as a function of angle; (2) with increasing charge transfer to the target nucleus, the observed strength becomes concentrated in broad Gaussian distributions centered at increasingly high excitation of the final nuclei; and (3) the quasielastic strength is most heavily concentrated among reactions involving transfer of four or fewer nucleons to the target nucleus (see Fig. 6). Superimposed on these smooth trends are features which clearly reflect the specific structure of the nuclei involved: (1) inelastic scattering to low-lying collective levels accounts for a substantial fraction of the total quasielastic cross section, and is dominant for ^{42}Ca and ^{44}Ca, which do not have closed neutron shells; (2) the total strength in the ^{13}N and ^{14}N channels decreases progressively from ^{40}Ca to ^{48}Ca, as the $f_{7/2}$ neutron shell is filled; and (3) the ^{12}C channel, which may be populated t

transfer of α-like clusters, is much stronger than all other multinucleon transfers for each Ca isotope.

Our results provide not only a test of the applicability of macroscopic models to the distribution of reaction strength for a relatively light system, but also important systematics relevant to the mechanism of individual quasielastic transitions. The measurements indicate which channels are important to include in coupled-channels treatments of individual transfers, but also suggest the coexistence with a conventional direct-reaction mechanism of a more complex process involving considerably longer contact between the two nuclei.

Similar measurements of both individual transitions and total reaction channels have been made for $^{16}O + ^{40}Ca$ at 75 MeV and for $^{18}O + ^{48}Ca$ at 56 MeV, and are in the process of being analyzed.

c. Study of the Reactions $^{16}O + ^{40,42,44,48}Ca$ at 56 MeV: Total Reaction Cross Sections

S. E. Vigdor, D. G. Kovar, Y. Eisen, W. Henning, T. R. Ophel, P. Sperr, and B. Zeidman

We have complemented our quasielastic cross-section data for $^{16}O + ^{40,42,44,48}Ca$ reactions at 56 MeV with measurements of the total fusion cross section.[1] The measurements are performed by detecting the heavy fragments left after compound-nucleus decay in a ΔE-E telescope with a thin (3.6 μm) silicon ΔE detector.[2] We have thus experimentally determined both the total reaction cross sections and the division of strength between compound and direct processes, information

---

[1] S. Vigdor, D. G. Kovar, Y. Eisen, W. Henning, T. Ophel, P. Sperr, and B. Zeidman, Bull. Am. Phys. Soc. 20, 1174 (1975).

[2] For experimental details see, P. Sperr, T. H. Braid, Y. Eisen, D. G. Kovar, F. W. Prosser, Jr., J. P. Schiffer, S. L. Tabor, and S. Vigdor, in Proceedings of Symposium on Macroscopic Features of Heavy Ion Collisions. Vol. II - Contributed Papers, Argonne National Laboratory, Argonne, Illinois, 1-3 April 1976, Physics Division Report ANL-PHY-76-2 (May 1976), p. 783.

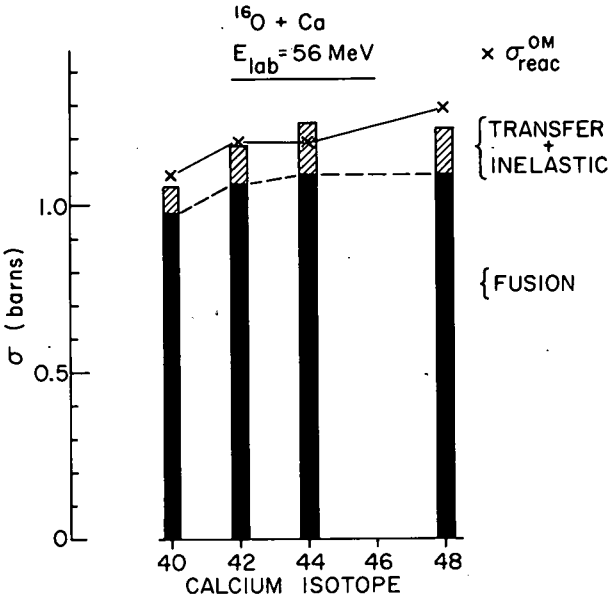

Fig. 7. Measured total reaction cross sections for ^{16}O + Ca and their decomposition in direct (σ_{dir}) and fusion (σ_{fus}) components. The experimental uncertainties are ~50—60 mb for σ_{fus} and ~20 mb for σ_{dir}. The x's represent the reaction cross sections calculated with optical-model parameters which fit the measured elastic scattering angular distributions.

basic to any general theory of heavy-ion interactions. The results of our cross-section measurements are shown in Fig. 7, where it may be observed that the fusion cross section increases by ~10% from ^{40}Ca to ^{42}Ca and is nearly constant for ^{42,44,48}Ca. There is also a sharp increase between ^{40}Ca and ^{42}Ca in the quasielastic strength which in all cases accounts for ~10% of the total reaction cross section. We are still in the process of reducing systematic uncertainties in the data analysis to the point where the experimental results provide a meaningful test for model predictions. At present the total reaction cross sections calculated from optical-model fits to elastic-scattering data reproduce each measured value within the experimental errors of 5—8%; however, there appears to be a systematic discrepancy between the predicted and observed trends across the Ca isotopes (see figure).

With the aid of optical-model and DWBA calculations, we have shown[3] that the direct reactions, while accounting for only ~10% of the total reaction cross section, exhaust a major fraction of the flux available in the surface partial waves. This result suggests the importance

[3] W. Henning, J. P. Schiffer, D. G. Kovar, S. Vigdor, B. Zeidman, Y. Eisen, and H.-J. Körner, Phys. Lett. 58B, 129 (1975).

of including coupling between different surface reactions in the theoretical treatment of direct processes. The effects of such coupling on total reaction cross sections calculated from fits to elastic-scattering data are being investigated.

d. Mechanism of Transfer Reactions Induced by ^{16}O on ^{48}Ca

D. G. Kovar, Y. Eisen, W. Henning, T. R. Ophel, B. Zeidman, J. R. Erskine, H. T. Fortune, and S. E. Vigdor

Angular distributions for inelastic scattering and for all strong transfer channels [$(d\sigma/d\Omega) \geq 20$ μb/sr] in the $^{16}O + ^{48}Ca$ reaction at 56 MeV have been measured using the ΔE-E (TOF) telescope[1] or the split-pole spectrograph.[2] With the failure of DWBA to reproduce the data for many transfer reactions,[3] it is crucial to provide measurements which can adequately test current coupled-channels models of multistep processes involving inelastic scattering or sequential transfer. Central to this study are the single-nucleon transfer reactions (^{16}O, ^{15}N) and (^{16}O, ^{17}O), where we observe simultaneously the excitation of states of both simple (single-particle or single-hole) and complex (multiparticle, multihole) configuration. Of particular interest are the transitions to the weakly populated (unresolved) $\frac{1}{2}^+$ and $\frac{3}{2}^+$ two-particle one-hole (2p-1h) states at $E_x \approx 2.23$ MeV in ^{49}Sc and to the $\frac{3}{2}^-$ one-particle two-hole (1p-2h) state at $E_x = 2.010$ MeV in ^{47}Ca. Because of their parentage, it was hoped that the magnitude and/or shape of the angular distributions for these states would be sensitive to contributions from sequential processes such as (^{16}O, ^{14}C)(^{14}C, ^{15}N) and (^{16}O, ^{18}O)(^{18}O, ^{17}O).

---

[1] B. Zeidman, W. Henning, and D. G. Kovar, Nucl. Instrum. Methods 118, 361 (1974).

[2] J. Erskine, T. H. Braid, and J. C. Stoltzfus (accepted in Nucl. Instrum. Methods).

[3] For example, Y. Eisen, H. T. Fortune, W. Henning, D. G. Kovar, S. Vigdor, and B. Zeidman, Phys. Rev. C 13, 699 (1976).

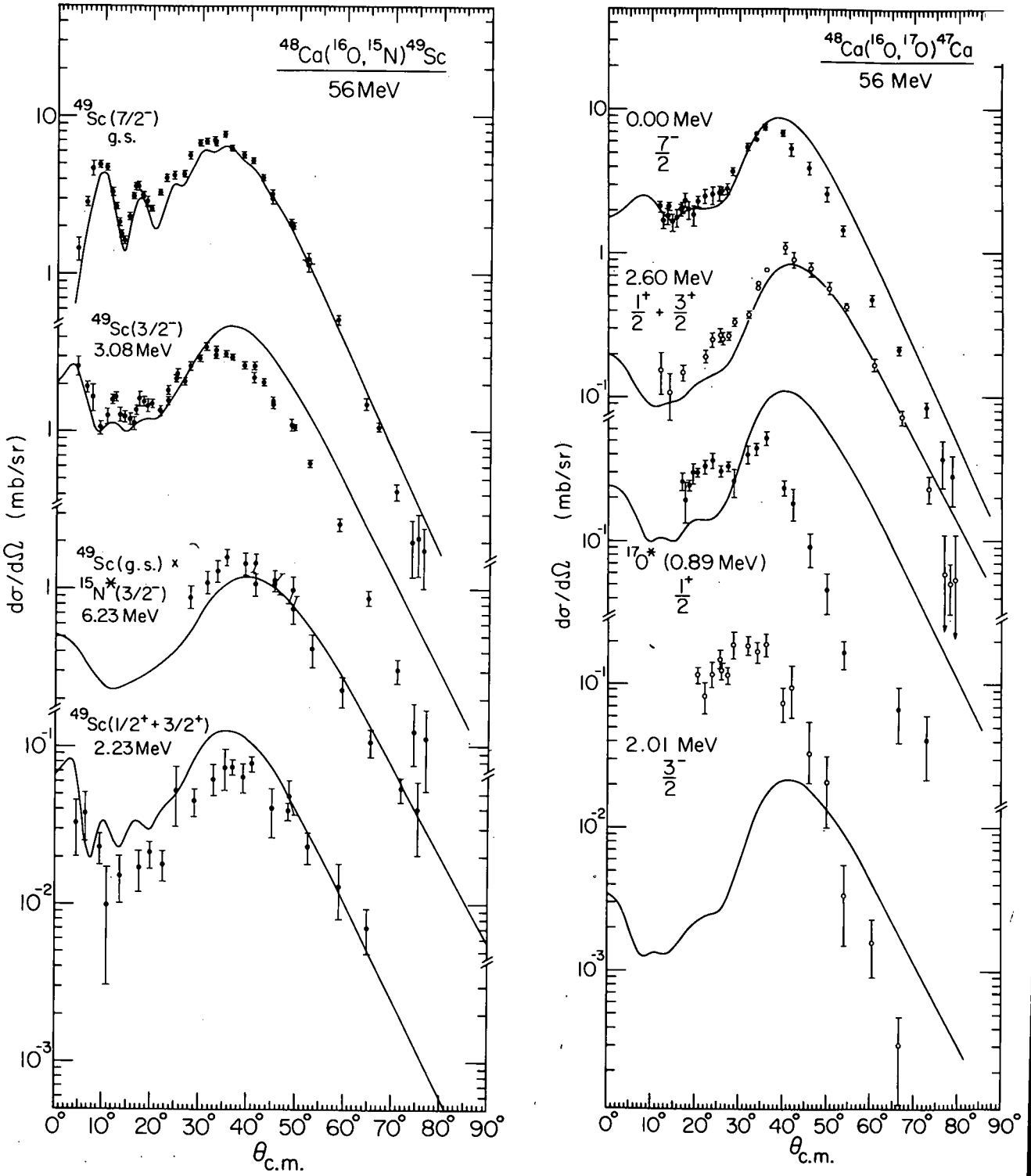

Fig. 8. Angular distributions measured for the $^{48}Ca(^{16}O, ^{15}N)^{49}Sc$ and $^{48}Ca(^{16}O, ^{17}O)^{47}Ca$ reactions. The solid curves are the predicted absolute cross sections predicted by the exact-finite range DWBA or the PTOLEMY [D. H. Gloeckner, M. H. Macfarlane, and Steven C. Piepe Argonne National Laboratory Topical Report ANL-76-11 (March 1976)] using spectroscopic factors extracted in light ion studies.

The angular distributions for the $^{48}Ca(^{16}O, ^{15}N)^{49}Sc$ and $^{48}Ca(^{16}O, ^{17}O)^{47}Ca$ transfer reactions measured are shown in Fig. 8. We found that DWBA calculations[4] reproduce fairly well the shapes and magnitudes of the ($^{16}O, ^{15}N$) angular distributions for transitions to the single-particle (hole) states in $^{49}Sc(^{15}N)$, as well as to the 2p-1h states. In the case of ($^{16}O, ^{17}O$), however, only the results for the single-hole states in ^{47}Ca resemble the predictions; the angular distributions for the transitions to the ^{17}O $\frac{1}{2}^+$ single-particle state and to the 1p-2h state in ^{47}Ca are not reproduced at all. Preliminary calculations for the $^{48}Ca(^{16}O, ^{15}N)^{49}Sc$ ($\frac{1}{2}^+, \frac{3}{2}^+$) transfer indicate that the sequential process is weak;[5] no calculations have been performed thus far for the $^{48}Ca(^{16}O, ^{17}O)^{47}Ca$ ($\frac{3}{2}^-$) transfer.

---

[4] D. G. Kovar, Y. Eisen, W. Henning, T. R. Ophel, B. Zeidman, J. R. Erskine, H. T. Fortune, P. Sperr, and S. E. Vigdor, in Proceedings of Symposium on Macroscopic Features of Heavy Ion Collisions. Vol. II - Contributed Papers, Argonne National Laboratory, Argonne, Illinois, 1-3 April 1976, Physics Division Report ANL-PHY-76-2 (May 1976), p. 645.

[5] G. Sherwood, Bull. Am. Phys. Soc. 21, 65 (1976).

e. Distribution of Reaction Strength Observed in $^{16}O + ^{40}Ca$ Collisions

S. E. Vigdor, D. G. Kovar, P. Sperr, J. Mahoney,* A. Menchaca-Rocha,* C. Olmer,* and M. Zisman*

The distribution of strength among all reactions channels in the interaction of $^{16}O + ^{40}Ca$ has been investigated over a wide range of bombarding energies, in collaboration with a group from Lawrence Berkeley Laboratory.[1] Angular distributions for transfer reactions and inelastic scattering, as well as for elastic scattering, were obtained at $E_{lab}(^{16}O)$ = 56 and 75 MeV at Argonne, and at 104, 140, and 214 MeV at the 88-in. LBL cyclotron. The complete fusion cross section was

---

* Lawrence Berkeley Laboratory, Berkeley, California.

[1] S. E. Vigdor et al., Bull. Am. Phys. Soc. 21, 680 (1976).

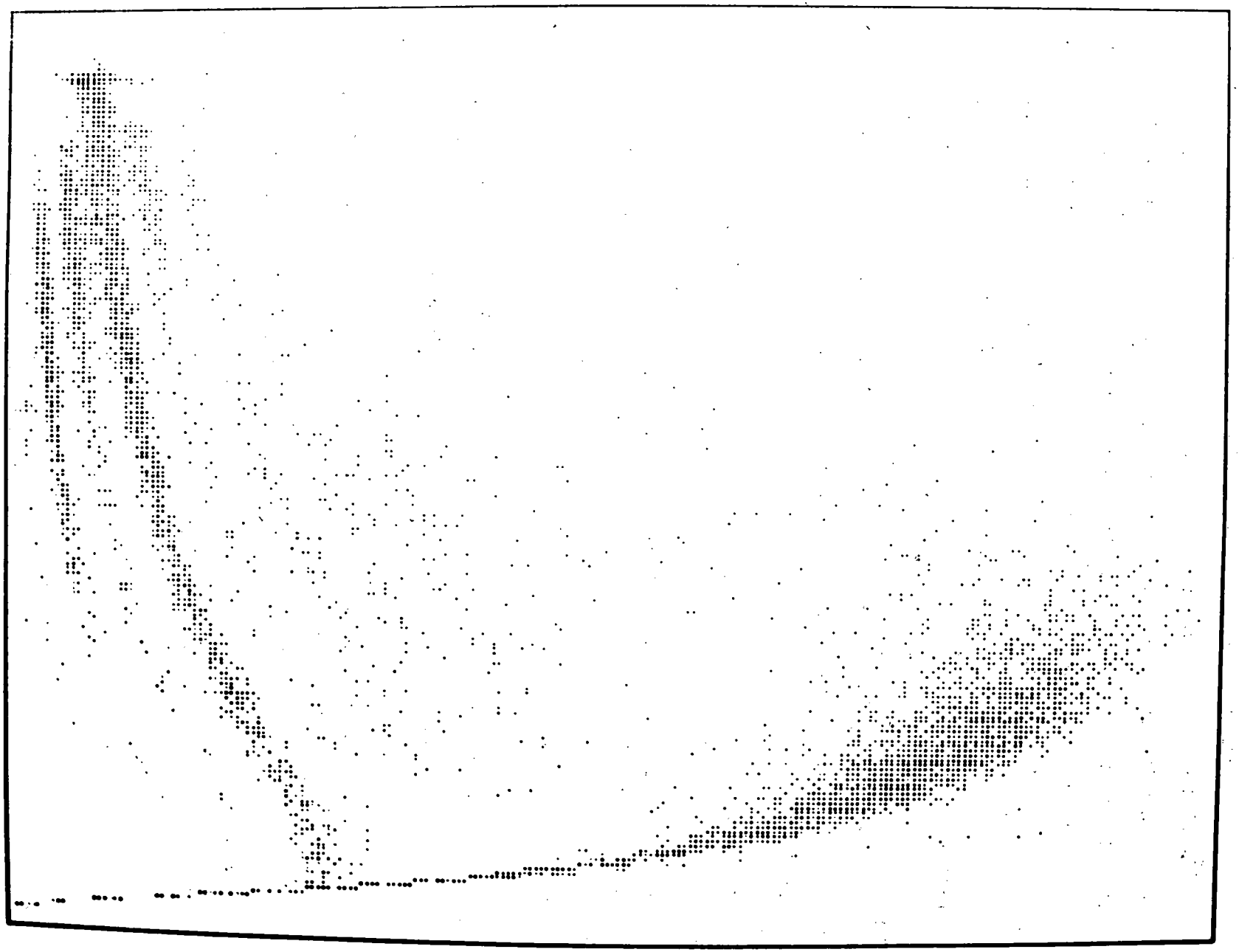

Fig. 9. Two-dimensional display of ΔE (horizontal) vs E_{total} (vertical) obtained at $\theta_L = 6^\circ$ for

measured at these energies and in addition at 40, 45, 50, and 63 MeV by detection of the heavy fragments (evaporation residues) remaining after particle decay of the compound nucleus ^{56}Ni. All the measurements were made with silicon-detector telescopes; for the fusion measurements, ΔE detectors of thickness 2.3 μm or 3.6 μm were used. A representative two-dimensional (E vs ΔE) spectrum acquired with the fusion telescope at E_{lab} = 140 MeV is shown in Fig. 9.

In Fig. 10 the measured fusion cross sections (σ_{fus}) are compared to the total reaction cross sections (σ_{reac}) as a function of bombarding energy. At energies up to about twice the Coulomb barrier height σ_{fus} accounts for most of σ_{reac}. However, whereas the fusion cross section saturates at $E_{lab} \approx 70$ MeV, the reaction cross section continues to rise rapidly toward higher energies. This "break" between σ_{fus} and σ_{reac} is consistent with the model of Glas and Mosel,[2] which assumes that fusion occurs only upon penetration to a critical distance R_c; the solid line through the fusion measurements in Fig. 10 is calculated using this model and the parameters indicated in the figure.

While the data analysis for the nonfusion reactions is still in progress, it is clear that most of the "missing" reaction cross section at high energies in Fig. 10 is accounted for by inelastic scattering and by stripping of relatively few nucleons into the target nucleus, accompanied by substantial (but not complete) damping of the initial kinetic energy into internal excitation of the fragments. The cross section for transfer of more than two units of charge increases with increasing bombarding energy, but remains a small fraction of σ_{reac} even at 214 MeV. The angular distributions of the transfer reaction products at the high energies are strongly forward peaked, as has been observed also for other light systems.[3]

---

[2] D. Glas and U. Mosel, Nucl. Phys. A237, 429 (1975).

[3] T. M. Cormier et al., Phys. Rev. C 13, 682 (1976); R. Albrecht et al., Phys. Rev. Lett. 34, 1400 (1975).

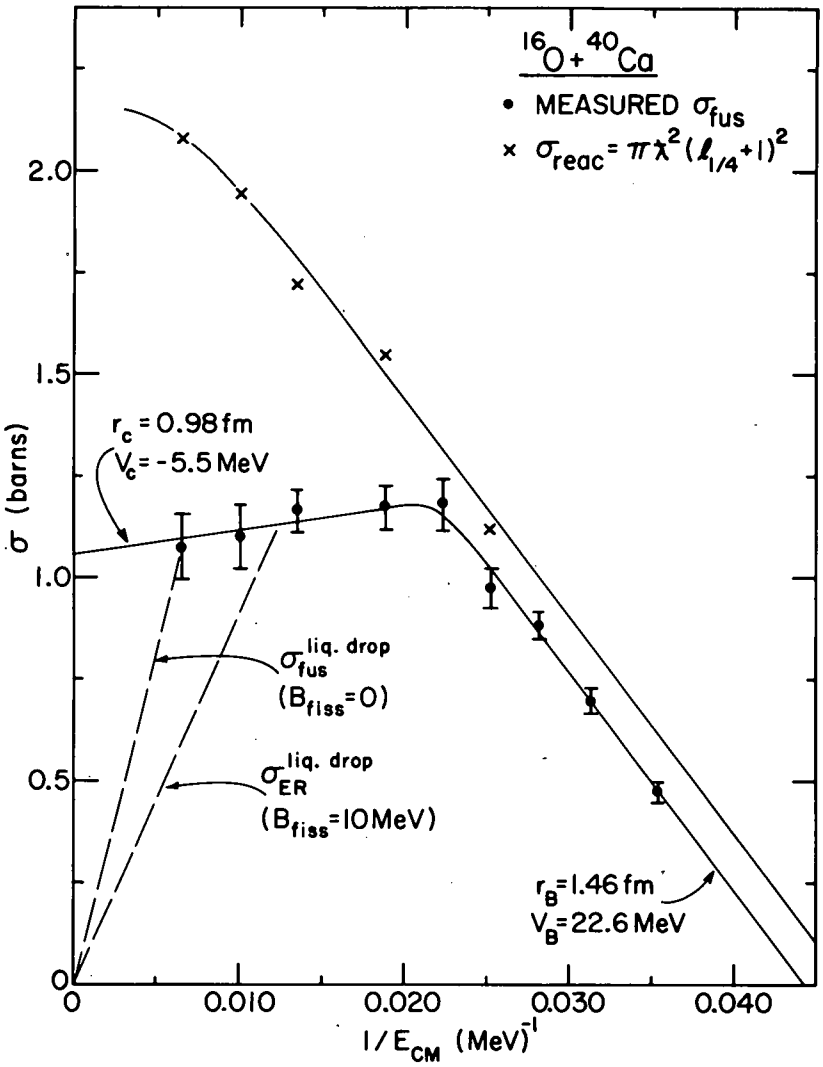

Fig. 10. Energy dependence of the fusion and total reaction cross sections for $^{16}O + ^{40}Ca$. Only evaporation residues (with $Z \geq 22$) have been included in the experimental determination of σ_{fus}; at the highest bombarding energies (E_{lab} = 140, 214 MeV) there may in addition be appreciable cross section for fusion followed by fission. The total reaction cross sections are determined from the measured elastic scattering quarter-points [$d\sigma_{el}(\theta_{1/4})/d\sigma_{Ruth}(\theta_{1/4}) = 0.25$; $\ell_{1/4} + \frac{1}{2} = \eta \cot(\theta_{1/4}/2)$]. The solid curve for σ_{reac} is only to guide the eye. The solid curve for σ_{fus} is calculated using the model of Ref. 2 and the parameters indicated in the figure. The dashed lines are estimates of the limiting total fusion and evaporation residue (ER) cross sections for formation of ^{56}Ni, based on fission barrier (B_{fiss}) calculations in the rotating liquid drop model (RLDM) of Ref. 5. Note that the measured σ_{ER} at E_{lab} = 214 MeV exceeds the RLDM estimate.

Little is yet known about the decomposition of the total reaction cross section in collisions between light nuclei at very high energies. Several models[4,5] predict that a compound nucleus cannot be formed with more than a certain critical angular momentum ℓ_{cr}; at energies above that for which the partial wave ℓ_{cr} first contributes to the fusion cross section, σ_{fus} is predicted to drop toward zero. In the rotating liquid drop model (RLDM) of Ref. 5, ℓ_{cr} is associated with the vanishing of the fission barrier ($B_{fiss} = 0$). The corresponding falloff predicted for the total fusion cross section, as indicated by a dashed line in Fig. 10, is not inconsistent with our measurements. However, the experimental results do exceed the estimated limit on the evaporation-residue cross section (see Fig. 10), which is considerably lower than the limit on σ_{fus} because fission is the favored decay mode of the compound nucleus for those angular momenta for which $B_{fiss} \leq 10$ MeV. The present results, together with other recent measurements,[6,7] suggest that the RLDM limits, based on calculations for rigidly rotating nuclei in thermal equilibrium, are not applicable to the highly excited composite systems formed in the fusion of light nuclei.

[4] R. Bass, Nucl. Phys. A231, 45 (1974).

[5] S. Cohen, F. Plasil, and W. J. Swiatecki, Ann. Phys. 82, 557 (1974).

[6] R. G. Stokstad et al., Phys. Rev. Lett. 36, 1529 (1976).

[7] M. N. Namboodiri, E. T. Chulick, and J. B. Natowitz, Nucl. Phys. A263, 491 (1976).

f. α-Particle and Proton Emission from the $^{16}O + ^{12}C$ System

S. L. Tabor, Y. Eisen, Z. Vager, and D. G. Kovar

This investigation of the emission of light particles following ^{16}O bombardment of a ^{12}C target was undertaken to complement a previous study[1] of the yield of fusion products from the same system.

[1] P. Sperr, S. Vigdor, Y. Eisen, W. Henning, D. G. Kovar, T. R. Ophel, and B. Zeidman, Phys. Rev. Lett. 36, 405 (1976).

The source of the fluctuations observed in the fusion cross section is not yet understood, and a search for similar structure in the light particle yields could provide further information about the effect.

Another phenomenon which the light ions can possibly elucidate is the observed saturation of the fusion cross section at higher energies. The fusion cross section ceases to increase and falls considerably below the total reaction cross section at higher bombarding energies. If an increasing fraction of the reaction cross section at higher energies leads to fragmentation of the colliding systems, this will be observed in the form of increased α production.

Beams at 30 to 74 MeV ^{16}O from the Argonne National Laboratory tandem accelerator were incident on self-supporting ^{12}C targets of 20 to 40 $\mu g/cm^2$ thickness. Reaction products were detected with two ΔE-E surface-barrier counter telescopes, using ΔE detectors of 7.2 and 15 μm thickness.

Excitation curves of proton, α and elastic ^{16}O yield were measured in steps of 0.5 to 2.0 MeV in the range E_{lab} = 30—64 MeV. In order to determine the total cross sections, complete angular distributions (10° to 170°) were measured at E_{lab} = 35, 49, 62, and 74 MeV.

The energy and angle-integrated α and proton total cross sections, σ_α and σ_p, are graphed as a function of incident energy in Fig. 11. To produce these curves, the differential cross sections, which were measured as a function of energy, were converted into total cross-section values by normalization factors interpolated between the energies at which angular distributions were measured. The interpolation of the normalization factors is justified by the fact that they change less than 10% between 35 and 62 MeV. Relative uncertainties in σ_α and σ_p are estimated to be about ±5% and the uncertainty in the absolute normalization is about ±15%.

Also shown in Fig. 11 is the fusion cross section σ_F reported by Sperr et al.[1] for the same colliding system. A corresponde

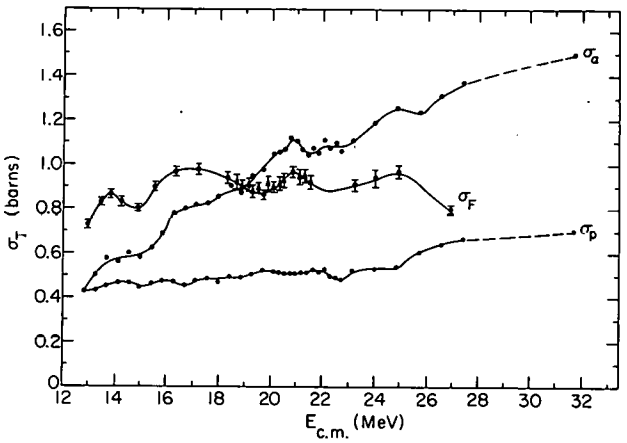

Fig. 11. Total cross sections for production of protons σ_p, α particles σ_α, and evaporation residues σ_F as a function of incident center-of-mass energy. σ_F is taken from Ref. 1 and the lines are drawn merely to guide the eye.

can be seen between the fluctuations in σ_F and σ_α. However, σ_α, unlike σ_F, increases by more than a factor of 3 in this energy range. The change in σ_α may reflect, in part, an increasing multiplicity of α particles emitted per interaction. σ_p shows less structure and increases only about 50% in this range.

Further work is in progress to understand the rapid increase in α yield with energy and to establish a more accurate calibration for the absolute cross sections.

g. Fusion Cross Sections of Light Heavy-Ion Systems

P. Sperr, T. H. Braid, Y. Eisen, D. G. Kovar, F. W. Prosser, Jr., J. P. Schiffer, S. L. Tabor, and S. Vigdor

In a recent study of the $^{16}O + ^{12}C$ system, unexpected oscillatory structure was seen in the energy dependence of the fusion cross section.[1] In the present study,[2] we bombarded ^{12}C targets with ^{12}C, ^{18}O, and ^{19}F beams in order to establish the range of nuclei over which structure is seen in the fusion excitation function and also to delineate the macroscopic features of the fusion process. The experimental procedure and uncertainties have been described previously.[1]

---

[1] P. Sperr, S. Vigdor, Y. Eisen, W. Henning, D. G. Kovar, T. R. Ophel, and B. Zeidman, Phys. Rev. Lett. 36, 405 (1976).

[2] P. Sperr, T. H. Braid, Y. Eisen, D. G. Kovar, F. W. Prosser, Jr., J. P. Schiffer, S. L. Tabor, and S. Vigdor (submitted to Phys. Rev. Lett.).

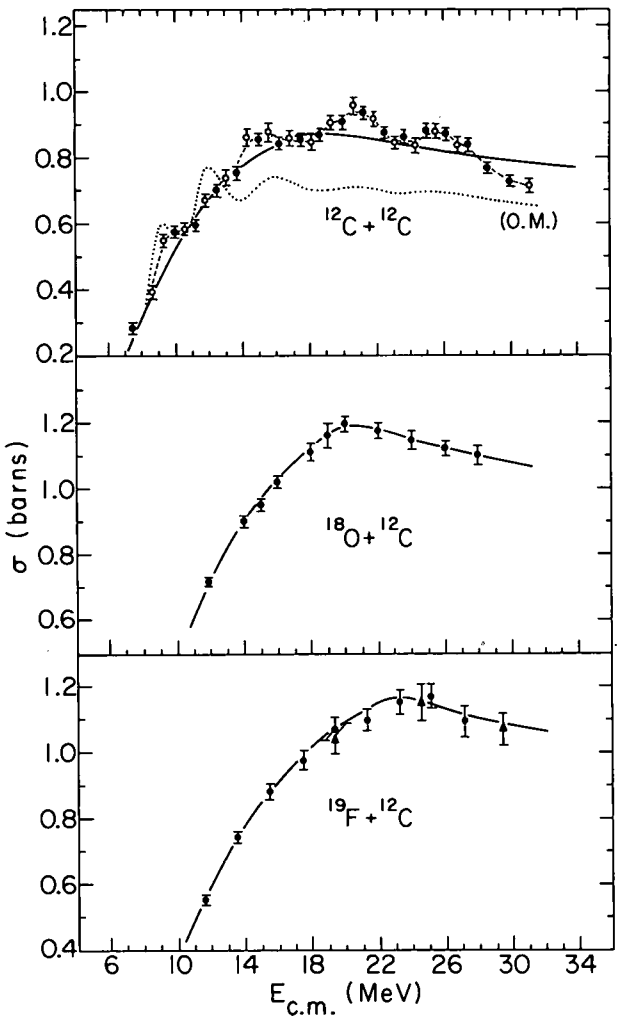

Fig. 12. Total fusion cross section for $^{12}C + ^{12}C$, $^{18}O + ^{12}C$, and $^{19}F + ^{12}C$, as a function of the c.m. energy. The open circles in the case of $^{12}C + ^{12}C$ represent measurements at $\theta_{lab} = 6^{\circ}$ only, where the total fusion cross section was estimated from the ratio $\sigma_{fus}/[d\sigma_{fus}/d\Omega(6^{\circ})]$ at neighboring energy points. The triangles in the case of $^{19}F + ^{12}C$ are values taken from F. Pühlhofer, W. Pfeffer, B. Kohlmeyer, and W. F. W. Schmeider, Nucl. Phys. A244, 329 (1975). The solid lines are model calculations (see text). For $^{12}C + ^{12}C$ the dotted curve is the reaction cross section calculated from the optical model.

All reaction products with Z higher than the incident ions were assumed to be evaporation residues and were included in defining the fusion cross section.

The fusion cross sections $[\sigma_{fus}(\sigma)]$ for the three systems studied are shown in Fig. 12 as a function of c.m. energy. The solid curves in Fig. 12 are calculated using the model of Glas and Mosel[3] which is based on the assumption that fusion occurs whenever the nuclei reach a critical separation distance R_c. The experimental results confirm the qualitative prediction of the model that σ_{fus} for such light systems saturates at some critical bombarding energy and then decreases or remains roughly constant at higher energies.

[3] D. Glas and U. Mosel, Phys. Rev. C 10, 2620 (1974).

There are two qualitative features in our experimental results which are striking. First, the excitation function for $^{12}C + ^{12}C$ exhibits oscillations similar to those observed previously for $^{16}O + ^{12}C$, while no such behavior is apparent in the measurements for $^{18}O + ^{12}C$ or $^{19}F + ^{12}C$. The second striking feature is that the structureless excitation functions observed for $^{18}O + ^{12}C$ and $^{19}F + ^{12}C$ are characterized by a significantly higher maximum value of σ_{fus} than the other systems (see Fig. 13).

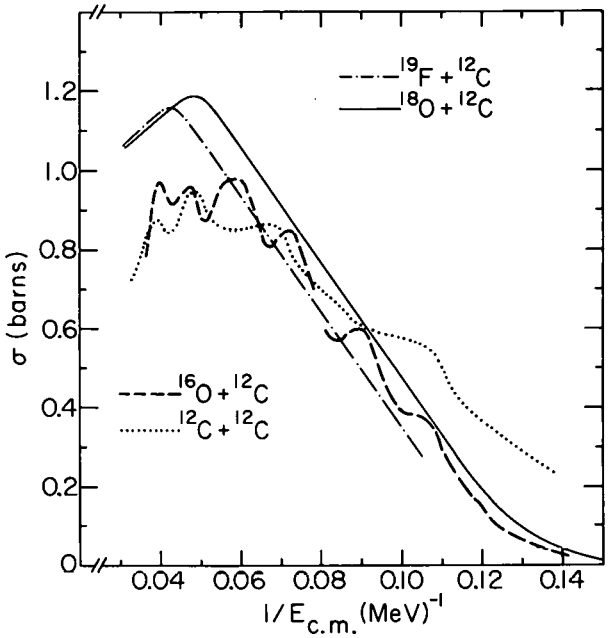

Fig. 13. Total fusion cross sections as a function of $1/E_{c.m.}$. For the sake of clarity only lines connecting the data points are shown. The low-energy part for $^{16}O + ^{12}C$ was taken from J. A. Kuehner and E. Almquist, Phys. Rev. 134, B1229 (1964).

The source of the oscillatory behavior in $\sigma_{fus}(E)$ is not clear at this point. There is no mechanism for generating resonances in the classical model of Ref. 3. However, it was noted that optical-model calculations[1] with weak surface absorption can give rise to shape resonances in the predicted total reaction cross section (e.g., see dotted curve, Fig. 12). While suggestive, it is premature at this point to make a connection between these shape resonances and the oscillations observed in the data.

In regard to the magnitude of the fusion cross sections at higher energies, Glas and Mosel[4] have predicted an anomalous decrease at higher energies whenever the interacting nuclei have closed-shell structure and are not easily excited. While the energy behavior of the data in Fig. 13 are in qualitative agreement with this prediction, a

[4] D. Glas and U. Mosel, Phys. Lett. 49B, 301 (1974).

TABLE I. Maximum values of the high-energy fusion cross section σ_{fus}^{max} for various systems.

System	σ_{fus}^{max} (mb)	Reference
$^{12}C + ^{12}C$	940 ± 30	a
$^{12}C + ^{14}N$	970 ± 100	b
	990 ± 70	c
$^{12}C + ^{16}O$	970 ± 30	d
$^{12}C + ^{18}O$	1200 ± 30	a
$^{12}C + ^{19}F$	1150 ± 40	a
$^{12}C + ^{27}Al$	1190 ± 120	e
$^{16}O + ^{40}Ca$	1180 ± 70	f

[a] This work.

[b] R. G. Stokstad, J. Gomez del Campo, J. A. Biggerstaff, A. H. Snell, and P. H. Stelson, Phys. Rev. Lett. 36, 1529 (1976).

[c] M. Conjeaud, S. Gary, S. Harar, and J. P. Wieleczko, in Proceedings of Symposium on Macroscopic Features of Heavy Ion Collisions. Vol. II - Contributed Papers, Argonne National Laboratory, Argonne, Illinois, 1-3 April 1976, Physics Division Report ANL-PHY-76-2 (May 1976), p. 499.

[d] Reference 1.

[e] R. R. Betts, W. A. Lanford, M. H. Mortensen, and R. L. White, in Proceedings of Symposium on Macroscopic Features of Heavy Ion Collisions. Vol. II - Contributed Papers, Argonne National Laboratory, Argonne, Illinois, 1-3 April 1976, Physics Division Report ANL-PHY-76-2 (May 1976), p. 443.

[f] S. Vigdor, D.G. Kovar, P. Sperr, J. Mahoney, A. Menchaca-Rocha, C. Olmer, and M. Zisman, Bull. Am. Phys. Soc. 21, 680 (1976).

possible alternative interpretation is suggested by comparison with results for other systems in which measured fusion excitation functions show a well-defined maximum (Table I). The systems involving the interaction of two 1p-shell nuclei have $\sigma_{fus}^{max} < 1.0$ b, while those systems in which a 1p-shell nucleus collides with another which has some nucleus in the s-d shell exhibit maximum fusion cross sections of ~1.2 b. These data make it tempting to associate the abrupt charge in σ_{fus}^{max} with the introduction of nucleons into a new major oscillator shell.

More data are clearly needed, but in any case the present measurements establish that large qualitative differences in the behavior of the fusion cross sections exist between light systems which differ only slightly in mass.

h. Oscillations in the Excitation Function for Complete Fusion of $^{16}O + ^{12}C$

Y. Eisen, W. Henning, D. G. Kovar, T. R. Ophel, P. Sperr, S. Vigdor, and B. Zeidman

The total fusion cross section for the $^{16}O + ^{12}C$ system has been measured in the energy range 13 MeV $\leq E_{c.m.} \leq$ 27 MeV with a conventional ΔE-E silicon-detector telescope.[1] Almost all the heavy fragments resulting from fusion and subsequent particle evaporation were able to pass through the thin (3.6 μm) ΔE detector without stopping. Two-dimensional (E vs ΔE) data storage facilitated identification of isotopes of different Z (see top inset, Fig. 14). All events identified as arising from isotopes of Ne, Na, Mg, and Al were included in determining the total fusion cross section; very few counts corresponding to F or Si nuclides were observed. Although many low-energy oxygen nuclei were detected, a negligible fraction of these are believed to result from complete fusion since the $^{28}Si \rightarrow 3\alpha + ^{16}O$ process (Q = -24 MeV) is unlikely at our energies (the available center-of-mass energy is insufficient to allow for appreciable α-particle penetration of the Coulomb and centrifugal barriers).

The total fusion cross section was derived by integration of the measured angular distributions (of which examples at two energies are shown in Fig. 14). As can be seen in the bottom inset of Fig. 14, a smooth extrapolation into the angular regions not measured indicates that $\sim$8% of the total cross section arises from angles smaller than 3°, while angles larger than 28° contribute $<$0.3%. The total fusion cross section (σ_{fus}) is plotted as a function of the center-of-mass energy in Fig. 15. The error bars ($\leq$2.5%) which are shown include uncertainties from counting statistics, from the estimate of the number of fusion residues stopped in the ΔE counter, from the extrapolation of the

---

[1] P. Sperr, S. Vigdor, Y. Eisen, W. Henning, D. G. Kovar, T. R. Ophel, and B. Zeidman, to be published in Phys. Rev. Lett.

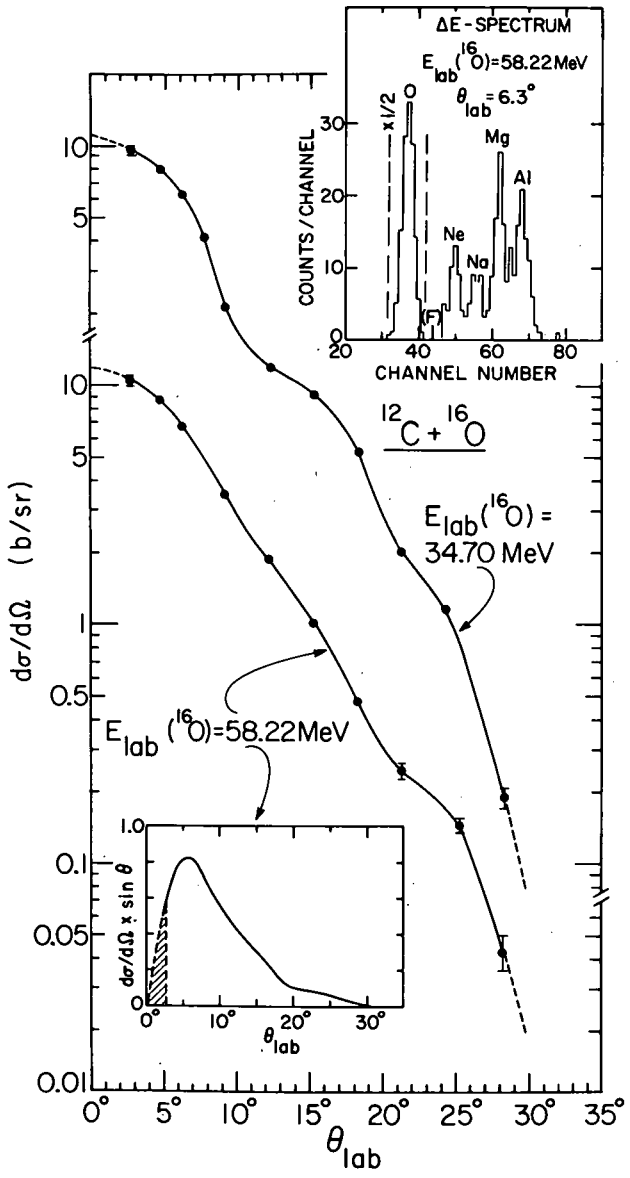

Fig. 14. Angular distributions at E_{lab} = 34.70 and 58.22 MeV summed over all outgoing energies and all fusion residues. The top inset shows a ΔE spectrum in coincidence with a narrow window on E. The bottom inset shows $(d\sigma/d\Omega) \times \sin\theta$ for E_{lab} = 58.22 MeV.

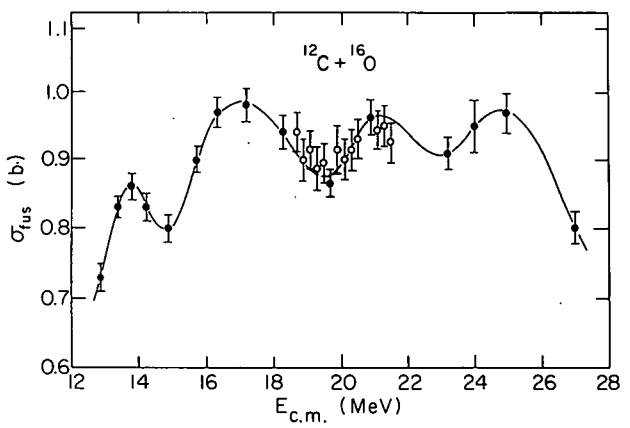

Fig. 15. Total fusion cross section as a function of the center-of-mass energy. The closed circles represent measurements of the complete angular distribution. The open circles represent measurements at $\theta_{lab} = 6^{o}$ only, where the total fusion cross section was estimated from the ratio $\sigma_{fus}/[d\sigma_{fus}/d\Omega(6^{o})]$ at neighboring energy points. The solid line serves only to guide the eye.

differential cross section to 0°, and from the normalization procedure for the absolute cross sections.

Our initial purpose in this experiment was to determine whether the fusion cross section asymptotically approaches an upper limit above some critical energy, as predicted by current theoretical models.[2,3] Our results (Fig. 15) show that above $E_{c.m.} \approx 17$ MeV the cross section does, on the average, remain roughly constant. However, superimposed on the average behavior, we observe unexpected oscillations with a period of 3—4 MeV (c.m. energy). The origin of these oscillations is not yet understood. The structure cannot easily be explained as arising from resonances in the nucleus-nucleus potential. Nor is there any clear correlation of the oscillations with resonances in other $^{16}O + ^{12}C$ channels. [Energies at which resonances have been observed in elastic and inelastic scattering correspond in one case ($E_{c.m.} = 13.7$ MeV) to a maximum in σ_{fus}, but in other cases ($E_{c.m.} = 19.7, 22.7$ MeV) to minima in σ_{fus}.] Furthermore, the oscillations in σ_{fus} are considerably broader than those in other channels. Additional measurements are necessary to determine whether the oscillations are peculiar to the present system or are a more general feature of fusion of "light" heavy ions.

---

[2] D. Glas and U. Mosel, Phys. Rev. C 10, 2620 (1974).

[3] M. Lefort, in Classical and Quantum Mechanical Aspects of Heavy Ion Collisions, edited by H. L. Harney, P. Braun-Munsinger, and C. K. Gelbke (Springer-Verlag, 1975), p. 275, and references therein.

i. Optimum Q Values in (^{18}O, ^{16}O) Reactions

Y. Eisen, W. Henning, H.-J. Körner, D. Kovar, J. P. Schiffer, S. Vigdor, and B. Zeidman

Several studies have been made of optimum Q values in heavy-ion reactions near the Coulomb barrier. In a semiclassical model the matched Q value is determined only by kinematic considerations ıd the matching of Coulomb energies; thus at back angles

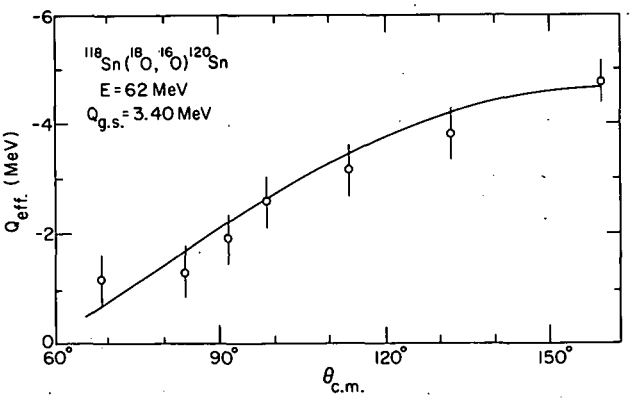

Fig. 16. Optimum Q value as a function of angle at E_{lab} = 62 MeV for $^{118}Sn(^{18}O,^{16}O)^{120}Sn$. The solid line indicates the trend in the data.

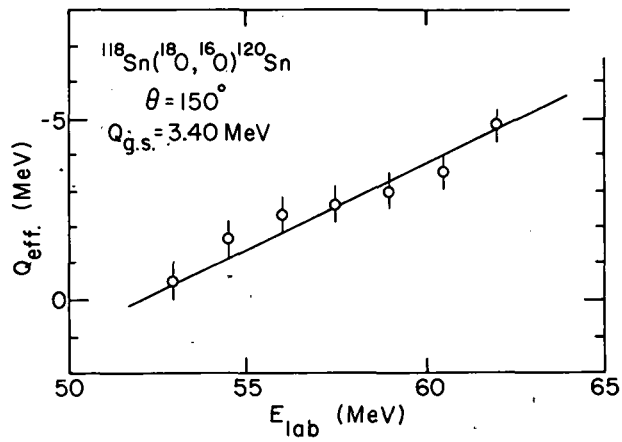

Fig. 17. Optimum Q value as a function of energy at $\theta = 150^{\circ}$ for $^{118}Sn(^{18}O,^{16}O)^{120}Sn$. The solid line indicates the trend in the data.

$$Q_{eff.} = \left(\frac{Z_1 Z_2}{Z_3 Z_4} - 1\right) E_{inc}.$$

Deviations from this expectation have been analyzed in terms of recoil effects and models involving friction. For transfer of neutral fragments the simple expectations are that $Q_{eff.} = 0$ and thus one may study other effects more carefully. Such data have been difficult to obtain because of the experimental problem of identifying a continuum of particles in the presence of strong elastic and inelastic scattering. The time-of-flight technique has allowed measurements of the $^{118}Sn(^{18}O,^{16}O)$ reaction, where the ground-state Q value is 3.4 MeV. The behavior of the centroid of ^{16}O particles indicates that the most favored Q value is increasingly negative as one goes to higher energies (with $\theta = 150^{\circ}$) or to larger angles (with E_{lab} = 62 MeV). The data are shown in Figs. 16 and 17. No simple explanation of this trend can be offered at present.

j. One- and Two-Nucleon Transfer Reactions Induced by ^{18}O on ^{48}Ca

Y. Eisen, K. Daneshvar, W. Henning, D. G. Kovar, T. R. Ophel, P. Sperr, S. L. Tabor, S. E. Vigdor, and B. Zeidman

The one- and two-nucleon transfer reactions initiated by 56-MeV ^{18}O ions incident on ^{48}Ca have been studied using the ΔE-E (TOF) telescope system.[1] The primary motivation was to gain further insight into the transfer mechanism and the structure of the nuclei involved from comparison with previous measurements for the corresponding transfers induced by ^{16}O ions on ^{48}Ca.[2] The most striking differences in the transfers induced by ^{16}O and ^{18}O appear in the two-nucleon transfers. Among the two-nucleon transfers studied [(^{18}O, ^{16}C), (^{18}O, ^{16}O), and (^{18}O, ^{20}O)], the well-matched reaction $^{48}Ca(^{18}O, ^{16}O)^{50}Ca$ is the strongest and exhibits a bell-shaped angular distribution for all transitions to states up to 5 MeV excitation in ^{50}Ca. In contrast the angular distributions for the well-matched $^{48}Ca(^{16}O, ^{14}C)^{50}Ti$ reaction oscillate strongly at forward angles with no pronounced strength at the grazing angle. Possible explanations for this difference are the larger binding energies for the two transferred nucleons in ^{16}O, and the larger surface absorption of ^{18}O which suppresses contributions from close trajectories. However, none of these angular distributions can be reproduced by conventional DWBA calculations which supposedly should account for usual binding energy and absorption effects, and so contributions from more complex processes should be considered. In contrast we observe that despite the fact that the reactions $^{48}Ca(^{16}O, ^{14}C)^{50}Ti$ and $^{48}Ca(^{18}O, ^{16}C)^{50}Ti$ differ by 7 MeV in Q value, the relative spectroscopic factors of the low-lying 0^+, 2^+, 4^+, and 6^+ states extracted from the two reactions are in good agreement, consistent with a simple reaction mechanism. It is the task

---

[1] B. Zeidman, W. Henning, and D. G. Kovar, Nucl. Instrum. Methods 118, 361 (1974).

[2] Y. Eisen, H. T. Fortune, W. Henning, D. G. Kovar, S. Vigdor, and B. Zeidman, Phys. Rev. C 13, 699 (1976).

of the more complex reaction models to satisfactorily explain such behavior, and the results gathered here for the single- and two-nucleon transfers, together with inelastic scattering, provide a complete set of data to stringently test such calculations.

k. Studies of Sub-Coulomb Neutron Transfers in the Region of Ca, Sr, and Zr Isotopes

Y. Eisen, J. P. Schiffer, and P. Sperr

The aim of the present study is to determine the rms radius of the excess neutrons in the Ca isotopes and the rms radii of the excess neutrons in the Sr and Zr isotopes. This may be done by studying the (^{18}O, ^{17}O) and the (^{14}N, ^{15}N) reactions, utilizing position-sensitive detectors in the focal plane of an Enge split-pole spectrograph. Measuring the transfer cross section at sub-Coulomb energies yields very accurate information on the size of the neutron wave function at large distances; this in turn determines the rms radius of the neutron orbit. It is of considerable current interest to compare this quantity to the rms radius of the excess neutrons found from Coulomb energy differences between nuclei and their analogs—work that was initiated at Argonne some years ago and that has produced much controversial discussion in the literature. The development of detection techniques has been very difficult because of the very low energies (~5 MeV) of the oxygen ions.

ℓ. Study of 2-Neutron Transfer Reactions on Vibrational Nuclei

J. Erskine and J. Schiffer

Exploratory data on the ^{106}Pd(^{18}O, ^{16}O)^{108}Pd reaction have been taken with the magnetic spectrograph and the heavy-ion focal-plane detector. The idea is to study the relative strength of vibrational levels under conditions where multistep processes should occur. This work is in progress.

B. MEASUREMENTS OF ASTROPHYSICAL INTEREST

The program involving the study of new isotopes of interest to astrophysics is continuing. Properties of proton-rich and neutron-rich isotopes near iron are under investigation by means of β- and γ-ray spectroscopy. Heavy-ion-induced reactions are used to form these short-lived species. New facilities for studying nuclei far from β stability have been constructed. A shell-model mass equation is being used to predict the masses of neutron-rich nuclides far from stability.

a. Facility for Observing Decay Properties of Isotopes Far from Stability

C. N. Davids, R. C. Pardo, and L. A. Parks

In addition to the pneumatic target-transfer system ("rabbit"), two additional pieces of apparatus are now available for decay studies on short-lived nuclides. These are a multiple-target rabbit and a helium-jet recoil-transport system (HEJRT).

The multiple rabbit allows eight separate targets held in a carrousel to be bombarded sequentially. In this way the buildup of long-lived isotopes is considerably reduced, thereby providing a higher sensitivity to weaker components of the desired short-lived isotopes. In a recent experiment, seven new γ rays following the decay of ^{53}Ti were observed; in previous single-target runs these γ rays were obscured by long-lived background.

The HEJRT system carries nuclides in a helium stream through a capillary tube to a low-background counting area. The nuclides are deposited onto a paper tape, which is then moved in front of the detectors. The advantage of this device is that a fresh source is counted after every bombardment. This system has been used for studies of the decay of ^{68}As.

b. New Isotopes of Interest to Explosive Nucleosynthesis

C. N. Davids, E. B. Norman, R. C. Pardo, L. A. Parks, and S. L. Tabor

(i) Neutron-Rich Isotopes. Neutron-rich isotopes are of interest to nucleosynthesis through their participation in the r process,

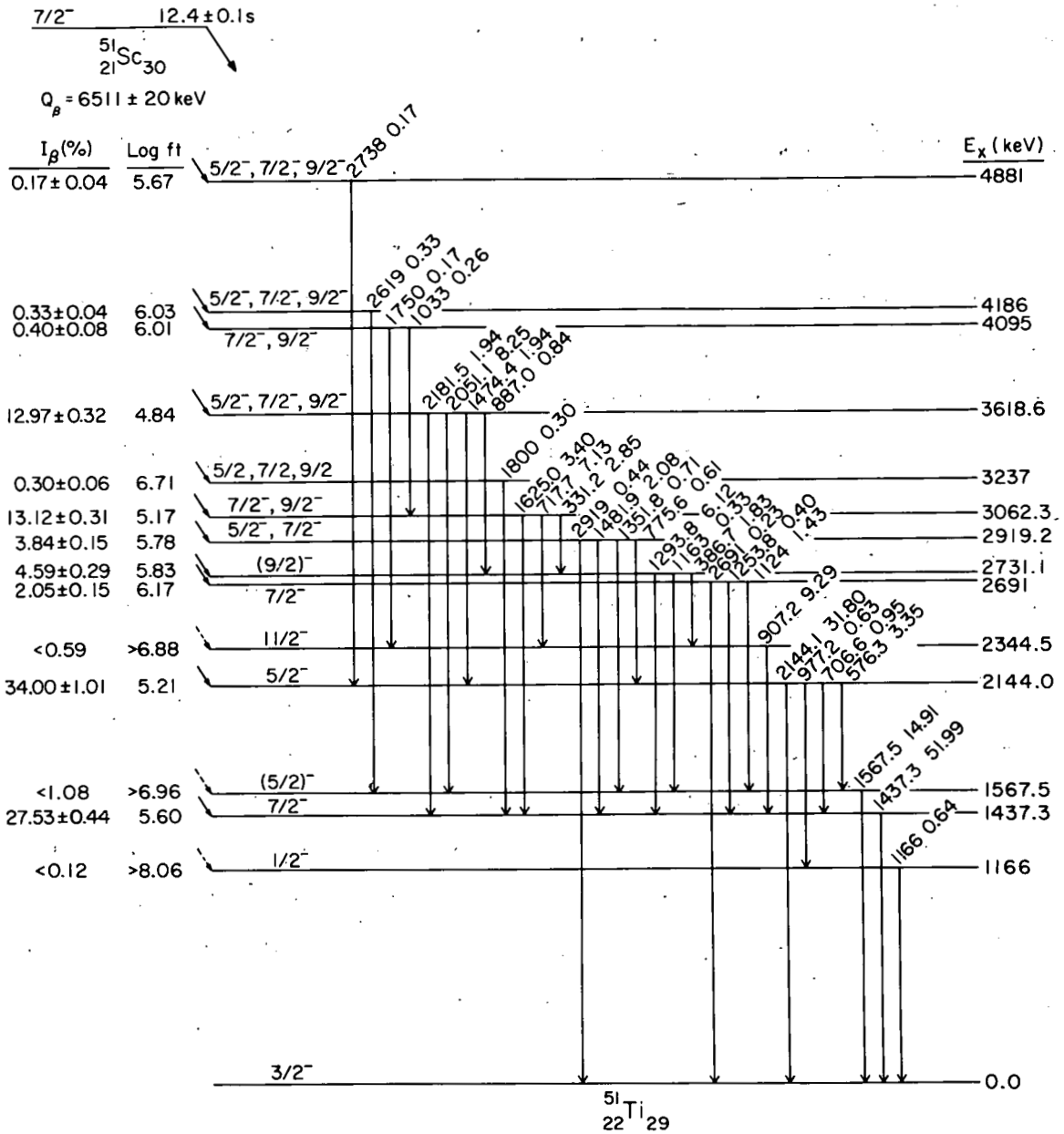

Fig. 18. Decay scheme for ^{51}Sc. Spin assignments for states above 2700-keV excitation are from the present work. Only ^{51}Ti states involved in ^{51}Sc decay are shown.

and by their conjectured presence in the crusts of neutron stars. We are searching for new isotopes near iron, in order to determine their β-decay properties and ground-state masses. This will enable comparisons with various mass predictions and provide information on nuclear systematics for extrapolation to large neutron excesses. Gamma-decay properties of states in the daughter nuclei are also obtained from these studies.

^{51}Sc. The β decay of ^{51}Sc to states in ^{51}Ti has been studied using the rabbit facility. ^{51}Sc was produced via the ^{48}Ca(α,p)^{51}Sc reaction at E_α = 18 MeV. Measurements of γ singles and γ-γ coincidences enabled the ^{51}Sc decay scheme shown in Fig. 18 to be constructed. This investigation yielded a more accurate determination of the ^{51}Sc half-life (12.4 ± 0.1 s), the observation of previously unknown β branches to ^{51}Ti levels at 2691, 2731, 2919, 3062, 3237, 3619, 4095, 4186, and 4881 keV, and the assignment of new levels in ^{51}Ti at 3062, 4095, and 4186 keV.

^{53}Ti. The β decay of 32.7 s ^{53}Ti has been studied using the multiple-rabbit system. The nuclide was produced by the ^{48}Ca(^{7}Li,pn)^{53}Ti reaction, with 14—20-MeV ^{7}Li ions. Gamma singles, γ-γ coincidence and β-γ coincidence measurements were performed, and the resulting preliminary decay scheme for ^{53}Ti is shown in Fig. 19.

A mass excess for ^{53}Ti of -46.89 ± 0.10 MeV was obtained from the β-γ measurements. Three separate β end points were determined by stretching or compressing a "standard" β spectrum having a known end point. The ^{52}V β spectrum was used for this standard shape. A typical fit to a ^{53}Ti β spectrum is shown in Fig. 20.

^{59}Mn. This nucleus was produced via the ^{48}Ca(^{13}C,pn)^{59}Mn reaction with a 26-MeV ^{13}C beam. ^{59}Mn decays with a half-life of 4.75 ± 0.14 s, and emits seven delayed γ rays. A preliminary decay scheme for ^{59}Mn is shown in Fig. 21. This scheme was constructed using the results of singles γ and γ-γ coincidence measurements.

pins and parities have been taken from the literature. β-γ coincidence

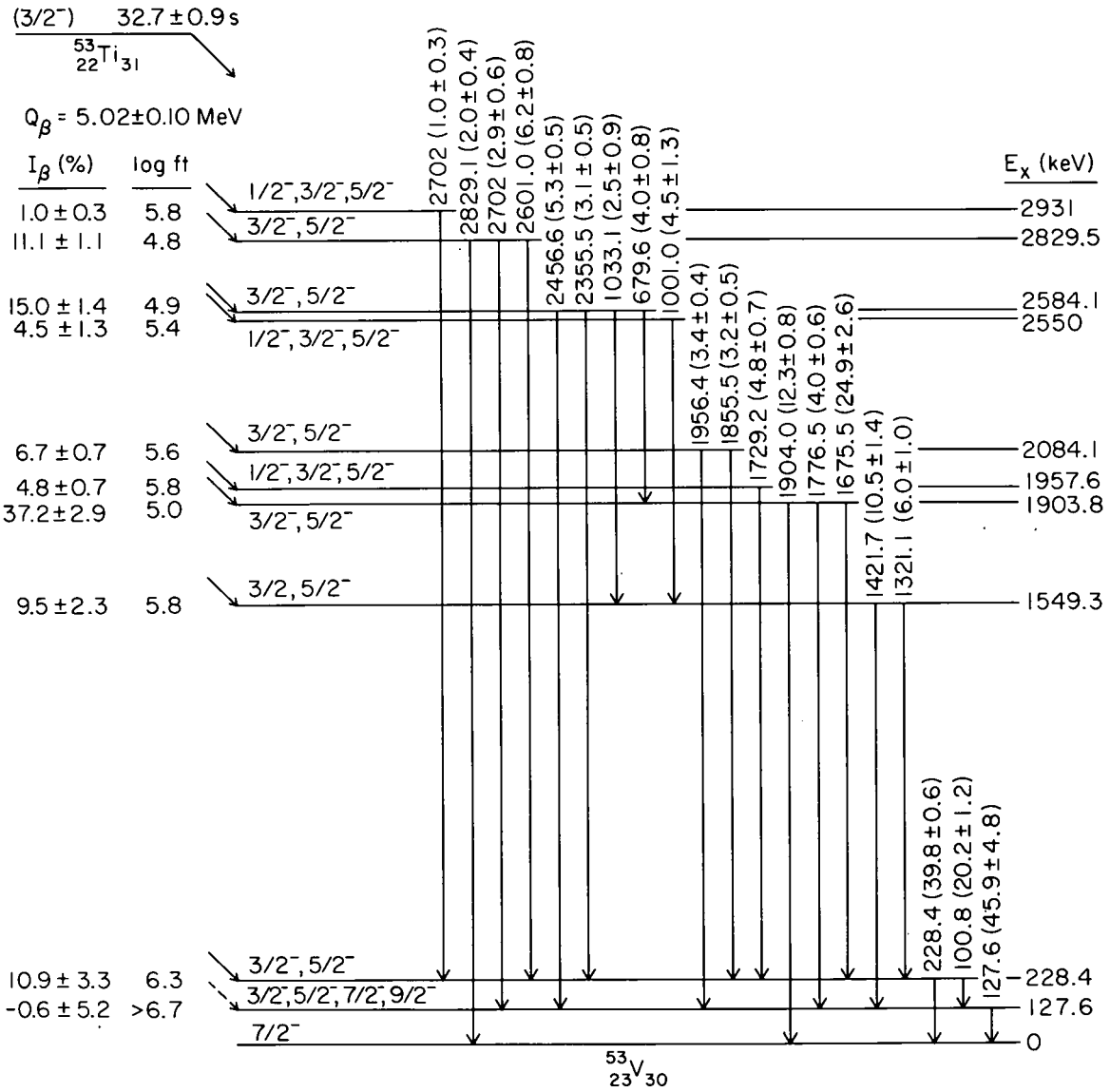

Fig. 19. Preliminary decay scheme for ^{53}Ti. Only ^{53}V states involved in ^{53}Ti decay are shown.

data are presently being analyzed, in order to obtain a mass excess for ^{59}Mn.

(ii) Proton-Rich Isotopes. Isotopes on the proton-rich side of β stability near iron are involved in low-density nucleosynthesis following a supernova explosion. Nuclides on the N=Z line are of prime importance, and one of these, ^{68}Se, has been the object of a search for some time. The reaction used was ^{58}Ni(^{12}C,2n)^{68}Se. A chemical

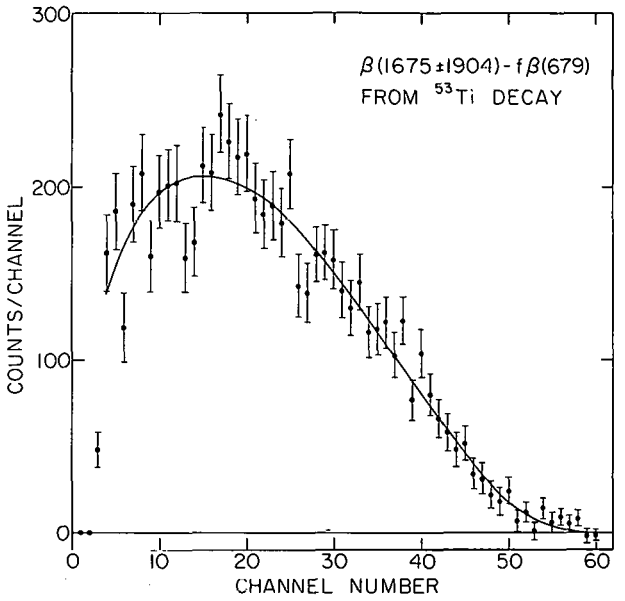

Fig. 20. β spectrum in coincidence with 1904- and 1675-keV γ rays in ^{53}Ti decay. Solid line represents a fit corresponding to a β endpoint energy of 3.09 ± 0.08 MeV.

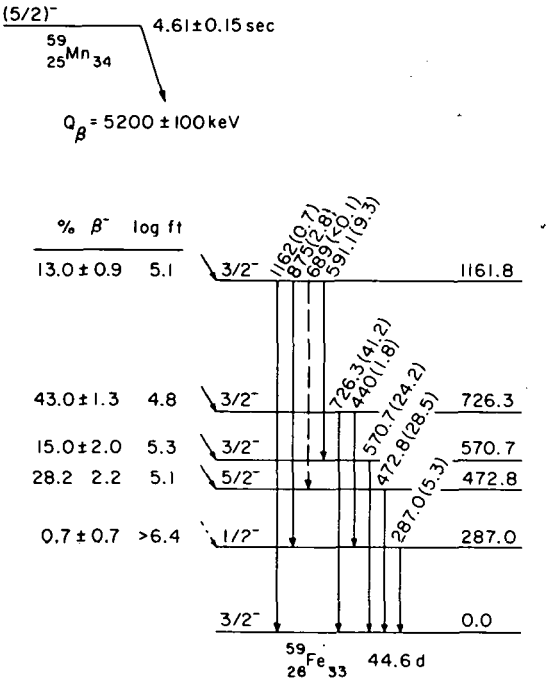

Fig. 21. Tentative decay scheme for ^{59}Mn. Only ^{59}Fe states involved in ^{59}Mn decay are shown.

separation technique was employed in conjunction with a helium-jet recoil-transfer system, but evidence for the decay of ^{68}Se was not obtained. Since little is presently known about the daughter nucleus ^{68}As, its decay has been studied.

^{68}As. This nuclide was produced via the ^{58}Ni(^{12}C,pn)^{68}As reaction at 32-MeV bombarding energy. γ singles, γ-γ coincidence, and β-γ coincidence measurements were made using both the rabbit and helium-jet systems. A decay half-life of 151.5 ± 0.9 s was observed, and the decay scheme obtained is shown in Fig. 22. A new state in ^{68}Ge at 1754.6 keV was found, and is postulated to be the 0^+ member of the 2-phonon triplet. The present measurements have determined that the ground-state spin of ^{68}As is 3, and the parity is most likely +. The mass excess of ^{68}As will be obtained from the β-γ coincidence data, which currently under analysis.

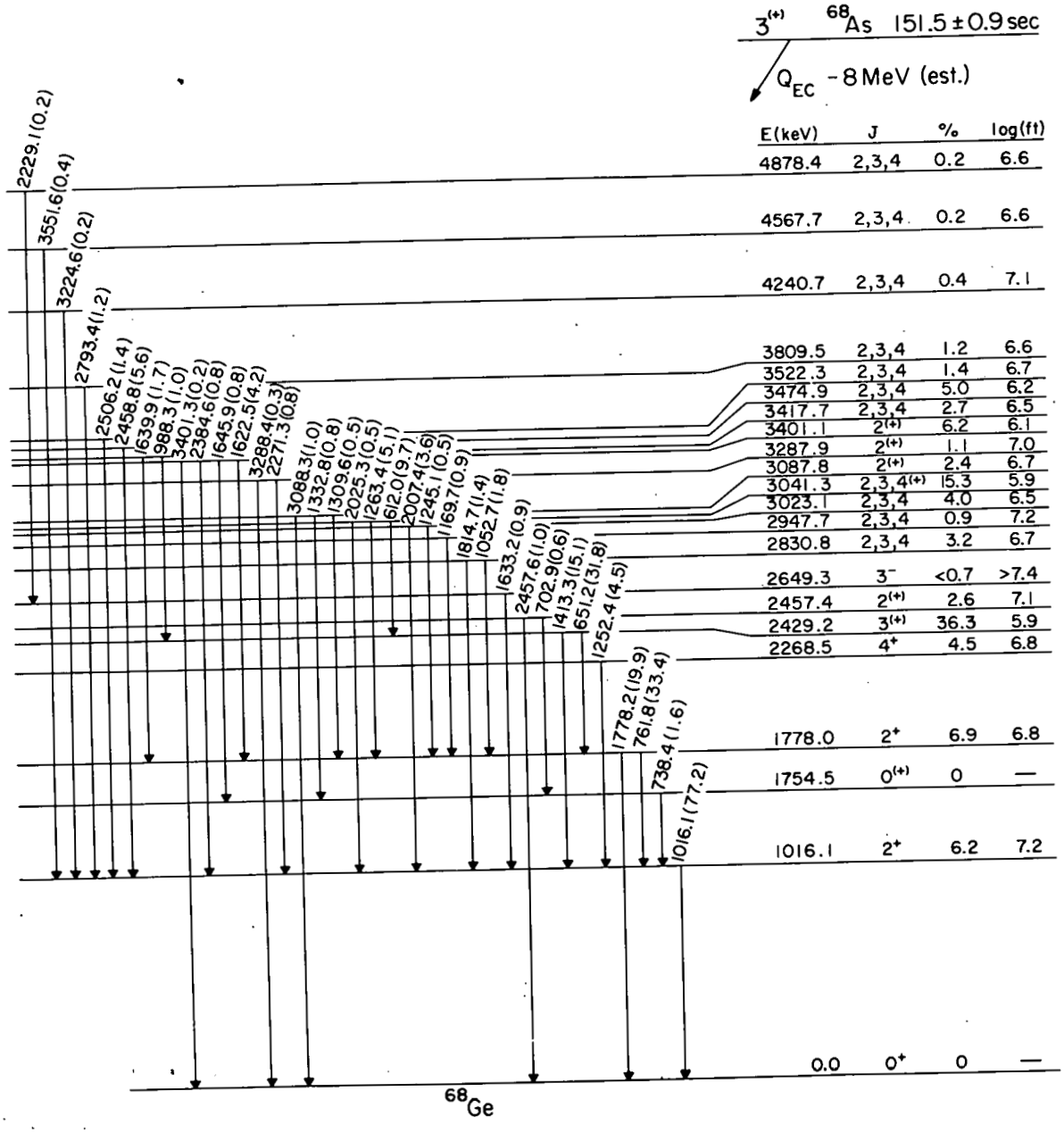

Fig. 22. Decay scheme for ^{68}As. Only ^{68}Ge states involved in ^{68}As decay are shown.

c. Mass-Excess Predictions Near Iron

C. N. Davids

In order to predict β-decay energies expected for the $T_Z = \frac{9}{2}$ nuclides ^{53}Ti, ^{55}V, ^{57}Cr, and ^{59}Mn currently under study, a modified shell-model mass equation has been used to predict the mass excesses of 42 isotopes near iron. Input data are 59 known mass excesses in the same region. Comparison with experimental data shows that this equation works quite well near the β-stability line. A paper has appeared in the Phys. Rev. on this topic.[1]

Further application of the mass equation is being pursued for higher atomic number, in the hope that predictions can be obtained for very neutron-rich isotopes involved in r-process nucleosynthesis.

---

[1] C. N. Davids, Phys. Rev. C 13, 887 (1976).

C. RESONANCES AND STRONGLY POPULATED STATES AT HIGH EXCITATION ENERGIES

a. Measurement of the Spin of a State at 23.85-MeV Excitation in $^{28}Si^*$

R. L. Boudrie and F. W. Prosser

A knowledge of the spins of two strongly populated final states in the $^{16}O(^{16}O,\alpha)^{28}Si^*$ reaction at 23.85- and 21.64-MeV excitation energy is necessary for understanding the reaction mechanism. With the $^{16}O(^{16}O,\alpha_1)^{28}Si^* \rightarrow {}^{24}Mg + \alpha_2$ reaction, three angular correlations of the second alpha particle were obtained simultaneously, in coincidence with the first alpha particle decaying to the 23.85-MeV state and to continuum states with slightly higher and lower excitation energy. The first alpha particle was detected in either of three surface-barrier detectors along the focal plane of the recently converted 0° magnetic spectrometer. The second alpha particle was detected in the target chamber with a position-sensitive detector, subtending a laboratory angular range of 50°.

Figure 23 shows a typical two-dimensional plot of alpha-particle energy versus its position along the detector, in coincidence with the first alpha particle decaying to the 23.85-MeV state. The first two excited states in ^{24}Mg are clearly seen, whereas the strength to the ground state is less by an order of magnitude. The broad band of counts with the lowest energy is associated with high-energy protons which lose only a fraction of their energy in the detector. The remainder of the counts are from random coincidences.

The resulting angular correlation to the ground state of ^{24}Mg is simply proportional to $|P_J(\cos\theta)|^2$, where J is the spin of the state of interest. Figure 24 shows this angular correlation with alpha particles decaying to the 23.85-MeV state in ^{28}Si. The dashed and dotted curves are least-squares fits to the background terms plus $|P_5(\cos\theta)|^2$ and $|P_9(\cos\theta)|^2$, respectively. The solid curve is a least-squares fit to the background terms plus a mixture of $|P_5(\cos\theta)|^2$ and $|P_9(\cos\theta)|^2$.

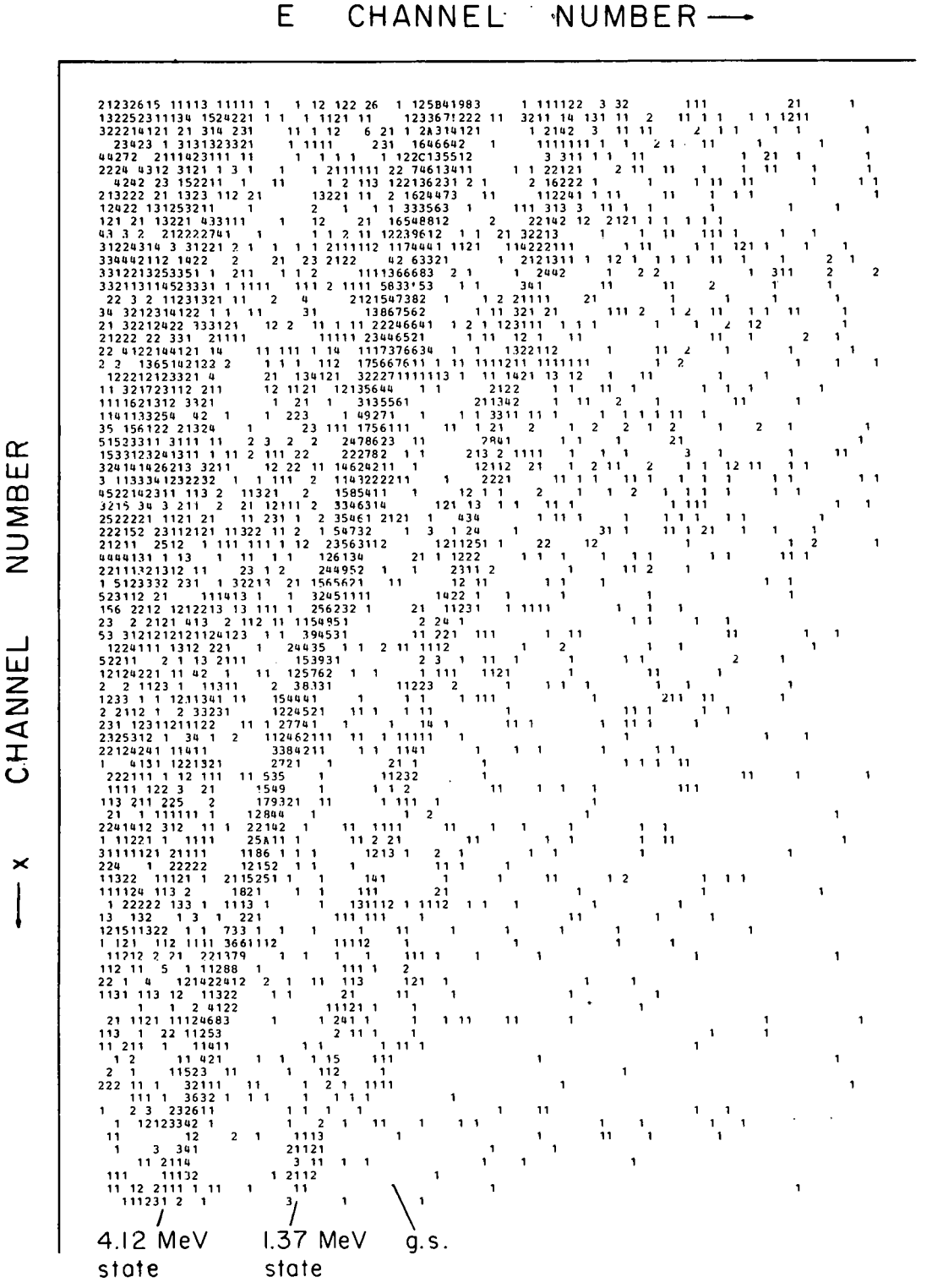

Fig. 23. Two-dimensional contour plot of E vs x for particles detected in the target chamber position-sensitive detector in coincidence with alpha particles detected in the focal-plane detector. Numbers represent the number of counts at each grid point. No background suppression has been used.

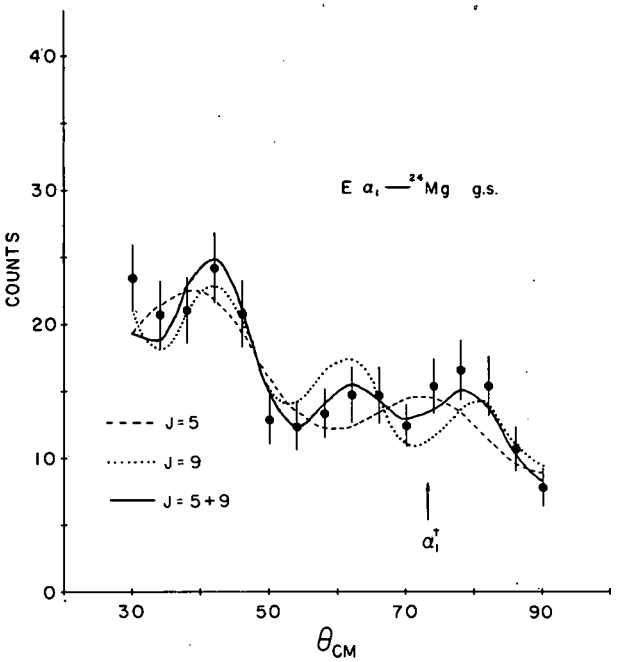

Fig. 24. Angular correlation of alpha particles, with alpha particles decaying to the 23.85-MeV state in $^{28}Si^*$, decaying to the ground state of ^{24}Mg. The solid curve is the best fit to the background terms plus $|P_5(\cos\theta)|^2$ and $|P_9(\cos\theta)|^2$. The dotted and dashed curves are best fits to the background terms plus $|P_5(\cos\theta)|^2$ and $|P_9(\cos\theta)|^2$, respectively. All the fits are integrated over the finite solid angle of each angular interval.

Similar fits were made for the angular correlation with alpha particles decaying to the continuum states with slightly higher and lower excitation energy than 23.85 MeV. Only a strong J = 5 dependence was seen in both cases. We propose that the spin of the state at 23.85 MeV is J = 9, while the J = 5 dependence is a result of a coherent contribution from the underlying continuum states.

b. Inelastic Scattering of $^{16}O + ^{12}C$ in the Region of the $E_{c.m.}$ = 19.7-MeV Resonance

J. R. Erskine, W. Henning, and P. Sperr

The analysis of the inelastic scattering experiment $^{12}C(^{16}O, ^{16}O^*)^{12}C$ in the region of the $E_{c.m.}$ = 19.7-MeV resonance has been completed and a report has been published.[1] The purpose of this work was to obtain information about the structure of the $E_{c.m.}$ = 19.7-MeV resonance through the study of excitation functions and oxygen-ion angular distributions associated with the inelastic excitations of the 6.050-MeV

[1] P. Sperr, W. Henning, and J. R. Erskine, Phys. Rev. C 13, 447 (1

(0^+) and 6.131-MeV (3^-) states in ^{16}O. In the excitation functions a strong enhancement of the cross section at the resonance energy near $E_{c.m.}$ = 19.7 MeV is seen only for the 3^- 6.131-MeV level. The 0^+ state showed a relatively smooth behavior. This result does not support the explanation that the resonance phenomenon is due to an α-exchange mechanism.

c. Study of the $^{24}Mg(^{16}O,\alpha)^{36}Ar^*$ and $^{28}Si(^{16}O,\alpha)^{40}Ca^*$ Reactions

F. W. Prosser, Jr., and J. P. Schiffer

Reactions induced in the interaction of "alpha-particle" nuclei [$^{12}C(^{12}C,\alpha)^{20}Ne^*$, $^{12}C(^{16}O,\alpha)^{24}Mg^*$, and $^{16}O(^{16}O,\alpha)^{28}Si^*$] have led to sharp, strongly-populated states in the residual nuclei at excitation energies of 10 to 25 MeV. These states have widths in the order of or less than the best experimental resolutions available, typically about 30 to 50 keV. Neither the nature of these states nor the reaction mechanism(s) by which they are populated are well understood. In an attempt to see whether this is a more general phenomenon, or characteristic only of systems restricted to ^{12}C and ^{16}O, we have looked for similar states in ^{36}Ar and ^{40}Ca using an ^{16}O beam at energies of 53 and 60 MeV on targets of ^{24}Mg and ^{28}Si.

Data analysis is in progress, but preliminary inspection of the data does not indicate the presence of strongly-populated states.

d. Experimental Proof for Binary Mass Division of a Composite System with $A \approx 80$

B. Zeidman* and collaborators

The reaction $^{32}S + ^{50}Ti$ was studied at 140-MeV laboratory energy with the Tandem accelerator of the Max-Planck Institute for Nuclear Physics at Heidelberg. By means of a multiparameter coincidence

*On assignment at Max-Planck Institute for Nuclear Physics, Heidelberg, Germany.

experiment in which two particles are detected and identified, the existence of a fission-like binary mass division of a composite system with mass $A \approx 80$ is proved. The reaction is accompanied by the evaporation of about three nucleons.

D. INSTRUMENTATION AND TARGETRY

a. A New Heavy-Ion Focal-Plane Detector for the Magnetic Spectrograph

J. R. Erskine, T. H. Braid, and J. C. Stoltzfus*

The key problem in the use of magnetic spectrographs for the study of heavy-ion-induced reactions is the focal-plane detector. A major development effort aimed at solving this problem has been completed and we now have a gas-counter system which has the excellent particle selectivity required. This means that the principal virtues of the magnetic spectrograph (energy resolution and solid angle) can now be applied to heavy-ion experiments.

The new detector is able to measure the total energy, the rate of energy loss, the angle of incidence, as well as the position along the focal surface for the incident heavy ion. The ion velocity could also be obtained from a time-of-flight measurement through the spectrograph by means of the timing signal from the detector if a pulsed beam or a start detector near the target were available. Knowledge of these parameters enables a unique determination of the ion mass, core charge, and charge state.

In tests made with a 56-MeV ^{16}O beam and the detector mounted in the focal plane of the split-pole magnetic spectrograph, typical position resolutions of 1.0 to 1.5 mm (FWHM) were observed over a 50 cm length of the detector. Special tests were made which suggest that the limiting position resolution is 0.76 mm or better. The resolution of the energy-loss signal was typically 4.5% (FWHM). The resolution of the total energy signal was 1.0—1.5% (FWHM) for small entrance apertures of the spectrograph, although 0.7% resolution was observed under special circumstances. The angle of incidence was measured with an uncertainty of about 1.2° (FWHM). A spectrum recorded with the counter is shown in Fig. 25.

* Beloit College, Beloit, Wisconsin.

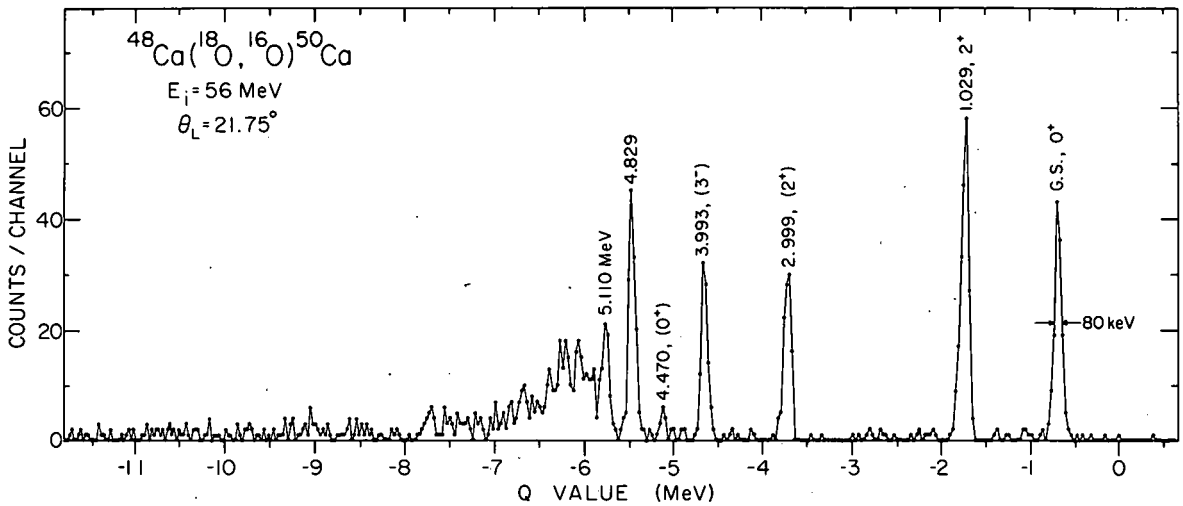

Fig. 25. A spectrum recorded by the heavy-ion focal-plane detector. This ^{16}O spectrum is one of many spectra for different heavy ions which can be processed from the same event-by-event data tape. The resolution was limited by the target.

Basically, the detector is a combination of a gridded ionization chamber and a proportional counter, but it also incorporates features of drift chambers. Some further details of the counter were given in last year's Annual Review and in the Addendum to the Annual Review. A report describing the counter and the associated development work has been submitted for publication.[1]

An essential part of the program to develop a heavy-ion detector has been the acquisition of the computer hardware and software needed for handling the multiparameter data. Until recently, we had no capability to place arbitrarily shaped two-parameter windows on contour plots of the data. The software to do this has now been written for the PDP computer, and this will enable the full capabilities of the new detector to be used.

---

[1] J. R. Erskine, T. H. Braid, and J. C. Stoltzfus, Nucl. Instrum. Methods (to be published).

b. Improvement of the ΔE-E Time-of-Flight Telescope System

S. E. Vigdor, Y. Eisen, W. Henning, D. G. Kovar, T. R. Ophel, P. Sperr, and B. Zeidman

We have addressed two problems inherent in the use of a ΔE-E (TOF) telescope: (1) the reduction in efficiency associated with multiple Coulomb scattering of the incident ions in the transmission detector, and (2) the misidentification of particles which undergo nuclear reactions in the stopping detector (giving rise to "reaction tails"). Calculation of the fraction of events which are multiply scattered out of the cone subtended by the E detector is necessary for determination of accurate relative cross sections for different particle types or energies and for different telescope geometries. We have written a computer code (MAZELTOF) which adjusts two parameters (the beam spot size and an overall normalization factor) to fit measurements of the absolute telescope efficiency for elastically scattered particles, and then calculates the efficiency for all other cases of interest. Excellent agreement with measurements for ^{16}O and ^{18}O scattered from Ca targets is obtained with reasonable values of the two parameters, and we believe that the calculated efficiencies are accurate in all cases within a few percent.

Nuclear reactions in the E detector are a nuisance primarily because the "reaction tail" from elastic scattering products often obscures desired reaction products of lower mass, energy, and (in some cases) atomic charge. We have improved the situation by replacing the particle identification parameter MZ^2 (derived from $\Delta E \times [k\Delta E + aE + E_0]$) with $Z\ (= [(1/M) \times MZ^2]^{1/2})$. While events in the reaction tail have uncharacteristically small values of mass ($M = t^2 \times E$) and of MZ^2, they take on spuriously large values of Z, and so can be largely eliminated with software or hardware rejection windows on the region of low mass coupled with high atomic charge, where no real particles are expected. More complete elimination of the reaction tail may be achieved in the ture by setting the rejection window not on Z, but rather on the

parameter $Z' (= \Delta E/(t - t_0)^2)$, which is also essentially proportional to the atomic charge of the detected ion. Real events can be made to deviate more rapidly from the tail in Z'-E space than in Z-E space.

c. Improvements in Experimental Facilities for Fusion Measurements

T. H. Braid, Y. Eisen, D. G. Kovar, J. P. Schiffer, P. Sperr, S. E. Vigdor, K. Daneshvar, J. J. Bicek, and W. Evans

In order to measure reliably absolute fusion cross sections to a precision of 2—3% in the 70-in. scattering chamber, it was necessary to reduce slit-edge scattering by a factor of 10—100, and to know the angle of the detector with respect to the beam to a few hundredths of a degree at all times. The first problem was addressed by the use of thin, carefully machined, electropolished slits in both the beam and detector collimators. The second problem was solved by precision alignment of the two-slit beam collimator, and installation of a left-right monitoring system which allows determination of beam-related angle shifts to better than $\pm 0.02^{\circ}$. To extend measurements to lower energies and heavier systems, we have constructed an ionization counter followed by a silicon E detector to replace the conventional silicon-detector telescope used presently. Preliminary results with this new system will be obtained shortly. Because of substantial carbon buildup on the target during exposure to the beam, many experiments are extremely difficult. To solve this problem we have designed a liquid nitrogen cryogenic trap to surround the target and hopefully to decrease the rate of carbon buildup significantly. It is now being fabricated and should be installed shortly.

d. Nuclear Target Making and Development

G. E. Thomas, P. J. Dusza, and J. N. Worthington

Over 650 different targets were evaporated during the last year varying in thickness from 0.01 monolayer to 2 mg/cm^2. The different elements, isotopes, or compounds evaporated included

Al, Au, Au (black), B, C, Ca, ^{40}Ca, ^{42}Ca, ^{43}Ca, ^{44}Ca, ^{48}Ca, Cd, ^{114}Cd, Cr, Cu, ^{74}Ge, ^{76}Ge, ^{6}LiF, $^{7}Li_2O$, Li, Mg, ^{24}Mg, Nb, ^{93}Nb, ^{60}Ni, Ni, $Pb^{37}Cl_2$, Pd, ^{106}Pd, ^{110}Pd, ^{45}Sc, Si, SiO_2, Sm, ^{148}Sm, ^{86}Sr, ^{122}Te, ^{48}Ti, V, W (smoked), WO_3. Some targets were self-supporting, some on backing such as Au, C, or Ni and some were in sandwich form.

New equipment systems were placed into operation such as a second 90 target capacity vacuum storage chamber for hygroscopic or readily oxidizing samples, an anodizing system, a controlled atmosphere drybox for mounting these hygroscopic or readily oxidizing materials, and fixtures for our system for resistive evaporation.

During the last year we produced over 125 targets using the various calcium isotopes. As a result we developed a system for routinely making the more expensive calcium-isotope targets in which we used only very small quantities of the source material. We also have a system for making several targets of various thicknesses in one evaporation.

Self-supporting calcium targets ≥ 300 $\mu g/cm^2$ have been produced by the technique of evaporating onto a glass slide and then removing the calcium with a razor blade. It is then carefully placed onto a standard target frame.

Niobium relative standards of 1.0 ± 0.05, 0.1 ± 0.005, and 0.01 ± 0.0006 monolayers have been produced in a single evaporation. A second evaporation with all parameters optimized produced an absolute standard of 0.1 ± 0.004 monolayer.

e. Fourth Annual International Conference of the Nuclear Target Development Society

G. E. Thomas and F. J. Karasek*

This conference was held at Argonne, Illinois on 30 September—2 October 1975. The conference was organized by the hysics Division and Materials Science Division of the Laboratory.

*Materials Science Division, ANL.

The total registration was 48. Of these, 28 were participants from other laboratories; 11 were from foreign countries. This relatively small group of people includes a significant fraction of all those who are target makers.

The subject matter of the conference was divided into four sessions, each introduced by an invited paper of a selected subject of general nature. The first dealt with general techniques for making evaporations and methods for measuring target thickness. Focused ion beam sputtering, a relatively new and interesting technique, was the next. The third discussed a topic of particular future concern for target makers: the manufacture of targets for high-resolution studies with heavy-ion reactions. The last invited paper was a discussion of making targets using electron gun systems.

A record of the conference has been published—Proceedings of the Fourth Annual International Conference of the Nuclear Target Development Society, Physics Division Informal Report ANL/PHY/MSD-76-1 (1976).

f. Physics Division Computer System

D. S. Gemmell and J. W. Tippie*

During the past year a PDP-11/45 computer system has been brought into operation at the Tandem accelerator. Additional systems have also been installed at the 4-MV Dynamitron accelerator, at an "off-line" location (for data analysis and program preparation purposes) and in a mobile trailer for use in LAMPF experiments.

Each system includes a PDP-11/45 computer with floating point hardware, additional fast memory, magnetic tape, disk, electrostatic printer/plotter, storage tube display, CAMAC, and a four ADC multiplex/interface. Much of this hardware has been installed and integrated into the system in the past year.

*Applied Mathematics Division, ANL.

The software for this system has reached operational status. A very primitive version was available in April of 1975, but was used primarily to demonstrate software techniques and was never extensively used. The first serious data acquisition with the new system began in September with the first release of the software system. This version supported pulse-height analysis of one- and two-parameter data as well as event-by-event data acquisition, data display, data recording, etc. This system was used to acquire 1-, 2-, 3-, and 4-parameter data. Approximately 48 different user functions were available on this release.

By December of 1975 sufficient confidence had been demonstrated in the PDP-11 system that the ASI computers were taken out of service (all except the off-line ASI which remains to analyze old data tapes).

The current PDP system now supports in excess of 97 standard functions, and in excess of 20 user-written functions. The most recent enhancements include:

(1) Real-time "filtering" of data where the experimenter is able to select data on the basis of a variable window which is a function of another parameter.

(2) Contour display of two-parameter data to facilitate setting of variable "filter" windows.

(3) Selective mapping of two-parameter data to permit clean separation of data, e.g., energy spectra for various nuclear charges (Z) or masses.

(4) Multiscale data acquisition with motor control.

A direct memory access interface-multiplex for ADC input is being incorporated into the system. This interface will greatly enhance data acquisition rates which are currently limited to about 1—2 K events/second. This interface will support data acquisition either in the "PHA" mode where the hardware will directly increment locations n memory as well as in the "LIST" mode where ADC data is entered directly into memory in a list.

Also under development is a refresh-type display unit with light pen. This unit is particularly adapted to display of spectra in that it has hardware which allows direct display of data with scaling of data in the CRT hardware. This feature is particularly useful in the intensive experimenter-data interaction encountered in these applications.

IV. LOW-ENERGY CHARGED-PARTICLE PHYSICS

A. CHARGED-PARTICLE RESEARCH AT THE TANDEM ACCELERATOR

This is a diverse program of experiments that is carried out by a number of people who are also involved in the heavy-ion and medium-energy programs. The program of research is an integral part of the activities in nuclear physics of the Argonne Physics Division and it has many ties to the theoretical program.

The research on effective interactions is the culmination of a long series of experiments and has resulted in a major definitive study.

The measurement of single-particle states in the actinides is a continuing activity. Relatively new is the study of the E2 giant resonance through the radiative capture of alpha particles on ^{54}Fe. A study of the anomalous nature of alpha-particle scattering from ^{40}Ca may result in some new insights regarding the structure of excited states in that nucleus.

The program of measurements of magnetic-moment g factors of short-lived nuclear states produces results that bear a close connection to other parts of the program, both theoretical and experimental. Previous work in this program has been concentrated primarily in the nuclear spectroscopy aspects of our measurements of g factors. Such measurements were made in liquid metal targets in order to reduce the complications from additional hyperfine fields present in solids. Further measurements have recently been made with solid targets as a function of temperature. As expected, one then observed a more complicated behavior which at least in part arose from the high probability that the isomeric nucleus is now in a region of high lattice disorder produced by the nuclear reaction which generated the isomer. Both aspects of the g-factor experiments (that is, the measurement of nuclear g factors and the observation of effects produced by radiation damage) will be improved by a new apparatus which has just now been installed. It will give more freedom in detector and magnetic field geometries, allowing, for example, the measurement of the longitudinal relaxation rate, a quantity of interest for the study of radiation damage. In the future we also expect to be able to pulse the magnetic field and thus extend, by an order of magnitude, the range of isomeric lifetimes which we can use.

1. REACTION MECHANISMS

Back-Angle α Scattering from ^{40}Ca and ^{44}Ca—Inelastic Scattering

K. A. Eberhard, T. H. Braid, T. Renner, J. P. Schiffer, and S. E. Vigdor

The back-angle enhancement in elastic scattering of alpha particles is well known for ^{40}Ca and has been a subject of a recent study at Argonne, where we established that this enhancement does not fluctuate with energy and must be attributed to a direct mechanism. Further work has now been done, using the split-pole spectrograph, in which the backward enhancement of inelastic scattering has been studied. A number of states show such enhancement in ^{40}Ca, none in ^{44}Ca. Back-angle excitation functions have been obtained at lab. energies between 21 and 27 MeV. Several states (e.g., the first 3^- state) are comparable in back-angle cross section to elastic scattering ~several mb/sr. The backward enhancement is not a constant feature; states of the same spin and parity exhibit different backward enhancements. This suggests that the backward inelastic cross section is sensitive to a different aspect of the wave function than the forward cross section.

2. NUCLEAR SPECTROSCOPY WITH CHARGED-PARTICLE REACTIONS

a. Studies of the Nucleus ^{39}Ar

R. E. Segel, W. C. Corwin, R. D. Lawson, P. Debevec,* L. Rutledge,† and T. Chen†

Several reactions leading to the nucleus ^{39}Ar have been studied with the objective of determining how well this nucleus can be described in terms of simple-shell model configurations built around a doubly-magic ^{40}Ca.

*Indiana University, Bloomington, Indiana.

†Northwestern University, Evanston, Illinois.

A study of the $^{40}Ar(p,d)^{39}Ar$ reaction has also been completed utilizing 35-MeV protons from the Michigan State University cyclotron. A number of spectroscopic factors for low-lying states were determined and confirmation that at least a part of the antianalog strength lies in the 3.38-MeV state was obtained. These single-nucleon transfer data appear to fit well into a simple picture of particle-hole states built around ^{40}Ca.

A study of the $^{37}Cl(^3He,p)^{39}Ar$ reaction has been completed. Here it was found that the analog state at 9.11 MeV is the most strongly fed. However, the even stronger transition expected to the antianalog state was not found. A group of states centered at around 4 MeV appear to share the antianalog strength but even the sum of all of the strengths feeding these states is not as large as expected. Angular distributions to these and other states were calculated with the distorted-wave Born approximation, two-nucleon transfer code TWOPAR, and it was found that this code gives at best a fair fit to the data.

A study of the $^{37}Cl(\alpha,d)^{39}Ar$ has also been completed. Some of the assignments made in the $(^3He,p)$ reaction appear to be substantiated by this study. In the (α,d) reaction, two states in the region of 5.5 MeV stand out strongly. These are believed to be high-spin states built around the $(f_{7/2})^2_{J=7}$ configuration.

Both the position of the analog state and the strength of this state in the two-nucleon transfer reaction appears to be well described by the simple particle-hole picture. However, the picture seems to fail rather badly for the antianalog state. It is fed too weakly in the $(^3He,p)$ reaction and, more importantly, it appears to lie at least 1 MeV too high an energy. The few other multiparticle multihole states of unstretched isospin in this mass region which have been identified also appear to be at too high an energy. The reason for this discrepancy is presently not known.

b. Effective Interactions from Two-Nucleon Spectra

J. P. Schiffer and W. W. True*

The spectrum of states in nuclei differing from closed shells by only two nucleons has been the subject of a continuing program of investigations at Argonne. The collection of data obtained here,

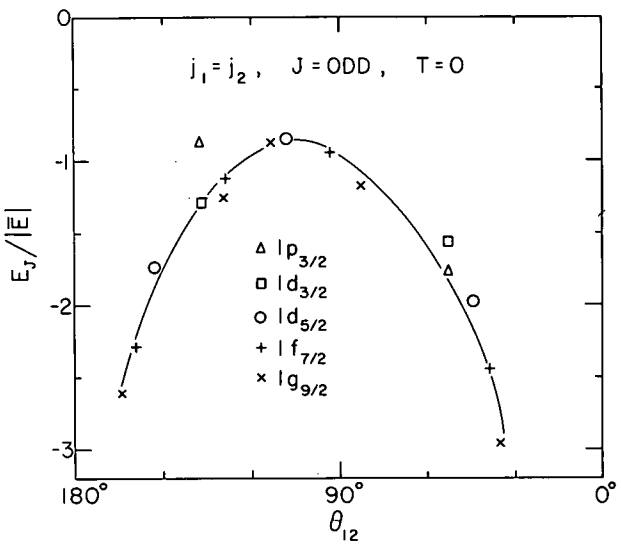

Fig. 26. The T=0 part of the normalized effective matrix element for $j_1 = j_2$.

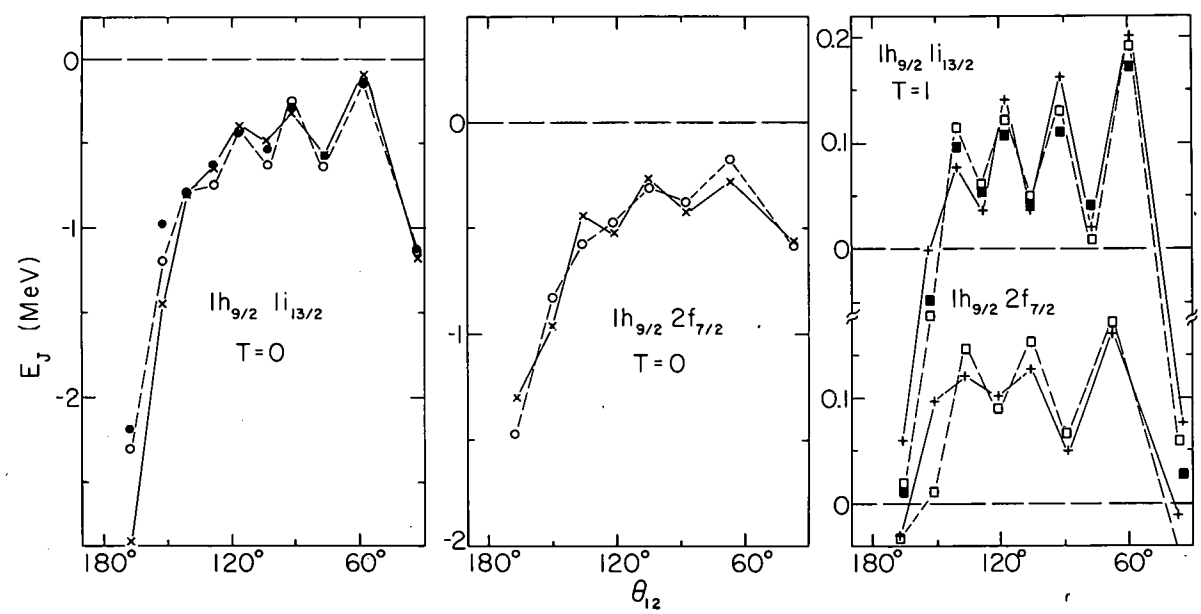

Fig. 27. The normalized effective matrix elements for some of the $j_1 \neq j_2$ multiplets.

*University of California, Davis, California.

together with all other such data, has been subjected to continuing analysis. In the latter part of 1975 this analysis was completed and a review paper has been published[1] on the subject. The results show that a single effective interaction can fit the data from nuclei throughout the periodic table remarkably well. The T=1 part of this interaction contains an attractive core with a repulsive tail, while the T=0 part is purely attractive. Figure 26 shows the normalized T=0, $j_1=j_2$ matrix element; Fig. 27 shows some of the $j_1 \neq j_2$ multiplets and the level of fit obtained.

[1] John P. Schiffer and William W. True, Rev. Mod. Phys. 48, 191 (1976).

c. High-Spin Yrast Levels in ^{47}Ti Populated by the ^{45}Sc(α,d)^{47}Ti Reaction

G. Hardie, L. Meyer-Schützmeister, D. Gloeckner, and T. H. Braid

The ^{45}Sc(α,d)^{47}Ti reaction at an alpha-particle energy of 25 MeV shows two strong deuteron groups which populate the states at 4.51 and 3.58 MeV. They are observed experimentally to be excited at least twice as strongly as all other states. Two states with similar excitation energies are predicted by $f_{7/2}$ shell-model calculations[1] to have spins $\frac{19}{2}^-$ and $\frac{17}{2}^-$. Both states are populated by deuterons whose angular distributions are consistent with L=6 orbital angular momentum transfer, so we conclude that the states at 4.51 and 3.58 MeV are indeed the yrast levels with spins $\frac{19}{2}^-$ and $\frac{17}{2}^-$. These two high-spin states are also strongly populated in the compound-nucleus reaction ^{45}Sc(α,np)^{47}Ti, which was used to study the gamma decay of these two states.[2] It was observed that the state at 3.58 MeV decays via two gammas in succession,

[1] A paper containing the details of the calculations and experiments by G. Hardie, L. Meyer-Schützmeister, D. Gloeckner, and T. H. Braid has been submitted to Phys. Rev.

[2] L. Meyer-Schützmeister, G. Hardie, and Terrence Sjoreen, to be ublished.

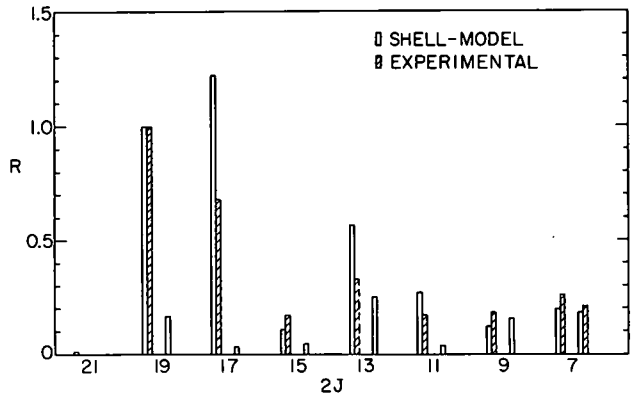

Fig. 28. A comparison between shell-model calculations and experimental results of the relative strengths for populating negative-parity states in ^{47}Ti by the (α,d) reaction. The open bars are the results of a calculation with an $(f_{7/2})$ shell model. The hatched bars are the experimental results. For each J value, the bars on the left are for the yrast levels and the ones on the right are for the first non-yrast levels. The symbol R is given by

$$R = \left[\sum_{5^\circ}^{50^\circ}\left(\frac{d\sigma}{d\omega}\sin\theta\right)^J\right] \Bigg/ \left[\sum_{5^\circ}^{50^\circ}\left(\frac{d\sigma}{d\Omega}\sin\theta\right)^{19/2^-}\right].$$

leading through the state at 2.748 MeV to the known $\frac{11}{2}^-$ state at 1.444 MeV.[3] This result ensures that for each gamma ray, $J_i > J_f$, where J_i is the gamma emitting state and J_f the final state. This conclusion, together with the measured gamma angular distribution, makes the spin assignment of $\frac{15}{2}^-$ to the state at 2.748 MeV unique. This $\frac{15}{2}^-$ state is also observed in the (α,d) work, and its relative yield and angular distribution (with a dominant L=6 transfer) agree with the shell-model calculations. A few other states are populated with similar angular distributions. Our $f_{7/2}$ shell-model calculations suggest that they are the yrast levels with spins $\frac{13}{2}^-$, $\frac{11}{2}^-$, $\frac{9}{2}^-$, and $\frac{7}{2}^-$. For all these states the measured and calculated yields in the (α,d) reaction are compared in Fig. 28. That the spin assignments adopted here are correct is also confirmed by other γ-ray studies.[3,4] Table II lists the observed yrast levels with negative parity and gives their energies and the cross sections obtained for the (α,d) reaction.

[3] J. J. Weaver, M. A. Grace, D. F. H. Start, R. W. Zurmühle, D. P. Balamuth, and J. W. Noé, Nucl. Phys. A196, 269 (1972).

[4] Z. P. Sawa, J. Blomquist, and W. Gullholmer, Nucl. Phys. A205, 257 (1973).

TABLE II. Experimental data on yrast levels of negative parity in ^{47}Ti as observed in $^{45}Sc(\alpha,d)^{47}Ti$ and in gamma-ray studies.

$^{45}Sc(\alpha,d)^{47}Ti$		Gamma-ray studies[a,b]	
E_x (MeV)	$(d\sigma/d\omega)_{c.m.}$[c] (μbarn/sr)	J^π[d]	E_x (MeV)
0.000	7 ± 1	$\frac{5}{2}^-$	
0.16	26 ± 2[e]	$\frac{7}{2}^-$	0.159 ± 0.001
1.26	19 ± 2	$\frac{9}{2}^-$	1.253 ± 0.001
1.45	18 ± 2[e]	$\frac{11}{2}^-$	1.444 ± 0.002
2.68	33 ± 2[e]	$\frac{13}{2}^-$	2.672 ± 0.001
2.77	16 ± 2	$\frac{15}{2}^-$	2.748 ± 0.002
3.58	68 ± 3	$\frac{17}{2}^-$	3.567 ± 0.005
4.51	92 ± 7	$\frac{19}{2}^-$	4.494 ± 0.005

[a] L. Meyer-Schützmeister, G. Hardie, and T. Sjoreen (to be published).

[b] Reference 4.

[c] Value at 22° (lab) unless otherwise noted.

[d] These assignments from Ref. a (this table) and from Refs. 3 and 4.

[e] Value at 7° (lab).

d. Investigation of the Nucleus $^{89}_{41}Nb_{48}$ by the $^{92}_{42}Mo_{50}$(p,α) Reaction

W. Henning and F. J. D. Serduke

The nucleus $^{89}_{41}Nb_{48}$ is of spectroscopic interest because of its proximity to the closed shell nucleus $^{88}_{38}Sr_{50}$. A major shell-model study of neutron-deficient nuclei in the mass-90 region here at Argonne stimulated this experimental investigation. Based on results of our

experiment, we find that the previous, scanty data on this nucleus are incorrect. We find the mass excess of ^{89}Nb to be -80600 ± 20 keV. In contrast to the remaining odd-niobium nuclei for which the ground states have $J^\pi = \frac{9}{2}^+$, there is evidence here for a ground state $J^\pi = \frac{1}{2}^-$. Our work has also yielded the identification of 25 previously unknown excited states. An account of this work will be submitted to the Physical Review.

e. Single-Particle States in Actinide Nuclei

J. R. Erskine, A. M. Friedman,* I. Ahmad,* and R. R. Chasman*

A program to study single-particle excitations in actinide nuclei has been underway for some time. Magnetic spectrograph data on the (d,p), (d,t), (^{3}He,d), and (α,t) reactions for many actinide targets have provided extensive knowledge of single-particle states. This basic knowledge is of crucial importance for the understanding of the complex nuclear excitations in deformed nuclei in the actinide region. An article for Reviews of Modern Physics which surveys single-particle excitations in actinide nuclei is in preparation.

In the past year an article about our work on ^{243}Pu has been submitted for publication in the Physical Review. This study (done in collaboration with R. F. Casten and W. R. Kane of Brookhaven National Laboratory) is based on (d,p) and (d,t) data from Argonne together with data on the ^{242}Pu(n,γ)^{243}Pu reaction recorded at the Brookhaven high-flux reactor. The rotational band structure of ^{243}Pu is now well known as a result of this study.

Recently new data with improved energy resolution have been taken with the ^{240}Pu(d,p)^{241}Pu and ^{242}Pu(d,t) reactions in order to study differences between the $\frac{1}{2}$-[501] and $\frac{1}{2}$-[750] states in ^{241}Pu and ^{243}Pu. Nonsingle-particle states with $K^\pi = \frac{1}{2}^-$ may play a critical role in explaining the differences between the two nuclei.

---

*Chemistry Division, ANL.

3. ELECTROMAGNETIC PROPERTIES

a. Search for the γ Decay of High-Spin States in ^{43}Ti

L. Meyer-Schützmeister, A. J. Elwyn, G. Hardie, and R. K. Smither

The study of high-spin states in fp-shell nuclei is continued by searching for the γ decay of ^{43}Ti. Hardly any information is available for this nucleus; only a few energy levels and no spin assignments are reported. No γ decay of any of these levels had previously been measured. Evaporation calculations have shown that for alpha-particle energies of 18—20 MeV the compound-nucleus reaction $^{40}Ca + \alpha \rightarrow {}^{44}Ti \rightarrow n + {}^{43}Ti$ should have a sufficiently large cross section to make the observation of gammas emitted by ^{43}Ti possible, although the gamma emission from other nuclei, in particular from ^{43}Sc produced in the reaction $^{40}Ca + \alpha \rightarrow {}^{44}Ti \rightarrow p + {}^{43}Sc$, is expected to be dominant. Indeed in the measurement of the γ-ray singles spectrum in the alpha bombardment of ^{40}Ca, no gammas belonging to ^{43}Ti could be identified. However, in a n-γ coincidence experiment the background of unwanted radiation was strongly reduced and γ rays were observed which, according to the known level scheme might belong to ^{43}Ti. These gammas could unfortunately not be identified in a γ-γ coincidence measurement. However, plans are underway to include the additional requirement of coincident neutrons in future experiments with the hope that the signal-to-background ratio will be sufficient to observe the ^{43}Ti transitions.

00475

b. Lifetimes of Some High-Spin States in ^{47}Ti

L. Meyer-Schützmeister, G. Hardie, and Terrence Sjoreen

In studying the gamma decay of high-spin states in ^{47}Ti, Doppler shifts for a few gammas were observed, and these data allowed us to determine the lifetimes of the six states given in Table III. The reaction $^{45}Sc(\alpha,np)^{47}Ti$ was used to excite the states. Since single

TABLE III. Comparison of measured and calculated transition strengths ($|M|^2$: strength in Weisskopf units).

Initial state		Final state	Measurements				Calculations					
							(^{42}Sc)		(^{48}Sc)		MBZ	
(MeV)	J^π	J^π (MeV)	E_γ (keV)	Multipolarity	τ[a] (psec)	$\lvert M\rvert^2$	Multipolarity	$\lvert M\rvert^2$	Multipolarity	$\lvert M\rvert^2$	Multipolarity	$\lvert M\rvert^2$
4.494	$\frac{19}{2}^-$	$\frac{17}{2}^-$	926.8	M1	$0.36^{+0.12}_{-0.10}$	0.11	M1	1.1	M1	0.88	M1	1.00
3.567	$\frac{17}{2}^-$	$\frac{15}{2}^-$	819.0	M1	$0.39^{+0.12}_{-0.10}$	0.15	M1	0.83	M1	0.68	M1	0.66
2.748	$\frac{15}{2}^-$	$\frac{11}{2}^-$	1304.5	E2	$3.2^{+2.8}_{-1.2}$	6.6	E2	12	E2	13	E2	13
1.444	$\frac{11}{2}^-$	$\frac{7}{2}^-$	1284.7	E2	$1.7^{+0.8}_{-0.6}$	13.3	E2	14	E2	15	E2	15
1.253	$\frac{9}{2}^-$	$\frac{7}{2}^-$	1093.7	$\delta^2 = 0.13$	$0.51^{+0.20}_{-0.15}$		$\delta^2 = 0.52$		$\delta^2 = 0.12$		$\delta^2 = 0.04$	
				M1: $\frac{1}{1+\delta^2}$	$0.58^{+0.23}_{-0.17}$	0.041	M1	0.005	M1	0.10	M1	0.026
				E2: $\frac{\delta^2}{1+\delta^2}$	$4.4^{+1.7}_{-1.3}$	11.3	E2	5.9	E2	2.7	E2	2.6
2.684	$(\frac{11}{2}^-)$[b]	$\frac{9}{2}^-$	1431.2	(M1)[c]	$6^{+\approx 5}_{-2.5}$	0.0018						
				(E2)[c]		2.2						
				(E1)[c]		4×10^{-5}						
				(M2)[c]		94						

[a] The measured lifetimes might be too large by a few tenths of a psec due to feeding times. This implies that for $\tau \leq 7 \times 10^{-13}$ sec, the given τ values might represent upper limits, the $|M|^2$ values lower limits. For $\tau > 7 \times 10^{-13}$ sec the uncertainties of the feeding times are included in the given errors.

[b] Reference 5.

[c] $\ldots\ldots^2$ is given for the indicated multipolarity of the transition.

gamma rays were detected, the possibility exists that the measured Doppler shifts may result from a higher state of longer lifetime which decays to the state of interest. However, a comparison of our data with earlier results[1] shows that the effect is negligible for $\tau > 0.7$ psec, although for $\tau \leq 0.7$ psec it might cause the measured value to be too large by 0.2—0.3 psec. We observed two M1 transitions between high-spin yrast levels, and these decays are fast, in that they have a strength of about 0.15 Weisskopf units; and one M1 transition between the yrast state $\frac{9}{2}^- \rightarrow \frac{7}{2}^-$ is somewhat hindered. This result is in agreement with $f_{7/2}$ shell-model calculations[2] and with measurements in neighboring nuclei.[3,4] E2 transition rates seem to be rather independent of spin and to have transition rates of about 10 ± 6 Weisskopf units. This again agrees with $f_{7/2}$ shell-model calculations and with experimental values observed in neighboring nuclei. An unusually slow M1 transition is seen for the 2.684-MeV state, which has been assigned[5] a spin of $\frac{11}{2}^-$. The reported gamma angular distribution[5] and our lifetime measurements suggest, instead, that this state probably has a spin of $J^\pi = \frac{7}{2}^+$ or $\frac{11}{2}^+$.

[1] J. J. Weaver, M. A. Grace, D. F. H. Start, R. W. Zurmühle, D. P. Balamuth, and J. W. Noé, Nucl. Phys. A196, 269 (1972).

[2] D. Gloeckner and F. Serduke, private communication.

[3] W. Kutschera, R. B. Huber, C. Signorini, and H. Morinaga, Phys. Rev. Lett. 33, 1108 (1974).

[4] S. L. Tabor and R. W. Zurmühle, Phys. Rev. C 10, 35 (1974).

[5] Z. P. Sawa, J. Blomquist, and W. Gullholmer, Nucl. Phys. A205, 257 (1973).

c. Study of the Giant Electric-Quadrupole Resonance (GQR) in ^{58}Ni by α Capture in ^{54}Fe

L. Meyer-Schützmeister, W. R. Wharton, P. T. Debevec, R. E. Segel, and K. Raghunathan

Excitation functions and angular distributions of the reaction $^{54}Fe(\alpha,\gamma_0)^{58}Ni$ allowed us to study the distribution of the E1

and E2 strength in ^{58}Ni in the energy region of 13.5—18.5 MeV. It has been found that, in this nucleus, the E2 strength seen by the alpha capture is concentrated in a narrow energy region of a few MeV, with a maximum yield at about 16-MeV excitation energy. In light nuclei (for example, ^{28}Si and ^{24}Mg), the E2 strength as measured[1,2] by the (α, γ_0) reaction is not concentrated in one well-defined giant resonance but is spread evenly over a wide energy range. In the inelastic scattering of alpha particles, an E2 giant resonance has been identified for nuclei with $A \geq 40$. In particular, for ^{58}Ni, such a resonance is observed[3—5] at an excitation energy of 16 MeV. But no E2 resonance above the underlying continuous background is seen in inelastic α scattering for nuclei with $A < 32$ and in particular not for ^{28}Si (Ref. 6). One should remember, however, that the (α, γ_0) reaction is known to excite the giant electric-dipole resonance predominantly through the compound nucleus, and therefore the cross section depends strongly on statistical factors. In contrast, there are indications that the (α, γ_0) reaction might excite the giant electric-quadrupole resonance, not only through the compound nucleus but also through direct-reaction processes. In Table IV, the integrated E2 and E1 strengths measured by the (α, γ_0) reaction and the E1 strength measured[7] earlier by (γ, p_0) are presented for ^{58}Ni. The strengths are

[1] L. Meyer-Schützmeister, Z. Vager, R. E. Segel, and P. P. Singh, Nucl. Phys. A108, 180 (1968).

[2] E. Kuhlmann, E. Ventura, G. R. Calarco, D. G. Mavis, and S. S. Hanna, Phys. Rev. C 11, 1525 (1975).

[3] J. M. Moss, C. R. Rozsa, J. D. Bronson, and D. H. Youngblood, Phys. Lett. 53B, 51 (1974).

[4] D. H. Youngblood, private communication.

[5] C. C. Chang, F. E. Bertrand, and D. C. Kocher, Phys. Rev. Lett. 34, 221 (1975).

[6] J. M. Moss, C. M. Rozsa, D. H. Youngblood, J. D. Bronson, and A. D. Bacher, Phys. Rev. Lett. 34, 748 (1975).

[7] H. Miyase, S. Oilawa, A. Suzuki, G. Vegaki, T. Saito, M. Suguwara and K. Shoda, Proc. Int. Conf. on Photonuclear Reactions and Applicatic..., Asilomar, March 1973, edited by B. L. Berman, Lawrence Livermore Laboratory, Livermore (1973).

TABLE IV. E1 and E2 strengths (in % of sum rule) as observed by the (α,γ_0) or (γ,p_0) reactions.

Nucleus	E1 $\int\sigma(\gamma,\alpha_0)dE$ %	E2 $\int(\sigma(\gamma,\alpha_0)/E^2)dE$ %	E1 $\int\sigma(\gamma,p_0)dE$ %
^{28}Si	1[a]	8[a]	13[b]
^{58}Ni	0.5[c]	2.5[c]	3.4[d]

[a] Reference 1.

[b] Reference 8.

[c] Present work.

[d] Reference 7.

given as a percentage of the sum-rule limits [E1: $\int\sigma(E1)dE = 60\ NZ/A$ mb MeV; E2: $\int(\sigma(E2)/E^2)dE = 0.22\ Z^2A^{-1/3}$ μb/MeV].

The (γ,α_0) reaction populates the giant quadrupole resonance relative to the sum-rule limit to the same extent that the (γ,p_0) reaction populates the giant-dipole resonance relative to its sum-rule limit. Similar remarks apply to the data[1,8] for ^{28}Si given in Table IV.

The (α,γ_0) reaction seems to be a useful technique for investigating the giant-quadrupole resonance, nearly as efficient as the (p,γ_0) reaction is for the giant-dipole resonance.

[8] P. P. Singh, R. E. Segel, L. Meyer-Schützmeister, S. S. Hanna, and R. G. Allas, Nucl. Phys. 65, 577 (1964).

d. Nuclear g Factors

R. E. Holland, F. J. Lynch, R. J. Mitchell,* T. V. Ragland,* and R. P. Scharenberg*

There are many interesting nuclear states with relatively long lives and well-defined configurations for which the nuclear g factor

* Purdue University, Lafayette, Indiana.

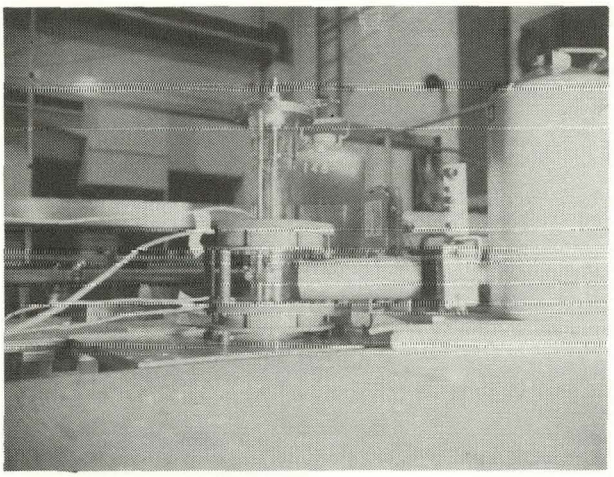

Fig. 29. New g-factor apparatus showing air core water-cooled magnets and suspended heated target assembly. Two intrinsic Ge detectors are placed at +135° to beam direction.

has not been determined because of the difficulty of the measurement. Since we have developed techniques which allow us to measure these states, we have continued to concentrate our effort on the measurement of g factors of isomers in the microsecond range. Measurements were made by the time-differential perturbed-angular-distribution method in liquid-metal targets. The most demanding of these, technically, was the measurement on the first excited state of ^{43}Sc, both because of the high chemical activity and the high vapor pressure of a molten-Ca target and because of the long lifetime of the state (630 μs).

Our present apparatus with iron-core magnet (designed by R. Scharenberg) which provides magnetic fields up to 25 kG, is suited for measurement of g factors of short-lived isomers. Much of our recent measurements have been made on states with lifetimes of 10—1000 μs, which require magnetic fields of less than 1 kG. We have constructed a new system with air-core magnets which have the advantages that: (1) The field can be monitored by measuring the current through the magnet coil. (2) The field can be turned on at the end of the beam pulse starting all the excited nuclei to precess synchronously. The new system will also provide much higher pumping speed greatly reducing the time to change targets. It will also provide for running targets at low temperatures as well as high temperatures. Figure 29 is a photograph of the new assembly.

(i) Nuclear g Factor for the $d_{3/2}$ Hole State in ^{43}Sc

R. E. Holland, F. J. Lynch, R. J. Mitchell,* T. V. Ragland,* and R. P. Scharenberg*

The isomeric first excited state of ^{43}Sc (E = 151 keV, τ = 620 μs) was produced by the reaction $^{40}Ca(\alpha,p)^{43}Sc$ in a liquid-metal target consisting of an alloy of Ca and Sn with a melting point of 625°C. Observations of the time-differential perturbed angular distributions in magnetic fields between 20 and 100 gauss gave a g factor of +0.232 ± 0.008 and relaxation times of the order of 500 μs. This g factor is close to that observed for a similar $d_{3/2}$-hole state in ^{47}Sc, but far from the g factor (0.35) calculated from the model of Lawson and Macfarlane. This model explained the inhibited M2 transition responsible for the isomerism of this state as arising from a wave function in which the predominant part consists of a $d_{3/2}$-proton hole coupled to the ground state of ^{44}Ti with a sizable admixture of a $d_{3/2}$-proton hole coupled to the first excited state of ^{44}Ti. Recent calculations by Lawson and Müller-Arnke indicate that if one also allows an $s_{1/2}$-proton hole coupled to the ^{44}Ti excited state as a component in the wave function, then agreement with the observed g factor can be obtained for quite reasonable values of the admixture.

(ii) Nuclear g Factor of the First Excited State of ^{99}Mo

R. E. Holland, F. J. Lynch, R. J. Mitchell,* T. V. Ragland,* and R. P. Scharenberg*

The isomeric first excited state of ^{99}Mo (E = 98 keV, τ = 24.5 μs) was produced with the reaction $^{96}Zr(\alpha,n)^{99}Mo$ in a liquid alloy target of Zr and Cu held just above its melting point at 875°C. Measurement of the time-differential perturbed angular correlation of the de-excitation γ rays in magnetic fields between 500 and 1000 gauss gave the value g = -0.312 ± 0.006. Although the single-particle g factor for a $d_{5/2}$ neutron is -0.764, core polarization effects are expected to reduce

*Purdue University, Lafayette, Indiana.

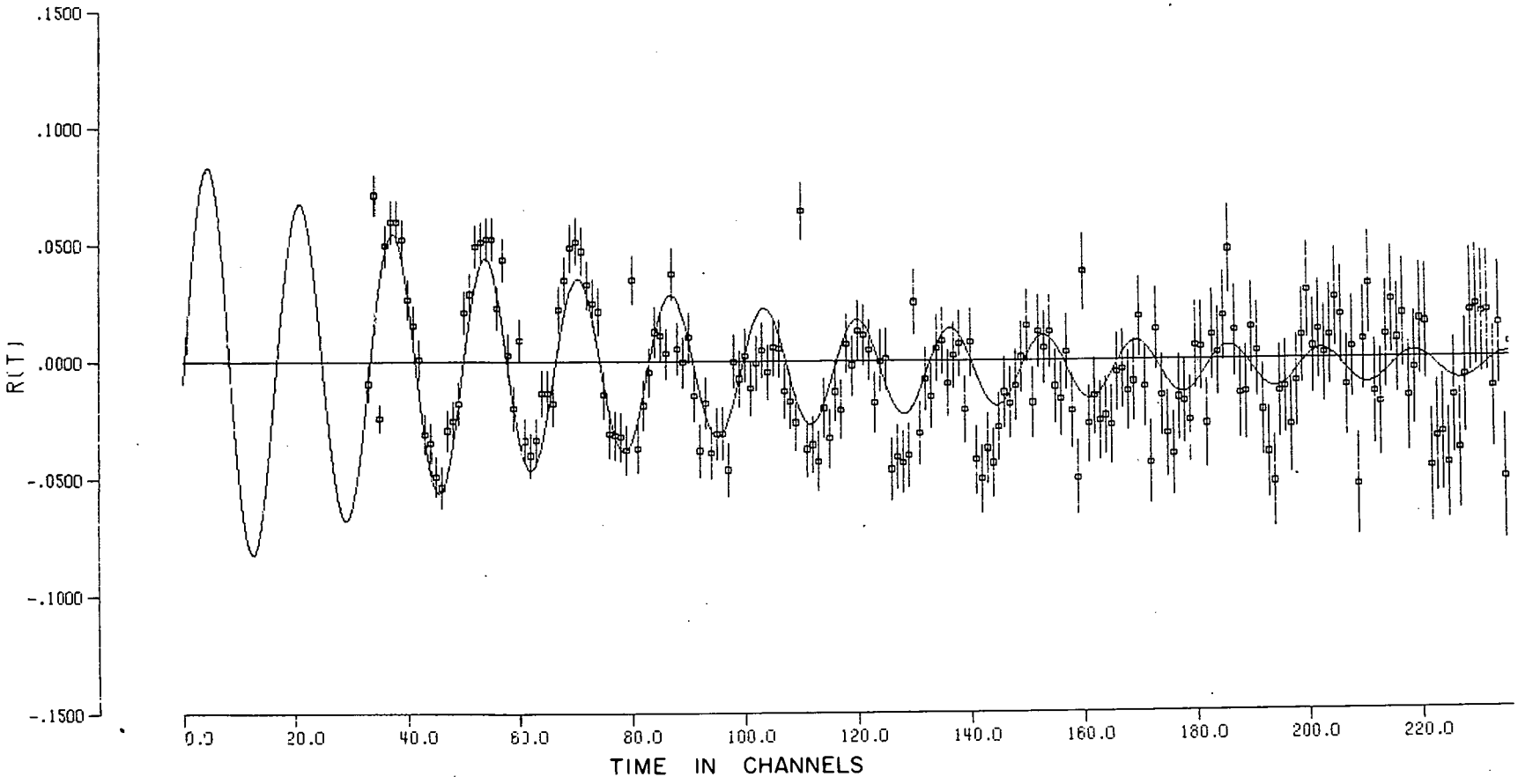

Fig. 30. The precession of ^{99}Mo first excited state in a magnetic field of 640 gauss in a solid Mo target at 1750°C. The count in a gamma detector at 43° and 133° was used to obtain the ratio of the difference divided by the sum of the count at these two angles as a function of time after the isomer was generated by the reaction ^{98}Mo(d,p)^{99}Mo. The time scale was 0.2 μs/channel.

the g factor to a value near that observed. The fact that nuclei in this region are well described by a pairing force model (which explains the isomerism of this state as resulting from an inhibited E2 transition) does not result directly in any modification of the single-particle g factor. However, the configuration mixing introduced by the pairing force would affect the amount of core polarization and in this way affect the calculated value of g. The observed g value is consistent with those observed for $d_{5/2}$ states in neighboring nuclei. This state was also excited by the reaction $^{98}Mo(d,p)^{99}Mo$ in a solid polycrystalline target heated from 1000°C to 1800°C. (A typical example is shown in Fig. 30.) In these data, a sudden increase in the number of nuclei participating in the Larmor precession occurred at ~1100°C. No change was apparent in the relaxation time (~20 μs) at 1100°C. These observations bear on the nature of damage to the crystal structure of a metal after nuclear recoil. We plan to investigate this further.

B. CHARGED-PARTICLE RESEARCH AT THE DYNAMITRON

This research effort was devoted mainly to experimental studies of charged-particle cross sections at low energies and the behavior of molecular ions in solids and gases.

1. CHARGED-PARTICLE CROSS SECTIONS

The major nuclear research activity at the Dynamitron, the program of charged-particle cross sections at low energy, was undertaken both for its intrinsic nuclear-physics interest and because of the parameters it provides for CTR. The effort is at present focused on the d+^{6}Li system, and cross sections are being measured in all channels.

a. Thermonuclear Reaction Rates for ^{6}Li+d Reactions

A. J. Elwyn, J. E. Monahan, and F. J. D. Serduke

The reaction-rate parameter associated with interacting ions in a hot plasma is the product of the reaction cross section and the relative velocity between the ions averaged over the distribution, usually assumed to be Maxwellian, of their relative velocities. Since the power released by nuclear reactions in such a plasma is proportional to these reaction rates, the feasibility of utilizing a particular fuel, such as ^{6}Li-D, in thermonuclear applications will depend in part on the values of

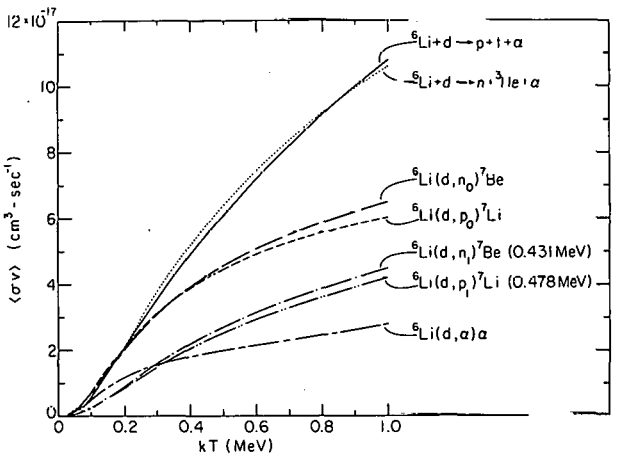

Fig. 31. Reaction rate parameters for all d+^{6}Li reactions as a function of kT. The results for d + ^{6}Li → p + t + α have been divided by a factor of 2.5.

the associated reaction rates and thus on the absolute reaction cross sections. Reaction-rate parameters for ^{6}Li+d reactions based on reaction cross sections recently measured at Argonne have been calculated, by numerical integration techniques, for temperatures that correspond to relative ion energies between 1 and 1000 keV. The results for temperatures greater than about 100 keV are shown in Fig. 31. For ion energies below the range of the measurements, extrapolated cross sections were obtained by use of an expression that has been shown to be an adequate representation of the cross section for all energies up to several hundred keV. Calculations of the power released into a heated plasma in ^{6}Li+d processes have been compared to similar quantities for the more usual d + t and d + d fusion reactions. The value for ^{6}Li + d surpasses that for the d + d reactions near relative ion energies of 100 keV, and is comparable to the d + t value at temperatures above 500 keV.

b. Cross Sections for Charged Particles from ^{6}Li+d Reactions at Low Energies

A. J. Elwyn, R. E. Holland, C. N. Davids, L. Meyer-Schützmeister, F. P. Mooring, and F. J. Lynch

As part of a program for determining absolute cross sections for various nuclear particles in charged-particle-induced reactions on light nuclei, we have measured the differential and total cross sections for the outgoing protons and alpha particles in the bombardment of ^{6}Li by ~0.1 to 1.0 MeV deuterons accelerated in the ANL Dynamitron. These experiments, along with recently completed measurements[1] of similar quantities for the outgoing neutrons in ^{6}Li+d reactions, provide nuclear cross sections of importance to the evaluation of ^{6}Li-D as a possible fusion fuel. At the same time, such studies can contribute to the understanding of the nuclear structure of light nuclei and of the

[1] A. J. Elwyn, R. E. Holland, F. J. Lynch, J. E. Monahan, and F. P. ooring, Nuclear Cross Sections and Technology, NBS Spec. Publ. 425 (U.S. Government Printing Office, 1975), p. 692.

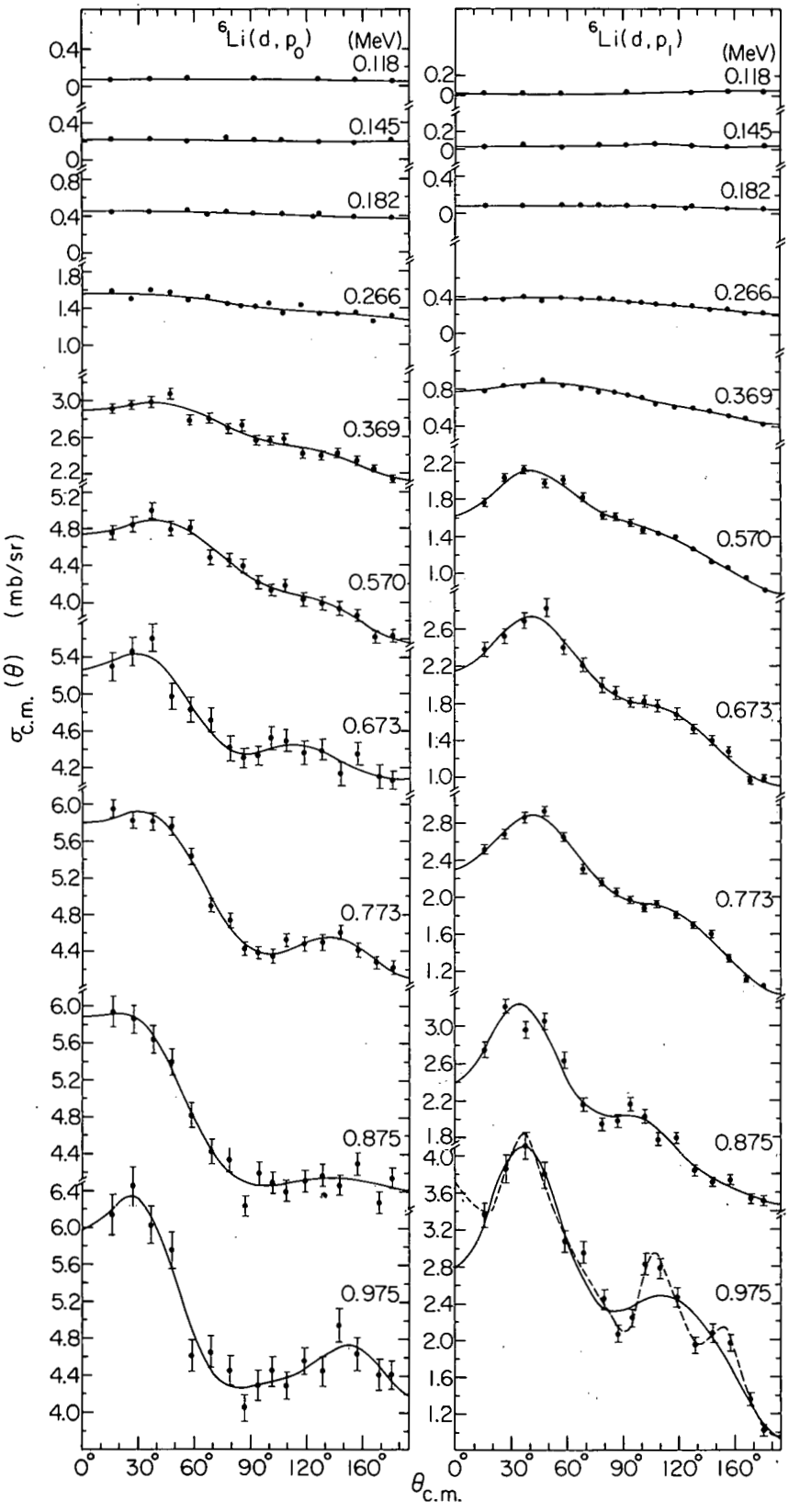

Fig. 32. Differential cross sections as a function of angle for both the gr d and first excited state protons in the ^{6}Li(d,p)^{7}Li reaction at various inc. dent deuteron energies.

relative importance of various reaction mechanisms. Differential and total cross sections of the protons in the ^{6}Li(d,p) reaction, both to the ground and first excited state in ^{7}Li, and the energetic alpha particles in the ^{6}Li(d,α)α reaction have been obtained by use of silicon surface-barrier detectors and a 30-in. scattering chamber. Figure 32 shows the differential cross sections for the ^{6}Li(d,p)^{7}Li reaction, while Fig. 33 presents the total reaction cross sections for both the ^{6}Li(d,p) and ^{6}Li(d,n) reactions. Targets of ^{6}LiF have been utilized, and target thickness and total integrated charge have been determined with sufficient accuracy to allow absolute cross-section measurements to 13—14%. Charged particles that arise in the breakup of ^{7}Li and ^{7}Be in the ^{6}Li + d reactions have been investigated by time-of-flight techniques using the post-acceleration pulsed beam from the Dynamitron. From two-dimensional analysis of both the energy and time of flight of low-energy charged particles over 20-cm flight paths, the spectra associated with the continuum protons can be extracted, and absolute cross sections for the ^{7}Li breakup process may be determined. Analysis of the raw data (both discrete and continuous-energy groups) and attempts to interpret the observed angular distributions in terms of various reaction mechanisms are currently in progress. Future measurements that involve the study of the interaction of some of the outgoing particles in ^{6}Li+d reactions with ^{6}Li [e.g., ^{6}Li(p,^{3}He)α reaction] are planned.

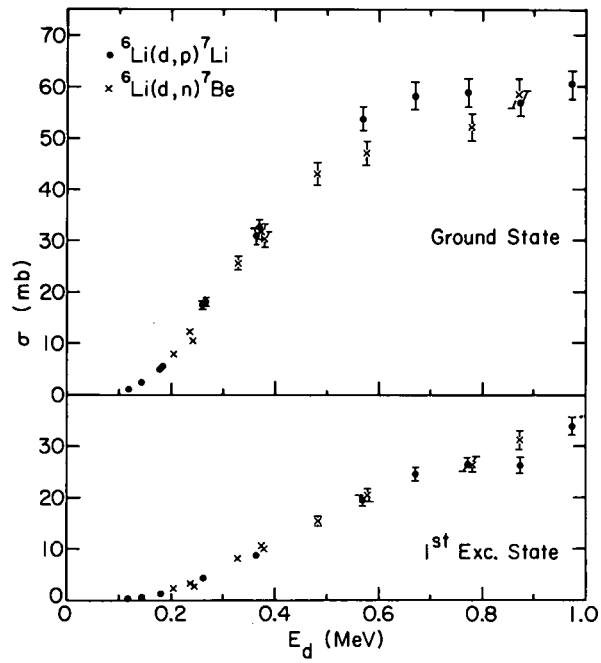

Fig. 33. Total reaction cross sections as a function of incident deuteron energy for the ground and first excited state particle groups for both the ^{6}Li(d,p)^{7}Li and ^{6}Li(d,n)^{7}Be reactions.

c. Three-Body Breakup in ^{6}Li+d Reactions

A. J. Elwyn, J. E. Monahan, and R. E. Holland

The interaction between particles in the final state modifies the cross sections and energy spectra in three-body breakup reactions. The interpretation of the continuous energy spectrum of the outgoing particles in, for example, ^{6}Li+d reactions may lead to an understanding of the reaction mechanisms that can produce a particle in the final state as well as the structure of the various light nuclei involved. The energy dependence of the neutron continuum distributions that arise from the breakup of ^{7}Be (based on ^{6}Li+d reactions recently measured at Argonne) have been compared with calculations based on the factored-wave-function method of treating final-state interactions. Preliminary results suggest that the 0° spectra at neutron energies between 750 keV and $\sim$2.5 MeV can be interpreted in terms of an s-wave Coulomb interaction between the ^{3}He and α particles in the final state. This interaction, furthermore, predicts phase shifts in good agreement with those previously obtained at other laboratories[1] for ^{3}He-α scattering. Attempts at a more complete interpretation of the neutron continuum distributions, particularly at neutron energies below 750 keV as well as a study of the outgoing protons in the three-body breakup of ^{7}Li, are in progress.

[1] See, for example, L. S. Chuang, Nucl. Phys. A174, 399 (1971).

d. Search for Direct Radiative α Capture in ^{16}O

A. J. Elwyn, L. Meyer-Schützmeister, F. P. Mooring, J. E. Monahan, and G. Hardie

Preliminary attempts to observe direct-capture γ rays from ^{20}Ne in the ^{16}O(α,γ) reaction have proved unsuccessful in spite of the use of high-intensity α-particle beams from the Argonne Dynamitron. Since the direct α-capture reaction may be able to provide more reliable α-particle spectroscopic factors for final states than can be obtained through α-particle stripping reactions, further experiments based on

modification of the experimental arrangement have been initiated. In order to reduce the background in the neighborhood of the expected nonresonant capture γ rays, a large NaI(Tl) anticoincidence annulus surrounding the main Ge(Li) detector was utilized. Although this system is not usable in its present form for the observation of the direct α-capture γ rays [because the available Ge(Li) detector reaches only part way into the anticoincidence annulus and cannot be brought close enough to the heavily-cooled target], backgrounds were improved by about a factor of 3, a reduction which in a proper experimental configuration may be sufficient for the observation of the extremely small cross section associated with direct capture. Further experiments must await modification of either the Ge(Li) detector or the NaI(Tl) anticoincidence crystal to allow positioning of the Ge(Li) detector closer to the target.

2. ENERGETIC MOLECULAR-ION BEAMS—DISSOCIATION AND INTERACTION IN TRAVERSING SOLID AND GASEOUS TARGETS

This program of measurements using the Argonne 4-MV Dynamitron accelerator is directed at studies of the physical processes involved when fast (~1 MeV/nucleon) molecular-ion beams traverse solid and gaseous targets. The work developed out of earlier channeling studies at the Dynamitron and many of the channeling experimental techniques are of great benefit. In particular, the use of very finely collimated beams permits angular resolutions of a few thousandths of a degree. Distributions in energy and angle are measured for the breakup products created when molecular ions dissociate in a target. This yields information not only on the initial properties of the molecular ions, but also on many new and interesting aspects of the interactions between fast charged particles and matter. For example, with beams of light diatomic molecular ions incident on thin foils, we have been able to observe the interaction between the trailing nuclear projectile (of the two created when the binding electrons are stripped off on entry into the foil) and the polarization oscillations generated by its partner ahead of it. A further field of interest lies in studies on the dissociation of fast heavy molecular ions. Our initial work on CH^+, OH^+, etc. indicates the great potential in this area for obtaining new information on effective charges and other properties of heavy nuclei traversing matter. There are good indications that this work will be of significant help in the problem of understanding

charge-state distributions for fast heavy ions emerging from foils and gas targets. This problem is of importance in many areas of physics but it is an especially crucial one in accelerator design and development.

a. Channeling of Fast Molecular Ions

D. S. Gemmell, J. M. Remillieux, and R. E. Holland

Angular distributions were measured for protons emerging near 0° from thin ($\sim$500 Å) gold crystals bombarded under (111)-planar channeling conditions by beams of H^+, H_2^+, H_3^+, $(^4HeH)^+$, D^+, D_2^+, D_3^+, and $(^3HeD)^+$ with energies in the range 0.15—2.0 MeV/nucleon. The shapes and widths of the measured angular distributions could not be accounted for in terms of a simple Coulomb explosion in which the constituent nuclei of an incident molecule repel each other apart after removal of their binding electrons on entering the target. A good quantitative fit was, however, obtained with computer calculations that included, in addition to the forces due to Coulomb repulsion and to the channeling potential, a "wake" force arising from the Coulomb effects of electron density oscillations trailing behind each charged projectile traversing the target. These oscillations are identified with volume plasmons excited by the projectiles.

b. Asymmetries in Energy Spectra

D. S. Gemmell, J. M. Remillieux, J.-C. Poizat,* and M. J. Gaillard*

A tightly-collimated ($\pm 0.06^{\circ}$ acceptance angle) Si counter was used to measure the energy spectra of protons that emerge in the beam direction when thin (100—500 Å) carbon foils are bombarded by H_2^+, H_3^+, and $(^4HeH)^+$ with energies of 0.5 to 2.0 MeV. Two peaks corresponding to protons emitted forwards and backwards in the CM frame were observed in the spectra. A previously unknown and unexpected

*University of Lyon, France.

esult was that the two peaks are asymmetrically populated, the lower-energy peak being up to a factor of three more intense than the higher-energy one. An explanation for the effect was given in terms of an interaction between trailing nuclei (in a given cluster created from an incident molecule) and the polarization oscillations generated in the target by other nuclei (from the same cluster) that precede.

c. $^{27}Al(p,\gamma)^{28}Si$ Studied with Molecular Ions

D. S. Gemmell and Z. Vager

The yield curve for γ rays from the 992-keV resonance in $^{27}Al(p,\gamma)^{28}Si$ was measured for protons emerging within $\pm 0.09^{\circ}$ of the beam direction when a 100-Å carbon foil was bombarded by ~2-MeV H_2^+ ions. The double-peaked yield curve showed the same sort of asymmetry discussed in the preceding paragraph.

d. Dissociation of Fast Molecular Ions in Thin Foils

D. S. Gemmell, Z. Vager, and B. J. Zabransky

We have begun using a 25° electrostatic analyzer and a set of four deflector plates to measure with greatly improved resolution (6×10^{-4} relative energy resolution, $\pm 0.008^{\circ}$ angular resolution) the distributions in angle and energy for the breakup products emerging from thin foils bombarded by ion beams of H^+, H_2^+, H_3^+, $(^4HeH)^+$, D^+, D_2^+, D_3^+, $(^3HeD)^+$, $^3He_2^+$, $^4He_2^+$, $(^3He^4He)^+$, CH^+, OH^+, and $(OH_2)^+$ with energies in the range 0.6 to 4.0 MeV.

The two main results obtained so far are:

(i) Light Molecular Ions. The measured distributions in energy and angle are not those expected on the basis of a simple "Coulomb explosion" picture (in which the nuclear fragments created after the incident ion loses its binding electrons fly apart under the influence of ir mutual Coulomb repulsion). There are large departures from the distributions expected from such a picture. For example, we find an

asymmetry in the intensities of the two peaks corresponding to particles emitted (in the COM system) parallel to or antiparallel to the beam direction. These asymmetries vary in magnitude [e.g., from ~5% for H_2^+ to a factor of 3 for $(^4HeH)^+$], but the sense of the asymmetry is always the same: Viz., for particles transmitted in the beam direction, the intensity of the peak corresponding to the case where the particle trails is always larger than for the peak corresponding to leading particles. On a simple Coulomb-explosion picture, these intensities should be equal. Simultaneous measurements of the distributions in angle and energy give further evidence for departures from a simple Coulomb explosion. An explanation for these effects has been offered in terms of a postulated interaction between the molecular constituents and polarization oscillations induced in the target electrons by the passage of the ions. Thus, a trailing particle experiences a force due to the electronic "wake" of a particle ahead of it, whereas this force does not influence the leading particle. Calculations have been made showing that the asymmetry in forces does in fact explain the asymmetries observed for the two energy groups. This interpretation of the results is reinforced by measurements with a double-layer carbon and aluminum target in which we see differences in the energy spectra obtained depending on whether the molecular ions enter the carbon or the aluminum first.

(ii) Heavy Molecular Ions. For 2.8-MeV $(OH)^+$ ions traversing a 100-Å carbon foil, the proton energy spectra, measured in the beam direction exhibit two sharp (width 1.4 keV) peaks separated by 10.3 keV. The oxygen ions emerging from the target have been measured to have a wide distribution in charge states (those from 2^+ up to 6^+ have large intensities). Since, inside the target the internuclear separation is expected to increase from about 1 to 1.8 Å, one would have expected that the Coulomb repulsion from the various integral charge states existing after emergence from the target would give rise to an easily observed splitting (~1-keV separation) of the peaks in the proton energy

spectra. The absence of this splitting taken together with other information on angular distributions suggests that the ions carry an electron cloud with them for at least several hundred angstroms after emerging from the foil into the vacuum. We hope that by studying these processes we can make valuable contributions to the problem of explaining the much higher charge-state distributions observed for fast heavy ions emerging from solid as compared with gaseous targets.

e. Transmission of Molecular Ions Through Foils

D. S. Gemmell, Z. Vager, and B. J. Zabransky

We have found that there is a finite probability ($\sim 10^{-6}$) for the transmission of energetic molecular ions such as 3-MeV HeH^+ and He_2^+ through carbon foils of a few hundred angstroms thickness. Precise measurements on the energy loss and angular distribution of the transmitted ions clearly rule out the possibility that they pass through pin holes in the target. It seems likely that the molecules dissociate on entering the foil and then, with low but finite probability, capture binding electrons at the exit. Experiments to measure the transmission probability as a function of target thickness and of incident ion velocity are planned to further elucidate the mechanism.

THIS PAGE

WAS INTENTIONALLY

LEFT BLANK

V. ACCELERATOR OPERATIONS

A. THE FN TANDEM VAN DE GRAAFF ACCELERATOR

The FN tandem is one of the principal research facilities of the Laboratory. It operates around the clock, seven days a week, with the following exceptions: (a) in 1976 there were several shutdowns (a total of 9 weeks) for accelerator development, and (b) the machine was run only five days weekly during part of the summer. In addition to use by the Physics Division staff and by graduate students and faculty members from physics departments in several universities, during 1976 the tandem has been used by members of the Chemistry Division, the Chemical Engineering Division, and the Radiological and Environmental Research Division at Argonne.

Numerous changes of the accelerator system were made during the past year in order to improve the reliability of the operation, increase the ability to respond to user needs, and improve the running efficiency. Ion-source development work has continued with the objective of producing high-intensity heavy-ion beams that have the good quality required when the tandem operates at high terminal voltages. Work on communication with the high-voltage terminal and with the dead sections between column sections has been initiated.

The continuing accelerator improvements are being guided by the need to upgrade the tandem so that it will be an acceptable heavy-ion injector for the planned superconducting-linac energy booster.

1. OPERATING EXPERIENCE

P. J. Billquist and J. L. Yntema

During the period 16 March 1975 to 15 March 1976 the accelerator operated 5462 hours. Of this time, 64% was used for the acceleration of ^{6}Li, ^{7}Li, ^{12}C, ^{13}C, ^{15}N, ^{16}O, ^{18}O, and ^{19}F ions; 33% was used for light ions; and 3% was used for machine-development work.

Because of the various technical developments outlined below, there was a general improvement in the efficiency and stability of operation during 1976.

2. ION-SOURCE SYSTEM

P. J. Billquist and J. L. Yntema

In July 1975 the configuration of the ion-source system was rearranged to allow injection into the tandem from three ion-source positions. This was achieved by using an old switching magnet. Since the magnet is not double focusing, there were some beam-optics problems. To overcome these, additional focusing elements were installed in order to match the emittance of the beam to the acceptance of the accelerator.

The rearrangement of the ion-source configuration has considerably reduced the time lost for ion-source changes, and it allows continued operation of the experimental program when one of the ion sources fails. Also, the improved beam optics has substantially increased the heavy-ion transmission through the accelerator.

3. ION-SOURCE DEVELOPMENT

P. J. Billquist, F. Munson, and J. L. Yntema

The new configuration of the ion-source system is expected to make it feasible to bring new ion sources into operation more rapidly than in the past, because a new source can be tested on line without the need to remove other sources in routine use.

Several source-development activities were carried out in the past year.

(1) A direct-extraction duoplasmatron and a sputtering PIG source (SPIGS) of the University of Wisconsin design have been built and are now in routine operation for H, O, and F ions. The good emittance of these sources results in excellent beam transmission through the tandem. Operation at 9.3 MV with 1 μA of analyzed $^{16}O^{6+}$ or with 0.1 μA of analyzed $^{16}O^{7+}$ is now common.

(2) The lithium-exchange duoplasmatron has been modified so as to reduce mechanical misalignments and in this way improve operation reliability. Also, a new power supply has been installed. These changes have caused a marked improvement in source performance.

(3) An inverted sputtering source similar to the one developed by Chapman at Florida State University has been constructed. The new source will be put into service in mid-1976.

4. INJECTION VOLTAGE

P. J. Billquist and J. L. Yntema

It is clear that the low injection voltage (30—50 kV) now in use makes it difficult to match most beams to our tandem. Moreover, a higher voltage is essential for the refined beam bunching required for the planned tandem-linac system. We expect to increase the voltage to an ultimate level of 150 kV in two steps, starting with an initial increase to a level of 80 keV. The new injection system is now being assembled and will be installed on the accelerator in July 1976. This system is expected to result in an important improvement in the usefulness of sputtering sources.

5. ANALYZING-MAGNET SUPPLY AND CONTROL

P. J. Billquist

In order to obtain better stability for the tandem beam, the power supply and control system for the analyzing magnet have been replaced. Three NMR probes are used in a system to monitor and compensate for the effects of magnet hysteresis.

6. PELLETRON CHAIN AND CORONA SYSTEM

P. J. Billquist and J. L. Yntema

Several changes that were required in order to keep up to date in this new technology have been made during the past year. The most significant of these has been the conversion of the enclosed-corona voltage-distribution system into one that operates on recirculated pure SF_6 rather than with the original mixture of N_2 and SF_6 without circulation. This change has resulted in greater stability of operation.

A single failure of the charging chain was repaired without difficulty, and the cause of the failure was eliminated.

7. TANDEM-TERMINAL CONTROL

J. J. Bicek and J. L. Yntema

A new kind of optical system to control equipment in the tandem terminal has been developed. The system transmits information by means of a modulated laser beam with a digital encoder, which in principle allows an unlimited number of control signals to be transmitted. This optical link has operated well in bench tests, and a preliminary test in the accelerator was successful. Bench tests on an expanded syste

that can transmit information out of the terminal are being prepared, and the planning for a complete control system for the tandem terminal is in progress. This system will be made of slightly-modified commercially-available equipment at a cost that is expected to be substantially lower than is involved in alternative approaches.

8. ACCELERATOR TUBE

We have undertaken a careful study of what is required to upgrade the capability of the tandem for heavy-ion acceleration. This study has led to the decision outlined below.

The present accelerator tube is a standard HVEC inclined-field (IF) tube with glass walls and aluminum electrodes. For heavy-ion acceleration, the main problems with this tube are that (a) the vacuum is poor because of the organic bonding agent, and (b) the IF structure causes the effective beam spot to be relatively large, and the interaction of the large area and multiple scattering in a foil stripper considerably deteriorates the beam emittance. Therefore, we plan to replace the present tube with one of improved design.

We will purchase a bakeable tube having axial symmetry from the National Electrostatic Corporation (NEC). There is space in the tandem to form an 8 UD accelerator, in NEC's nomenclature. Pumping will be required in the terminal and perhaps in the midsections. The modulus of the NEC tube is 0.500 in., whereas that of the HVEC support column is 0.999 in. Thus, it is necessary to install a second corona-discharge system to distribute the voltage. The two corona systems are expected to require only a rather small increase in total corona current, and this will not be an important additional drain on the charging chain.

The main objective of the tube change is to improve the current-carrying capacity of the machine for ions with masses in the

range $20 < A < 100$. The maximum terminal voltage is less critical, because the maximum output energy of the planned tandem-linac system is rather insensitive to the tandem voltage for a wide range of projectiles—although not for the heaviest ones. On the basis of experience elsewhere, it is believed that an 8 UD accelerating structure will operate reliably with ~10 MV on the terminal.

Procurement and installation of the new tube is the main part of an Accelerator Improvement Project for the coming year.

9. BEAM-BUNCHING SYSTEM

F. J. Lynch, R. N. Lewis,* and L. M. Bollinger

The design of an advanced system for bunching heavy ions has been completed, and construction is in progress. The system will consist of (1) a pretandem normally-conducting buncher, (2) a post-tandem superconducting buncher, and (3) a bunch-phase detector that dynamically links the two bunchers. The design objective is to bunch a large fraction (~80%) of the dc ion beam from the source into pulses <100 psec wide with a frequency of ~50 MHz. The system will be used both for time-of-flight experiments with ions from the tandem and for injection into the planned superconducting linac.

The pretandem buncher will consist of a single gridded accelerating gap located about 1.2 meters in front of the low-energy accelerator tube. Its function is to compress most of the dc beam from the source into approximately 1 nsec bursts at the tandem terminal. The wide range of low velocities of the heavy ions entering the pretandem buncher present some unusual design challenges. The buncher electrodes consist of two grids closely spaced and aligned to reduce transverse acceleration. The ideal sawtooth waveform for modulating the ion

*Electronics Division, ANL.

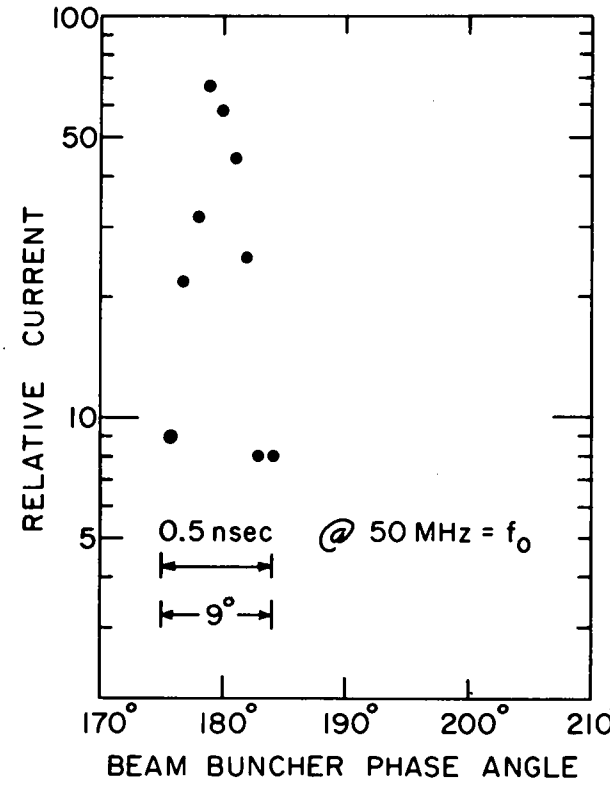

Fig. 34. Graph of beam current vs time for quasi-sawtooth waveform excitation. Excitation waveform is $V_m(t) = -0.454 (\sin \omega t + 0.4045 \sin 2\omega t + 0.18 \sin 3\omega t + 0.06 \sin 4\omega t)$, where $\omega = 2\pi \cdot 50 \cdot 10^6$ radians per sec. The calculation is for a singly charged ^{58}Ni ion injected at 100 keV, and a drift distance of 1.5 meters. 76% of dc beam falls within 0.5 ns. Random energy spread is assumed to be negligible.

velocities will be approximated by superimposing the first four harmonics of one-half the linac frequency (~96 MHz). Figure 34 is a graph of beam current vs time calculated on the assumption that there is no energy modulation uncorrelated in time. This calculation shows that 75% of the dc beam falls within a time interval of 0.5 ns.

The beam-pulse phase detector is a resonant system that is excited by the beam.

Post-tandem bunching will be carried out with an existing $\lambda/2$ superconducting-helix resonator that will be modified so as to have greater mechanical rigidity. This accelerating structure will be suitable for all ions in the mass range $10 < A < 110$.

The construction of special electronics for the bunching system is being done in the Argonne Electronics Division. The work is being carried out as part of an Accelerator Improvement Project for 1976.

10. UNIVERSITY USE OF THE TANDEM ACCELERATOR

The academic community's interest in the user program continues to remain high. A large number of scientists from many institutions base a significant portion of their research program on the availability of the Argonne tandem Van de Graaff complex. They periodically visit the Laboratory to conduct experiments at the tandem and to make use of its support facilities in analyzing and processing their raw data as well as to exchange views and information with local investigators. Representatives from ten institutions have conducted experiments at the tandem during the past year. All but one group have chosen to collaborate with local scientists.

Several predoctoral students are conducting their thesis research at the tandem. Some of these come with university user groups and work directly under the auspices of a university professor. Others have chosen to participate in Argonne's Resident Student Program, in which a student comes to the Laboratory after he finishes his formal course work and works under the joint direction of a local staff member and a thesis advisor from the parent university.

During the past year about 20% of the available time at the tandem was used by groups from neighboring institutions, and 14% of the time by students in the Resident Student Program. A list of those institutions whose staff members have performed experiments at the tandem during the past year, together with the names of the principal investigators and the title of the research done, is given below. The names of local collaborators are enclosed in parentheses.

(1) East Texas State University

Transfer Reaction Cross Sections in the Region of the Malmin Resonance

D. S. Gale, (W. Henning, D. G. Kovar, and B. Zeidman)

(2) University of Kansas

A Study of States in ^{28}Si Excited in the Reaction $^{16}O(^{16}O,\alpha)^{28}Si$; $^{28}Si \rightarrow {}^{24}Mg + \alpha$

R. W. Krone, F. W. Prosser, (R. L. Boudrie, and J. R. Erskine)

An Investigation of States in ^{40}Ca Produced in the Reaction $^{28}Si(^{16}O,\alpha)^{40}Ca$

F. W. Prosser and (J. P. Schiffer)

(3) Northern Illinois University

Production of a Mössbauer Source by the $^{54}Cr(^{4}He,p)^{57}Mn$ Reaction

R. S. Preston and (B. J. Zabransky)

Coulomb Excitation of ^{148}Sm

D. L. Bushnell, (R. E. Holland, L. Meyer-Schützmeister, and R. K. Smither)

(4) Northwestern University

Giant-Dipole Resonance Studies with Alpha-Particle Capture

L. L. Rutledge, Jr., (L. Meyer-Schützmeister, K. Raghunathan, and R. E. Segel)

(5) Ohio University

Energy Levels of ^{108}Ag Produced in the $^{107}Ag(d,p)^{108}Ag$ Reaction

C. E. Brient and K. R. S. Devan

(6) University of Pennsylvania

A Study of High-Spin States in ^{20}Ne Excited by the $^{12}C(^{12}C,\alpha)^{20}Ne$ Reaction

H. T. Fortune, (T. H. Braid, K. Raghunathan, R. E. Segel, and J. F. Tonn)

A Measure of the Q Value of the $^{84}Sr(d,{}^{3}He)^{83}Ru$ Reaction and the Assignment of Spins to the Excited States

L. R. Medsker, (R. L. Boudrie, and J. L. Yntema)

(7) Purdue University

Gyromagnetic Ratios of High-Spin States

R. J. Mitchell, T. V. Ragland, R. P. Scharenberg, (R. E. Holland, and F. J. Lynch)

(8) University of Washington

Excitation Function of Alpha Particles Elastically Scattered at Back Angles

K. A. Eberhard, (T. H. Braid, T. Renner, J. P. Schiffer, and S. E. Vigdor)

(9) Western Michigan University

A Search for the ^{43}Ti Isotope

G. Hardie and (L. Meyer-Schützmeister)

Deuteron Groups from the ^{45}Sc(^{4}He,d)^{47}Ti Reaction

G. Hardie, (T. H. Braid, and L. Meyer-Schützmeister)

(10) Wright-Patterson Aerospace Research Laboratory

An Investigation of the Reactions ^{42}Ca(^{4}He,d)^{44}Sc and ^{44}Ca(^{4}He,d)^{46}Sc

J. C. Manthuruthil, C. P. Poirier, (T. H. Braid, and L. Meyer-Schützmeister)

The following is the current list of students participating in the Resident Student Program together with their local advisor.

(1) R. L. Boudrie: University of Kansas

J. R. Erskine, adv.

(2) W. Corwin: Illinois Institute of Technology

R. E. Segel, adv.

(3) K. Daneshvar: University of Illinois, Chicago Circle Campus

D. G. Kovar, adv.

(4) M. Murphy: University of Chicago

C. N. Davids, adv.

(5) E. B. Norman: University of Chicago

C. N. Davids, adv.

(6) R. C. Pardo: University of Texas

C. N. Davids, adv.

(7) L. A. Parks: University of Texas

C. N. Davids, adv.

(8) K. Raghunathan: Northwestern University

R. E. Segel, adv.

(9) T. Renner: University of Chicago
J. P. Schiffer, adv.

(10) J. F. Tonn: Northwestern University
R. E. Segel, adv.

During the past year, J. F. Tonn received his doctorate working under this program.

B. OPERATION OF THE DYNAMITRON ACCELERATOR

The 4-MV Dynamitron accelerator and associated facilities support a wide range of research programs that include nuclear research, atomic physics research and materials science research. The accelerator is operated by the Physics Division and costs are shared on the basis of the fraction of time devoted to each program. In 1976, nuclear science research accounted for about 55% of the use of the accelerator. Other research carried out at the Dynamitron included atomic physics, materials science, and applied CTR research.

1. OPERATIONAL EXPERIENCE

F. P. Mooring, D. S. Gemmell, A. Langsdorf, Jr., and R. L. Amrein

During the past year, the experimental program at the Dynamitron has been hampered by pressure-sensitive leaks in the accelerator tube. Early in the year leaks began to develop and their number increased with time. They all occurred through the walls of the ceramic insulators separating the electrodes. Numerous insulators have developed leaks, and a total of 50 leaks have been repaired. At least 7 leaks have opened twice, and 4 three times. The leaks were sealed with a commercial polyurethane varnish sold as a vacuum sealant. Until the high-voltage properties of the sealant could be ascertained, it was used sparingly. After it became evident that the number of leaks was increasing at a rising rate and that no trouble was experienced in using the varnish in large voltage gradients, the tube was removed from the accelerator and all insulators painted with two or three heavy coats of the sealant. In April 1976 tests were made on one tube section with an epoxy sealant which will hopefully provide a longer-term solution to the problem of tube leaks.

The Dynamitron ran for 80% of the scheduled running time during the year. Among the atomic ions that were accelerated are $^{1}H^{+}$, $^{2}H^{+}$, $^{3}He^{+}$, $^{4}He^{+}$, $^{12}C^{+}$, $^{14}N^{+}$, $^{16}O^{+}$, $^{20}Ne^{+}$, $^{35}Cl^{+}$, $^{37}Cl^{+}$, $^{40}Ar^{+}$, ^{51}V,

$^{56}Fe^+$, $^{58}Ni^+$, $^{60}Ni^+$, $^{84}Kr^+$, Xe^+. Molecular ion beams included $(^1H\text{-}^1H)^+$, $(^1H\text{-}^1H\text{-}^1H)^+$, $(^2H\text{-}^2H)^+$, $(^2H\text{-}^2H\text{-}^2H)^+$, $(^1H\text{-}^4He)^+$, $(^2H\text{-}^4He)^+$, $(^1H\text{-}^3He)^+$, $(^2H\text{-}^3He)^+$, $(^3He\text{-}^3He)^+$, $(^3He\text{-}^4He)^+$, $(^4He\text{-}^4He)^+$, $(^1H\text{-}^{12}C)^+$, $(^1H\text{-}^{16}O)^+$, $(^1H\text{-}^1H\text{-}^{16}O)^+$, and $(^{16}O\text{-}^{16}O)^+$. Ion currents in the range 0.1 nA—100 μA were produced and terminal voltages ranged from 400 kV to 4.0 MV. Both dc and pulsed beams were generated.

More than thirty scientists used the machine last year. About half were from the Physics Division, the rest included members of other Argonne divisions, scientists from six other laboratories and visitors from two foreign countries. Physicists from the University of California at Los Angeles, Westinghouse Electric Corporation Research Laboratories, the Advanced Reactor Division of Westinghouse Electric Corporation, and the Hanford Engineering Development Laboratory of Westinghouse Hanford Company have used the facility to study the damage induced in materials by energetic heavy ions.

The Dynamitron ran 24 hours per day, five days per week. Except for the vacuum problems, the machine ran well. Ion-source changes still account for most of the scheduled down time. A new terminal, now under construction and slated to be installed this summer, will facilitate ion-source changes. The Dynamitron continues to be an important facility for Argonne's research program.

2. IMPROVEMENT OF ACCELERATION TUBE FOR THE DYNAMITRON

A. Langsdorf

The performance of the acceleration tube in our 4-MV Dynamitron has been improved by a very simple change in the location of the thirteen "decoupler" diaphragms in the twelve-feet-long tube assembly. Such diaphragms are an integral part of the overall design of this tube manufactured by National Electrostatics Corporation), which was installed

in the Dynamitron in June of 1974. The essence of this new and original arrangement is merely the physical displacement of these diaphragms (in the downstream direction of ion-beam particle flow) so as to strongly accentuate the asymmetry of electric field strength on the two sides of each diaphragm. In consequence there is a substantial area on the upstream face of each diaphragm, and surrounding the central hole, where electric field lines start out from the diaphragm surface pointing oppositely to their usual sense, and then turn around and pass through the central hole. The key function of this reversed sense of electric field on the diaphragm is to inhibit escape from the diaphragm surface of secondary low-energy negative ions and electrons which are produced whenever high-energy positive ions strike this surface. (There are always some stray high-energy positive ions present because some finite fraction of the ion beam is scattered by residual gas in the imperfect vacuum in the tube. There may also be stray positive ion bombardment for other reasons.)

The concept of backbiasing as here applied is not in itself original; many accelerators have employed a few diaphragm apertures "backbiased" by actually reversing polarity of some nearby electrodes. In our tube, which has 12 sections, decoupled by eleven diaphragms between them, such a form of backbiasing could not have been practical to apply consistently to all of them, and would have been complicated to apply even to a few. This new method is, on the contrary, simple, practical, and effective. It may well be called "self-backbiasing." The self-backbiasing would not be effective if too small an area of diaphragm had reversed field sense. Therefore, calculations of the surface fields were made prior to adopting the scheme. For the geometry actually used the reversed region reaches out to more than 1.9 times the aperture diameter. Since the apertures are 1.5 in. diameter, the emission of negative particles should be highly suppressed out to 2.85 in. diameter, in a system where the full aperture of electrodes is 3.25 in.

The motivation of this work has been to achieve successful operation of an acceleration tube made by National Electrostatics Corporation (NEC). Their tube of unique design was procured to begin with because the more common type of tube made with glass insulators and steel electrodes glued together with organic cement had not shown long life. The primary trouble with these glass tubes had seemed to be an incurable one: electrical breakdown decomposed the organic cement and the gaseous products created a plasma that sputtered metal onto the glass wall which in consequence short-circuited; cleaning and rebuilding such tubes at frequent intervals seemed completely uneconomic. Because the NEC tube has no organic material in it, it seems to be proof against such rapid failure after a relatively few breakdown events; our experience with the NEC tube seems to confirm this opinion. However, we have experienced modes of failure of the NEC tube that were new and not experienced in their prior use. This is not surprising because no NEC tube was ever previously installed in a Dynamitron, and in addition, no Dynamitron has ever previously been employed extensively with such high-current beams of heavy ions of nickel, nickel chloride ions, etc. (Heavy ions greatly intensify the problems encountered compared to lighter ions of hydrogen, helium, etc.) The Dynamitron, furthermore, has much more power capability than ordinary electrostatic generators electrically charged by belts or chains, so it can much more easily be so employed as to overstress its acceleration tube. Our experience with the NEC tubes demonstrated two serious problems: many small punctures through the ceramic walls developed, and ion-plus-electron bombardment of the decoupler diaphragms actually heated some of them so hot that they warped severely. The latter effect showed conclusively that, whereas the diaphragms may "decouple" by preventing many stray ions produced within one section from reaching other sections, the diaphragms themselves couple to each other. By this it is meant that positive ions striking one

aphragm create negative ions and electrons at the surface of another;

some of these flow back to the diaphragm from which the positives came and produce more positive ions. Conditions arise where this chain reaction comes close to divergence. The evidence for this by direct visual observation of damaged electrodes seems dramatically convincing. The cause of the punctures through the ceramic is less certain, but there is some evidence that it is a consequence of intense x rays which are in turn generated by the electron component of the total current flow within the tube system. A reasonable conjecture, based upon data in the literature, is that the intense directional x-ray irradiation actually causes a net migration of charge within the ceramic, so great that the resulting space charge causes electric puncture through it. This is a problem that needs further study.

The NEC acceleration tube was repaired by varnishing its exterior surface quite heavily to seal the small leaks. (There were about 24 punctured spots; none was large enough to be visible.) The new diaphragms were installed; the orientation of the ion source was adjusted to improve the aiming of the ion beam so it was closer to being on the axis of the tube than before; and since reassembly we have consistently limited the maximum beam current so that the maximum x-ray flux generated by electrons within the tube is only about one-fourth as much as we previously allowed. These last two steps inevitably compromise a simple comparison of behavior of the system prior to and after the basic modification, namely, the new diaphragm design. However, the steps were deemed essential to maintaining operation. Nevertheless, there are several signs that the new diaphragm design actually made a very significant improvement in machine performance. Among these are the following: (a) The machine "conditions" so that it can be raised to full voltage more quickly than before. (b) When accelerating heavy ions like nickel, there is no longer a noticeable component of ions in the beam ascribable to lower-energy heavy ions produced part way down the acceleration tube. (c) The new diaphragms have not warped. (d) The

accelerator operated steadily for over three months before a number of the old leaks through the acceleration tube reopened sufficiently to require repair, and very few, if any, new leaks have been formed. There is no way as yet to ascertain whether this achievement, limited as it may be, is mainly ascribable to the new diaphragms, the varnishing, the limiting of x-ray flux, or some combination thereof. (Before these steps had been taken, leaks had been forming or reopening within but a few days of operation after stop-gap repairs.)

The present status is that we now have on hand a new NEC tube which will be installed with the self-backbiased type of diaphragms. Certain minor modifications to these new diaphragms will be made a part of a continuing effort to further improve accelerating-tube performance. Two as yet unresolved problems now stand out as deserving immediate attention. One is that with the presently installed NEC tube, the ion-beam trajectory through it has consistently failed to remain sufficiently accurately centered on the tube axis. This problem apparently has not been experienced with other NEC tubes. Since our tube has insert electrodes within it of a design not previously employed in NEC tubes, it seems likely that this difficulty relates to imperfections in this new electrode design. The other problem is to achieve a substantial improvement in the quality of the vacuum in the acceleration tube, especially in the region near the ion-source end of the tube. Success in these two directions, together with the new diaphragm design, should hopefully be sufficient to achieve further improvement in tube lifetime and overall performance.

THIS PAGE

WAS INTENTIONALLY

LEFT BLANK

VI. NEUTRON PHYSICS

The neutron research effort has had two principal components: a high-priority program of photonuclear studies using photons from an electron linac and other sources, and a program of nuclear-structure studies based on neutrons from the CP-5 reactor. The work with reactor neutrons will end in July 1976.

A. PHOTONUCLEAR RESEARCH

The cornerstone of the photonuclear program is Argonne's very intense ultrahigh resolution electron linac. This unique facility has been developed by the ANL staff into a probe of unexcelled sensitivity and precision for the study of photoneutron spectra in the threshold region. These experiments in which the neutron spectra are observed with excellent energy resolution have become a powerful tool in the study of highly-excited nuclear states. They complement traditional (n,γ) measurements and in many cases extend experimentation to previously inaccessible classes of nuclei. They have been a major factor in recent progress in our understanding of the interaction of neutrons with complex nuclei, and have provided results relevant to the long-range needs of the U.S. applied energy program. Results in the past 18 months have contributed to the resolution of major questions in nuclear physics such as the search for radiative giant resonances.

For the moment the technical performance of the ANL facility remains unexcelled and the program is the only effort of its kind in operation. The development of a polarimeter for measurement of polarization of neutrons generated in (γ,n) reactions has been particularly successful and has given added dimension to our research capability.

1. THRESHOLD PHOTONEUTRON EXPERIMENTS AT THE ANL LINAC

The threshold-photoneutron experiments to study the ground-state radiations of highly excited nuclear states are carried out at the high-current electron linac operated by the Chemistry Division. The very intense nanosecond pulsed bremsstrahlung for incident electron energies f 6—14 MeV which characterize this source make it unique for such studies. ..n additional capability of generating 50 picosecond wide pulses of 200 amps

of electrons can be used to observe photoneutron spectra with resolution limited only by the detector system. These features of our source permit one to study a large number of excited states in a given nuclear target in a manner that is not possible using the techniques currently employed in the study of neutron induced reactions. In contrast to capture reactions, measurement of photoneutron angular distributions is simple and direct. When coupled with polarization measurements of the same excited states, these data constitute an unambiguous spectroscopy of highly excited nuclear states, which can determine many features of nuclear interactions and nuclear structure, which involve neutrons or photons.

The threshold method is an ideal technique for isolating "intermediate structure" in the distribution of reaction strength among photoneutron resonances. At the present time, this aspect of the program has been given primary emphasis in measurements whose objective is to search for local concentrations of strength for M1 transitions. Such giant M1 resonances have been predicted, but to date their existence has not been established, except in very light nuclei. In addition, those problems which have been studied in the past by neutron capture are pursued: the dependence of radiative strength of transitions on resonance spin and parity, radiative strength functions, statistical distributions of ground-state radiation widths and possible correlations between neutron and radiative widths. In all of these areas, this class of measurement constitutes a major advance.

a. Photodisintegration of the Deuteron Near Threshold

H. E. Jackson, R. J. Holt, R. M. Laszewski, and W. M. Wilson

The simplest and most basic threshold measurement is the photodisintegration of the deuteron. This experiment is of particular interest because the deuteron is the one nuclear system for which the effects of meson exchange currents and virtual isobaric states can be calculated accurately. The photomagnetic disintegration amplitude of the deuteron is particularly sensitive to these phenomena and it is in the threshold region that photomagnetic disintegration is strongest. The only information comes from the inverse reaction, i.e., thermal capture cross section is observed to be enhanced over predicted values by 10%. This enhancement can be explained in terms of mesonic effects.

The experiments are performed by irradiating a deuterium target with pulsed bremsstrahlung. Initial efforts have been focused on

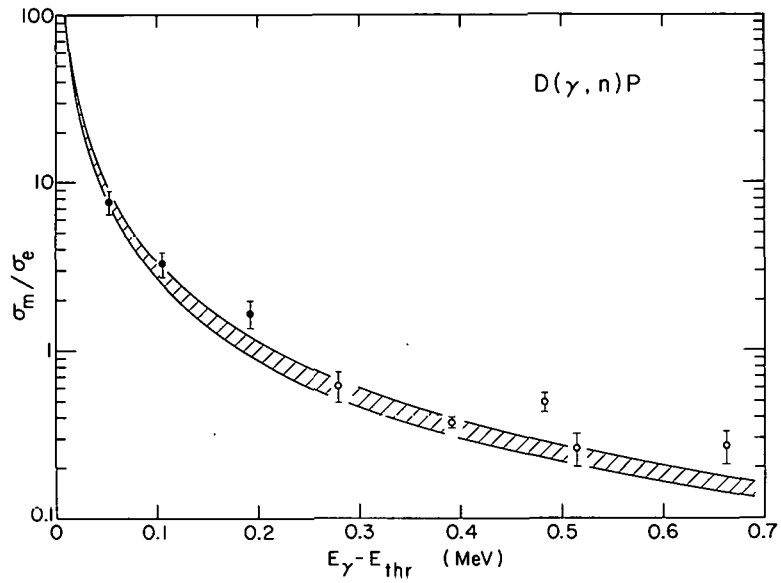

Fig. 35. The solid circles represent the present measurements, while the open circles represent all previous photodisintegration studies. The smooth curves indicate the limits of the present uncertainty of the effective range theory.

determination of the angular distribution of the photoneutrons. To date a precision of about 10% has been achieved, which is adequate for testing the simple effective-range theory. The measured magnetic-to-electric dipole cross-section ratio is shown in Fig. 35. Future measurements of increased precision should permit a comparison with this theory which will place limits on any final-state interaction or momentum-dependent component in the nucleon potential. Such effects would cause spin mixing and lead to an interference term in the photoneutron distribution. Such terms are absent in the predictions of the effective-range theory.

b. Threshold Photoneutron Spectroscopy of ^{17}O

R. J. Holt and H. E. Jackson

The ^{17}O nucleus is particularly well suited for the study of single-particle M1 transitions ($1d_{5/2} \rightarrow 1d_{3/2}$) from many points of view. (i) The ^{17}O nucleus is thought to be well represented by an ^{16}O core plus a neutron in the $1d_{5/2}$ orbital. (ii) Most (~70%) of the $1d_{3/2}$ strength is believed to be concentrated in the 5.08-MeV level. (iii) It is unnecessary to renormalize the single-particle M1 operator since the magnetic moment of ^{17}O is given almost completely by the Schmidt estimate. The primary objective of the present study is to determine the

extent to which the $1d_{5/2} \rightarrow 1d_{3/2}$ M1 excitation (5.08 MeV) can be represented by a transition between two single-particle states.

The threshold photoneutron spectra for the $^{17}O(\gamma,n_0)^{16}O$ reaction were observed, for the first time, throughout the excitation energy range 4.3 to 6.2 MeV and at reaction angles of 90° and 135°. A tentative value for the M1 reduced transition probability for the 5.08-MeV resonance was observed to be $B(M1, d_{3/2} \rightarrow d_{5/2}) = 0.9\ \mu_0^2$. A value of $B(M1) = 2.0\ \mu_0^2$ was deduced from the single-particle model. In order to compare in detail the present observation and calculation, it is necessary to determine the proper normalization for the unbound $d_{3/2}$ radial wave function. Further refinements in the experiment and theory are necessary in order to determine the source of the discrepancy.

c. Nonresonant (γ,n) Reactions and Channel Transition in Medium-Weight Nuclei

H. E. Jackson, R. J. Holt, R. M. Laszewski, and W. M. Wilson

A particularly striking example of a doorway state common to both the entrance and exit channel has been observed in studies of the (γ,n) reaction for ^{29}Si performed at the ANL threshold photoneutron facility. A preliminary analysis has established complete correlation between photon and neutron partial widths and an unexpectedly large nonresonant background cross section for a group of $\frac{3}{2}^+$ resonances near 750 keV. The strong correlation of partial widths and the "anomalous" background cross section are precisely the features that are associated with dominance of simple single-particle configurations in the initial and final nuclear states. In the case of ^{29}Si, these results can be attributed to the presence of a common doorway state consisting of a $2p_{3/2}$ neutron coupled to a ^{28}Si core.

A similar study has been made for targets in the Cr-Ni region in an effort to determine the magnitude of channel transitions, that is, radiative transitions which involve direct emission of valence

nucleons into the continuum. As in the case of ^{29}Si, strong correlations are observed for s-wave resonances in both ^{53}Cr and ^{61}Ni. In addition, the strength of nonresonant processes displays a mass dependence in exact agreement with the predictions of the channel-capture theory of radiative transitions. A complete analysis of the data will be used to establish the degree to which the radiative widths can be explained in terms of channel transitions.

d. Measurement of Ground-State Radiation Widths Near Photoneutron Threshold in ^{140}Ce

R. M. Laszewski, R. J. Holt, and H. E. Jackson

The ground-state transition strengths of levels near the photoneutron threshold in ^{140}Ce have been studied by means of the $^{140}Ce(\gamma,n)^{139}Ce$ reaction. The angular distribution of photoneutrons was measured at laboratory angles of 90° and 135° with high-energy resolution (0.5 ns/m). The time-of-flight spectra are shown in Fig. 36. The angular distribution enables E1 and M1 transitions to be distinguished. For nuclei with $A \sim 140$, M1 ground-state radiation widths are expected to be enhanced because of the possibility of collective spin-flip transitions between the filled $\nu(1h_{11/2})$ shell and the vacant $\nu(1h_{9/2})$ orbital. It is also possible for protons in the $\pi(1g_{9/2})$ orbital to be excited into the vacant $\pi(1g_{7/2})$ orbital by M1 radiation. A total M1 strength of $B(\uparrow M1) = 0.39\ (e\hbar/2Mc)^2$ was observed over a 40-keV interval of excitation centered at 9.08 MeV. This unusually large amount of integrated M1 strength suggests the proximity of a collective M1 resonance. A total E1 strength of $B(\uparrow E1) = 6.6\ e^2fm^2$ was observed over the same excitation interval.

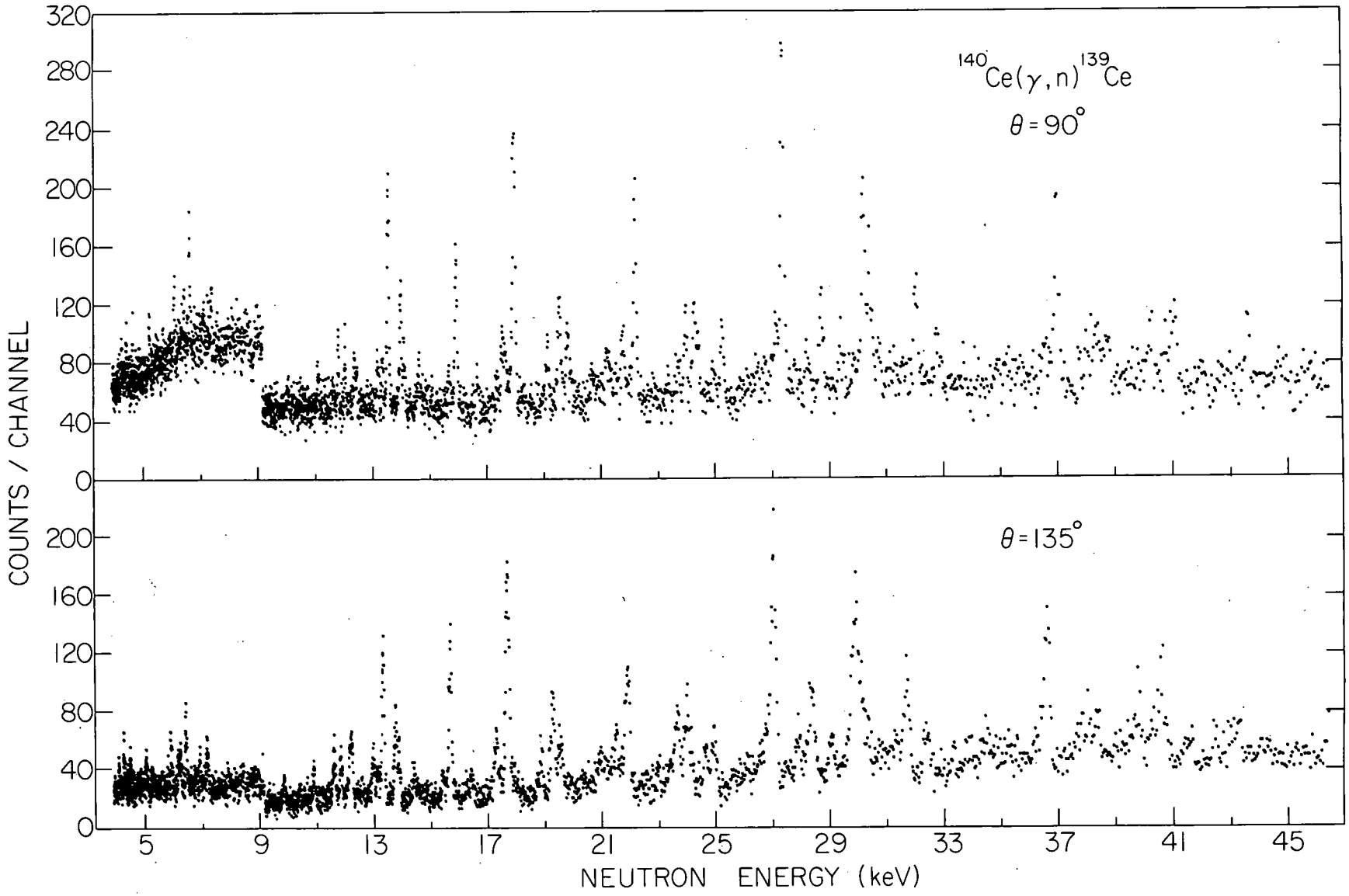

ig. 36. Photoneutron spectra for the $^{140}Ce(\gamma,n)^{139}Ce$ reaction at reaction angles of 90° and 135°

e. Development of Polarimeter and Instrumentation for Threshold Photoneutron Polarization Studies

R. J. Holt, H. E. Jackson, J. R. Specht, and R. M. Laszewski

(i) Polarimeter System. It is well known[1] that photonucleon polarization studies provide a powerful method for determining the existence and magnitude of E1-M1 and E1-E2 admixtures in photoexcitations of nuclei. In order to determine the nature of the giant M1 and isoscalar E2 resonances in nuclei, a photoneutron polarimeter system was developed which is suitable for use with continuous energy spectrum of neutrons in the energy range 170 keV to 3 MeV. The feasibility of measuring the polarization of photoneutrons from resonances near threshold was demonstrated for the first time for the case of the $^{208}Pb(\gamma,\vec{n}_0)^{207}Pb$ reaction.

In order to observe the polarization over this broad energy range Mg, ^{16}O and ^{12}C were used as analyzing targets in separate experiments. A neutron spin-precession solenoid, designed for use with a continuous energy spectrum of neutrons, was developed in order to minimize systematic errors.

(ii) Absolute Calibration of the Polarimeter: Neutron Double Scattering. In order to determine the absolute analyzing power of the polarimeter in the energy range 170 to 320 keV the polarization of neutrons elastically scattered from Mg was measured using a true neutron double-scattering method. The present work represents the first attempt at establishing an absolute calibration standard for neutron polarization studies in this energy region. Intense pulsed beams of unpolarized neutrons were obtained by allowing a 20-MeV electron beam to impinge on a target of natural uranium. These neutrons scatter elastically from the first Mg target at an angle of 45° and become

[1] F. W. K. Firk, Ann. Rev. Nucl. Sci. 20, 39 (1970); H. F. Glavish, S. S. Hanna, R. Avida, R. N. Boyd, C. C. Chang, and E. Diener, ıys. Rev. Lett. 28, 766 (1972).

polarized. The amount of polarization is measured by allowing the polarized neutrons to scatter again from a second target, identical to the first, at the same reaction angle, 45°. A preliminary analysis of the data indicates that the observed polarizations are in general agreement with a previous study of the $Mg(n,\vec{n})Mg$ reaction.

f. Search for the Giant M1 Resonance in ^{208}Pb

R. J. Holt, H. E. Jackson, and R. M. Laszewski

The ^{208}Pb nucleus should provide an ideal example of the giant M1 resonance since it has more nucleons which are available for spin-flip transitions than any other nucleus. It is widely believed that a collective M1 resonance exists at an excitation energy of 7.9 MeV, is fragmented, and is spread over 700 keV in ^{208}Pb. Thus far, the large spreading cannot be explained within the framework of current theories. For these reasons, we observed the polarization of photoneutrons emitted from resonances in the expected giant M1 resonance region of ^{208}Pb in order to deduce the multipolarities of these resonances. The photoneutron polarizations were measured at reaction angles of 90° and 135° throughout the excitation energy range 7.56 to 8.40 MeV (E_n = 180 to 1000 keV). Definitive multipolarity assignments for 12 resonances were made on the basis of these polarization observations. The resonances observed at photoneutron energies of 7.56, 7.70, 7.92, 7.98, 8.03, and 8.23 MeV, previously believed to comprise a major part (~75%) of the giant M1 resonance, are shown to be E1 excitations. Only one M1 resonance, located at 7.99 MeV, was found in this energy region. This single resonance accounts for only 28% of the M1 strength expected from calculations based on the collective vibrational model of Bohr and Mottelson. The search for the giant M1 resonance in ^{208}Pb has been completed above the photoneutron threshold.

Discovery of Large sd-Wave Admixtures for 1^- Resonances in the ^{207}Pb+n System

R. J. Holt, R. M. Laszewski, and H. E. Jackson

A recent shell-model calculation of Harvey and Khanna indicates that segments of the $|^{207}\text{Pb} \otimes 3d_{3/2}\rangle$ and $|^{207}\text{Pb} \otimes 4s_{1/2}\rangle$ basis states in ^{208}Pb are expected to occur in 1^- resonances near the photoneutron threshold. Furthermore, Harvey and Khanna predict that the ratios of d-to-s-wave amplitudes of these basis states should be $\gg 1$. Hence, these shell-model calculations can be tested by searching for abnormally large ratios of the neutron reduced widths γ_d^2/γ_s^2. The signature of large sd-wave mixing for 1^- resonances in the ^{207}Pb+n system is a large photoneutron polarization for the $^{208}\text{Pb}(\gamma, n_0)^{207}\text{Pb}$ reaction at a suitable reaction angle, say 135°.

Photoneutron polarizations were observed at 135° for the 180- and 254-keV resonances for the $^{208}\text{Pb}(\gamma, n_0)^{207}\text{Pb}$ reaction. The observed polarizations are shown in Fig. 37. The lower graphs indicate the raw photoneutron spectra from ^{208}Pb after the emitted neutrons scatter from a Mg analyzer at angles of ± 45. A large polarization effect is signified by the difference in the spectra with and without the field of the neutron spin-precession solenoid. On the basis of these measurements and previous angular-distribution studies, the ratios γ_d^2/γ_s^2 were found to be 9 and 21 for the 180- and 254-keV resonances. These results support the shell-model calculations for ^{208}Pb. Although the polarization studies are essential in order to identify resonances with large sd-wave mixing, the exact magnitude of γ_d^2/γ_s^2 was found to be sensitive to angular distribution measurements. More accurate angular-distribution studies are necessary in order to determine the amount of the $|^{207}\text{Pb} \otimes 3d_{3/2}\rangle$ configuration above the photoneutron threshold.

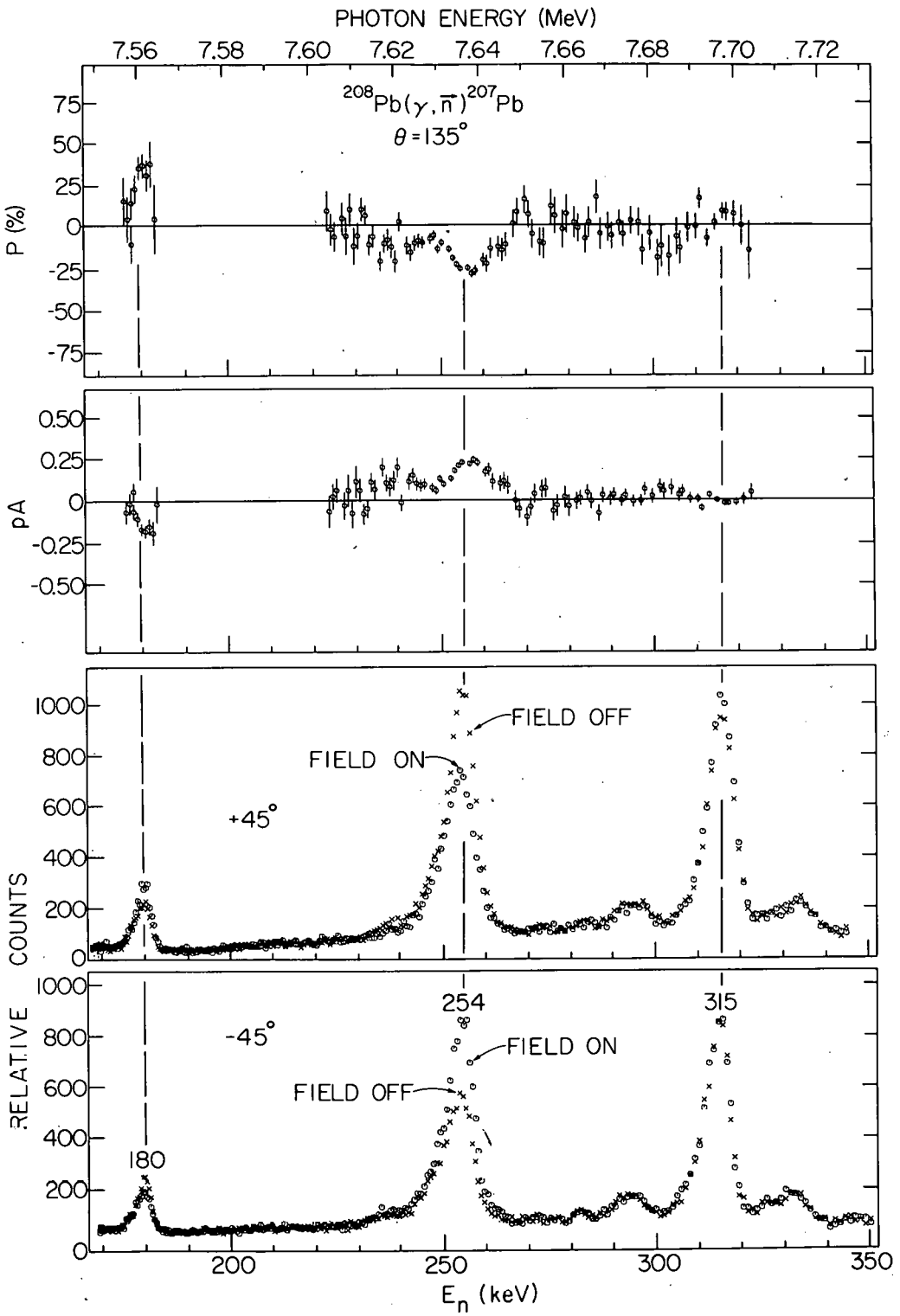

Fig. 37. Upper graphs represent the observations of the photoneutron polarization p and the asymmetry product pA. Lower graphs indicate the photoneutron spectra from ^{208}Pb after scattering from a Mg analyzer at angles of $\pm 45^{\circ}$ and with and without the field of the neutron-spin-precession solenoid.

. Studies of the Distribution of E2 Transition Strength in ^{208}Pb Using Photoneutron Polarization Measurements

R. M. Laszewski and R. J. Holt

Preliminary measurements of the polarization of neutrons in the energy range 1.4 to 2.0 MeV from the ^{208}Pb$(\gamma, \vec{n}_0)^{207}$Pb reaction have been made in order to examine the distribution of E2 ground-state transition strength in ^{208}Pb. Inelastic electron and hadron scattering experiments have shown broad resonances in many nuclei including ^{208}Pb at excitations near those predicted for the isoscalar monopole and quadrupole giant resonances. The photoneutron polarization technique enables the location of quadrupole excitations to be determined unambiguously and with much greater energy resolution than was previously possible. The preliminary measurements show E2 resonances at excitations of 9.04 and 9.12 MeV. The measurements are currently being extended to neutron energies above 2.0 MeV and below 1.4 MeV.

2. NUCLEAR STRUCTURE STUDIES AT CP-5

Nuclear structure studies were performed at the Argonne research reactor CP-5 using both thermal (n, γ) studies and average resonance neutron-capture experiments. The work was done in three different mass regions: (1) the mass region just above the closed neutron shell at N = 82 (Sm and Nd isotopes), (2) the mass region halfway between the closed neutron shells at N = 50 and N = 82 (Cd and Te isotopes), and (3) the mass region halfway between the closed neutron shells at N = 82 and N = 126 (Hf and W isotopes). These three regions contain nuclei whose level schemes are classified as characteristic of transitional nuclei, vibrational nuclei, and rotational nuclei, respectively. The object of this work was to compare the level scheme systematics and γ-ray branching ratio systematics in these regions. The detailed information about γ-ray transition strengths, ratios, B(E2)'s, etc. is needed to distinguish between the many nuclear theories that could apply to these nuclei. For example, both the recently-developed phonon model of Arima and Iachello (interacting boson model) and the older rotational model with
cited-state bands built on two-quasiparticle levels, and including
mplete Coriolis coupling calculations, can reproduce the level energies

of many nuclei equally well. The predictions of these models for γ-ray branching ratios and transition strength will in most cases be different and allow one to select a preferred model. The cluster-vibration model of Paar and Alaga coupled with their GVISR method for calculating γ-ray transition strength give still different values. The microscopic calculation of Janssen using the Strutinski method also gives different values as do the quasiparticle-random-phase calculations of Maramoi, Kuriyama, Yamamura, Sorensen, Kisslinger, etc. The perturbative boson expansion methods of Marshalek will give another set of numbers. In order to sort out these many theories, one needs at least 5 or 6 γ-ray branching ratios plus transition strengths if possible, in addition to complete information on spins, parities and energy levels; and ten sets of additional information would be preferred in case some of the level assignments are wrong. The profusion of models makes it important that the experimental data be as complete as possible and considerable effort was expended in identifying all low spin levels ($J < 6$) and all E1, E2, and M1 γ transitions between these levels up to 3-MeV excitation. The energy range covered in the (n, γ) spectra was 20 keV to 10 MeV. Crystal diffraction measurements covered the region from 20 keV to 2 MeV, while the Ge(Li) detector measurements concentrated on the 500-keV to 10-MeV region. The scientific question that is trying to be answered is whether or not a systematic γ-decay pattern is present for the low-lying levels of all the nuclei in each group; and, if so, how does it change from group to group. Completeness is important in this work because we must be able to identify the same transitions in all the nuclei if we wish to have anything to compare. This is difficult because the level spacings change as we move from nucleus to nucleus. In one level scheme the energy separation between two levels might be 500 keV, while the same level spacing in a nucleus with 4 or 6 more neutrons might be only 100 keV. Assuming the values of the B(E2)'s for these transitions are the same, this variation in γ energy changes the speed of the transition by a factor of ~3000. When this happens, a transition that was one of the strongest in the level scheme can become one of the weakest. Thus, it is essential that the γ spectrometers used have a large dynamic range both in γ energy and sensitivity. Without both the diffraction spectrometer and the Ge(Li) γ-detector spectrometer, these experiments would not have been possible. The closing down of the Argonne γ-diffraction spectrometer in 1975 made it necessary to go to Grenoble, France to complete some of the work. Grenoble is the only other place in the world that has a γ-diffraction spectrometer with comparable energy resolution and sensitivity.

1. Nuclear Structure of ^{148}Sm, ^{150}Sm, and ^{152}Sm

R. K. Smither and D. L. Bushnell

The (n,γ) reaction has been used to study the level structure of ^{148}Sm, ^{150}Sm, and ^{152}Sm. Special care was given to identifying and measuring the γ intensity of all possible E1, M1, and E2 transitions between the low-lying states. This emphasis on completeness has made it possible to identify a characteristic γ-decay pattern for many of the low-lying states that can be followed from nucleus to nucleus. What is surprising is that these decay patterns, i.e., relative values for B(E2)'s, etc. do not change very much; the patterns in ^{148}Sm are not much different from those found in ^{152}Sm. (See Fig. 38.) The general structure of the level scheme also remains the same, while the energies of the individual levels change dramatically; e.g., the excitation energy of the first 2^+ state changes by a factor of 5. The selection rules for the γ decays are found to be of a yes/no nature. The B(E2) values found for competing transitions are either quite similar or very much slower, differing by a factor of 10 or 100. This is just the γ-decay pattern that is predicted by a simple phonon or boson model. The transitions that change the phonon number by zero or one are allowed, while those that change the phonon number by two or more are retarded by a factor $R^{(\Delta n-1)}$. The predictions of the phonon model are compared to the rotor model in Fig. 39. The level structure of the Sm nuclei changes smoothly with neutron number from a rotational-type structure, i.e., rotational bands with an I(I+1) energy dependence, to a vibrational type structure, i.e., quasibands with a $E_L = n \cdot \Delta E$ energy dependence. We have, therefore, the difficult problem of finding a model that will change the level structure and absolute values of the B(E2)'s from those typical of a rotational level scheme to those typical of a vibrational level scheme without changing the relative values of the B(E2)'s. As difficult as this problem may seem, it is also quite encouraging because the smooth dependence of all the observables suggests that a single theory could be used to describe all of

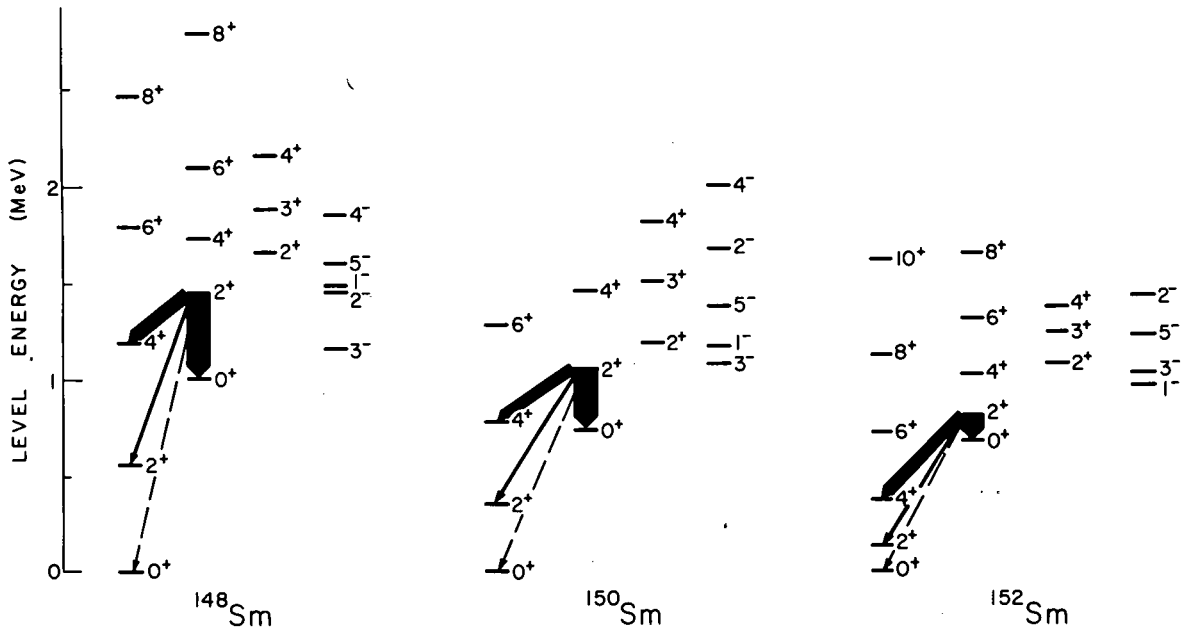

Fig. 38. Comparison of the low-lying level structure and B(E2) gamma-ray branching ratios in ^{148}Sm, ^{150}Sm, and ^{152}Sm. The widths of the lines are meant to suggest the relative values of the B(E2) component of the transitions. The dashed lines are about a factor of 10 weaker than the narrowest solid line.

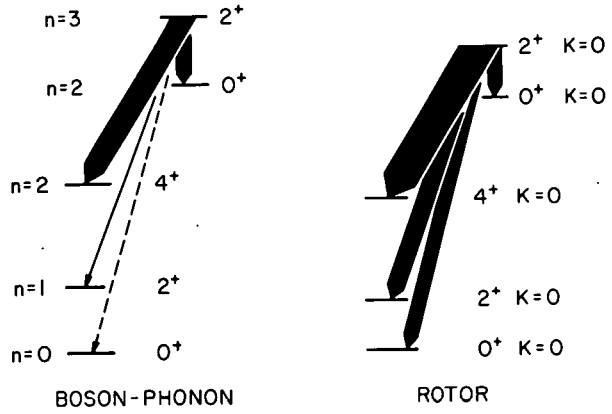

Fig. 39. Theoretical predictions for the gamma-decay branching ratios shown in Fig. 38, based on the phonon and rotor models. The widths of the lines are meant to suggest the relative value of the B(E2) component of the transitions. The dashed line is 10 times weaker than the thin solid line.

the Sm level schemes. The data taking is complete except for some conflicting data in the ^{148}Sm level scheme. Further Ge-detector data should resolve these problems. Also missing are good values for the B(E2)'s of the transitions from the second and third 2^+ excited states in ^{148}Sm. Experimental work is in progress at the Argonne Tandem to measure these B(E2)'s through Coulomb excitation with ^{16}O ions. (See Sec. VI. A2b below.)

b. Coulomb-Excitation Experiments in ^{148}Sm

R. K. Smither and Luise Meyer-Schützmeister

The object of this work is to measure the values of the B(E2)'s of the transitions from the ground state to the second and third 2^+ states in ^{148}Sm. Natural and enriched targets were bombarded with ^{16}O ions at three different energies, 35, 45, and 55 MeV. The trouble with the previous Coulomb excitation experiments is that the complete level scheme was not known and transitions to nearby levels were not resolved from the transitions of interest. This resolution problem coupled with the very weak nature of these forbidden E2 transitions, $\Delta n = 2$ and 3, respectively, resulted in a poor signal-to-background ratio, and thus inaccurate values for the B(E2)'s. The experiments calibrated the sensitivity of the system. One long run using the natural Sm target gave us relative B(E2) values for the stronger E2 transition in ^{148}Sm compared to the corresponding transition in ^{150}Sm and ^{152}Sm. The next experiment will use a thick target of separated isotope material (^{148}Sm metal) and will take both singles and coincidence spectra using two Ge(Li) detectors. This should result in appreciably more precise values for the B(E2)'s and based on them, more accurate values for the B(E2)'s of the other transitions that depopulate the second and third 2^+ levels in ^{148}Sm. The data suggest that the B(E2)'s of all the transitions in each nucleus decrease with decreasing neutron number. The B(E2) of one of the ^{148}Sm transitions had previously appeared to be anomalously large, but our results suggest that it is smaller than previously reported and consistent with the general trend.

c. Nuclear Structures of the Odd-N Sm Isotopes ^{145}Sm, ^{149}Sm, ^{151}Sm, ^{153}Sm, and ^{155}Sm

R. K. Smither, D. L. Bushnell, and G. D. Loper*

The (n,γ) reaction has been used to develop the level schemes of the even-Z, odd-N nuclei of ^{145}Sm, ^{149}Sm, ^{151}Sm, ^{153}Sm, and ^{155}Sm. Both thermal-neutron capture and average-resonance neutron capture data have been used. The Argonne gamma-ray diffraction spectrometer was used to investigate the low-energy portions of the spectra, while Ge(Li) and intrinsic-Ge-detector spectrometers were used to study the medium- and high-energy portions of the (n,γ) spectra. The last set of diffraction measurements on the low-energy portion of the ^{154}Sm(n,γ)^{155}Sm spectra were taken with the three diffraction spectrometers located at the high-flux reactor of the Institut Max von Laue-Paul Langevin in Grenoble, France, during a six-week visit in January-February 1976. A conversion-electron spectrum for the ^{154}Sm(n,e$^-$)^{155}Sm reaction was also taken with the high-resolution magnetic spectrometer BILL at the ILL high-flux reactor. The data taking and much of the data analysis is now complete on the ^{150}Sm(n,γ)^{151}Sm, ^{152}Sm(n,γ)^{153}Sm, and ^{154}Sm(n,γ)^{155}Sm reactions. Some medium- and low-energy data are still lacking for the ^{144}Sm(n,γ)^{145}Sm and ^{148}Sm(n,γ)^{149}Sm reactions. The intrinsic-Ge-detector spectrometer located at the Argonne research reactor will be used during next year to complete the medium-energy work. It is hoped that the missing low-energy data can be taken at Grenoble. This work complements the similar studies underway at Grenoble on the even-Z, odd-N, Nd nuclei. It is hoped that enough detailed information on the level schemes and gamma-ray-branching ratios in the Sm and Nd isotopes can be obtained from these experiments to sort out what is happening in this transition region. Based on results of the present work, the Nilsson model does a reasonable job of describing the level scheme of ^{153}Sm and ^{155}Sm. The level scheme of ^{151}Sm is not so well described

*Wichita State University, Wichita, Kansas.

by this model and the level schemes of ^{149}Sm and ^{145}Sm suggest that another approach is needed.

d. Nuclear Structure of ^{112}Cd and ^{114}Cd

R. K. Smither and D. L. Bushnell

Diffraction data were taken on the low-energy portions of the (n, γ) spectra from the ^{111}Cd(n, γ)^{112}Cd and ^{113}Cd(n, γ)^{114}Cd reactions. These reactions had been studied previously with the Argonne diffraction spectrometer, so this work concentrated on obtaining better precision for the intensities of γ transitions that have been placed in the level schemes of ^{112}Cd and ^{114}Cd. (See Fig. 40.) Some time was also spent searching for missing lines and setting upper limits on their intensities if they could not be found. The major objective of this work is to see if corresponding levels in ^{112}Cd and ^{114}Cd γ decayed in the same manner; and, if so, could this decay pattern be reproduced by any of the current nuclear models. In particular, we were interested in comparing the predictions of the "interacting boson model" of Iachello and Arima with our results. Iachello has had some success with this model in the level scheme of ^{110}Cd. A major puzzle in the even-Z, even-N Cd isotopes has been the character of the negative parity states. The present data are consistent with the lowest 3^-, 2^-, and 1^- states

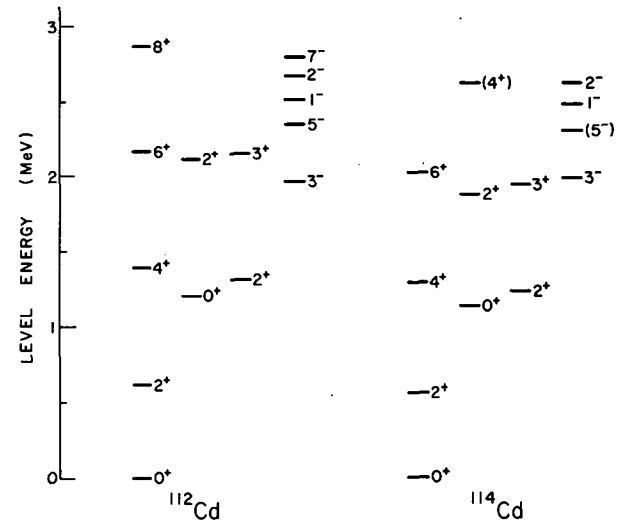

Fig. 40. Partial level scheme of ^{112}Cd and ^{114}Cd showing some of the low-lying levels that can be explained by the "interacting boson" model.

being band heads for three quasibands ($K = 3$, $J_i = 3^-, 5^-, 7^-$, etc.; $K = 2$, $J_i = 2^-, 4^-$, etc.; $K = 1$, $J_i = 1^-, 3^-, 5^-$, etc.). The 7^- and 9^- members of the K=3 band have been identified in ^{110}Cd and ^{112}Cd level schemes with heavy-ion reactions so this picture appears to be correct. The connection between this work in the Cd isotopes and the previously reported work in the Sm and Nd isotopes is that all of these nuclei have the same basic level structure and rather similar γ-decay patterns for the low-lying levels, so it is conceivable that they could all be fit by the same model.

e. Neutron Capture in Isomeric States in Te Isotopes

R. K. Smither, B. Hamermesh, and D. L. Bushnell

The thermal-neutron-capture γ-ray spectra resulting from neutron capture in the $\frac{11}{2}^-$ metastable states in ^{125}Te and ^{127}Te were studied with the Argonne (n, γ) facility using an intrinsic-Ge-detector γ-ray spectrometer. The metastable states were produced by irradiating samples of ^{124}Te and ^{126}Te in the Oak Ridge high-flux reactor. S-wave neutron capture in the $\frac{11}{2}^-$ states can produce a 5^- or 6^- state in the even-Z, even-N ^{126}Te and ^{128}Te isotopes. These states will make E1 transitions to 4^+, 5^+, 6^+, and 7^+ states and M1 transitions to 4^-, 5^-, 6^-, and 7^- states and will therefore give information about the high-spin states in ^{126}Te and ^{128}Te. The experiment must be repeated with the same samples after the isomeric states have decayed. This will be done during this fiscal year. A comparison of these two runs will allow an unambiguous assignment of the appropriate γ rays to neutron capture in these metastable states.

Nuclear Structure of ^{144}Nd and ^{146}Nd

R. K. Smither, D. L. Bushnell, G. Tassotto, S. Ledvina,* and J. Hawkins

A level scheme for ^{146}Nd containing 33 excited states up to 2528 keV has been developed based upon both thermal-neutron-capture and average-resonance neutron-capture-gamma-ray spectroscopy. (See Fig. 41.) In addition, a preliminary level scheme for ^{144}Nd has been prepared based on similar (n,γ) spectra. Isotopically enriched targets of ^{145}Nd and ^{143}Nd were used for the thermal-capture experiments to produce both high-energy (4 to 7 meV) and medium-energy (0.4 to 2.8 mcV) γ-ray spectra. The average-resonance neutron-capture experiments were performed using two different thicknesses of boron absorber (0.32 cm and 0.95 cm) and large (~26 g) natural targets. Comparison of the (n,γ) spectra obtained with thermal-neutron capture is used to assign the γ transitions in the average-resonance-capture data to the appropriate isotopes of Nd. The spin and parity assignments are based on the average-resonance neutron-capture data and the medium-energy (0.4 meV—2.8 meV) thermal-capture data. The analysis of γ spectra recently obtained with resonant capture in a target enriched in ^{145}Nd is in progress. This new work with the enriched sample will greatly simplify the resonance-capture spectrum and make it possible to identify many more of the negative-parity states (fed by M1 transitions) in level schemes. A new medium-energy spectrum with better resolution was also obtained with the new intrinsic-Ge-detector system. The new data have resulted in a greatly improved level scheme that shows much more information about γ transitions between the low-lying levels. The level scheme is being compared with the predictions of the interacting-boson model of Arima and Iachello. Additional average-resonance neutron-capture experiments using an enriched sample of ^{143}Nd are planned. It is hoped that a similar improvement in the level scheme of ^{144}Nd will be obtained.

*Northern Illinois University, DeKalb, Illinois.

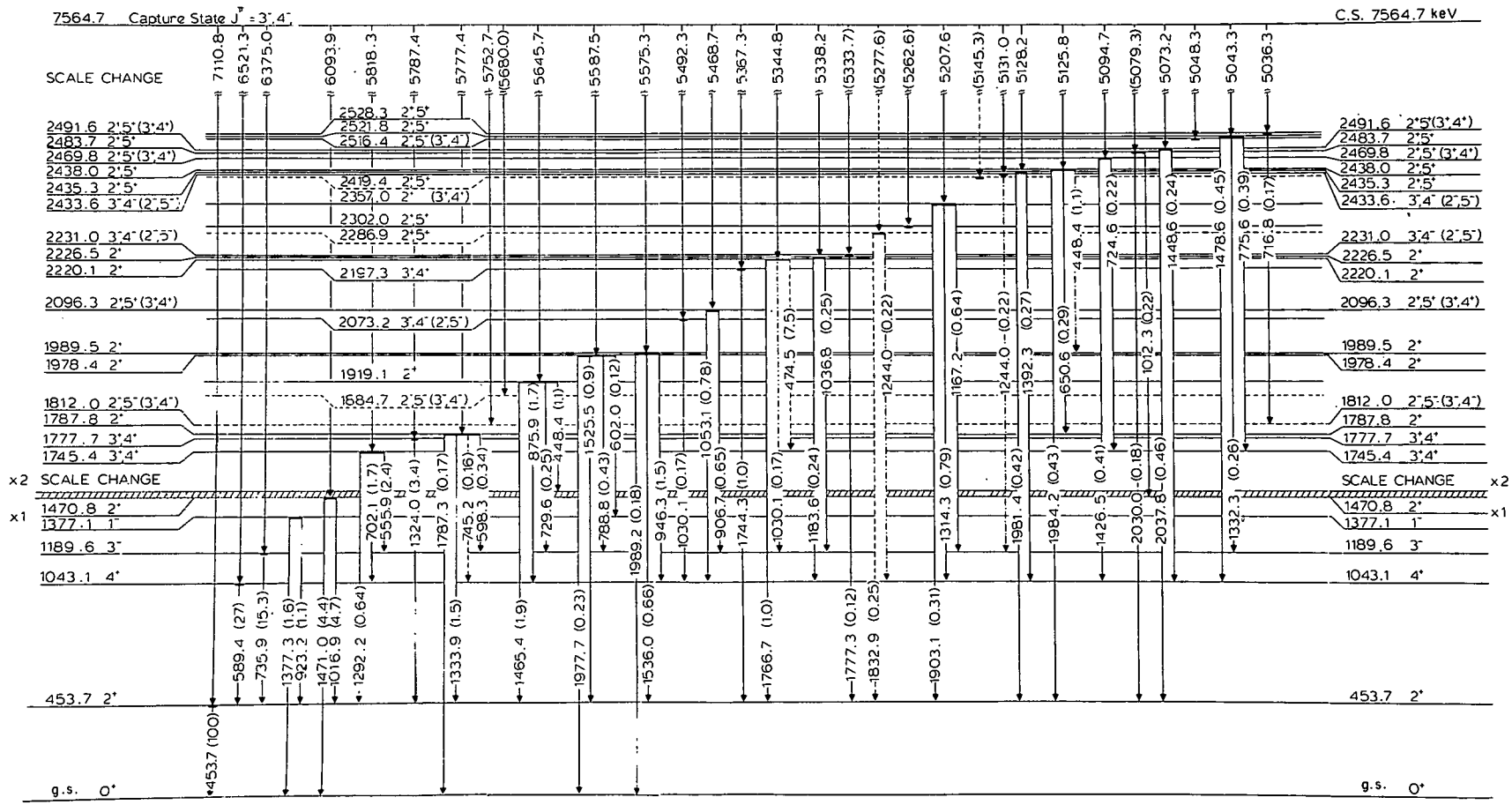

Fig. 41. Partial level scheme for ^{146}Nd based on neutron-capture γ-ray spectroscopy. The first label on the transitions is the gamma-ray energy in keV and the second number in parentheses is the relative gamma-ray intensity. A transition shown with a dot-dash line is located twice in the level scheme. A dashed line depicts a special intensity problem or marginal energy fit. A pair of J^{π} values in parentheses indicate a less favored choice which nevertheless cannot be ruled out. A primary γ-ray energy listed along the top of the diagram in a parenthesis means the energy was not available from thermal capture so the average-capture value is adopted for the diagram. The corresponding thermal-capture transitions will be 0.2—0.5 keV lower in energy. A dashed level implies marginal evidence or its existence.

g. Nuclear Structure of ^{178}Hf

R. K. Smither and D. L. Bushnell

The Argonne 7.7-m bent-crystal γ-ray diffraction spectrometer and the intrinsic-Ge γ-ray spectrometer at the CP-5 research reactor were used to measure the ^{177}Hf(n,γ)^{178}Hf gamma-ray spectrum from 20 keV to 7.6 meV. Both thermal-neutron capture and average-resonance neutron-capture experiments were performed using enriched samples. Two thicknesses of boron were used in the average-resonance neutron-capture experiments (0.16 cm and 0.32 cm). A detailed level scheme up to 2050-keV excitation energy was developed from this data for ^{178}Hf. It contains 44 levels with the parity of 35 of these states being defined uniquely by the average-resonance neutron-capture data. Approximately 150 low-energy γ transitions are placed in the level scheme. The level structure is being analyzed assuming that it consists of a series of overlapping rotational bands based on intrinsic excited states. The relative intensities of the intraband and interband γ transitions are being compared to the Alaga rules to determine the amount of mixing that takes place between the different configurations. This work extends the earlier work of Smither based solely on low-energy spectra taken with the Argonne diffraction spectrometer shortly after it was built. The new level scheme is more complex and has more accurate values for the gamma-ray energies and intensities. The basic question that one is trying to answer is just how far up in the level scheme can one recognize any special character in the individual levels that make it possible to associate them with a particular configuration or with a single value of K for the member of a rotational band.

3. OTHER NEUTRON PHYSICS

a. Search for Collapsed Nuclei

R. J. Holt, L. M. Bollinger, A. M. Friedman,* S. M. Fried,* J. P. Schiffer, J. R. Specht, and G. E. Thomas

In 1972 A. Bodmer in the ANL Nuclear Theory program postulated the existence of "collapsed" nuclei that have properties entirely unlike normal nuclei. One such property is an extremely high binding energy for neutrons. In early 1973, a search for the possible existence of collapsed nuclei in nature was carried out by looking for neutron-capture γ rays with energies much greater than any known neutron-binding energy. Such gamma rays would also be expected if the binding energy were sufficient for pion production. The 1973 measurement was carried out in graphite. The renewed interest in this field was due to the work of Lee and Wick in 1974 which suggested such abnormal nuclei, possibly in heavy elements. Radon is a noble gas with no normal stable isotopes and a sample was obtained which would have contained any abnormal radon nuclides. The sample was placed in the through-hole facility at CP-5. The gamma rays were observed with a spectrometer consisting of an array of NaI detectors which efficiently counted γ rays in the 25—100-MeV region and effectively rejected cosmic-ray background. No effect above background was seen. A very low limit may be set from these results: the amount of abnormal radon (or other heavy noble gas) is less than 10^{-29} of the earth's mass, by weight.

*Chemistry Division, ANL.

b. Neutron Elastic Scattering from ^{12}C and ^{6}Li Below 4 MeV

R. J. Holt, A. B. Smith,* P. A. Guenther,* and J. F. Whalen*

This work is the result of a collaboration between the Physics and Applied Physics Divisions. Studies of neutron scattering from light

*Applied Physics Division, ANL.

uclei are important for fundamental nuclear-structure information, reactor applications, radiological physics and neutron-flux calibration standards. Measurements of the angular distributions of neutrons elastically scattered from ^{12}C were completed below 4 MeV. In addition, an R-matrix analysis of the observations was completed and the results were published.

Almost no measurements of the angular distribution of elastic neutron scattering from ^{6}Li exist in the MeV range. However, previous polarized-neutron scattering studies[1] of ^{6}Li indicate that several resonances in the $^{6}Li+n$ system have anomalously large neutron reduced widths (>1 MeV) in the energy region below 5 MeV. Therefore, we have initiated angular distribution studies of the $^{6}Li(n,n)^{6}Li$ reaction below 4 MeV in order to determine the reaction mechanisms of the postulated resonances. In addition, it is expected that the present measurements will play an important part in the design of the ^{6}Li heating element in proposed fusion-powered reactors.

[1] R. J. Holt, F. W. K. Firk, G. T. Hickey, and R. Nath, Nucl. Phys. A237, 111 (1975).

4. HIGH-ENERGY PHOTON SCATTERING

High-Intensity Monochromatic Photon Source for Photonuclear Studies

R. J. Holt, H. E. Jackson, R. M. Laszewski, and J. R. Specht

In order to study basic photonuclear phenomena such as Delbrück scattering and nuclear Raman scattering in the region of the giant resonance, it is necessary to develop high-energy (10—20 MeV), high-intensity monochromatic sources of photons. Currently, the most widely used sources of monoenergetic photons consist of photons produced in (n, γ) reactions at reactor facilities. Unfortunately, these urces are practical only below 11 MeV.

In a preliminary investigation, we demonstrated the feasibility of using the ZGS preinjector as a proton source in the $^{7}Li(p,\gamma_0)$ reaction in order to generate 17.6-MeV photons. However, in order to achieve a sufficient photon intensity for photonuclear studies, the preinjector must be operated in a mode which produces high proton currents (1—5 mA, dc). Hence, we have developed a technically advanced ^{7}Li target assembly in which the effects of sputtering and beam heating of the target material are minimized. The present target assembly is a modified and updated version of the rotating tritium target at Livermore. The photon intensity that can be achieved with the present target is expected to surpass that of the (n, γ) sources previously employed at the CP-5 reactor through-hole facility. The target is constructed and will be installed at the ZGS facility later this year.

VII. THEORETICAL NUCLEAR PHYSICS

INTRODUCTION

The nuclear-theory program attempts to deal in a comprehensive way with most of the central problems of theoretical nuclear physics. The theoretical research is strongly coordinated with our experimental program in the areas of heavy-ion reactions, nuclear-structure studies, and to some extent in intermediate-energy research. A major resource and a common thread of much of the nuclear-theory program is our investment in the development of advanced computational methods for theoretical physics.

The current highlights and trends are the following.

(1) The heavy-ion-reaction work continues to be emphasized. We have now produced a single-channel DWBA code (PTOLEMY) which calculates angular distributions and parameter searches an order of magnitude faster than previous DWBA codes. The use of PTOLEMY makes feasible detailed analyses of large quantities of heavy-ion scattering and reaction data, analyses which would otherwise have been prohibitively expensive in many cases. PTOLEMY is being thoroughly engineered and documented to make it available to workers in other heavy-ion research laboratories.

(2) Classical "molecular dynamical" calculations for high-energy heavy-ion collisions have been carried to the point where shock-wave phenomena are seen in the results.

(3) The nuclear-structure-theory effort continues to play a major role. Isospin-violating effects and structure effects related to clump transfer in heavy-ion reactions are being emphasized.

(4) The nuclear-matter program is focusing primarily on the open questions about the reliability of calculations based on the Bruckner-Bethe-Goldstone expansion and of those based on the variational method. Also, the effects of including baryon resonances in the calculations have been shown not to provide an escape from the general failure of calculations based on phenomenologically-favored two-body forces to agree with the experimental binding energies and densities of heavy nuclei.

(5) A new project has been started to understand the pion-nucleus optical potential in terms of pion-nucleon scattering information.

(6) Studies of nuclear phenomena and quantum electrodynamical phenomena under exotic conditions that may obtain in heavy-ion collisions are continuing, as are related quark-model studies based on numerical solutions of nonlinear field equations.

(7) The development and maintenance of the Argonne computer language, Speakeasy, is now supported by an external user group.

A. HEAVY-ION REACTION THEORY

The report on heavy-ion reaction theory given last year was based on a view of heavy-ion interactions that had begun to emerge from experiments then recently completed or still in progress at various laboratories in the U. S. A., Europe, and Japan. This view, which has been confirmed by a stream of experimental results in the past year, distinguishes three classes of heavy-ion reactions.

(1) Quasielastic reactions: direct, peripheral and resulting in the transfer of small amounts of energy and matter.

(2) Strongly-damped collisions: also direct, and probably predominantly peripheral resulting in the transfer of hundreds of MeV of energy into internal excitation of the reaction products.

(3) Compound nucleus: collisions leading to complete fusion of the reacting ions.

Recent experiments indicate that as the bombarding energy increases and as the masses of the colliding ions increase, a larger fraction of the total reaction cross section goes into direct-reaction channels. Thus the study of direct reactions between heavy ions encompasses a large fraction of what happens when two large nuclei collide. It is also clear that the boundary between quasielastic and strongly-damped direct reactions is not sharply drawn. Most heavy-ion direct-reaction phenomena are likely to involve the strong coupling of a number of channels.

Theoretical heavy-ion studies at Argonne now center

(1) on detailed comparisons of theory and experiment in situations wherein single-channel DWBA can reasonably be expected to be adequate;

(2) on studies of the optical-model potentials that underlie any description of at least the quasielastic interactions between heavy ions. Such studies include both phenomenological fits to data and microscopic calculations in terms of the force between free nucleons;

(3) on the computational problems associated with the large Coulomb fields and large angular momenta that occur in heavy-ion collisions. Such problems must be thoroughly tamed in the single-channel framework to make possible numerically-reliable multichannel extensions.

The continuing long-term thrust of our efforts is towards a fully quantum-mechanical multichannel approach to heavy-ion direct reactions with the channels corresponding not to individual nuclear states but to energy-averaged nuclear excitations or giant resonances.

a. PTOLEMY: A Computer Program for Heavy-Ion Direct Reactions

D. H. Gloeckner, M. H. Macfarlane, and Steven C. Pieper

The DWBA program PTOLEMY has been extended, improved, and, perhaps more importantly, fully documented (Argonne Report ANL-76-11). It is being used extensively at Argonne to analyze heavy-ion reaction data taken at the tandem Van de Graaff and is in use at Rutgers University and Oak Ridge National Laboratory. During the past year an optical-model parameter-fitting procedure has been built into PTOLEMY; this procedure is an order of magnitude faster than other optical-model search programs available at Argonne (see Sec. VII. Ac below). Extensive work has been done (see Sec. VII. Ab) to permit PTOLEMY to handle the enormous Coulomb fields and angular momenta that are encountered in reactions such as ^{136}Xe on ^{208}Pb at 1.12 GeV (recently studied on the Berkeley HILAC).

b. Functions of Mathematical Physics

M. H. Macfarlane and Steven C. Pieper

Calculations of heavy-ion scattering require the evaluation of functions of mathematical physics (such as Coulomb wave functions, Clebsch-Gordan coefficients, and spherical harmonics) for large values of one or more arguments. The existing computer subroutines for such functions have often been designed for different applications and may not return correct values for such large arguments. During the past few years we have constructed new subroutines or improved existing subroutines with the special needs of heavy-ion scattering in mind. In the past year, we have extended the range of the Argonne Applied Mathematics Division's subroutine for the regular Coulomb function by an order of magnitude in each of its three variables. We demonstrated the reliability of the existing subroutine for the irregular Coulomb function at considerably larger arguments than it was designed for. We are currently working on a revision of the Manchester Coulomb wave function

subroutine that will provide accurate answers for the region inside the turning point. A completely new routine for the evaluation of points and weights for Gauss-Legendre integration was written. This routine is very rapid and accurate over a large range of mesh densities. It has been tested for one to 2000 points. Routines for the evaluation of 3-J, 6-J and 9-J coefficients that had been written in the previous fiscal year were documented and incorporated into the standard Argonne subroutine library. These routines are the fastest we know of and provide reliable values for angular momenta up to several thousand.

c. Optical-Model Search Procedures

D. H. Gloeckner, M. H. Macfarlane, and Steven C. Pieper

Many of the optical-model fitting programs in current use are slow, either because information about first derivatives of χ^2 is acquired by difference methods, or because second-derivative information is introduced inefficiently. The first difficulty can be circumvented by application of first-order perturbation theory to the Schrödinger equation for elastic scattering; we find that first derivatives of χ^2 can be calculated in this fashion more than five times as fast as is possible by difference methods. The second difficulty can be removed by using a linear approximation to the second-derivative matrix in which only the first derivatives of the individual terms in the χ^2 function appear. In extensive tests using standard minimization procedures, it was found that use of the linearized second derivatives is greatly superior to alternative methods (such as variable-metric methods) of introducing second-derivative information. The resulting least-squares minimization procedure has been incorporated into PTOLEMY (see Sec. VII. Aa) and permits, for example, energy-dependent eight-parameter fits to data on the elastic scattering of ^{16}O on ^{208}Pb at five energies from 104 to 216 MeV in running times of less than 1 minute on the BM 370/195. A paper on optical-model fitting methods is being submitted for publication.

d. Elastic Scattering and Single-Nucleon Transfer Induced by ^{16}O Ions on ^{208}Pb

D. H. Gloeckner, D. Kovar, M. H. Macfarlane, and Steven C. Pieper

Elastic scattering of ^{16}O from ^{208}Pb, together with the reactions (^{16}O, ^{15}N) to single-proton states in ^{209}Bi and (^{16}O, ^{17}O) to single-hole states in ^{207}Pb were studied at Berkeley some three years ago at bombarding energies of 104, 140, and 216 MeV. The 216-MeV transfer had not been analyzed because of the prohibitive size of the necessary DWBA calculations. We have undertaken a detailed study in which the optical-model parameters are first determined by simultaneous energy-dependent fits to data at five energies—the Berkeley data at 104, 120, and 216 MeV were augmented by Oak Ridge studies of elastic scattering at 129 and 192 MeV. The resulting potentials, together with the best available spectroscopic factors determined by light-ion transfer experiments, are then used to calculate the (absolute) heavy-ion transfer cross sections. We have completed the study of (^{16}O, ^{15}N) and are currently studying (^{16}O, ^{17}O). The main conclusions of this study are as follows.

(1) Inclusion of data over a wide range of energies with the requirement of sensible energy dependence of the optical-model parameters tends to eliminate the deep potentials ($V \gtrsim 100$ MeV) often encountered in single-energy fits.

(2) All of the optical-model parameter sets that reproduce elastic scattering yield peak DWBA cross sections which increase between 104 and 216 MeV more rapidly than the experimental cross section (by factors of 2 to 4).

(3) The absolute normalization of the DWBA calculation is roughly correct at 216 MeV, but too small by factors of 2 to 4 at the lower energies.

e. Finite-Range DWBA Calculations for $^{13}C(^{3}He, ^{6}He)^{10}C$

G. Delic* and D. Kurath

The three-neutron pickup reaction ($^{3}He, ^{6}He$) offers a test of whether or not the reaction proceeds by direct transfer of a cluster with spatial symmetry [21], the maximum symmetry allowed by the Pauli principle. As the result of a zero-range DWBA analysis of their data, the investigators concluded that such cluster transfer could not account for their results, particularly the ratio of cross sections for transfer to the ground state and first excited state.

We find that a finite-range DWBA calculation differs strongly from the zero-range calculation since the most important contributions come from amplitudes not present in the zero-range treatment. The result is that transfer to the first excited state should be favored over transfer to the ground state, in agreement with observation and in contradiction to the zero-range result. Therefore, it is possible to interpret the reaction mechanism as direct cluster transfer.

*Lawrence Berkeley Laboratory, Berkeley, California.

f. Microscopic Optical Potentials for Heavy-Ion Elastic Scattering

G.-H. Göritz* and U. Mosel

The real part of the optical-model potential for the reactions α-α, ^{16}O-^{16}O, and ^{40}Ca-^{40}Ca has been calculated at several scattering energies. The nuclei are represented by ground-state wave functions of an oscillator shell model localized at a given separation distance. The relative motion of the nuclei is approximated by a plane wave. A variant of Skyrme's density-dependent force is used for the nucleon-nucleon interaction. The two most striking results of this study are the following.

*University of Giessen, Giessen, Germany.

(1) Rather shallow potentials emerge ($V \sim 20$ to 50 MeV).

(2) The real potential depths increase slowly with increasing energy.

This energy dependence is a sensitive matter since it results from a balancing of two competing tendencies; the decrease in the Pauli repulsion with increasing energy counteracts the explicit energy dependence of the two-body interaction (which yields a nucleon-nucleus potential that decreases with energy).

A paper based on this study has been submitted for publication. Section VII. Ah of this report describes a somewhat different way of taking exchange effects in folded potentials into account. It will be of interest to compare the energy dependence predicted by each of the two methods.

g. Momentum-Space Folding Techniques and Heavy-Ion Coulomb Potentials

M. H. Macfarlane and S. C. Pieper

We have formulated the "folding" model for heavy-ion interaction potentials in momentum space and are currently applying the numerical techniques developed in connection with the DWBA approach to π-nucleus reactions. To date only Coulomb interactions have been studied; the main results are as follows.

(1) Fourier-transform methods lead directly to a simple analytic formula for the folded Coulomb potential $V_c(r)$ between two uniform spherical charge distributions. (The expression involves $1/r \times$ [Polynomial in r].)

(2) Folded-Coulomb potentials between diffuse charge distributions fitted to electron-scattering data have been computed. It is found that if the diffuse distributions are replaced by uniform distributions of the same rms radius, the resulting Coulomb potentials agree to within less than 2% at all r and to less than 0.2% in the region probed in heavy-ion peripheral reactions. The folded potential between the

equivalent uniform distributions will be used as the default option for the Coulomb potential in the next version of the computer program PTOLEMY (Sec. VII. Aa).

(3) The Coulomb potential of a point charge interacting with a uniform spherical distribution can approximate the folded potentials to less than 0.5% in the peripheral region but only if somewhat smaller radii ($R_c \sim (A_1^{1/3} + A_2^{1/3}) \times 1.0$ fm) than is common in heavy-ion optical-model studies are used.

h. Importance of the NN Force and of the Exchange Potential for Elastic Scattering of Alpha Particles

Y. Eisen and B. Day

The microscopic description of the real part of the optical potential between composite systems is of great interest because it provides insight into the matter distributions of the colliding nuclei and into the nucleon-nucleon (NN) force. Several attempts have been made in the past to calculate the real part of the optical potential by folding an effective NN interaction with the density distributions of the colliding nuclei. However, the strength of the optical potential near the interaction radius has typically been overestimated by as much as a factor of 2.

The present study includes the exchange as well as the direct part of the alpha-nucleus potential. The exchange term comes from antisymmetrization with respect to the two interacting nucleons, one from the alpha particle and the other from the target nucleus. Both parts of the alpha-nucleus potential are generated from a density-dependent effective interaction acting in both even and odd states. This effective interaction is calculated using nuclear-matter theory from the Reid potential and from modifications of it that preserve the quality of fits to the NN phase shifts. The resulting optical potential is tested by analysis of elastic scattering of alpha particles from ^{90}Zr and ^{208}Pb at w energies (10—24 MeV).

The results of this work are: (a) Near the interaction radius, the exchange contribution to the optical potential is 20—25% of the direct term and cannot be neglected. (b) The optical potential generated microscopically from a realistic NN force gives an excellent fit to low-energy elastic alpha scattering. (c) Elastic scattering is sensitive to that part of the NN force that does not contain the one-pion-exchange potential. The P-wave potentials that fit the data have shorter ranges than the P-wave parts of the Reid potential.

It is planned to extend the calculations to higher energies, which will probe the alpha-nucleus interaction at shorter distances. One paper has been published on this work, and a second has been submitted for publication.

B. DENSE NUCLEAR MATTER AND HIGH-ENERGY COLLISIONS OF HEAVY IONS

The present investigations arose from our interests in "collapsed" nuclei, i.e., conceivable superstable nuclei, whose phenomenological implications we considered several years ago. More recently there has been much interest in collapsed nuclear states as a result of a dynamical scheme proposed by T. D. Lee and G. C. Wick which involves nonlinear meson interactions and which could lead to "abnormal" nuclear matter and nuclei whose phenomenology has much in common with that of collapsed nuclei.

On the one hand there are questions concerning the possible properties of nuclear matter under unusual conditions. Our approach has been to consider relativistic Hartree calculations and an associated phenomenology.

On the other hand, there are questions related to the possibility of producing dense states of nuclear matter in general. The only apparent possible means of production seems to be in the high-energy collision of heavy nuclei (greater than about a lab. energy of 100 MeV/nucleon) which may lead to shock-wave type phenomena and associated dense and hot nuclear matter.

a. Relativistic Hartree Calculations of Nuclear Properties

A. R. Bodmer and John Boguta

We have studied the surface properties of nuclear matter in the relativistic Hartree approximation. The original motivation was to study the surface properties of Lee-Wick abnormal nuclear matter as these are of crucial importance for the stability of finite abnormal nuclei. However, it became clear that it was necessary first to consider ordinary nuclear matter, in particular its surface properties. We have studied these properties for equal numbers of neutrons and protons, i.e., $N = Z$, and for semi-infinite nuclear matter, i.e., for an infinite slab of nuclear matter with a free surface. Our results so far are mainly for the Walecka model where the nucleons, described by the Dirac

ation, are coupled to scalar and vector-meson fields without self-interactions.

The Hartree problem for the semi-infinite case is solved self-consistently. We have also studied the Thomas-Fermi (TF) approximation which is itself an approximation to the Hartree approximation. The two agree well for not-too-small surface thicknesses. Variation of either the vector-meson mass m_V or the scalar-meson mass m_S leads to approximately the same relation between the surface energy E_s and thickness t. For the empirical value of t, the corresponding E_s is somewhat too large. This is most probably because the Walecka model gives too-incompressible nuclear matter—possibly because of neglect of correlations. For accepted values of m_V, we obtain reasonable values of m_S of around 500 MeV.

b. Classical, Molecular-Dynamics, Approach to High-Energy Collisions of Nuclei

A. R. Bodmer and C. N. Panos

We have made classical Newtonian calculations of high-energy collisions of heavy ions using the approach of molecular dynamics. This work was motivated by classical hydrodynamic considerations which imply shock-wave phenomena leading to very hot transitory regions of very high density. However, hydrodynamics assumes that the relevant mean free path is short compared to the nuclear dimensions and that thermal equilibrium is attained during the collision; both these requirements may not be realized. The Newtonian approach, which calculates the classical trajectories of all the nucleons assuming some two-body force, makes no such assumptions and thus supplements as well as tests the hydrodynamic approach. The validity of classical mechanics (assumed by both approaches) may not be too unreasonable at the relevant energies.

Extensive calculations have been made at laboratory energies of 120 MeV and 300 MeV/nucleon for collisions between two nuclei with A = 50 and rather less completely between nuclei with A = 50 and 200 and A = 200 and 200. Averages are taken over a number of ini

listributions of positions and velocities in each nucleus. The trajectories provided by the dynamical calculations are analyzed to give hydrodynamic-type averages such as densities, collective velocities, and internal energies, as a function of position and time. The nucleon-nucleon potential used is a sum of attractive and repulsive Yukawa potentials based on the Reid potential. The parameters are adjusted to give reasonable binding energies and to reproduce the essential features of the scattering by a classical two-body calculation. These features are taken to be the cross section appropriate for the viscosity and therefore for shock phenomena. This cross section emphasizes the transverse momentum transfer much more strongly than does the total cross section. For moderate impact parameters less than about a nuclear radius (central-type collisions), there are pronounced shock-wave phenomena. Thus after the nuclei have penetrated a distance of about a nucleon mean free path, there is rapid randomization of the initial translational energy associated with large compressions and internal energies; this is followed by an adiabatic-like expansion. For larger impact parameters (peripheral-type collisions), shock phenomena are much less pronounced and the two nuclei go past each other with much less change. Since in the overall angular distribution large impact parameters are heavily weighted, this leads to a large forward/backward peaking in the C.M. system. In general it is clear that mean-free path, i.e., viscous effects, play a very important role in modifying shock-wave phenomena.

C. NUCLEAR STRUCTURE THEORY

The properties of nuclei near closed shells have been studied utilizing the Argonne shell-model programs, and vibrational nuclei were treated with a model of interacting bosons. These efforts, described in the following paragraphs, had a threefold purpose.

(1) To correlate existing data, determine the nature of the effective nuclear interaction, and suggest experiments which would assess the validity of the models employed. Typical of this aspect of the research are the calculations with the model of interacting bosons used to interpret the data in the Cd isotopes, the continued exploration of the 1p shell, and the shell-model calculations for nuclei near A = 90.

(2) A number of experiments in recent years have been concerned with violation of accepted isospin properties which would be manifest in electromagnetic transitions. Examples are isospin dependence in the residual nuclear interaction resulting in asymmetry in mirror gamma decays, or the occurrence of an isotensor component in the electromagnetic interaction resulting in $\Delta T=2$ transitions. Since these are generally small effects, careful nuclear structure analysis is needed to see whether the observations can be attributed to more conventional sources. Such analysis is typified by the treatment of the E1 decays in ^{13}C and ^{13}N and the interpretation of the $\Delta T=2$ transition in ^{44}Ti.

(3) Nuclei with well-understood nuclear structure are useful for testing reaction mechanisms with light or heavy ions. Examples of this are the triton-like (p,α) reaction and the (^{6}Li,^{8}B) reaction for 1p-shell targets as well as the still-to-be-exploited well-determined structure of the low-lying states of ^{18}O.

a. Interacting Boson Model of Vibrational Nuclei

A. Arima* and F. Iachello

A description of vibrational nuclei is given in terms of a model of interacting bosons. The Hamiltonian is similar to a shell model with bosons, and the resultant group-theoretical classification leads to explicit analytic expressions for the energy spectra and transition probabilities. A detailed description for ^{110}Cd is given in terms of

*University of Tokyo, Tokyo, Japan.

uadrupole bosons in excellent agreement with observation. Symmetry-breaking terms are calculated by perturbation theory and enable one to account for the observed weak magnetic transitions as well.

b. Spectrum of ^{13}B

D. Kurath

Aside from the $\frac{3}{2}^-$ ground state whose properties are well described by a $(1p)^9$ configuration, little is understood about the spectrum of ^{13}B. Excited states of both parities, as determined by the ^{11}B(t,p)^{13}B reaction, are found starting at 3.5 MeV. Some limits on gamma-decay lifetimes are known, and some information from ^{14}C(d, ^{3}He) experiments is available. A study has been made for levels of both parities, allowing promotion of two neutrons to $(2s_{1/2}, 1d_{5/2})$ levels, or a single nucleon to the (2s,1d) region. The particle-hole interaction was that determined in an earlier study of ^{14}B. Calculated levels of both parities are found in the low excitation-energy region, including normal parity levels from the $(1p)^7(2s_{1/2}, d_{5/2})^2$ configuration. This should help in the identification of the excited states and offer a good test of the particle-hole interaction.

c. Allowed Beta Decay of the N=49 Isotones

D. H. Gloeckner,* R. D. Lawson, and F. J. D. Serduke

We have shown that the properties of the low-lying states of the N=49 isotones ^{88}Y, ^{89}Zr, ^{90}Nb, ^{91}Mo, ^{92}Tc, and ^{93}Ru can be understood when one assumes $^{88}_{38}Sr_{50}$ is an inert core and the valence nucleons occupy the $2p_{1/2}$ and $1g_{9/2}$ single-particle levels. As a further test of this model the beta decay of these nuclei to the N=50 isotones has been examined. Decays between yrast positive-parity states exhibit large variations in their transition rates—for example, the ^{93}Ru$(\frac{9}{2}^+) \rightarrow {}^{93}Tc(\frac{9}{2}^+)$ decay is about 100 times faster than the ^{91}Mo$(\frac{9}{2}^+) \rightarrow {}^{91}Nb(\frac{7}{2}^+)$ transition. This large variation can be understood

*Rutgers University, New Brunswick, New Jersey.

within the $2p_{1/2}, 1g_{9/2}$ model space and moreover the absolute values of the decay rates can be well reproduced if one uses a state-independent Gamow-Teller $g_{9/2}$ beta-decay matrix element that is about half the single-particle value. In addition it is shown that $g_{9/2}$ and $p_{1/2}$ nucleons contribute about equally to $\frac{1}{2}^- \rightarrow \frac{1}{2}^-$ decays and because these contributions interfere destructively, the model provides a simple explanation for the strongly inhibited $^{89}Zr(\frac{1}{2}^-) \rightarrow {}^{89}Y(\frac{1}{2}^-)$ transition. This work has been accepted for publication in Nuclear Physics.

d. Shell-Model Study of N=48 Nuclei

D. H. Gloeckner* and F. J. D. Serduke

Nuclear properties of the N=48 isotones with $Z > 38$ have been calculated using the shell-model effective interactions determined from the N=49 and N=50 isotone studies described earlier. There is excellent agreement with the experimental spectra for the known low-lying states of ^{87}Y, ^{88}Zr, ^{89}Nb, and ^{90}Mo. Of particular interest are states in ^{88}Zr that will soon be investigated at the ANL FN tandem with the $^{86}Sr(^{16}O, ^{14}C)^{88}Zr$ reaction. Our model predicts unambiguously that a two-proton transfer reaction should strongly populate the second state of a given spin in this nucleus. This is in contrast to two-neutron pickup on ^{90}Zr which should preferentially excite the first state of a given spin. Our shell model of the neutron-deficient nuclei in the mass-90 region also should prove useful in interpreting the data for other nuclei in forthcoming heavy-ion studies. The results of these calculations have been submitted to Nuclear Physics.

*Rutgers University, New Brunswick, New Jersey.

e. E4 Gamma Decays

R. D. Lawson and A. Müller-Arnke*

Three E4 gamma transitions have been identified in the $f_{7/2}$ nuclei. The one at the beginning of the shell, the $6^+ \rightarrow 2^+$ decay in ^{44}Sc, is enhanced by a factor of about 50% over the Weisskopf estimate. On the other hand, the two observed at the end of the shell are hindered—the $2^+ \rightarrow 6^+$ decay in ^{52}Mn is inhibited by a factor of 6 compared to the Weisskopf estimate and the $\frac{19}{2}^- \rightarrow \frac{11}{2}^-$ is slowed down by a factor of 4. If one assumes that the major part of the residual nucleon-nucleon interaction can be taken into account by allowing nucleons to move in a single-particle potential with quadrupole deformation, one can show that admixtures into the $(f_{7/2})^n$ wave function corresponding to one nucleon in the $f_{5/2}$, $p_{3/2}$ or $p_{1/2}$ orbits interfere constructively at the beginning of the shell and destructively at the end. To find the expected magnitude of these interference effects we have carried out a shell-model calculation that included all states within the model space $(f_{7/2})^n$ and $((f_{7/2})^{n-1}j)$, where j denotes either a neutron or a proton in the $f_{5/2}$, $p_{3/2}$ or $p_{1/2}$ orbit. The interference effects have the expected sign. Several interactions have been considered and in all cases, if the $f_{5/2}$-$f_{7/2}$, $p_{3/2}$-$f_{7/2}$ and $p_{1/2}$-$f_{7/2}$ single-particle energy splittings are chosen to agree with those observed in the Ni nuclei, the calculated interference is not large enough to fit the experimental data. Thus even when this extended model space is used, one must introduce an additional polarization charge. If one chooses this to be isoscalar ($e_\pi = e(1 + \delta)$ and $e_\nu = e\delta$), one must take $\delta = +0.42$ for ^{44}Sc, whereas $\delta = -0.32$ for ^{52}Mn and $\delta = -0.18$ for ^{53}Fe.

*Technische Hochschule, Darmstadt, West Germany.

f. Asymmetry of Mirror E1 Transitions in ^{13}C, ^{13}N

D. Kurath

Measurements of analogous E1 transitions in the mirror nuclei ^{13}C and ^{13}N exhibit large differences for those cases involving the

$\frac{1}{2}^+$ first excited state. While this might be a manifestation of a charge-dependent nuclear interaction, a more likely source is a nuclear effect based on the difference in binding energy with respect to nucleon emission. It is not, however, simply due to a different radial matrix element in the E1-transition calculation. The E1-transition probability is strongly affected by the extent to which the odd nucleon in the $\frac{1}{2}^+$ state is coupled to the deformed ^{12}C core. In ^{13}N the nearly unbound proton is physically farther from the ^{12}C core and thus more weakly coupled to the deformation through nuclear forces, resulting in a much smaller inhibition of the E1 transition probability than is true for ^{13}C. The observed difference is likely due to this sensitive nuclear effect, and not to violation of charge independence in the nuclear interaction itself. This explanation was reported in a comment [Phys. Rev. Lett. 35, 1546 (1975)].

g. ΔT=2 Gamma-Ray Transitions

W. R. Dixon,* R. S. Storey,* J. J. Simpson,† and R. D. Lawson

ΔT=2 nuclear gamma decay is forbidden if isospin is a good quantum number and if there is no isotensor component in the electromagnetic interaction. In order to test this selection rule the decay of the 9.338-MeV T=2, $I=0^+$ state in ^{44}Ti was studied. It was found that the level decays predominantly to the 7.216-MeV T=1, $I=1^+$ state and that the upper limit for branching to the T=0, $I=2^+$ level at 1.083 MeV was 0.16%. When this result is combined with the measured value of $\Gamma_a \Gamma_\gamma/\Gamma$, one finds, on the assumption that $\Gamma_a >> \Gamma_\gamma$, B(E2; 0^+ T = 2 → 2^+ T = 0) is less than 1.4×10^{-3} Weisskopf units (W.u.). To see whether this is consistent with the expected isospin mixing brought about by Coulomb effects, a shell-model calculation was carried out using the $f_{7/2}$ model space. Instead of explicitly calculating the Coulomb matrix elements,

*National Research Council of Canada, Ottawa, Ontario, Canada.

†University of Guelph, Guelph, Ontario, Canada.

he proton-proton interaction energies were taken from the spectrum of ^{42}Ti, the neutron-proton and the neutron-neutron interaction from the energies of the T=1 states in ^{42}Sc. With these matrix elements B(E2; 9.338 MeV → 1.038 MeV) = 1.16×10^{-3} W.u., in agreement with the experimental limit. Thus this experiment provides no evidence for an isotensor part of the electromagnetic interaction. Moreover, since the calculated value of B(E2) is extremely sensitive to the input two-particle matrix elements and to the assumed model space, a more exact measurement is not likely to shed light on the possible existence of an isotensor operator. This work has been accepted for publication in Physical Review.

h. 1p Shell

D. Kurath

The 1p shell is one of the few regions of the periodic table for which there is an accurate and detailed shell-model description. It remains a region of active interest as evidenced by requests from more than a dozen universities and national laboratories during the past year for information relevant to particular experiments or theoretical treatments of reaction processes. The latter category includes inelastic electron scattering, pion charge-exchange reactions and multistep processes in heavy-ion transfer reactions. Various matrix elements were also provided for a careful study of isospin mixing of the 1^+ states in ^{12}C which is related to the isospin purity of nuclear forces.

Particular experiments relative to the model include measurements of static moments of the beta-unstable nuclei ^{8}Li and ^{9}Li. An interesting study of two-proton pickup via (^{6}Li, ^{8}B) on 1p-shell targets was carried out at the Lawrence Berkeley Laboratory. It was found that transfer in a spatially symmetric state is much the dominant mode, even though calculated values would allow a spatially-asymmetric state.[1]

[1] R. B. Weisenmiller et al., Phys. Rev. C 13, 1330 (1976).

TABLE V. The $^{14}N(p,\alpha)^{11}C$ reaction at E_p = 43.7 MeV. The integrated cross section and probable J of transfer are from C. C. Maples, LBL-253, University of California Thesis (1971), unpublished. The calculated summed spectroscopic strength and dominant J are from D. Kurath and D. J. Millener, Nucl. Phys. A238, 269 (1975). The last column lists the strength normalized to the ground-state cross section.

		Exp.		Calc.		Norm.
E	I	$\sigma(12^\circ$ to $90^\circ)$ μb	(J)	SUMSQ	(Dominant J)	SUMSQ
0	$\frac{3}{2}$	580 ± 29	$(\frac{5}{2})$	1.88	(89% $\frac{5}{2}$)	580[N]
2.00	$\frac{1}{2}$	303 ± 21	$(\frac{1}{2})$	0.82	(99% $\frac{1}{2}$)	253
4.32	$\frac{5}{2}$	545 ± 28	$(\frac{5}{2} + \frac{3}{2})$	1.37	(53% $\frac{5}{2}$)	423
4.80	$\frac{3}{2}$*	358 ± 23	$(\frac{5}{2} + \frac{3}{2})$	0.85	(62% $\frac{3}{2}$)	263
6.48	$\frac{7}{2}$	467 ± 24	$(\frac{7}{2} + \frac{5}{2})$	1.66	(93% $\frac{7}{2}$)	513
8.42	$\frac{5}{2}$*	929 ± 35	$(\frac{5}{2})$	3.52	(83% $\frac{7}{2}$)	1088
12.58	$\frac{7}{2}$*	764 ± 35	$(\frac{7}{2} + \frac{5}{2})$	2.79	(92% $\frac{7}{2}$)	862

Calculated structure amplitudes for triton-like transfer in the 1p shell were reported last year. Since then experimental evidence for $(1p)^3$ pickup was found which agrees remarkably well with our calculations. An example is given in Table V. The comparison was reported at the Conference on Clustering Phenomena in Nuclei, College Park, Maryland.[2]

[2] D. Kurath, ORO-4856-26, 439-449 (1975).

i. Structure of ^{18}O

R. D. Lawson, F. J. D. Serduke, and H. T. Fortune*

The structure of the lowest three 0^+, the lowest three 2^+, and the lowest two 4^+ states is described using the $1d_{5/2}, 2s_{1/2}$ model space plus one intruder (core excited) state of each spin. Linear

* University of Pennsylvania, Philadelphia, Pennsylvania.

combinations of these basis states can be found that reproduce quite accurately all the existing one- and two-nucleon transfer data and the static and dynamic electromagnetic properties. Only for a few isolated quantities is the $d_{3/2}$ configuration important and even in these instances its contribution can be treated in perturbation theory. It is then possible to invert the problem and construct the Hamiltonian matrix that yields the fitted wave functions and the experimentally observed energies of these positive-parity states in ^{18}O. Consequently one now has an example of a model-space Hamiltonian that reproduces not only the energies of the system but also the dynamic properties. Further, since ^{18}O is a projectile that is often used, a detailed knowledge of its low-lying state structure will help to assess the validity of assumed reaction mechanisms in heavy-ion physics. This work has been submitted to Physical Review.

D. NUCLEAR MATTER AND NUCLEAR FORCES

The formulation of any complete physical theory involves three interrelated steps: (1) identification of the relevant degrees of freedom, (2) determination of the dynamical equations (equations of motion), and (3) methods of solution (approximations). Steps (1) and (2) provide the foundation of the theory. In nuclear theory steps (1) and (2) involve the explicit assumption that nuclei consist of nucleons governed by a many-body Schrödinger equation. Other degrees of freedom are buried in the Hamiltonian or they may be superimposed ad hoc when needed explicitly. In this context the fundamental problem of nuclear theory is the determination of the Hamiltonian.

The nucleon-nucleon potential must, of course, reproduce the empirical scattering phase shifts. The only firm theoretical constraint is that the one-pion-exchange potential should dominate at large distances. These requirements do not, by any means, determine the potential. The properties of the ground state of homogeneous nuclear matter depend sensitively on features of the interaction that do not affect nucleon-nucleon scattering. This fact has been the primary motivation for our work on nuclear-matter theory.

It is therefore essential to have a mathematically precise formulation of the general theory (Coester 1968). It encompasses the widely-used Brueckner-Bethe-Goldstone (BBG) theory as a special approximation scheme. The following major questions must be answered. (1) Is the BBG approximation scheme valid? (2) If it is valid, can the higher-order correction terms produce the empirical values or are many-body forces required? (3) If it is not valid, what is a valid approximation scheme for the general equations?

It would be essential to investigate these questions in any case in order to rule out spurious agreement of the wrong potentials with the empirical data. Fortunately the theoretical problem was not obscured by such a spurious agreement. We found (1970) that in the lowest-order BBG approximation the calculated saturation points for all phase-shift-equivalent potentials lie on a narrow band in the energy-density plane. This band, which we call the saturation band, does not include the empirical saturation point. We have explored the possibility that inclusion of $\Delta(1236)$ components in the nuclear wave functions might permit an escape from this saturation band. The result was negative. An earlier study showed that a proper treatment of relativistic kinematics does not help either.

The validity of any approximation scheme depends on the properties of the potential and on the density. The BBG scheme is

manifestly invalid for purely repulsive potentials at any density. There are plausibility arguments for its validity for potentials like the Reid $^1S_0$ potential. For the full Reid potential including the tensor force, the BBG approximation could only be justified by the experience that approximations are often better than we have a right to expect.

An accurate calculation of the first correction in the BBG scheme (the 3-body correlation term) should give a more definite indication of its validity. For realistic potentials only one reasonably complete calculation exists (Dahlblom), and it gives a small result. But the calculation involves approximations that are not necessarily reliable and does not include the full effect of the tensor force. For S-wave potentials we found qualitatively similar results by more accurate calculations. In that case the 3-body correlation energy does not move the saturation point out of the band.

Comparison of the general equations for bosons and fermions shows that the boson equations are simpler and the 3-body correlation effects can be obtained much more rapidly. If the BBG approximation is valid for bosons, it is plausible that it is also valid for fermions. On the other hand, it is quite possible that it fails for bosons but succeeds for fermions.

The validity of the BBG approximation has been challenged recently by variational calculations with Jastrow wave functions (Clark, Pandharipande, and Bethe). These calculations predict more binding, and saturation at much higher density, than the lowest-order BBG calculations. However, the evaluation of the expectation value of the Hamiltonian for variational wave functions involves approximations that have not been fully tested. It is advantageous to investigate this discrepancy for Bose gases. The variational calculations with Jastrow wave functions are more reliable in that case. We find that, for a Bose gas interacting through the Reid $^1S_0$ potential, the first two terms in the BBG expansion for the energy indicate satisfactory convergence and agreement with a variational calculation. However, signs of lack of convergence show up in the next order and in the two-body wave functions.

a. Variational and Lowest-Order Brueckner-Bethe-Goldstone Calculations for Simple Systems

B. Day, V. R. Pandharipande,* and R. W. Wiringa*

The discrepancy between lowest-order Brueckner-Bethe-Goldstone (BBG) and variational calculations of nuclear matter shows

* University of Illinois, Urbana, Illinois.

that a critical study of both approaches is needed. It is sensible to start with the simpler case of a Bose gas. Therefore, the binding energy of the Bose gas was calculated over a range of densities for two different central potentials. The radial shapes of these two potentials were the same as those of the Reid $^1S_0$ potential and the central part of the Reid $^3S_1$ potential, respectively. But, for the Bose gas, each potential was assumed to act in all partial waves, not just in S waves. For each potential, one set of calculations used the lowest-order BBG approximation. The other used the variational method, with the hypernetted chain (HNC) approximation for the evaluation of the expectation value of the Hamiltonian.

For the Reid $^1S_0$ potential, the HNC calculation gave substantially more binding than lowest-order BBG over a wide range of density. In the Reid $^3S_1$ case, the two calculations were in fairly good agreement at densities low enough that the BBG scheme could be expected to work. Thus a large discrepancy between the HNC and lowest-order BBG results can occur for a Bose gas. However, the Reid $^3S_1$ result shows that the discrepancy is potential dependent.

The situation was partially understood by a theoretical argument. This argument shows that, if the 2-body potential is changed by adding a weak, long-ranged part, then the additional binding energy that results is underestimated in the lowest-order BBG approximation. However, inclusion of the next (3-body) BBG term repairs the error.

The two main conclusions of this work are: (1) The large difference between lowest-order BBG and variational results can occur for the simple case of a Bose gas. Hence it can be studied without the complication of tensor forces and Fermi statistics. (2) There are theoretical indications that the BBG result cannot be trusted unless the 3-body term is included. A paper describing this work has been published.

b. Three-Body Correlations in the Bose Gas

B. Day and F. Coester

Because of the large discrepancy between variational and BBG calculations for nuclear matter, both approaches should be critically examined. For the variational calculations, the question is whether the approximations used to evaluate the expectation value of the Hamiltonian are adequate. In the BBG scheme, we must investigate the 3-body and higher-order terms. As a first step it may be helpful to study these questions for the simpler case of a Bose gas. The general equations are simpler for bosons than for fermions. Thus numerical results and theoretical understanding can be obtained more quickly for bosons. Also, the Bose gas is expected to provide a stringent test for the BBG expansion; if it works for bosons, it will almost certainly work for fermions with central forces (tensor forces are another matter, however).

We have therefore extended the boson calculations described in the previous subsection by making accurate calculations of the 3-body term in the BBG scheme. For the Reid $^1S_0$ potential, the large difference between the variational and lowest-order BBG results is almost completely eliminated by inclusion of the 3-body BBG term. In the Reid $^3S_1$ case, the already-good agreement between the variational and lowest-order BBG results is made even better by the 3-body term. We conclude that, at least for the simple case of a Bose gas, the first two terms of the BBG expansion agree well with a variational calculation.

For the Reid $^1S_0$ potential, we have calculated some of the 4-body BBG terms, as well as the 3-body contribution to the 2-body wave function. Here, signs of nonconvergence show up. Further work on this problem is in progress.

c. Perturbation Corrections to Variational Calculations of Nuclear Matte

J. W. Clark, P. M. Lam,* and W. J. Ter Louw*

The discrepancy between lowest-order BBG and variational calculations for nuclear matter raises the following questions. (1) Will inclusion of the 3-body term in the BBG scheme repair the discrepancy? (2) Is the evaluation of the energy expectation value with variational wave functions sufficiently accurate? If (2) is answered affirmatively, so that the variational energies are true upper bounds, the following question becomes of great interest: How far below the variational result is the true ground-state energy? This question can be answered by taking the variational wave function as the unperturbed ground state and evaluating perturbation corrections to the energy. The additional binding energy obtained is a measure of how far the exact ground-state energy lies below the variational result.

We have done the perturbation calculation for two realistic central potentials, for which we had previously made variational calculations. The perturbation corrections gave additional binding energy of 3—5 MeV.

The implications of this result depend on the assumption that the expectation value of the Hamiltonian has been accurately calculated for the variational wave function. Assuming this to be true, we conclude that the exact ground-state energy is about 3—5 MeV below the variational result. Under the same assumption, we can also draw the following conclusion about the BBG calculation, for which the lowest-order energy is about 10 MeV above the variational result for the present 2-body potentials: If the BBG expansion is correct, then its 3-body and higher terms must not only make up the difference of 10 MeV between the lowest-order BBG and variational results, but must give 3—5 MeV of additional binding. A calculation of the 3-body BBG term for these potentials would therefore be of great interest. A paper describing this work has been published in Nucl. Phys. A255, 1 (1975).

*Washington University, St. Louis, Missouri.

1. Isobar Configurations in Nuclear Matter

B. Day and F. Coester

Conventional nuclear-matter calculations assume that the two-body potentials can satisfactorily reproduce all important effects of the suppressed meson degrees of freedom. Explicit inclusion of some important meson degrees of freedom into the nuclear-matter wave function provides a partial check of the validity of this assumption. We have treated the $\Delta(1236)$ pion-nucleon resonance as an excited state of the nucleon in order to see whether the saturation properties of nuclear matter are changed significantly. In this model the two-body potential has components that change a nucleon-nucleon (NN) pair into a nucleon-Δ (NΔ) pair. The couplings $^1S_0$ (NN) $\rightleftarrows$ $^5D_0$ (NΔ) and $^3P_1$ (NN) $\rightleftarrows$ $^5P_1$ (NΔ) were studied in detail. In each case a coupled-channel potential was found that gives an excellent fit to the nucleon-nucleon phase shifts. In all other partial waves we assumed the Reid or Ueda-Green potentials with no coupling to the Δ state.

The effective interaction in nuclear matter in this model is weaker than the effective interaction for two free nucleons for two reasons: (1) in nuclear matter the energy denominators are larger than in scattering (dispersion effect), and (2) the exclusion principle forbids NΔ states in which the nucleon momentum is below the Fermi level (Pauli effect).

The NΔ coupling was found to cause substantial shifts of 5—10 MeV in the saturation points. But the calculated saturation points remained on the saturation band. The question arises of whether this behavior would be different for a different choice of 2-body interaction. The NN potential and the coupling potential to the NΔ state are determined by one-pion exchange at large distances, but both could be varied at short distances. We investigated this by deriving approximate analytic formulas for the Pauli and dispersion effects. Using these formulas, we found that, although the size of the energy shift depends on the

short-range behavior of the potential, its density dependence does not. Hence no reasonable model of NΔ coupling will permit an escape from the saturation band.

Thus the main conclusions from this work are as follows. First, inclusion of NΔ coupling has a big effect on the equilibrium energy and density of nuclear matter that depends sensitively on the short-distance behavior of the 2-body interaction. Second, the NΔ coupling does not permit an escape from the saturation band, regardless of the short-range behavior of the potential. Hence the effects of NΔ coupling are no different from those obtainable by using different phase-shift-equivalent NN potentials without NΔ coupling. A paper describing this work has been accepted for publication.

E. PION PHYSICS

a. Pion-Nucleon Interaction, Pion-Nucleus Potential

As a probe of nuclear structure, the pion is qualitatively different from other projectiles. Thus, the study of π-nucleus interactions can yield distinctively new information about the structure of nuclei. This promise and the expected rich π-nucleus reaction data motivate us to seek a theoretical method to describe the π-nucleus interactions in the energy region $E_\pi \leq 300$ MeV. In our approach, we emphasize the requirement that the theoretical model must provide a practical and accurate means of extracting nuclear-structure information from the data.

Within present computational limits, the most reliable method to study π-nucleus reactions such as $A(\pi^+,\pi^-)B$ and $A(p,\pi^\pm)B$ is probably the distorted-wave method. This method is based on a π-nucleus optical potential. Despite extensive study, the current π-nucleus optical potentials constructed from the π-nucleon t matrix fail to describe recent π-^{4}He and π-^{12}C elastic scattering data in the energy region $E_\pi \leq 80$ MeV. To clarify the experimental situation and as a first step toward placing the distorted-wave method on a firmer footing, we have focused attention on the derivation of the π-nucleus optical potential. This is done within the framework of multiple-scattering theory, with a correct treatment of the basic π-nucleon interaction and of the relativistic π-nucleon relative motion inside the nuclei.

Because of the nature of the basic π-nucleon interaction, the π-nucleus interaction potentials are intrinsically nonlocal. Phase-shift equivalent local potentials can be constructed from the nonlocal π-nucleus optical potentials. But the resulting local potentials are not expected to be reliable for the study of the large momentum-transfer

reactions such as $A(p,\pi^+)B$. In order to extract correct nuclear-structure information from the forthcoming data, it is necessary to include nonlocal effects exactly in the distorted-wave method. A momentum-space distorted-wave program developed by T.-S. H. Lee and F. Tabakin can serve this purpose. However, their program is still not very efficient. We will improve this program by incorporating various momentum-space computation methods developed at ANL.

(i) Exactly Soluble Resonance Model for Pion-Nucleon Interaction

T.-S. H. Lee and F. Coester

As a first step in the study of the pion-nucleus optical potential, we have devised a simple soluble model of the pion-nucleon interaction in which nucleon recoil and relativistic invariance are treated exactly within the framework of relativistic particle Hamiltonian theory. We assume that for low pion energies ($E_\pi \leq 300$ MeV) the pion-nucleon interaction is dominated by the lowest resonances N^* and Δ. The resonance energies and widths are the only adjustable parameters. The model provides a good fit to the empirical pion-nucleon phase shifts. A paper for publication is in preparation.

(ii) A Calculation of the First-Order π-^{4}He Optical Potential

T.-S. H. Lee

In order to determine whether the first-order π-nucleus optical potential in the multiple-scattering theory is applicable in the low-energy region $E_\pi \leq 80$ MeV, a calculation of the π-^{4}He first-order optical potential has been carried out with correct treatment of various many-body aspects of the problem. Compared with previous optical-model calculations, the main features of this study are: (1) The π-nucleon interaction model of Lee and Coester [see Sec. VII. Ea(i)] is used to generate the π-nucleon off-shell t matrix. (2) The dependence of the π-nucleon t matrix on the π-nucleon total momentum in the π-nucleus

c.m. frame is rigorously determined by the relativistic particle Hamiltonian theory. (3) The nucleon motion is treated exactly by folding the nonstatic π-nucleon t matrix into the ^{4}He wave functions. And (4) the binding and Pauli effects on the π-nucleon interaction inside the nuclei are treated by including the first-order corrections to the impulse approximation in the calculation.

Our calculations have shown that previously-used simplifying assumptions about the many-body aspect of the first-order optical potential become unreliable in the low-energy region. The discrepancy between the data and our results is much smaller than that obtained by current optical potentials, and is mainly in the large momentum-transfer region where the N-N correlation effects are expected to be important. A paper describing these calculations is in preparation.

(iii) Second-Order π-Nucleus Optical Potential

S. Chakravarti and T.-S. H. Lee

In order to describe the large-angle elastic scattering and to investigate the N-N correlation effects on the π-nucleus relative wave function, it is necessary to study the π-nucleus second-order optical potential. The second-order optical potential is expected to be important in determining the short-range part of the π-nucleus relative wave function which must be accurately known for the distorted-wave study of the large-momentum-transfer π-nucleus reactions.

We have constructed the pion-nucleus second-order optical potential from the π-N interaction model of Lee and Coester. To facilitate the practical calculations, the second-order potential is formulated in such a way that the nuclear structure information and the π-N interaction are clearly separated. The N-N correlations are parameterized by assuming a Jastrow wave function for the nuclear ground state. Attempts are being made to see whether the large angle π-^{4}He elastic-scattering data at $E_\pi \leq 80$ MeV can be explained, if the second-order optical potential is included in the calculations.

b. Pion-Nucleus Reactions

J. E. Monahan and F. J. D. Serduke

Events in which the mass of the pion is absorbed seem to account for a large fraction of the cross section for pion-nucleus reactions. This is particularly true for those reactions that involve the removal of several nucleons. This suggests the following (oversimplified) description of the multinucleon removal processes. Consider pions incident on a target with mass number A and assume that pion absorption with the emission of two nucleons is the primary initial (prompt) process. Ratios of the initial absorption cross sections are taken to be those predicted by the isobar model and the emission of additional nucleons is described by an evaporation model. Final-state nucleon-nucleon interactions are taken into account by assuming that the A-2 intermediate nuclei have excitation energies distributed uniformly up to some maximum. Recent measurements of the cross sections for the production of nuclei with mass number less than A-4 for $\pi^{\pm}$ on ^{58}Ni and ^{60}Ni were reproduced (to within the accuracy of the data) in this model. Although this result indicates that statistical processes (evaporation) play a role in these reactions, the major conclusion is that the production cross sections alone do not permit a unique determination of the initial pion interactions. The model predicts a substantially larger number of high-energy protons than are observed in the particle spectrum measured for π^{+} on nickel targets. Two possible explanations are: (i) large final-state interactions involving nucleon-nucleon scattering to the continuum and (ii) pion absorption on clusters of more than two nucleons. It is interesting that Monte Carlo cascade-evaporation calculations, which take (i) into account, at least approximately, also predict a significantly larger number of high-energy protons from the π^{+}-Ni reaction.

F. OTHER THEORETICAL PHYSICS

a. Approximately Relativistic Particle Interactions

F. Coester and P. Havas*

Equations of motion for the world lines of classical particles with direct interactions can be derived from Fokker action principles. A canonical form for such equations of motion exists only approximately to order $1/c^2$. Such action principles have been investigated extensively by Havas and collaborators. Fully relativistic, canonical direct-interaction theories are possible if the requirement of observable invariant world lines is abandoned for the interacting particles. That is reasonable for the quantum mechanical description of strongly interacting particles, for which only scattering amplitudes are actually observable. It is then sufficient to require the existence of an S matrix and the dynamic and kinematic independence of separated clusters. Such theories have been used by Coester et al. to investigate relativistic effects in nuclear structure. In the classical limit, and an expansion to order $1/c^2$, the Hamiltonian can be compared with those derived from Fokker action principles in the same approximation. To order $1/c^2$ it is possible to satisfy the world-line condition in the canonical theory if the nonrelativistic limit of the potential is velocity independent. A paper for publication in Phys. Rev. D is in preparation.

*Temple University, Philadelphia, Pennsylvania.

b. Extrapolation of Low-Energy Reaction Cross Sections

J. E. Monahan, A. J. Elwyn, and F. J. D. Serduke

Many applications in astrophysical and controlled-fusion research require values of nuclear-reaction cross sections at interaction energies considerably below the range in which absolute measurements re practical. Measured cross sections must be extrapolated to the

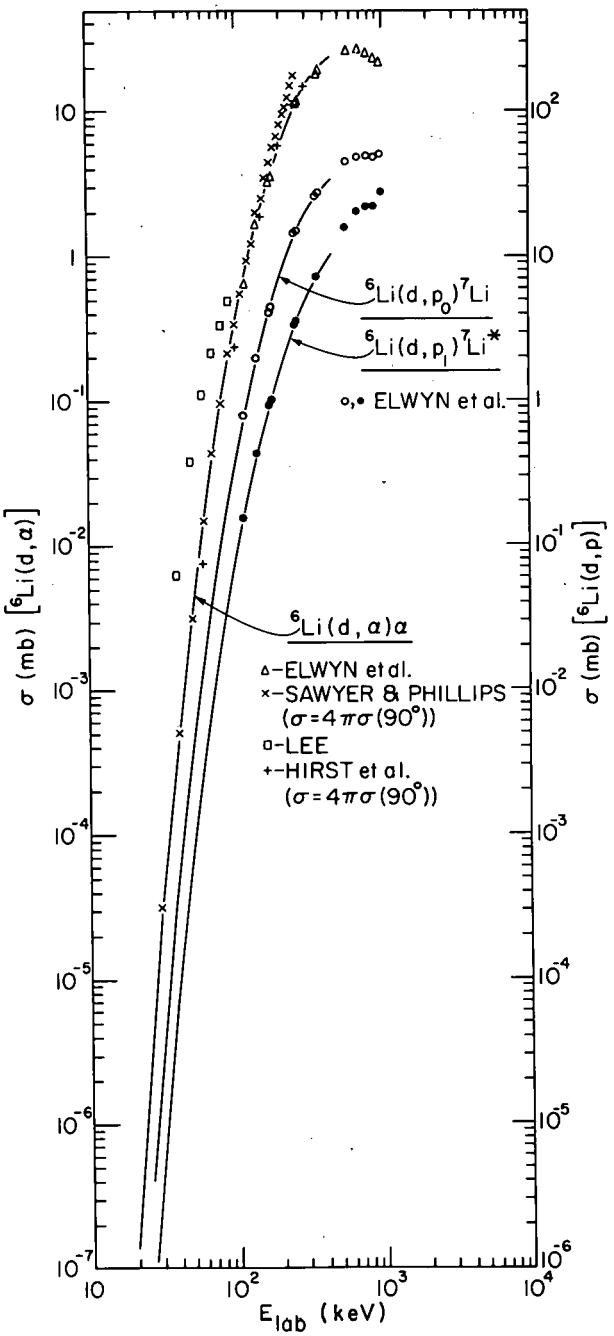

Fig. 42. Cross sections for charged particles emitted in d+^{6}Li reactions as functions of incident deuteron energy. The smooth curves are cross-section calculations based on the extrapolation formula and the data of Elwyn et al. for E ≤ 400 keV.

energies of interest. The extrapolation formulas that are used for this purpose are empirical and thus introduce uncertainty in the extrapolation procedures. For exoergic reactions, which are not dominated by resonances in the range of measurement, a physically meaningful extrapolation formula can be derived from the R-matrix theory. For energies such that only incident s waves contribute to the reaction, the resulting formula contains two "free" parameters. This procedure has been used to extrapolate cross sections for various d+^{6}Li reactions, measured at energies above ~100 keV, to energies in the range of one keV. The resulting fits are consistent with the assigned "relative error" (i.e., the error obtained by neglecting uncertainties in overall normalization) of 5% for the measured cross sections and a relative error of ~12% at the extremity of the extrapolation range. Extrapolations of the ^{6}Li(d,p)^{7}Li, ^{6}Li(d,p)^{7}Li*, and ^{6}Li(d,α)^{4}He cross sections to energies below 400 keV were based on the measurements of

Elwyn et al.[1] and are shown in Fig. 42. Also shown in the figure are other low-energy measurements of the (d, α) cross section. In view of the considerable uncertainty in the data at lower energies, the agreement between the measured and extrapolated cross sections is considered to be quite good.

A tacit assumption of any cross-section extrapolation procedure is that there exist no undetected resonances at energies below the interval in which the measurements are made. For charge numbers Z_1 and Z_2 in the incident channel such that $Z_1 Z_2 \geq 3$, it can be shown that, for any reaction, a resonance with observable strength at an energy less than ~100 keV will also give rise to measurable effects at energies greater than 100 keV.

[1] A. J. Elwyn, R. E. Holland, C. Davids, F. J. Lynch, L. Meyer-Schützmeister, and F. P. Mooring (to be published).

c. A Three-Body Model for Deuteron-Nucleus Scattering

T.-S. H. Lee and R. D. Amado*

In conventional nuclear spectroscopic studies, the deuteron-nucleus optical potential plays an important role. The adiabatic deuteron-nucleus optical model of Johnson and Soper has been extensively used in analyzing experimental data. However, recent studies of Farrell, Vincent, and Austern, and of Rawitscher have raised doubts about the validity of the model. The above two studies disagree with each other because of differences in their approximate treatments of the basic three-body problem. In order to clarify the situation, we are studying a three-body model of deuteron-nucleus scattering. In our approach, we emphasize a consistent treatment of the three-body aspects of deuteron-nucleus interaction. This is done by using Noble's integral-equation formalism for direct nuclear reactions. From this study, we hope to

* University of Pennsylvania, Philadelphia, Pennsylvania.

develop a more accurate empirical parameterization of the deuteron-nucleus optical model; this can then be incorporated in DWBA treatments of direct reactions involving deuterons.

d. Quark Confinement and Hadronic Structure

The spectroscopic information available at present leaves little doubt that the hadronic spectrum satisfies rules consistent with an underlying SU(3) symmetry group [or SU(4) ⊃ SU(3), etc.]. However, this observation leads us to request the existence of the fundamental particles—quarks—which so far have escaped detection in laboratory and cosmic-ray experiments.

One of the possible explanations of this vexing phenomenon (once we abandon the bizarre quantum numbers in favor of an additional internal quark symmetry as required by some experiments) is the assumption that the free quark mass is very large, as compared to the mass of a proton.

The above approach implies a quark-shell model of hadrons with the additional (as compared to nuclear physics) difficulty of finding the proper interaction in a strong binding theory in which the properties of the bound states have little in common with (eventually existing) bare particles entering into the theoretical description.

(i) Model of Quark Confinement with Scalar Gluons

Johann Rafelski

The forces between the quarks are not understood. It has been suggested that the structure of hadrons may be described by a theory in which the forces between quarks are mediated by scalar mesons (gluons) and the coherent (mean) field approximation is used. In our model we adopt the simplest choice for the Lagrangian $\mathfrak{L}$ of the interacting quark-gluon system and investigate the properties of solutions in the lar

coupling constant, $g^2 \gg 10$, limit:

$$\mathcal{L} = \bar{\Psi}(\gamma \cdot p - m_q)\Psi - \tfrac{1}{2}(\partial\Phi \cdot \partial\Phi + \mu^2\Phi^2) + g\Phi\bar{\Psi}\Psi,$$

where Ψ is the quark field, all quarks have mass m_q, and μ is the mass of the scalar gluon field.

The existence of confined spherically symmetric solutions in our model is demonstrated and the limit of infinite quark mass is considered. The structure constants of hadrons are calculated as functions of the coupling constant and the gluon mass. Good agreement with experiment has been found. This schematic model is not to be taken as an ultimate phenomenological description of hadrons, which would perhaps include other mesons than the scalar gluon and a detailed treatment of the internal quark variables. However, it appears to provide a useful test case for finding the general consequences of the coherent field approximation and it has some advantages of conceptual simplicity over similarly motivated models based on Lagrangians containing higher powers of the field variables. (Phys. Rev. D, November 1976.)

(ii) Nonspherical Bags in Theories of Quark Confinement

Johann Rafelski and Berndt Müller

In the theories of hadronic structure the constituent particles (quarks) are normally assumed to move in a "shell potential" with spherical symmetry. We have investigated numerically the questions connected with possible deformed solutions. Cylindrical symmetry has been assumed allowing for prolate or oblate deformation. As a test case of our considerations we have chosen the theory of temporary quark confinement discussed above [Sec. VII. Fd(i)]. Our preliminary results indicate that a deformed stable solution can be possibly found only in strongly deformed bags (strings). However, no solution of lower energy, than that of the spherical solution, has been found. Work is being prepared for publication.)

(iii) Vector Coupling and Bound States of Fermions in Three-Space Dimensions

Johann Rafelski and Berndt Müller

In the recently proposed theories of strong quark coupling via colored gluons ("chromodynamics"), the interaction of a fermion field with a non-Abelian vector field of the Yang-Mills type plays an important role. In this work we make a step into this direction and consider an Abelian, massive vector field in interaction with a spinor field. This is the simplest case, in which we can study the consequences of soliton-like solutions in three-space dimensions involving vector fields.

The main problem which is encountered even in a schematical model of quark-vector gluon interaction is closely related to the questions concerning Klein's paradox. It is well known that a three-dimensional fermion field subject to a sufficiently strong external potential can exhibit particle states of negative energy. This may lead to the spontaneous production of pairs, where the energy of the process is provided by the external field. We have been able to show, using the mean (coherent) field approximation, that in our case in which no external forces are acting, the energy content of the mean boson field raises the total energy above zero. Spontaneous particle creation does not occur, although the eigenvalues associated with the Dirac equation can lie below the critical threshold $E_D < -m$. (Phys. Rev. D, in press.)

e. Thomas-Fermi Theory Revisited

The application of the Thomas-Fermi-(Dirac) theory to molecular and solid-state structure has been hesitant after a "no binding" conjecture was proposed by E. Teller. Since the immediate use of heavy-ion accelerators makes a study of inner quasimolecular electronic states possible, interest has been revived in the performance of many-electron relativistic calculations of two-center molecules. The experien- with Thomas-Fermi calculations in atomic systems suggests that an

adequate description of the inner molecular levels can be achieved. Molecular binding could then be investigated by further Hartree-Fock iterations. The dynamics of quasimolecular electronic orbits in heavy-ion collisions will, however, be described correctly without any further effect.

The relativistic generalization of the Thomas-Fermi theory can be used to calculate the spontaneous neutralization of charged nuclear matter. This success of the Thomas-Fermi theory suggests strongly its application to nonhomogeneous "nuclear charge" distributions. This is especially true for highly compressed lattices, as probably found on the surface of neutron stars.

(i) Inner Electronic Shells in U-U Collisions

Johann Rafelski, Eberhard Gross,* and Berndt Müller*

In sub-Coulomb heavy-ion collisions the inner electron shells create quasimolecular orbits, since the motion of the electrons is much faster than $v_{ion} \sim c/7$. One of the fundamental problems in the description and prediction of the phenomena involved is the calculation of the quasimolecular electronic orbits.

We have carried out a numerical Thomas-Fermi calculation to determine a self-consistent Coulomb potential as a functional of the internuclear distance. We then solve the two-center Dirac equation using this self-consistent Thomas-Fermi potential and obtain electronic wave functions.

*Institute for Theoretical Physics, Frankfurt, Germany.

(ii) Coulomb Energy and the Stability of the Charged Vacuum

Johann Rafelski and Berndt Müller

When the binding of an electron in an external Coulomb eld exceeds twice its mass, spontaneous pair production will occur

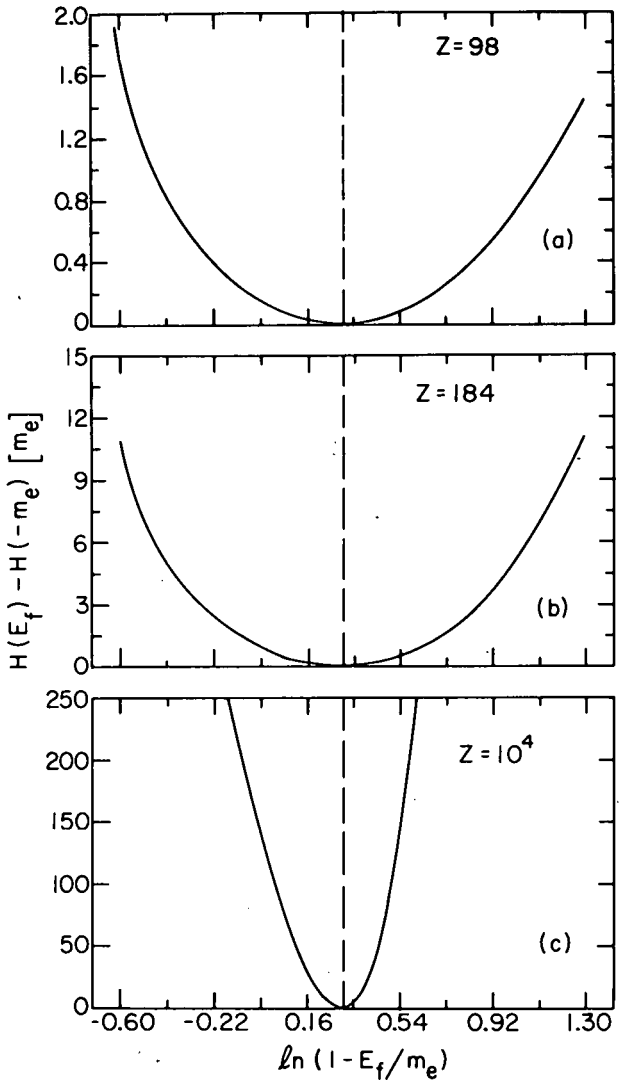

Fig. 43. The Coulomb energy as a function of Fermi surface in supercritical nuclei.

whenever this particular state is not occupied. Therefore, there is no stable state consisting of bare external "nuclear" charge—instead all electronic states below a Fermi energy $E_F = -m$ (energy includes the mass of the electron) are occupied.

We show that the state with $E_F = -m$ is the state of lowest energy of our system within the Thomas-Fermi theory. Calculating the Coulomb energy of the charged state as a function of E_F, we find ($\hbar = c = m_e = 1$)

$$E_c = \alpha [\ln(1 - E_F)]^2 + \beta,$$

where α and β depend on the value of the nuclear charge density and are obtainable numerically. Examples of this behavior are shown in Fig. 43.

The most interesting consequence arising from the above result may be the possibility of collective oscillations of the vacuum charge. While E_c represents the potential energy in the collective parameter $\ln(1 - E_F)$, the kinetic energy could possibly be obtainable from a crank-like approach to the collective motion. (Work is being prepared for publication.)

Quantum Electrodynamics of Strong Fields

(i) Review of the Theory of Elementary Particles Interacting with Arbitrarily Strong Classical Fields

Johann Rafelski, L. Fulcher,* and A. Klein†

We have written a review paper, "Theory of Elementary Particles Interacting with Arbitrarily Strong Classical Fields," for Physics Reports. In this paper, we review and consolidate the recent work that deals with the spontaneous creation of particles and antiparticles by strong static external fields. An example of this kind of phenomenon, which has stimulated much of the current interest, would be the spontaneous production of positrons in the vicinity of a superheavy nucleus with a charge $Z > 170$. This example of spontaneous particle production should be realizable during the collision of two very heavy ions, such as the collision of a uranium nucleus with another uranium nucleus, provided that the two nuclei come close enough together. (In this case, the spontaneous production mode is only one of several which contribute. The others involve time-dependent electromagnetic fields.) The heavy-ion experiment mentioned above will soon be attempted at GSI in Wixhausen near Darmstadt.

Research on the theory of bosons bound to strong potentials is also discussed in the review. Further applications of the theory to related subjects in strongly coupled field theory and spontaneous particle production in gravitational fields are considered.

(ii) Bose Condensation in Supercritical External Fields

Johann Rafelski and Abraham Klein†

In strong external electromagnetic fields the energy necessary to bind an additional boson-antiboson pair may disappear

*Bowling Green State University, Bowlling Green, Ohio.

†University of Pennsylvania, Philadelphia, Pennsylvania.

allowing for creation of Bose condensates. As an augmentation of our previous work, we have discovered a new mechanism that might favor a charged condensate over the previously preferred neutral one. Such condensates may appear in some astrophysical situations or in another (theoretical) form in strong binding theories of hadronic matter.
[Published as Comment in Phys. Rev. D 12, 1194 (1975).]

(iii) Magnetic Splitting of Quasimolecular Electronic States in Strong Fields

Johann Rafelski and Berndt Müller

In order to test the behavior of matter in very strong magnetic fields, an experiment has to fulfill two conditions: (1) extremely high currents are needed as the source of the magnetic field and (2) the probing charge must be in the close vicinity of the current because of the dipole character of the magnetic field.

In sub-Coulomb-barrier heavy-ion collisions the magnetic field created in the vicinity of the colliding nuclei is of the order of 10^{14} Gauss, however over a rather small volume. (In a constant magnetic field of this size the Zeeman splitting of the spin states of an electron would be comparable to its rest mass.) It is important to recognize that the inner-shell electrons move in the force field generated by the colliding heavy ions: these electrons are bound by both nuclei and form quasi-molecular states. This leads to the localization of the inner-shell electronic wave functions in the region of strong magnetic fields.

In the quasimolecule the main binding is provided by the electrostatic potential of the two nuclei, while the magnetic "hyperfine" splitting of the electronic states may reach 0.2 m in selected systems. This is the case because the effective electric coupling constant is Ze^2, whereas it is Ze^2v/c for the magnetic interaction.

The spinor wave functions of relativistic electrons in the collision system are found by solving the two-center Dirac equation ($\hbar$ =)

$$\left(\vec{\alpha} \cdot \vec{p} + \beta m - \frac{Z_1 e^2}{|\vec{r} - \vec{R}/2|} - \frac{Z_2 e^2}{|\vec{r} + \vec{R}/2|} \right) \psi = E\psi. \qquad (1)$$

$\vec{\alpha}$ and β are the Dirac matrices, and R is the internuclear distance. (The electron-electron interactions are neglected here; we will discuss their effects below.) E is the total energy of the electron and is related to the binding energy E_B by $E = m - E_B$. The energy spectrum of Eq. (1) consists of discrete bound states in the interval $-m < E < +m$, electron scattering states for $E > m$, and positron scattering states for $E < -m$. For $Z_1 + Z_2 > 137$ and for separations $R < R_{cr}(Z_1 + Z_2)$, electronic bound states can exist as resonance states in the negative energy continuum. R_{cr} is the critical distance between the nuclei at which the binding energy of most strongly bound electrons exceeds 2 m.

The vector potential $\vec{A}$ present in the heavy-ion collision (as seen from the c.m. system) is given in the Lorentz gauge by

$$e\vec{A} = -Ze^2 \frac{\vec{V}_1}{|\vec{r} - \vec{R}/2|} - Ze^2 \frac{\vec{V}_2}{|\vec{r} + \vec{R}/2|}. \qquad (2)$$

(We have restricted our calculations to symmetric collisions and $\vec{V}_i$ are the heavy-ion velocities.) It is important to realize that the corresponding magnetic field cannot be transformed away by a choice of a suitable inertial frame.

In the basis of Eq. (1) the magnetic states of opposite spin are degenerate. Therefore, the calculation of the magnetic splitting due to H_{mag} proceeds via degenerate-state perturbation theory.

To evaluate the necessary matrix elements we have to solve Eq. (1) which, in contrast to its nonrelativistic counterpart, is not separable in two coordinates. We have developed a new approach in which the Dirac wave function is expanded in spinor multipoles. The two-dimensional equation reduces then to an infinite system of coupled first-order differential equations in one dimension. This system was truncated at sufficiently large angular momentum j_{max}. The resulting system of

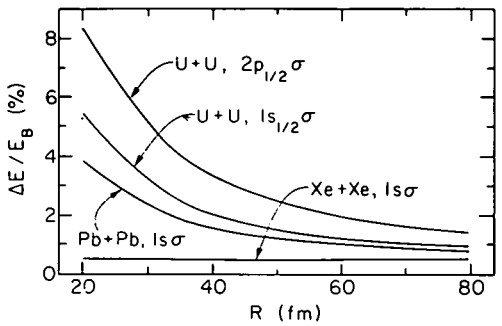

Fig. 44. The relative magnetic splitting $(E\downarrow - E\uparrow)/E_B$ for the four selected quasimolecular states. Collision parameters are: E_{kin}/N = 9 MeV/nucl and b = 13 fm.

$2(2j_{max} + 1)$ coupled differential equation was solved iteratively for the energy eigenvalue and $2j_{max}$ coefficients describing the behavior of the wave function at the origin. In order to obtain good wave functions we required convergence of the $2j_{max} + 1$ eigenvalues to better than 10^{-10}. However, because of the truncation of the Hilbert space the true eigenvalue was only established to a relative precision of 0.1%. The direction of the iteration was determined by the use of the $(2j_{max} + 1)$ dimensional steepest descent method. We have tested the accuracy of our new code and found it significantly superior to other calculational techniques for solving the nonspherical Dirac equation.

We have used these new wave functions to calculate the splitting ΔE of the opposite spin states using the collision parameters: b = 13 fm and E_{kin}/N = 9 MeV/nucl. The relative splittings $\Delta E/E_{Binding}$ are shown in Fig. 44 as a function of R for the above-mentioned scattering systems. We find that the relative magnetic splitting of the $2p_{1/2}\ \sigma$ level in U + U is very large and exceeds that of the 1s σ state because the binding energy is considerably smaller, while the magnetic interaction is of the same size. The energies of the U + U molecular states are shown in Figs. 45a and 45b. The relative splitting of the 1s σ state in Xe + Xe may be too small to be detectable.

In view of these results we feel that any experiment to test the behavior of electrons in such a strong magnetic field should be carried out in a system as heavy as Pb + Pb. As the system becomes heavier, an investigation of the splitting of the $2p_{1/2}\ \sigma$ level seems to be advantageous, since it is much easier to have this state ionized in the co ɔn.

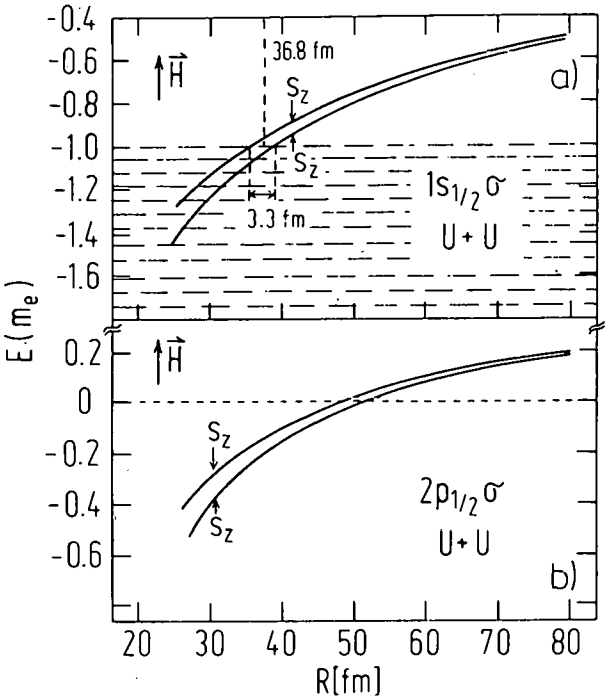

Fig. 45. The four quasimolecular states with magnetic interaction which are discussed in the text. Collision parameters are: E_{kin}/N = 9 MeV/nucl and b = 20 fm. (a) U + U, $1s_{1/2}\sigma$: the spin parallel state reaches the negative energy continuum 3.3 fm earlier than the state with anti-parallel spin. (b) U + U, $2p_{1/2}\sigma$.

The U + U molecular levels were calculated without the inclusion of electron screening and virtual vacuum polarization. Also, the finite size of the U nuclei has not been considered. Those effects combined would shift the energies by approximately 100 keV upwards parallel to the plotted curves in Fig. 45. We estimate the shift in R_{cr} due to the neglected effect to be 3 fm. The magnetic interaction causes the spin-up state to join the negative continuum 3.3 fm earlier than the spin-down state. The true critical radius lies at 36 fm for the spin-up state in the U + U system including the above-mentioned corrections.

We have investigated the various dynamic couplings within the two-state system and found the rearrangement of vacancies between the spin states is negligible. Therefore, the distribution of vacancies in the magnetic substates of the K shell after the heavy-ion collision is determined by the dynamical coupling of the substates to higher electronic states. This causes the degree of polarization of the subsequent K_{α} radiation to be sensitive to the ionization mechanism for the molecular ates. If the ionization occurs in the region of strong magnetic splitting ... $\leq$ 200 fm), then the ratio between the two photon polarization states

after the collision will be $\sigma_{\downarrow}/\sigma^{\uparrow} \approx e^{+\Delta E/\Gamma} \sim \left(1 + \frac{\Delta E}{\Gamma}\right) > 1$. Γ is the dynamic collision broadening of the molecular 1s σ state, and we estimate $\Delta E/\Gamma \sim 0.2$. On the other hand, if ionization occurs in the periphery of the collision, then the two spin states will be differently refilled and $\sigma_{\downarrow}/\sigma^{\uparrow} \leq 1$. Here the deviation from unity should be much smaller than in the first case: the density of vacancies is much lower in the inner shell.

In conclusion we find that the strong magnetic fields generated in a heavy-ion collision produce a splitting of one-fifth of the electron mass in the quasimolecular states. An experimental confirmation of this effect may extend the proven region of validity of quantum electrodynamics to include external magnetic field strength up to 10^{14} Gauss. The polarization of the characteristic radiation from inner-shell electronic transitions contains information on the mechanism for vacancy production in the heavy-ion collision. This work has been published in Phys. Rev. Lett. 36, 517 (1976).

g. New Systematics in Hadron Total Cross Section

Harry J. Lipkin

Analysis of total cross-section data from 2 to 200 GeV/c shows striking regularities in the discrepancies between the experimental data and predictions based on two-component duality with exact exchange degeneracy, universality, and SU(3) symmetry. These regularities suggest that the discrepancies are not due to a number of unrelated breaking effects, but are all related and described by a single universal third component which has even-signature isoscalar exchange in the t channel, has exactly the same energy dependence for kaon-nucleon, pion-nucleon, and nucleon-nucleon scattering processes, and scales in the ratio $1:2:\frac{9}{2}$. This new component suggests a common origin for the strangeness dependence of the total cross sections and the deviations from quark-model additivity, and gives a unified description

f the following apparently unrelated effects: (1) The $\sigma(\pi N)-\sigma(KN)$ difference, (2) the deviation of $\sigma(\pi N)/\sigma(NN)$ from $\frac{2}{3}$, (3) differences in energy behavior of cross sections, particularly the decrease in $\sigma(pp)$ at low energies, and (4) the differences among $\sigma(K^+p)$, $\sigma(pp)$, and $\sigma(\phi p)$, which are all pure Pomeron in two-component duality.

h. Strangeness Analog States

J. P. Schiffer and H. J. Lipkin

In hypernuclei, that is to say in nuclei containing a Λ particle, interesting coherent features may be obtained. Since the Λ is a baryon which may occupy different shell-model orbits, in much the same way as a nucleon does, it had been thought that there may be a coherent analog of the ground state of a normal nucleus, in which the Λ replaces a nucleon, with all other aspects and symmetries unchanged. These "strangeness analog states" were expected to appear in the low-momentum-transfer strangeness-exchange reactions (K^-,π^-). Recently-published data[1] from CERN have been reanalyzed from this point of view. The expectation for the analog state was that it occur at a fixed Q value, regardless of target. The Q value for the analog state would be a measure of the difference in the Λ-N and the N-N interaction. The CERN data for ^{16}O, ^{12}C, and ^{9}Be were all found to show a prominent bump at a Q value of $\sim$-20 MeV. Figure 46 shows a comparison of smooth curves drawn through the data.

The possibility of using the (π^+,K^+) reaction as an alternative method for populating these hypernuclei was explored. The intensity of π^+ beams would make this an attractive reaction. The momentum mismatch was worse than for (K^-,π^-), but it was hoped that this difference would not lower the cross section to a prohibitive level. More careful estimates

---

[1] W. Brückner, M. A. Faessler, K. Kilian, U. Lynen, B. Pietrzyk, Povh, H. G. Schürlein, H. Schröder, and A. H. Walenka, Phys. Lett. B, 107 (1975).

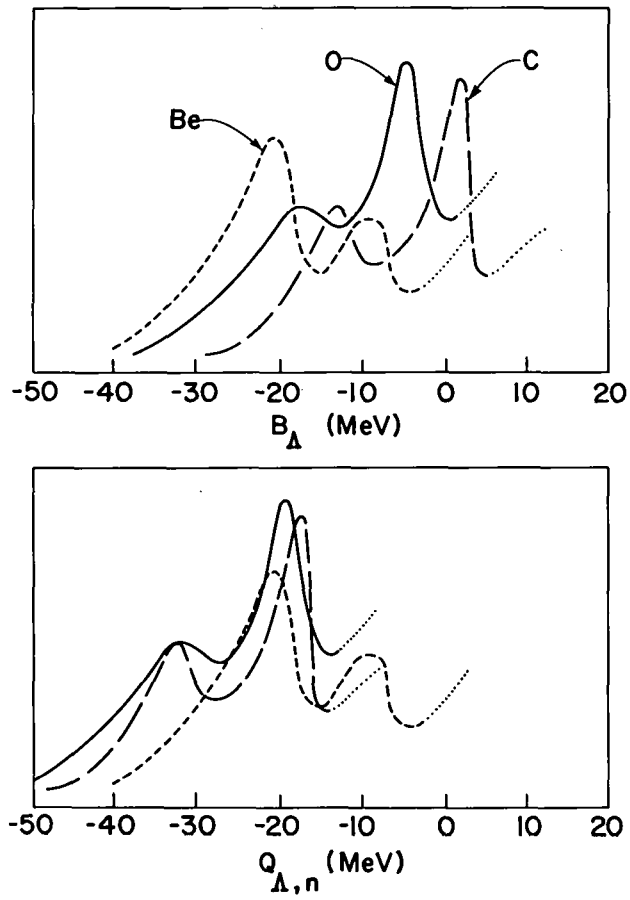

Fig. 46. (a) Smooth curves drawn through the data in Ref. 1 for π^- spectra (counts/MeV in arbitrary relative units) from low-momentum-transfer (K^-,π^-) reactions as a function of the binding of the Λ. (b) The same data plotted against the (Λ,n) Q_value. The rise on the right-hand side is from the $K^-\rightarrow 2\pi$ process.

indicate that the loss in yield is indeed ~two orders of magnitude and that this alternative technique is not particularly attractive.

i. The Speakeasy Center

S. Cohen

Speakeasy (a user oriented computer language originally developed in the Physics Division) has gained widespread acceptance throughout the world. At present over 70 different installations are making use of this language, including many government agencies, several universities, and a large number of commercial firms. Although Speakeasy was conceived as a tool for researchers in the physical sciences, the general nature of this language has led to its use by economists, engineers, and students in many fields.

The Speakeasy Center is the maintenance and development site for the program. The Center is funded by the Speakeasy Users Group through a yearly membership fee. The yearly meeting of the User Group is held at Argonne and has proven to be a meeting of substantial importance in the computing community.

THIS PAGE
WAS INTENTIONALLY
LEFT BLANK

ATOMIC AND MOLECULAR PHYSICS RESEARCH

INTRODUCTION

The research program in Atomic and Molecular Physics is comprised of eight ongoing research projects, described below as follows:

A. Photoionization and Photoelectron Physics and Chemistry

B. Interactions of Energetic Particles and Photons with Surfaces of Solids

C. Laser and Radiofrequency Spectroscopy of Free Atoms and Molecules

D. Low-Energy Positron Source Development

E. Mössbauer Effect

F. Scanning Secondary-Ion Microprobe

G. Beam-Foil Measurements of the Radiative Spectra, Decay Times, and Collision Dynamics of Heavy Ions

H. Theoretical Research

THIS PAGE

WAS INTENTIONALLY

LEFT BLANK

VIII. ATOMIC AND MOLECULAR PHYSICS

A. PHOTOIONIZATION AND PHOTOELECTRON PHYSICS AND CHEMISTRY

This research involves detailed investigations of the interaction of electromagnetic radiation with gaseous matter, from the vicinity of the first ionization threshold to the highest photon energy achievable with existing equipment. In some studies, the highly excited or ionized species are permitted to react with other gases (chemi-ionization, ion-molecule reactions) and the products and cross sections are measured as a function of photon energy.

Two photoionization mass spectrometers are currently in use for studies of ions produced in these various processes: (1) a one-meter, normal incidence vacuum-ultraviolet monochromator (VUV) combined with a magnetic-sector mass spectrometer, and (2) a three-meter, normal incidence VUV monochromator mated with a quadrupole mass spectrometer.

The concomitant production of electrons in the photoionization process is studied by photoelectron spectroscopy (PES). A cylindrical-mirror electron energy analyzer has been utilized in the past few years for such measurements and recently a hemispherical analyzer capable of measuring photoelectron spectra as a function of angle has been put into operation.

From PES, one determines the various molecular-ion states that can be formed by photoionization and their relative cross sections. Photoionization mass spectrometry then tells us whether the molecular ion survives as a unit or as fragments, the thresholds for such processes, and the variation of cross section with photon energy. Accurate bond energies can be deduced from fragmentation thresholds, and accurate ionization potentials from photoelectron spectroscopic bands. In the latter case, the shapes of the bands provide valuable information about the bonding character of the respective molecular orbitals, which differ drastically in ionic and covalent molecules. Other information which can be gleaned from these bands includes the structure of the molecules and spin-orbit splitting.

A great deal can be learned about the dynamics of the ıotoionization process from observations of autoionization phenomena in ıotoionization mass spectrometry and from wavelength-dependent PES, examples of which are given below.

During the past year, the one-meter photoionization apparatus has been employed to explore higher-energy processes in the more common gases, and to study more reactive species. For the examination of higher energy processes, a hollow cathode lamp is used to generate lines between 743 Å (16.7 eV) and 304 Å (40.8 eV), thereby doubling the energy range accessible to most previous investigators. With this capability, we have measured the fragmentation behavior of O_2, N_2, CO, NO, CO_2, H_2O, NH_3, and CH_4, and correlated these results with photoelectron spectra and ion kinetic-energy spectra. One of the goals of such an investigation is to determine what factors govern the modes of decomposition of specific states of a molecular ion.

In the program to study the photoionization behavior of reactive species, we have measured the photoionization mass spectrum of ozone. The adiabatic ionization potential has been obtained more accurately, the relative probability of decomposition into O_2^+ and O^+ has been determined, and a surprisingly intense O_5^+ peak has been observed, generated by the reaction

$$O_3^+ + O_3 \rightarrow O_5^+ + O.$$

We are currently trying to assess the possible importance of this reaction in the dynamics of the upper atmosphere.

A major effort was made with the three-meter apparatus to compare the relative merits of synchrotron radiation and intense laboratory light sources for photoionization and photoelectron spectroscopic measurements. Measurements were made with this apparatus at the electron-synchrotron storage-ring facility in Stoughton, Wisconsin, and compared with our relatively potent helium-continuum lamp. Many useful parameters were obtained, which will enable us to accurately pinpoint which experiments can be usefully performed in our laboratory, and which require a synchrotron. In addition, with this bench-mark study, we shall be able to "calibrate" future improvements in synchrotron intensity and/or lamp design, and to compare our capability with those of synchrotron users at the other major synchrotrons in the world.

An obvious advantage of the synchrotron over the helium continuum lamp is that the latter has a short wavelength cutoff at ~600 Å. We have utilized the extended wavelength capability of the synchrotron source to measure the autoionization structure between the $^2P_{3/2}$-$^2P_{1/2}$ thresholds of Ne^+, which occurs below 600 Å.

In the domain of photoelectron spectroscopy, we are still in the process of trying to develop a heating system that will generate vapors in the 1000°—2000°C region without disturbing the performance of the electron energy analyzer. In the meantime, we have continued our studies in the temperature range below 1000°C.

The apparatus for the study of photoelectron angular distributions, which utilizes a hemispherical electron energy analyzer, has produced its first published results.

a. The Photoelectron Spectrum and Structure of Tl_2F_2

D. G. Streets and J. Berkowitz

A previous photoelectron spectrum had been used to infer a linear F-Tl-Tl-F structure for Tl_2F_2. We have found that three of the peaks in this older spectrum were due to CO_2, generated from a Tl_2CO_3 impurity in the sample. A pure sample of TlF was then used to obtain spectra of both TlF and Tl_2F_2, using different heating techniques. The new spectrum of Tl_2F_2 is consistent with a rhombic structure, analogous to the structures of alkali halide dimers.

b. The Photoelectron Spectra of Se_2 and Te_2

D. G. Streets and J. Berkowitz

Our earlier work on the photoelectron spectra of diatomic chalcogens (S_2 and Te_2) has been extended to include the other member (Se_2) and several peaks previously unobserved have been detected in the Te_2 spectrum. The anomalous intensity ratio of $^2\Pi_{g,1/2}$ and $^2\Pi_{g,3/2}$ peaks in the Te_2 spectrum is also seen for Se_2. Whereas this ratio is close to unity for O_2 and S_2, it becomes $\sim$2.5:1 for Se_2 and $\sim$10:1 for Te_2.

c. Photoelectron Spectra of Sulfur Molecular Species

J. Berkowitz, E. H. Appelman,* M. J. Weiss, and K. Lehmann

Unlike oxygen, which forms O_2 readily and O_3 weakly, sulfur (next row in the periodic chart) has a strong propensity to form polyatomic molecules. In saturated sulfur vapor, the molecules S_n (n = 2, 3, · · · 10) have been observed. In an attempt to understand the molecular structure and electronic arrangement that provides

*Chemistry Division, ANL.

stability for this large range of sulfur molecules, we had previously obtained the 584 Å photoelectron spectra of isolated S_2, and now have also taken data for S_6 and S_8. The next step in the understanding of the changes in electron arrangement that are occurring will likely be the development of sufficiently accurate calculations to enable the interpretation of these experimental results. Although a number of semiempirical calculations of the CNDO and extended Hückel type have been performed, our data indicate that none of these calculations are of sufficient accuracy to enable us to proceed further in the analysis. A comparison of the bonding, structure and spectra of various oxygen, sulfur-oxygen, and sulfur containing molecules is currently being prepared. This study may be of some use in the elucidation of sulfur-containing pollutants in the atmosphere.

d. Photoelectron Spectra of Transition Metal Dihalides

D. G. Streets and J. Berkowitz

These materials vaporize at relatively high temperatures, and little is known of their structure and gas phase electronic spectra. We have succeeded in obtaining the 584 Å photoelectron spectra of the chlorides and bromides of Mn, Fe, and Co. Analysis of these data awaits the availability of some molecular calculations. At least two theoretical groups are currently working on these problems.

e. Electronic Structures of Fulvalene and Octachlorofulvalene

D. G. Streets and J. Berkowitz

Most organic compounds are volatile, and the measurement of various gas phase properties (including photoelectron spectra) is readily achieved. In a few cases of structural interest, the samples need to be volatilized, and our spectrometer is particularly appropriate for such cases. We have recently obtained the 584 Å photoelectron spectrum of octachlorofulvalene, and an interpretation of this spectrum with the aid

f semiempirical calculations of the extended Hückel type. An optimum fit occurs when the two cyclopentadienyl rings are twisted with respect to one another by 39°. The analysis enables one to deduce orbital energies, charge densities, and π/σ mixing.

f. High-Resolution Photoionization Mass Spectrometry Using Synchrotron Radiation

K. Radler and J. Berkowitz

The ejection of an electron from the outermost occupied orbitals in Ne, Ar, Kr, and Xe gives rise to a spin-orbit pair, $Ng^+ (^2P_{3/2}, ^2P_{1/2})$ (Ng refers to noble gas). Rydberg series can be observed converging to each of these levels. Some of the higher Rydberg levels converging to the upper $^2P_{1/2}$ state occur at energies above the $^2P_{3/2}$ threshold of ionization, and hence these Rydberg levels can autoionize. The autoionization structure has been extensively studied in Ar, Kr, and Xe, and manifests a sharp s component and a broad d component. (We have recently re-examined the Ar spectrum at sufficiently high resolution to observe natural line widths.) The corresponding spectrum of Ne occurs at wavelengths below 600 Å, and is thus outside the range of the helium continuum. It has heretofore only been studied spectrographically, with correspondingly poor intensity profiles. We have now succeeded in extending the Ng^+ measurements by photoionization techniques to Ne, using the synchrotron radiation together with our 3-meter photoionization apparatus. The fine structure of the Ne spectrum is rather different from that of the heavier noble gases, displaying s and d components of comparable width.

g. Photoionization Mass Spectrum of Carbon Diselenide

K. Radler and J. Berkowitz

Although fairly high-resolution photoionization measurements exist for CO_2, and CS_2 and COS have been investigated at moderate

resolution, such studies have not yet been extended to CSe_2. In fact, even thermochemical information relating to the strength of the C-Se bond is very poor. We are currently in the midst of examining this molecule, and have observed thresholds for the reactions

$$CSe_2 + h\nu \rightarrow CSe^+ + Se + e^-$$

and

$$CSe_2 + h\nu \rightarrow Se^+ + CSe + e^-.$$

From the threshold of the latter reaction, we deduce that the SeC-Se bond energy is 3.834 eV; when combined with other data, this measurement favors the lower [$\Delta H_f^0(CSe_2)$ = 39.4 kcal/mole] of two competing values for the heat of formation of carbon diselenide. From the first reaction, we can infer that the first ionization potential of CSe = 11.06_5 eV.

This molecule was also deemed to be a good candidate for exploiting the advantages of the synchrotron radiation, since the ionization forming parent ion (CSe_2^+) extends to much longer wavelength than the helium continuum and hence a complete study using laboratory light sources requires patching, whereas the synchrotron radiation produces a smooth continuum well beyond the threshold for CSe_2^+. We have, in fact, obtained preliminary data for the entire energy range of CSe_2^+ and its fragments. The spectrum is very rich in autoionization structure. Its analysis will be the subject of future work.

h. Photodissociative Ionization in the 21—41-eV Region

P. L. Kronebusch and J. Berkowitz

With the one-meter instrument, branching ratios have been measured for the photodissociative ionization of O_2, N_2, CO, NO, CO_2, H_2O, NH_3, and CH_4 between 16.8 and 40.8 eV, using line sources. Inconsistencies in previous photoionization fragmentation patterns for NO and H_2O at 21.2 eV, and for CH_4 at 16.8 eV, have been clarified.

The high-energy state of CO^+ has been found to decay predominantly to $O^+ + C$, in contrast to a recent study. Partial cross sections for formation of high-energy states in O_2^+ and CO_2^+ deduced from this study are substantially lower than those reported in a recent 304 Å photoelectron spectroscopic investigation. The NO^+ decomposition at higher energy favors $N^+ + O$, although the lower-energy channel is $O^+ + N$. Ionization from the inner (2s-like) valence states of CO_2 and H_2O leads to C^+ and O^+ fragments, respectively, with probable shattering of the molecular ion into atomic and ionic fragments.

Preliminary results have also been obtained for C_2H_2, C_2H_4, C_2H_6, C_6H_6, SF_6, N_2O, COS, CS_2, and H_2S.

i. Photoionization of Reactive Species; the Photoionization Mass Spectrum of O_3 and the Reactive Formation of O_5^+

M. J. Weiss, J. Berkowitz, and E. H. Appelman*

Although three different groups have recently published 584 Å photoelectron spectra of O_3, the photoionization mass spectra heretofore presented are severely limited, either in energy range studied or in resolution and accuracy. In our study, we find step-like structure in the near threshold region, probably correlating with vibrational states of O_3^+. The weakness or absence of autoionization structure suggests that predissociation is a dominant decay mode of "super-excited" states just above the ionization threshold. We are currently extracting a precise value for this threshold. The dissociative ionization processes forming $O_2^+ + O$ and $O^+ + O_2$ occur at or very near their thermochemical thresholds. At ~19—20 eV, the O_2^+ and O_3^+ are comparable in intensity, the O^+ much weaker.

We have observed O_5^+ with an apparently large cross section produced by the reaction

$$O_3^+ + O_3 \rightarrow O_5^+ + O_1.$$

*Chemistry Division, ANL.

Its threshold appears to be about the same as that for formation of O_3^+ an hence the reaction is either thermoneutral or exothermic. The existence and apparent stability of O_5^+ relates to our studies of the bonding and comparative stabilities of larger molecules containing sulfur and oxygen. (See Sec. VIII. Ac above.) Recent calculations indicate that the positive ions of sulfur rings may be relatively more stable than their neutral counterparts, and this suggests a ring structure for O_5^+. The corresponding neutral species O_5 (and O_4) are unstable in their ground states.

j. Wavelength Dependence of the Photoelectron Angular Distributions of the Rare Gases

J. L. Dehmer,* W. A. Chupka, J. Berkowitz, and W. T. Jivery

Photoelectron angular distributions for the valence p shells of the rare gases have been measured up to a photon energy of 40.8 eV (48.4 eV for Ne) using resonance radiation from a hollow-cathode discharge lamp. This work extends the range of existing absolute measurements on Ne, Kr, and Xe. Comparison with Hartree-Fock and RPAE (random-phase approximation with exchange) calculations indicates excellent agreement for Ne. However, the present results, particularly for Xe, add to earlier evidence that data for Ar, Kr, and Xe show systematic deviations from theory, especially at the higher photoelectron kinetic energies. For Kr and Xe, we report asymmetry parameters separately for processes leading to the $^2P_{3/2,1/2}$ spin-orbit states of the residual ion. The Xe results indicate that $\beta_{3/2}-\beta_{1/2}$ is positive for $\lambda \geq 461$ Å, but changes sign in the range $\lambda \sim 350-400$ Å. At 304 Å, $\beta_{3/2}-\beta_{1/2} = -0.30$, which agrees with a recent calculation based on the Dirac-Slater model.

---

*Radiological and Environmental Research Division, ANL.

k. Very High Resolution Study of Photoabsorption, Photoionization, and Predissociation in H_2

P. M. Dehmer and W. A. Chupka

Relative photoabsorption and photoionization cross sections for H_2 (para and ordinary) have been measured at 78°K from 715—805 Å for para-H_2 and from 745—805 Å for ordinary H_2, with a wavelength resolution of 0.016 Å. This resolution represents a factor of three improvement over the previous data reported from this laboratory, and in addition, the new data have significantly improved statistics. This enables observation and identification of the R(0) $np\sigma$ and $np\pi$ Rydberg series in para-H_2 to principal quantum numbers of approximately 40 for series converging to $H_2^+(^2\Sigma_g^+, v = 1—6)$. Line widths and relative intensities were measured for a large number of these levels and the results are compared to calculations using a quantum defect theory (QDT) approach. Two-channel QDT is used to assign nearly all the prominent structure in the para-H_2 spectrum. The ionization efficiency for these Rydberg states is always close to unity for states which autoionize with $\Delta v = -1$. Decay by predissociation and/or emission competes to varying degrees with autoionization for those states which cannot autoionize with $\Delta v = -1$. For example, for certain low n $^1\Pi_u$ states which can only autoionize via large changes in Δv, the P and R rotational branches decay primarily by predissociation, while the Q rotational branch decays primarily by photon emission. A paper describing this work has been submitted for publication in J. Chem. Phys.

B. INTERACTIONS OF ENERGETIC PARTICLES AND PHOTONS WITH SURFACES OF SOLIDS

The overall purpose of this project is to study specific atomic- and molecular-physics phenomena that occur when energetic particles (keV-MeV range) and photons (15—50-keV range) interact with the surfaces of solids. For example, studies of the basic mechanisms underlying the release of atomic and molecular species, and the changes in the surface structure under energetic-particle and photon impact are being conducted; and the results are compared with theoretical models. Other studies deal with the reflection of energetic light particles (e.g., H^+, He^+) from surfaces.

These studies are undertaken to provide a better understanding of the basic mechanisms underlying those phenomena which can cause, for example, plasma contamination and cooling, and the erosion of components in plasma devices, accelerators, and satellites.

At the present the particle and photon irradiations are being conducted with a 2-MV Van de Graaff accelerator and an intense x-ray source, respectively. However, a unique, three-component irradiation facility is under construction which will allow the simultaneous bombardment of target surfaces by ions of two different species (e.g., D^+ and He^+) at a given energy, or ions of the same species at different energies, together with photons. This facility will permit, for example, studies of synergistic effects on particle release by sputtering and blistering.

a. Sputtering and Blistering

S. K. Das and M. Kaminsky

During the impact of energetic light ions (e.g., He^+ ions with energies ranging from 0.03—1.5 MeV) on surfaces, both physical sputtering and blistering processes occur simultaneously above certain flux and fluence levels and contribute to the erosion of surfaces and the release of gas. Experiments to determine the relative contributions of physical sputtering and blistering to the total erosion yield and the release of particles were conducted by bombarding the surfaces of polycrystalline V and Nb with ^4He ions with energies ranging from ~0.03—1.5 MeV.

For a determination of erosion rates due to radiation blistering, measurements of the skin thickness and of the area from which the skins have been lost have been made. It was discovered that for helium-ion energies from 0.08—1.5 MeV the measured skin thicknesses for V and Nb correlate well with the calculated maxima in the projected-range probability distributions (i.e., the maxima in the helium-implant concentration) and not with the maxima in the damage-energy distributions. This finding is important because it allows one to calculate blister skin thicknesses for the energy range studied. Reports of this work appear in Applied Physics Letters 27, 521 (1975); J. Nucl. Materials 59, 86 (1976); J. Nucl. Materials (to be published); in Proceedings of International Conference on Application of Ion Beams to Materials, Warwick, England, September 8-12, 1975; and Proceedings of the International Conference on Surface Effects in Controlled Fusion Devices, San Francisco, California, February 16-20, 1976.

Studies of the physical sputtering of polycrystalline V and Nb targets under He-ion bombardment with energies ranging from 0.15—1.5 MeV have been conducted under high-vacuum conditions. A quantitative determination of the amount and the spatial distribution of the sputtered deposits on the Si (111) collector surfaces was obtained by three independent techniques, Rutherford backscattering, scanning Auger spectroscopy, and ion-microprobe analysis (IMMA), using vapor deposited standards. Total sputtering-yield values are being evaluated and they will be compared with values calculated according to various sputtering theories (e.g., Sigmund, Brandt and Laubert, Goldman and Simon, and Pease). The data are being prepared for publication in 1976.

b. Photon-Impact and Secondary-Electron-Emission Studies

M. S. Kaminsky, S. K. Das, and S. B. Brumbach

With a recently constructed ultrahigh-vacuum apparatus, photodesorption studies of the type of gas species and the amount of gas

released from stainless steel, Al_2O_3 and gold surfaces under x-ray impact (18—24-keV photon energy) were started. These studies are the first of their kind since all other photodesorption studies known today have been conducted at photon energies which were approximately four orders of magnitude smaller; yet, studies in the x-ray range are of great interest for the operation of plasma devices and future fusion reactors since the bremsstrahlung radiation in such facilities is expected to cover part of the x-ray range.

The results obtained, for example, for stainless steel surfaces reveal: (a) That the dominant gas species released are O_2 and CO_2 and not H_2, H_2O, or CO, which are typically observed in thermal desorption. (b) That mean quantum yields for O_2 and CO_2 are in the range 8×10^{-5} to 2×10^{-3} molecules per photon for the bremsstrahlung spectrum studied. (c) That the energy dependence on the mean quantum yield for CO_2 release reveals an increase in the yield with decreasing mean photon energy. This energy dependence can be correlated with the photon-energy dependence of the photon-absorption coefficient of the substrate material. (d) In order to explore the possibility of photon-induced CO oxidation as a mechanism for the CO_2 production, the intensity of the photon-induced CO_2 signal was measured for various partial pressures of CO. The amount of CO_2 released from stainless steel surfaces was found not to be a function of the CO partial pressure in the 10^{-10} to 10^{-8} torr range.

Results of this work have been reported in the Proceedings of the Sixth Symposium on Engineering Problems of Fusion Research (published by the Nuclear and Plasma Sciences Society of the IEEE), San Diego, California, November 18-21, 1975, in the Journal of Applied Physics (in press), and has been submitted for publication to the Journal of Nuclear Materials.

Reflection of D^+, D^0, He^+, and He^0 from Surfaces

M. S. Kaminsky and P. J. Dusza

Measurements of the reflection coefficient for He^+ from highly polished Nb surfaces held in a high-vacuum environment have been started. The reflection coefficient is measured as a function of the helium-ion energy (0.1—1.0-MeV energy range) and the scattering angle.

C. LASER AND RADIOFREQUENCY SPECTROSCOPY OF FREE ATOMS AND MOLECULES

This research uses laser and radiofrequency techniques to study in detail the structure of atoms and molecules in beams and vapors. Traditional atomic-beam procedures are combined with the new techniques of laser spectroscopy to greatly increase the scope of the investigations. The principal goal is a continuing improvement in our understanding of atomic and molecular structure. The effort is focused primarily on the heaviest atoms (or molecules containing them) because of the increased difficulties structure theorists have with such systems. A secondary goal is to make certain that heavy, complex systems are probed in detail with the rapidly evolving and sophisticated laser techniques now being so widely applied elsewhere to lighter systems.

a. Laser-Quenching Spectroscopy of Actinide Molecules

W. J. Childs and L. S. Goodman

It has been known[1] for several years that placement of a vapor phase absorber inside the cavity of a laser can reveal absorption lines with 10^2—10^5 times the sensitivity found if the sample is placed outside. The increase in sensitivity, though partly due to multiple passes through the absorber, arises mainly from the fact that all photons absorbed by the vapor are no longer free for stimulating emission in the active (lasing) medium. In the present system, a broadband, flashlamp-pumped dye laser is used so that absorption by the vapor at discrete wavelengths quenches the lasing action only at those wavelengths. The Argonne 9-meter grating spectrograph is then used to analyze in detail the quenched spectra at high resolution.

The extreme sensitivity of the technique was clearly shown by our observation[2] of the $6\ ^2S_{1/2} \rightarrow 7\ ^2P_{3/2}$ transition in ^{133}Cs, with

[1] N. C. Peterson, M. J. Kurylo, W. Braun, A. M. Bass, and R. A. Keller, J. Opt. Soc. Am. 61, 746 (1971); R. J. Thrash, H. von Weyssenhoff and J. Shirk, J. Chem. Phys. 55, 4659 (1971).

[2] W. J. Childs, M. S. Fred, and L. S. Goodman, Appl. Optics 13, 2297 (1974).

learly resolved hyperfine structure, using a sample of fewer than 10^8 atoms of Cs. Molecular vapors are also easily detected. For example, extremely weak vibration-rotation H_2O lines are clearly seen from the air drifting through the laser cavity in a dehumidified room.

Observation[3] of very weak but sharp lines in the visible region of the spectrum of PuF_6 by conventional multi-pass techniques using very long exposures suggested that the laser-quenching technique might be ideally suited for a further investigation. In an experiment[4,5] that included the full cooperation of the Argonne Chemistry Division, quenching spectra were taken of $^{242}PuF_6$ in several spectral regions. The upper trace in Fig. 47 shows the results for one region; a great deal of very fine structure can be clearly seen. The resolution of individual lines far exceeds that of the earlier conventional spectra, and the improvement is probably due to the nonlinear nature of the quenching process as well as to other factors such as the greatly reduced exposure times required. The spectrum of a second absorption cell containing $^{239}PuF_6$ is shown in the lower section of Fig. 47. Although a substantial isotope shift is clearly seen for nearly every identifiable feature in this region of the spectrum, the shift varies from feature to feature, and in addition several other nearby regions show virtually no features with isotope shifts. This is the first observation of an isotope shift in an actinide molecule in the visible region of the spectrum. The bands observed are presumably due to vibronic superstructure on f^2 optical transitions, and the variation of the isotope shift from band to band shows

---

[3] M. Fred, private communication, 1974 (unpublished work performed in 1954).

[4] R. Kugel, C. Williams, M. Fred, J. Malm, W. T. Carnall, J. C. Hindman, W. J. Childs, and L. S. Goodman, "Isotope Effects in the Molecular Spectrum of Plutonium Hexafluoride," submitted to J. Chem. Phys., 1976.

[5] W. J. Childs, L. S. Goodman, R. Kugel, C. Williams, J. Malm, T. Carnall, M. Fred, and J. C. Hindman, "Isotope Shift in PuF_6 Observed by Laser-Quenching Spectroscopy," submitted to Fifth International Conference on Atomic Physics, Berkeley, California, July 26-30, 1976.

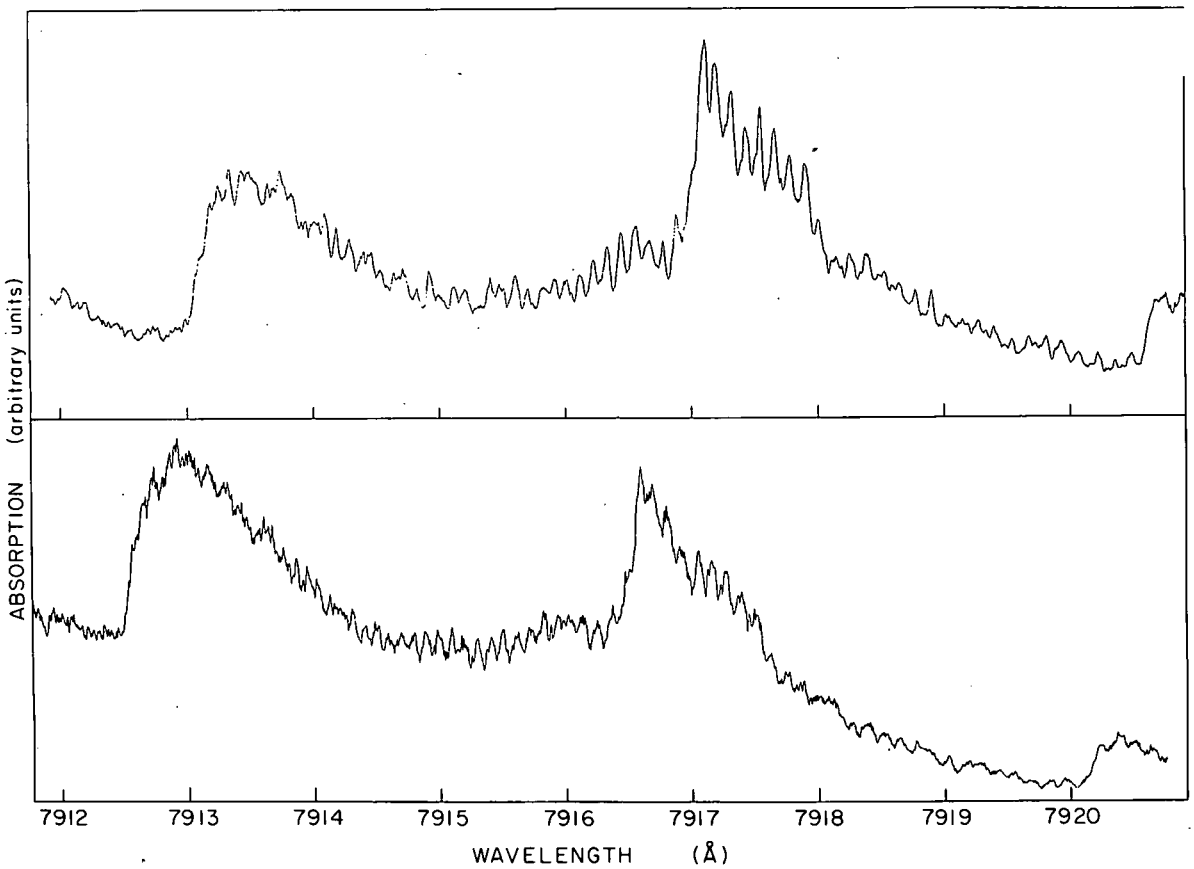

Fig. 47. Near-infrared section of the spectrum of PuF_6, obtained by intracavity laser-quenching spectroscopy. Upper trace $^{242}PuF_6$; lower trace $^{239}PuF_6$. The resolution of fine detail is considerably better than that previously achieved with conventional methods, and the isotope shifts shown are the first observed in the visible-near-infrared region for any actinide molecule.

great promise as a key to understanding the spectra (and structure) in detail. New theoretical attacks on the spectrum of PuF_6 and other small molecules containing heavy atoms can now be expected.

Preliminary work on IrF_6, for which the structure is much better understood theoretically, shows sharp lines in its quenching spectra, and an effort to observe isotope shifts with separated isotopes is underway. The interpretation may well be more straightforward than for PuF_6 for which even a preliminary analysis of the spectrum is not yet available.

Actinide Spectroscopy with Tunable Dye Lasers and Atomic Beams

W. J. Childs and L. S. Goodman

The very recent development of tunable, single-frequency dye lasers has suggested a rapidly increasing number of applications to atomic-beam studies of atomic structure. A well-collimated beam is clearly an ideal target for Doppler-free laser spectroscopy. Because of the extremely strong fluorescence that can be induced in atoms by laser light, laser fluorescence is often the most sensitive means of observing an atom. For this reason, laser-induced fluorescence may well be the most sensitive and selective (because of the ultranarrow linewidth) means of detecting atoms that have undergone resonance in a Rabi-type atomic-beam magnetic-resonance apparatus.

Preliminary tests with a beam of sodium irradiated by one component of the D_2 line showed very high sensitivity (a beam of density 10^5 atoms/cm^3 gave fluorescence easily visible to the naked eye). Rapid fluctuations of the laser frequency over a region broader than the Doppler width were very troublesome; however, the dye laser wavelength was then servoed to an external confocal Fabry-Perot interferometer, thus eliminating the rapid fluctuations and leaving only slower thermal changes. When proper collimation had been provided to shield the fluorescence-detecting photomultiplier from scattered laser light, the signal-to-background ratio increased to 10^5 for a sodium beam of about 2×10^{-10} amp. It was found straightforward to detect a beam of density 200 atoms/cm^3, since each atom can scatter many photons each second. When it is recognized that the Doppler width (30 MHz) for the geometry used is much greater than the laser linewidth ($\sim$1 MHz), it is seen that the fluorescence from less than one atom is being observed. The development of the laser system has now reached the stage that it is ready to be applied to heavy atoms.

In addition to serving as a detector for atoms that have undergone magnetic resonance, the laser system can of course be used in

other ways. For example, if the laser wavelength is swept, one observes the hyperfine components of both the lower and excited states of beam atoms without Doppler broadening, and then high precision hfs and isotope shift studies become possible. A number of other uses of the laser in connection with the atomic beam have been suggested and demonstrated by others for lighter atoms, and will be applied to the heavy atoms here at Argonne.

D. LOW-ENERGY POSITRON SOURCE DEVELOPMENT

L. S. Goodman and B. L. Donnally

Positronium is an excellent system in which to test quantum electrodynamical calculations because it is a completely leptonic system, and is uncomplicated by nuclear structure questions which arise in other hydrogenic systems. The major focus of this work is to measure the fine structure of excited states of positronium. It was only recently, after about 25 years of searches by various groups, that a group at Brandeis was able to detect an excited state of positronium, and make a relatively crude measurement of its fine structure. In the Brandeis work the excited positronium atoms are formed at surfaces and there exists the possibility that the atoms are not always completely free of the surfaces and are therefore perturbed by them. To avoid this potential difficulty, and to provide a measurement by an independent method, we seek to produce the positroniums by charge exchange in a beam and observe them in a region of sparse population of atoms.

To do this we must produce a beam of slow positrons (in the range of a few electron volts) substantially more intense than has been achieved before. In order to obtain low-energy positrons, fast positrons from a radioactive source or from pair production are thermalized in a moderator and the slow positrons emerging from the surface are transported to a region far away from the source where experiments can be done. Before we can optimize the intensity of such a source, we must learn something about the factors affecting positron emission at surfaces, a poorly understood phenomenon at this time. The question of what happens when positrons are emitted from some surfaces is important not only to try to get a better slow positron source, but also, in its own right, to try to develop new sources of understanding of surface properties.

In order to facilitate these studies, a bent solenoidal gnetic-field transport system was constructed. Experiments were

carried out that show that positrons first backscattered from a high-Z material are much more effective in producing slow positrons at surfaces, apparently because there are many more low-energy positrons than when the positrons are emitted directly from the radioactive source. There are found to be no substantial differences among the very high-Z materials in their effect in backscattering. Using the information gained already, a moderator assembly using lead as a backscatterer and magnesium oxide powder as an emitter surface, was constructed. This unoptimized-design assembly provided a yield of slow positrons (ratio of the number of slow positrons emitted at the surface to the number of positrons emitted by the radioactive sources) of 8×10^{-5}, about 2—3 times that best achieved previously.

Intense positron sources can be produced from the radioactive decay of appropriate isotopes made on line with either the cyclotron or the Dynamitron. The reactions which appear most promising are $^{10}B(d,n)^{11}C$, $^{11}B(p,n)^{11}C$, $^{12}C(d,n)^{13}N$, and $^{13}C(p,n)^{13}N$, with the $^{10}B(d,n)^{11}C$ reaction being the most likely prospect at low energy. However, the total reaction cross sections are poorly known, reported values for the same reaction differing by more than an order of magnitude, and experiments must be carried out to determine the optimum reaction and accelerator for low-energy positron production. The experiment has been designed, and equipment constructed, for the measurement of cross sections as a function of energy for positron-source-producing charged-particle reactions at the Tandem accelerator.

E. MÖSSBAUER EFFECT

Our Mössbauer Effect program stresses pioneering ventures in a wide range of fundamental scientific problems. A major fraction of the research lines of development radiating from the original discovery have begun at ANL. Six projects are being pursued or explored at present.

(1) Studies with ^{67}Zn. The principal technical superiority of the Mössbauer effect is the unique sharpness of the resonance, and among the nuclear transitions for which the effect has been observed, the 93.26-keV state in ^{67}Zn emits the narrowest line. Its width is 5×10^{-16} of its energy. We have studied a variety of properties of the transition and of a zinc oxide host in the past, by Doppler and by radio-frequency spectrometry. These methods are being applied to other hosts at present. A future plan is to measure the ether drift in the sense of the Michelson-Morley experiment with at least an order of magnitude greater sensitivity than has been done by other means.

(2) Coherent Phenomena in γ-Ray Emission. The recoil-free radiation possesses long coherence times associated with its narrow width. The radiation can be frequency modulated, or amplitude modulated, transmitted through resonant filters and subsequently demodulated with results calculable by classical optics and traditional methods of radio engineering. We are using frequency modulation in three ways: first as a means of detecting direct acoustic generation by microwaves in metals at low temperatures, second as a technique of spectrometry, and third as an intermediary to obtaining amplitude-modulation γ radiation.

(3) Local Structure in Liquids and Glasses. Examining the hyperfine structure of a given nucleus provides the most local probe of matter available. It is valuable to apply this to disordered materials for which detailed structural information is not available by other techniques. Our efforts to clarify the local structure should help in the understanding of such important processes as ionic diffusion and ionic mobility.

(4) x-Ray Mirrors. With visible light, such processes as microscopy, interferometry, and holography are of great importance. There is much to be gained by extending these methods to higher frequencies. Both excellent monochromaticity and intense fluxes in sharply defined directions are needed. Gamma rays, although superb in energy resolution, are too few in number. However, the present synchrotron ring SPEAR extends the available luminance more than a factor of 100, and future rings with wigglers will give another factor of more than 100. But such radiation comes buried in vast amounts of ff-resonance undesired intensity. Quite special x-ray mirrors composed

in part of the appropriate Mössbauer isotope, will be able to diffract just the desired frequencies into a new direction, thus creating the needed intense and monochromatic source.

(5) One-Dimensional Conductivity. A new kind of electrical conductivity has recently been found in certain layered inorganic and organic crystals. It requires the presence of partly oxidized bromine or iodine atoms. The conductivity is perpendicular to the layers and is so strongly anisotropic as to be called 'one dimensional.' Mössbauer studies of the local structure and the charge states of the iodine atoms in a few of these compounds has made an important contribution to the understanding of this phenomenon. Further measurements are needed to help design better crystals.

(6) Lake Michigan Sediments. The Mössbauer effect provides a method of nondestructive chemical analysis sensitive to the chemical composition of the sample studied. We have used the resonance in ^{57}Fe to study the distribution of iron oxide pollutants in Lake Michigan sediments.

a. Mössbauer Measurements with the 93.26-keV Transition in ^{67}Zn

G. J. Perlow, W. Potzel, and A. Forster

Experiments have been continued in order to detect the narrow resonance in other materials than zinc oxide. Samples of enriched zinc aluminum spinel and of the cubic form of enriched zinc sulfide have been tested. A broad resonance has been found in the former by Doppler spectrometry. The radio-frequency technique that we have used previously to make a precision measurement of the zinc oxide quadrupole coupling appears to be suited for further use here, and is to be tried. Experiments with ^{67}Zn involve some difficulties. The samples must have a high degree of local crystalline perfection, the source lifetime is relatively short and requires cyclotron bombardment for its preparation, and the experiments require liquid helium temperature. An interesting source of difficulty is that the relativistic time dilatation difference between source and absorber due to the difference in atomic zero point motion results in a line shift of one line width for each 1.3° difference in Debye temperature.

b. Coherent Phenomena in γ-Ray Emission

G. J. Perlow, W. Potzel, and W. Koch*

A major effort was the study of the direct generation of acoustic waves by microwaves in a metal at low temperature. The phenomenon has been observed by acoustic techniques in the past, but it was felt that the Mössbauer effect would lead to new insights. Experiments were done with a 700-MHz half-wave line terminated by a source of ^{57}Co in a copper foil. The direct generation process produces FM sidebands which are not absorbed by a Mössbauer absorber and result in an increase of counting rate during the pulse. The effect occurs but is masked by a very much larger effect which we believe to be due to an oscillator low temperature expansion phenomenon. Some puzzling features of the observations remain unexplained, however, and the experimentation is continuing.

A second set of measurements is connected with the possible production of coherent amplitude modulation of a γ ray through the intermediary of frequency modulation. The latter is produced by the Doppler effect in a source moved at high frequency by a piezo crystal. The emitted γ radiation is filtered through a resonant medium which alters the phase and amplitudes of the FM sidebands. The transmitted radiation is amplitude modulated in the process. This is detected by fast timing techniques.

*Technical University, Munich, Germany.

c. Atomic Motions in Liquids and Glasses

S. L. Ruby, J. C. Love, and P. A. Flinn*

To understand our test systems, we have utilized Mössbauer, Raman, and diffusion measurements. We have been able to show that the rapid increase in the vibration displacements as the glass

*Carnegie-Mellon University, Pittsburgh, Pennsylvania.

is heated into a supercooled liquid is consistent with the creation of very soft modes. The number of such new modes is proportional to the temperature above the glass transition temperature t_g, and the frequency of the mode (not separately detected yet) is related simply to the proportionality constant. Simultaneously, the diffusion constant is also increasing very rapidly, but a theory combining the vibration and diffusive processes is not available.

d. x-Ray Mirrors and Spatially Coherent Nuclear Scattering

S. L. Ruby

There are two major experimental problems delaying the progress of this work. One is a suitable detector, and the second is suitable crystals. During this year, we have made a careful study of all x-ray detection methods suitable to the requirements of this experiment. It is required to measure the arrival time of an infrequent single 10-keV photon in the midst of intense nanosecond wide, repetitive bursts of the same photons every microsecond. A new style detector has been designed, with which experiments demonstrating spatially coherent nuclear Bragg scattering can be performed, using merely enriched single crystals of iron. This will be the first demonstration of Bragg dispersion in time, in addition to the conventional dispersions in energy and angle.

e. One-Dimensional Conducting Iodides

S. L. Ruby and T. J. Marks*

Earlier Mössbauer studies of iodine in starch had initiated the problem of one-dimensional halide 'metals.' In solution, iodine atoms enter the hollow helix created by the starch molecules. Once oxidized, these iodine atoms strongly absorb light whose electric field is oriented parallel to the direction of the helix. Mössbauer studies had shown that the simplest picture—merely a chain of equivalent iodine—w

*Northwestern University, Evanston, Illinois.

ot appropriate. The results fit a model of distorted I_3^- ions. The new materials, e.g., $(bqd)_2Ni\ I_{.6}$ (closely related to Krogman's salt and TTF-TCNQ) synthesized and studied by conductivity and Raman techniques at Northwestern, showed very similar iodine Mössbauer spectra to the starch. The disproof of the presence of I_2 and I^- was particularly helpful. x-ray diffraction techniques had not been useful because of the non-stoichiometric disordered occupancy of the iodine positions.

f. Study of Lake Michigan Sediments by Mössbauer Spectroscopy

G. J. Perlow, W. Potzel, and A. Forster

Our earlier work established the existence of a magnetically ordered ferric oxide component in lower Lake Michigan sediments. Its depth dependence showed it to be associated with air pollution from the steel mills. We have since studied samples from other sediments, more remote from the mills. The component is present but in lesser abundance.

One consequence of the work is that it furnishes a method for dating recent sediments in areas not too remote from iron processing facilities.

F. SCANNING SECONDARY-ION MICROPROBE

Microscopic Location of Stable Tracer Isotopes

V. E. Krohn and G. R. Ringo

The aim of this project is to improve the present ion-microprobe analyzer very significantly in two respects—(1) space resolution and (2) mass resolution—to make it a much more useful instrument, particularly in biology. The ion-microprobe analyzer generally uses a beam of primary ions focused to a point whose diameter determines the space resolution of the instrument and is at present 1 to 2 μm. The primary beam is scanned over the specimen and a map of the distribution of an element or isotope of interest in the specimen is built up by detection of the secondary ions produced in the specimen and analyzed by a mass spectrometer of appropriate resolution, usually around 300.

We believe this instrument could be very useful in biology to map stable isotopes such as ^{13}C, ^{17}O, etc. used as tracers. However, for full usefulness it will be necessary to have enough mass resolution to distinguish ion pairs such as ^{17}O and ^{16}OH—about 5000—and the best practical space resolution—which we expect to be less than 50 nm.

The critical problem in this development is the achievement of these improvements in resolution without sacrificing too much of the intensity in the secondary-ion peaks of interest. In the first phase of this project we devised an extraction system for efficient collection of the secondary ions and their injection into the small phase space accepted by a high-resolution (25 000) mass spectrometer.[1] Next, using the arrangement shown in Fig. 48, we showed that a field-evaporation source emitting ions from the tip of a liquid metal cone, a source which is often called an electrohydrodynamic (or EHD) source, could produce a primary ion beam of very high brightness.[2] The maximum brightness we have

[1] V. E. Krohn and G. R. Ringo, Rev. Sci. Instr. 43, 1771 (1972).

[2] V. E. Krohn and G. R. Ringo, Appl. Phys. Lett. 27, 479 (1975).

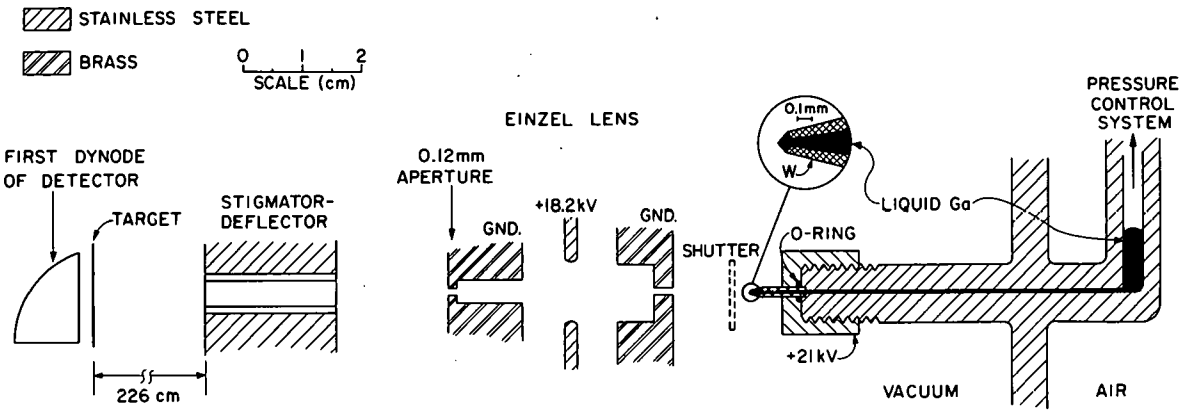

Fig. 48. Optical test bench for ion sources as arranged for the test of gallium.

achieved with this source[3] is 1.4×10^6 A $cm^{-2} sr^{-1}$ at 21 kV using gallium.

We are now planning a demonstration microprobe[3] which will have a gallium ion source of this kind. We are also planning a separate experiment in a commercial ion microprobe to determine the extent of the enhancement of the negative ion yields from sputtered biological substrates when neutral cesium is evaporated onto them.[4,5]

---

[3] V. E. Krohn and G. R. Ringo, submitted to Int. J. Mass Spectry. Ion Phys.

[4] Victor E. Krohn, Jr., J. Appl. Phys. 33, 3523 (1962).

[5] V. E. Krohn, Int. J. Mass Spectry. Ion Phys. (in press).

G. BEAM-FOIL MEASUREMENTS OF THE RADIATIVE SPECTRA, DECAY TIMES AND COLLISION DYNAMICS OF HEAVY IONS

This research program is aimed at developing a comprehensive understanding of multiply-ionized heavy ions; on the one hand, their atomic parameters such as the energy levels and radiative lifetimes, and on the other hand, their production, de-excitation and re-excitation by collisions in gases, solids, and at surfaces. One aspect of this study is to explore the systematic variation in energy of x-ray resonance radiation and fluorescence at lower energies (the vacuum-ultraviolet region). This information will also be valuable as a diagnostic tool in the analysis of thermonuclear plasmas. We hope to demonstrate which of the various decay channels for an excited, multiply-charged ion are most easily detectable and distinguishable from those of other species.

We can observe the photon spectrum from x rays to the visible region from the multiply-charged ions produced in ion beam impact on solid and gas targets. Wavelength shifts of resonance x-ray lines will reveal the ionization and excitation of the ions. Transition probabilities are obtained from lifetime studies: both the metastable levels and also allowed electric-dipole transitions of highly-stripped ions with lifetimes in the picosecond range.

Two accelerators, the 4-MeV Dynamitron and the Tandem, provide ions at energies from 1 MeV up to about 70 MeV.

Considerable collaboration with theoretical physicists at Argonne and elsewhere has been initiated for the interpretation of both the collision phenomena and the observed atomic transitions.

a. Orientation and Alignment of Fast Ion Beams

H. G. Berry, J. M. G. Desesquelles, and C. H. Batson

A thin carbon foil, with its surface tilted at an angle to the fast-beam direction, induces both orientation and alignment of excited atomic states, which are deduced from measurements of the polarization of the light emitted in radiative decays.

We have extended our neon-ion polarization measurements from normal incidence to 80° incidence angle, and show that the orientation (zero at normal incidence) increases monotonically with incidence angle

ur results are being compared in detail with the theory of Y. Band (see Sec. VIII. Hd). A spherical-tensor development of the bulk and surface interactions is able to reproduce the various observed angular dependences.

b. Orientation in Heavy Ions

H. G. Berry, J. M. G. Desesquelles, and C. H. Batson

A preliminary measurement in vanadium V has shown a 5% orientation signal in a ^2P-^2D transition for a tilted foil of 45° angle of incidence. As previous measurements in such heavy-ion beams with perpendicular foils have shown no alignment, the experiment promises new developments for quantum beat measurements in heavy ions.

One of these possibilities, under development, is the measurement of orientation of the fast beam scattered from a solid surface both with and without prefoil ionization and excitation.

An ultrahigh vacuum system is being prepared for observations of clean surfaces.

c. Circularly Polarized Quantum Beats in ^{14}N IV

H. G. Berry, R. M. Schectman, L. J. Curtis,* and D. G. Ellis*

The first circularly polarized zero-field quantum beats were observed in the 3s ^3S-3p ^3P transition of ^{14}N IV after excitation in a thin carbon foil tilted at 45° to the beam axis. Observations of both orientation and alignment light modulations verified the predictions of D. G. Ellis (Toledo) and also resulted in a measurement of the 3p ^3P state hyperfine constant A = 690 ± 15 MHz.

*University of Toledo, Toledo, Ohio.

d. Electric-Field Quantum Beats

H. G. Berry, J. M. G. Desesquelles, R. M. Schectman, and G. Gabrielse*

Application of an electric field after foil excitation of close-lying hydrogenic excited states has enabled us to observe coherence of opposite parity states (e.g., the 2s-2p states of H I). This excitation coherence is most easily shown as a change in phase of the quantum beats when a longitudinal electric field is reversed in sign.

We have continued our measurements in both H I (Ly α at 1216 Å and Ly β at 1025 Å) and He II, where the radiation occurs in the grazing incidence region (Ly β at 256 Å, Ly γ at 243 Å).

A comprehensive computer fitting program has been written by Gabrielse to aid in the analysis in terms of the initial excitation matrix. This program will also handle future measurements in electric fields and magnetic fields of arbitrary direction.

*University of Chicago, Chicago, Illinois.

e. Heavy-Ion Spectroscopy and Lifetimes

H. G. Berry and C. H. Batson

Lifetime measurements in vanadium V, an alkali-like ion, have been completed and published (for wavelengths between 500 Å and 5000 Å). Many identifications have been made for both this ion and other charge states in this same wavelength region, and preliminary spectra have been obtained for wavelengths down to 100 Å.

Similar spectra of foil-excited nickel show a great many unidentified lines in the spectral region 700 to 1500 Å and at higher wavelengths; we have thus far identified only the hydrogenic transitions. These latter have given approximate measurements of the core polarization for the ions V to IX.

. Grazing Incidence Spectra and Lifetimes (30—500 Å)

H. G. Berry, J. M. G. Desesquelles, R. M. Schectman, C. H. Batson, P. J. Tryon, and P. D. Schnur

We have modified the entrance optics of our McPherson grazing-incidence monochromator to obtain improved spatial resolution of the excited-ion beam. Thus, our observation lengths are now 40—100 microns, and we can observe the very fast decays expected in this short wavelength region.

Initial measurements in chlorine and argon have shown that we can now measure lifetimes of excited heavy ions down to a few picoseconds at the Dynamitron accelerator. A systematic investigation of the lifetimes of the ions Cl VI, Cl VII and Ar VII, Ar VIII was undertaken and completed. Comparisons were made with existing theoretical results and predictions of a Bates-Damgaard Coulomb approximation program written and run at the Argonne computer by Gerald Gabrielse (student at University of Chicago).

Further lifetime measurements are in progress in the Ne-I-like resonance lines of Cl and Ar. These transitions occur near 58 Å and 48 Å, respectively.

This work will be continued at the Tandem Van de Graaff accelerator where higher beam velocities should enable us to further improve our lifetime-measurement resolution to below one picosecond.

g. x-Ray Spectroscopy

J. M. G. Desesquelles and H. G. Berry

The resonance transitions of the more-highly-stripped ions occur in the soft to medium x-ray region. Thus, a bent-crystal high-resolution monochromator is on order and a target chamber is in preparation to extend our wavelength capability limit from 40 Å down to ' or 2 Å. We plan for the first experiments to be underway at the Tandem _ccelerator by summer of 1976. An essential part of the system is high

spatial resolution to enable us to continue our picosecond lifetime measurements into the x-ray region.

h. Excitation Amplitudes for Electron Impact of Hydrogen

Y. B. Band, H. G. Berry, and G. Gabrielse*

Electron excitation of close-lying hydrogen states produces coherence similar to that seen in foil-excitation (see Sec. VIII. Gd) and hence our analysis program has been similarly applied to such experiments on H_α emission by Mahan et al. at JILA. A published calculation of these coherence effects by Krotkov was incomplete in that it omitted $\ell, \ell+2$ coherence and hyperfine structure.

The foil-excitation analysis program has been adapted to analyze the electron-impact data using a Born-approximation calculation of the scattering amplitudes and to predict the intensity and polarization asymmetries observable from such excitation amplitudes.

Krotkov's results for the intensity variations have been reproduced, but in addition strong asymmetries have been found in the expected polarizations. From this preliminary work it appears that (a) a more accurate calculation would be useful and (b) several experiments can be suggested for measurements of these excitation amplitudes.

*University of Chicago, Chicago, Illinois.

i. Doubly-Excited States of 3-Electron Ions

H. G. Berry, J. M. G. Desesquelles, and R. M. Schectman

The beam-foil technique has previously been applied to classify transitions between multiply-excited states in the 3-electron systems of Li I, Be II, and B III, while electron spectra have provided low-energy-resolution data for isoelectronic O VI and F VII.

We have investigated spectra from the 3-electron systems of C IV and N V using a grazing-incidence monochromator at wavelengt

f 30 to 500 Å, and a normal-incidence monochromator for wavelengths up to 3000 Å. We have been able to verify other recent work in C IV at the higher wavelengths, but with much improved precision in determination of the energy levels.

H. THEORETICAL RESEARCH

The principal areas of investigation are collision/reaction theory, which relates to photoelectron-photoionization research, and studies of charge-exchange processes, which relate to experiments at higher energies.

A possibly important sidelight of the theoretical effort has been the development of a simple model which, although crude in its assumptions, appears to give a useful interpretation of the polarizations and alignments of beams produced by the passage of ions through tilted foils.

a. Dissociation Processes of Polyatomic Molecules

Yehuda B. Band and K. F. Freed*

We have developed a theory of the product energy dependence in photodissociation processes in polyatomic molecules, the primary initiation step in wide classes of photochemical reactions. The theory is of particular interest because the vibrational energy of the photoproducts can be used to do useful work, such as the development of photochemical lasers, the use of this energy to overcome activation barriers for subsequen chemical reactions, and the introduction of possible mechanisms for laser isotope separation. The description of the primary photodissociation process is, of course, of general scientific interest in the elucidation

---

*Department of Chemistry and James Franck Institute, University of Chicago, Chicago, Illinois.

of this important photochemical step, in the analysis of chemical dynamics, and in the general understanding of unimolecular decomposition reactions.

Early investigations of primary photochemical processes involved the analysis of the secondary, tertiary, etc. reactions of the photoproducts with various scavengers. Besides the inherent difficulties in this unraveling process, information concerning product energy distributions was often lost in collision processes. Recently, technological developments have begun to enable experimentation on the primary photodecomposition step.

Theoretical interest in photodissociation in polyatomic molecules has paralleled developments in the experiments. The available theories were generally predicated on the assumption that the bond that breaks in the photodissociation is also a normal coordinate in the initial bound molecular state. Furthermore, the changes in the remaining vibrational degrees of freedom, between the initial bound molecular state and the photofragments, was likewise generally not considered. An analysis of simple molecular models readily demonstrates the often drastic changes in these vibrations and the coupling of the dissociation coordinate to a number of the initial state vibrational normal modes. These two features of real molecular systems can be anticipated to have a significant influence on the nature of the energy distribution among the degrees of freedom of the photo products.

The current theory[1,2] incorporates the correct, and often known, normal modes of vibration for both the initial bound molecular state and for the final states of the fragments. The dissociation process is viewed as a two-step process; first there is a sudden Franck-Condon

[1] Y. B. Band and K. F. Freed, Chem. Phys. Lett. 28, 328 (1974).

[2] Y. B. Band and K. F. Freed, J. Chem. Phys. 63, 3382 (1975).

rearrangement process wherein the molecule makes a rapid transition from the bound to the dissociative electronic surface. This is followed by a vibrational relaxation process which occurs during the "half-collision" that ensues as the repelling fragments recede from each other. The latter has been widely studied in theories and experiments on vibrational relaxation processes, while the former is the new element of the theory.

A simple pictorial representation has been devised to summarize the energy distribution produced in the first Franck-Condon rearrangement step. It is shown how this part of the dissociation mechanism can lead to the occurrence of large vibrational population inversions in the photofragments, thereby providing potential candidates for photochemical lasers and for vibrationally excited molecules to enable the occurrence of subsequent chemical reactions that would otherwise be impossible. Although the vibrational relaxation process may alter this distribution, the simplicity of the theory of the sudden rearrangement process makes it an enormously useful screening tool for selecting potentially interesting cases. (In numerical studies of photodissociation processes in HCN and ICN, these vibrational relaxation effects are found to be negligible at the radiation wavelengths employed in the experiments. In CO_2,[3] on the other hand, the vibrational relaxation modifies the distributions only by about 15%.)

The sudden rearrangement process has also been shown to predict the occurrence of very large isotope effects in photodissociation processes.[4] These isotope effects vary exponentially as the difference of the square roots of the reduced mass of the departing atom with respect to the other fragment. This mechanism is probably responsible for the well known large deuterium isotope effect on predissociation rates in small organic molecules. It also provides a new possibility for laser isotope separation.

---

[3] Y. B. Band and K. F. Freed, J. Chem. Phys. 64, 4329 (1976).

[4] Y. B. Band and K. F. Freed, J. Chem. Phys. 63, 4479 (1975).

The full quantum theory of dissociation processes in polyatomic molecules has been converted into a form enabling the isolation of a selected fragment vibration.[5] This form enables the easy evaluation of the probability distribution of energy partitioning between this vibration and all other degrees of freedom that results from the sudden Franck-Condon rearrangement process. The resultant Franck-Condon factors involve the square of the one-dimensional overlap integral between effective oscillator wave functions and the wave functions for the selected fragment vibration, a form that resembles the simple golden rule model for polyatomic dissociation and reaction processes. The full quantum theory can, therefore, be viewed as providing both a rigorous justification for certain generic aspects of the simple golden rule model as well as providing a number of important generalizations thereof. Some of these involve dealing with initial bound state vibrational excitation, explicit molecule, fragment and energy dependence of the effective oscillator, and the incorporation of all isotopic dependence. In certain limiting situations the full quantum theory yields simple, readily usable analytic expressions for the frequency and equilibrium position of the effective oscillator. Specific applications are presented for the direct photodissociation of HCN, DCN, and CO_2 where comparisons between the full theory and the simple golden rule are presented. We also discuss the generalizations of the previous theory to enable the incorporation of effects of distortion in the normal modes as a function of the reaction coordinate on the repulsive potential energy surface.

[5] Y. B. Band and K. F. Freed, J. Chem. Phys. (to be published).

b. Photofragment Rotational-Population Distributions

Michael Morse,* Karl F. Freed,* and Yehuda B. Band

Although several theories have been proposed to predict fragment vibrational distributions in photodissociations,[1—3] a full quantum theory for rotational distributions has not been developed. This report presents a theory for rotational distributions arising from photofragmentations of a linear triatomic molecule.[4]

The probability of producing fragment state f from initial state i is given by

$$P_{fi} = \left| \sum_{\bar{f}} S_{ff\bar{}} \langle \psi_{\bar{f}} | V_{int} | \psi_i \rangle \right|^2,$$

where $\underset{\sim}{S}$ is the half-collision S matrix and V_{int} the coupling leading to photodissociation.[1] Because there is an extensive literature on the evaluation of collisional S matrices, for the moment ignore $\underset{\sim}{S}$ (i.e., take $\underset{\sim}{S} = \underset{\sim}{1}$). We start with Born-Oppenheimer wavefunctions for the initial and final states. For the initial state this consists of a product of an electronic function, a vibrational function for the three normal modes of vibration, and a wavefunction for the overall rotation of the molecule. For the final state there is a product of an electronic function, a vibrational function for the diatom stretch, a continuum function describing the relative translational motion of the fragments, a rotational function for the diatom, and a function describing the relative rotation of the fragments. After integration over the overall rotational degrees of freedom, and over electronic coordinates, a complicated three-dimensional

*Department of Chemistry and James Franck Institute, University of Chicago, Chicago, Illinois.

[1] Y. B. Band and K. F. Freed, J. Chem. Phys. 63, 3382 (1975).

[2] M. J. Berry, Chem. Phys. Lett. 27, 73 (1974).

[3] S. Mukamel and J. Jortner, J. Chem. Phys. (submitted).

[4] M. Morse, Y. Band, and K. Freed (to be published).

›ound-continuum vibrational integral remains because we have employed the normal coordinates appropriate to the different vibrations in the bound state and the diatomic fragment. Accurate analytical approximations have been devised to these bound-continuum generalized Franck-Condon factors which describe the sudden rearrangement when the molecule is excited from the bound to the repulsive electronic surface.

We have calculated distributions for the diatom rotational angular momentum j, and for the orbital angular momentum ℓ. It is found that, for the triatomic initially in its ground rotational state, the distributions for $j(j+1)$ and $\ell(\ell+1)$ are identical. For this case the diatomic fragment is found to have an average energy

$$\overline{E}_{rot} = \frac{\kappa^2 B}{(1-A)^2}(v+1)$$

and a dispersion

$$\sigma(E_{rot}) = \frac{\kappa^2 B}{(1-A)^2}\left[\frac{v^2}{2} + v + 1\right]^{1/2},$$

where κ, B, and A depend on bond lengths, force constants, etc. of particular molecule and v is the number of quanta initially excited in the bending mode of the triatomic. Thus, there will generally be considerable rotational excitation accompanying the photodissociation of linear triatomic molecules. The distribution for ℓ is independent of the initial triatomic rotational state, indicating that for high initial rotational states, most of the initial angular momentum is carried off as rotation of the diatomic fragment. We expect this result to be quite general, and are now proceeding to the case of bent triatomics and to an evaluation of the S matrix.

c. Theory of Alignment and Orientation in Beam-Foil Experiments

Yehuda B. Band

Preferential population of magnetic quantum states of an excited atomic state (n, ℓ) with a given angular-momentum quantum number ℓ is known to be produced in beam-foil collisions. Light emitted by decay of this excited state manifold is thereby partially polarized, and the Stokes parameters of the light are related to the alignment and orientation of the excited-state manifold. We employ a density-matrix formulation for describing the processes which lead to the production of the excited-state manifold.[1] The symmetry properties of the beam-foil interaction are analyzed to obtain the dependence of the alignment and orientation of the excited-state manifold as a function of the angle α between the beam direction and the foil normal when the foil is tilted relative to the beam.

In the interior of the foil, the density matrix for the atomic system has come into quasiequilibrium with the surrounding medium, so that it is axially symmetric about the beam direction and symmetric under reflections in any plane containing the axial symmetry axis. Thus, the density matrix may be written as

$$\rho = \sum_{n^{\ell}, n'^{\ell'}} \sum_{k=0}^{\ell+\ell'}{}' T_0^{[k]y}(n^{\ell}, n'^{\ell'}),$$

where $[k]$ is the rank of the irreducible tensors which all have the component of angular momentum along the beam axis (taken as the y axis) to be zero, and the prime on the sum over k restricts the k values such that $\ell + \ell' + k$ is even. This density matrix is propagated through the down-beam foil surface using an evolution operator which is constructed using a surface-interacting potential which depends upon the distance of the atomic electrons from the foil surface, and is therefore

[1] For a full account of this work see Y. B. Band, Phys. Rev. A 13, 2061 (June 1976).

axially symmetric about the foil normal $\hat{u}$. The α dependence of the evolved density matrix is analyzed using symmetry arguments. From the density matrix, the α dependence of the Stokes parameters for the light emitted normal to the $\hat{y}$-$\hat{u}$ plane is found to be of the form

$$S/I = c \tan \alpha / f(\alpha),$$

$$C/I = 2d \tan \alpha / f(\alpha),$$

$$M/I = -[e + (f + d \cos 2\alpha)/\cos^2 \alpha]/f(\alpha),$$

where $f(\alpha) = 1 + a/\cos^2 \alpha + b \cos 2\alpha/\cos^2 \alpha$, and the constants are related to reduced matrix elements $\langle n^{\ell} \| T^{[k]} \| n'^{\ell'} \rangle$, $\langle n^{\ell} \| r^{[1]} \| n'^{\ell'} \rangle$, and the detailed shape of the surface interaction potential.

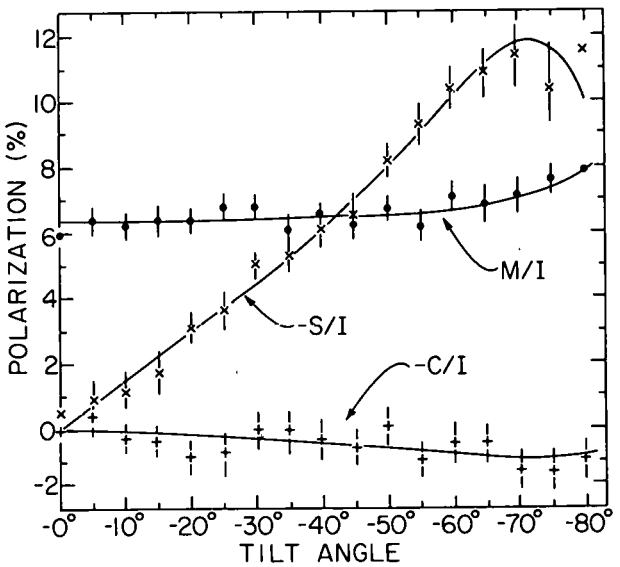

Fig. 49. Percentage polarizations S/I, C/I, M/I as a function of tilt angle for the NeIII 2866 Å $3p'^1F \rightarrow 3s'^1D$ transition with incident 1-MeV energy beam. Curves are the least-squares fit to the data.

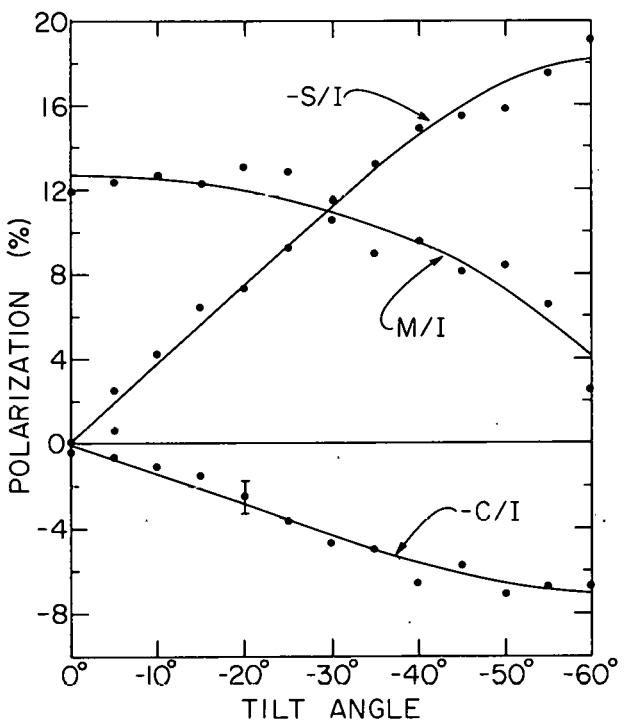

Fig. 50. Percentage polarizations S/I, C/I, M/I as a function of tilt angle for the HeI 5015 Å $3p^1P \rightarrow 2s^1S$ transition with incident 245-keV energy beam. Curves are the least-squares fit to the data. Representative error bar on data is shown.

Production of the excited state manifold by the process of capture of an electron from the surface when the atom is near the surface does not change the α dependence of the Stokes parameters in the above expressions.

Figures 49 and 50 compare the above expressions with data, where the constants were determined from a least-squares fit.

d. Differential Cross Sections for Electron Capture in Proton-Atom Collisions

Yehuda B. Band

Besides the usual questions concerning the criteria for validity of first-order perturbation theory (FOPT) for high-energy electron capture processes in proton-atom collisions, and the effects of non-orthogonality corrections upon FOPT,[1] there are two further crucial factors which must be considered in proton-multielectron-atom capture collisions: the effect of full inclusion of the proton-core interaction in FOPT (Full FOPT), thus taking into account the screening due to the distribution of the atomic electrons, and the difficult (unsolved) problem of determining the effect of the remaining electrons of the target atom upon the hydrogen atom once capture has occurred (final state interactions). Cocke et al.[2] measured the differential total capture cross section of K-shell Ar electrons by fast protons and found that it did not agree with several FOPT calculations which either totally neglected the proton-core interaction potential, including only the proton-electron interaction (OBK approximation), or only partially accounted for it.

Here we report the results of Full FOPT calculations for differential capture cross sections of protons on Ar and He.[3] Using the

---

[1] Y. B. Band, Phys. Rev. A 8, 2857 (1973).

[2] C. L. Cocke et al., Phys. Rev. Lett. 36, 782 (1976).

[3] Y. B. Band, to be published.

coordinate system introduced in Ref. 1, the Full FOPT amplitude for capture is given by

$$T_{fi} = \frac{\langle f|V_{Ae} + V_{AB}|i\rangle - \langle f|i\rangle\langle i|V_{Ae} + V_{AB}|i\rangle}{1 - |\langle f|i\rangle|^2},$$

where

$$|i\rangle = (2\pi)^{-3/2} e^{i\vec{k}_i \cdot \vec{R}'_A} \varphi_i(\vec{r}_B),$$

$$|f\rangle = (2\pi)^{-3/2} e^{-i\vec{k}_f \cdot \vec{R}'_B} \varphi_f(\vec{r}_A),$$

$$V_{Ae} = -r_A^{-1},$$

and the proton-core interaction

$$V_{AB}(\vec{R}) = Z_B R^{-1} - \sum_{j=1}^{Z_B - 1} |\psi_j(r)|^2 |\vec{R} - \vec{r}|^{-1} d^3r.$$

For Ar we have used a Thomas-Fermi electron distribution in the second term of V_{AB}. Figure 51 shows results of calculations with the OBK approximation, the Full FOPT, with $V_{AB} = 1/R(R^{-1}\text{FOPT})^2$, and the data of Cocke et al.[2] The OBK curve has a much steeper slope than the data points, the R^{-1}FOPT has a dark angle produced because of the cancellation of V_{Ae} and V_{AB} at the impact parameter corresponding to the dark angle and Full FOPT has the same general slope as the data but two orders of magnitude too large. The electron screening in V_{AB} accounts for the filling of the dark angle. Capture into excited states does not change the slope of the cross section and accounts for only a fraction of the total cross section. Given the poor agreement with theory, we might speculate that the final state interaction with the outer Ar electrons is responsible for the strong depletion of flux from the charge capture channel. This flux would be redistributed into the ionization channel for K-shell acancy producing processes. In the forward peak where the Full FOPT

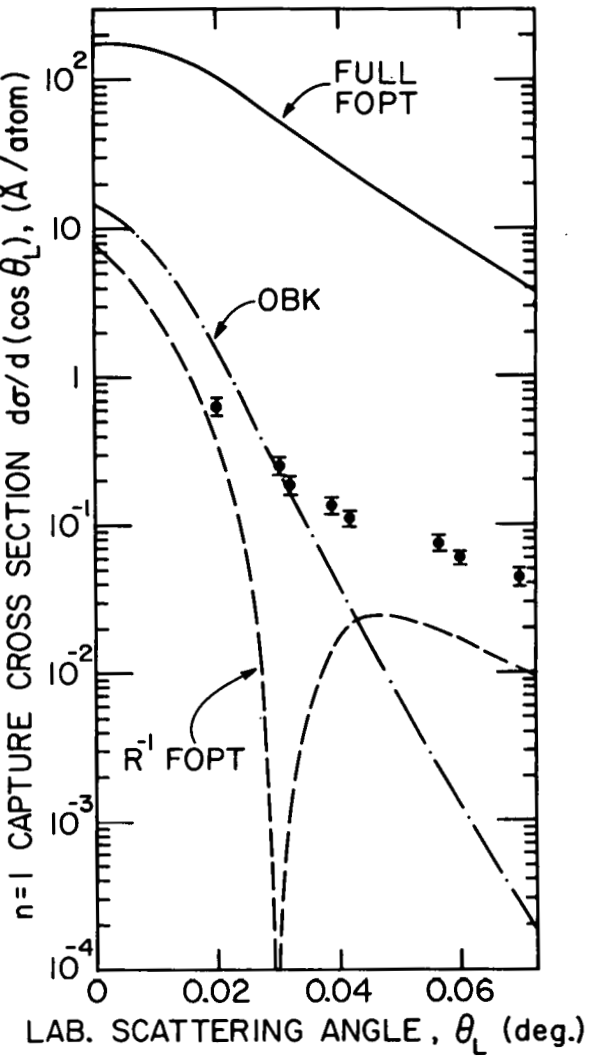

Fig. 51. Calculated differential cross sections p + Ar → H(1s) + Ar^+ for 6-MeV incident protons. Φ, data of C. L. Cocke et al.

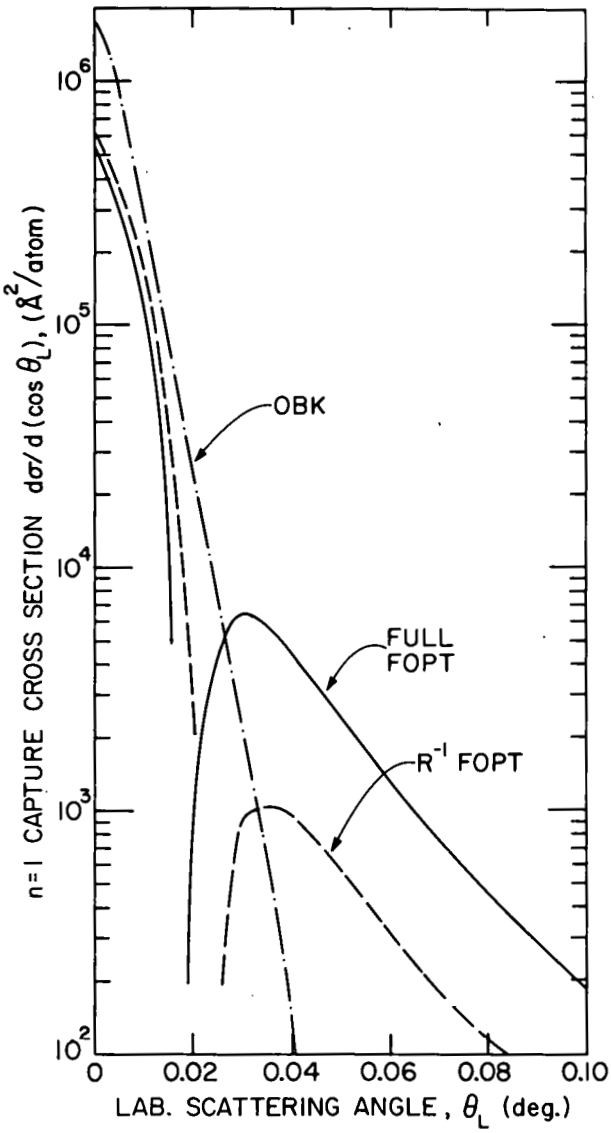

Fig. 52. Calculated differential capture cross sections p + He → H(1s) + He^+ for 300-keV incident protons.

angular distribution is large, the depletion would be weakly dependent upon scattering angle, and the shape of the capture cross section would remain unaltered. The cross section for K-shell vacancy production is several orders of magnitude larger than the K-shell capture cross section, so there is no inconsistency in speculating that the large capture cross section is converted into ionization by the final state interactions and accounts for at least part of the flux into K-shell ionization.

For proton-He capture collisions the final state interactions should produce only minor effects upon the differential capture cross section. Figure 52 shows the calculated differential cross sections for capture into H(1s). Excited state capture does not significantly alter the shape of the curves and is about 20% of ground-state capture. Differential cross-section experiments with a He target should be performed to test the theory and determine if there is a dark angle.

THIS PAGE
WAS INTENTIONALLY
LEFT BLANK

PUBLICATIONS FROM 1 APRIL 1975 THROUGH 31 MARCH 1976

The papers listed here are those whose publication was noted by the reporting unit of the Laboratory in the 1-year period stated above. The dates on the journals therefore often precede this period, and some dated within the period will be listed subsequently. The list of "journal articles and book chapters," which also includes letters and notes, is classified by topic; the arrangement is approximately that followed in the Table of Contents of this Annual Review. The "reports at meetings" include abstracts, summaries, and full texts in volumes of proceedings; they are listed chronologically.

A. PUBLISHED JOURNAL ARTICLES AND BOOK CHAPTERS

1. ABSOLUTE CROSS SECTIONS FOR PRODUCTION OF PROMPT NUCLEAR γ RAYS BY FAST PIONS
   H. E. Jackson, D. G. Kovar, L. Meyer-Schützmeister, S. E. Vigdor, T. P. Wangler, R. E. Segel, J. P. Schiffer, R. L. Burman,* P. A. M. Gram,* D. M. Drake,* V. G. Lind,† E. N. Hatch,† O. H. Otteson,† R. E. McAdams,† B. C. Cook,‡ and R. B. Clark§
   Phys. Rev. Lett. 35, 1170-1172 (27 October 1975)

2. SYSTEMATICS OF PION AND PROTON INTERACTIONS WITH Ni NUCLIDES
   H. E. Jackson, D. G. Kovar, L. Meyer-Schützmeister, R. E. Segel, J. P. Schiffer, S. Vigdor, T. P. Wangler, R. L. Burman,* D. M. Drake,* P. A. M. Gram,* R. P. Redwine,* V. G. Lind,† E. N. Hatch,† O. H. Otteson,† R. E. McAdams,† B. C. Cook,‡ and R. B. Clark §
   Phys. Rev. Lett. 35, 641-644 (8 September 1975)

---

*Los Alamos Scientific Laboratory, Los Alamos, New Mexico.

†Utah State University, Logan, Utah.

‡Iowa State University, Ames, Iowa.

§Texas A & M University, College Station, Texas.

3. SEARCH FOR EXOTIC MESON AND HYPERON FINAL STATES IN K^- INTERACTIONS AT 5.5 GeV/c
   R. Davis,* R. Ammar,* W. Kropac,* H. Yarger,* B. Werner,† Y. Cho,‡ D. Johnson,§ B. Musgrave,§ and T. Wangler
   Nucl. Phys. B96, 426-434 (29 September 1975)

4. OSCILLATIONS IN THE EXCITATION FUNCTION FOR COMPLETE FUSION OF $^{16}O + ^{12}C$
   P. Sperr, S. Vigdor, Y. Eisen, W. Henning, D. G. Kovar, T. R. Ophel, and B. Zeidman
   Phys. Rev. Lett. 36, 405-408 (23 February 1976)

5. $^{12}C(^{16}O, ^{12}C)^{16}O^*$ INELASTIC SCATTERING IN THE REGION OF THE $E_{c.m.}$ = 19.7-MeV RESONANCE
   P. Sperr, W. Henning, and J. R. Erskine
   Phys. Rev. C 13, 447-449 (January 1976)

6. STUDY OF DIRECT-REACTION CROSS SECTIONS IN COLLISIONS BETWEEN HEAVY IONS
   W. Henning, J. P. Schiffer, D. G. Kovar, S. Vigdor, B. Zeidman, Y. Eisen, and H.-J. Körner
   Phys. Lett. 58B, 129-131 (1 September 1975)

7. $^{12}C(^{12}C, \alpha)^{20}Ne$ EXCITATION FUNCTIONS AND ANGULAR DISTRIBUTIONS
   L. R. Greenwood, R. E. Segel, K. Raghunathan, M. A. Lee, H. T. Fortune, and J. R. Erskine
   Phys. Rev. C 12, 156-178 (July 1975)

8. TRANSFER OF THREE IDENTICAL NUCLEONS IN $^{16}O + ^{48}Ca$
   H. T. Fortune, W. Henning, D. G. Kovar, B. Zeidman, and Y. Eisen
   Phys. Lett. 57B, 445-446 (4 August 1975)

9. TWO-NUCLEON TRANSFER REACTIONS INDUCED BY ^{16}O ON ^{42}Ca AND ^{48}Ca
   Y. Eisen, H. T. Fortune, W. Henning, D. G. Kovar, S. Vigdor, and B. Zeidman
   Phys. Rev. C 13, 699-711 (February 1976)

---

*University of Kansas, Lawrence, Kansas.

†Community College of Allegheny County, Pittsburgh, Pennsylvania.

‡Accelerator Research Facilities Division, ANL.

§High Energy Physics Division, ANL.

10. EVIDENCE FOR A $^{12}C+^{12}C$ COLLECTIVE BAND IN ^{24}Mg
E. R. Cosman,* T. M. Cormier,* K. Van Bibber,* A. Sperduto,* G. Young,* J. Erskine, L. R. Greenwood, and Ole Hansen†
Phys. Rev. Lett. 35, 265-268 (4 August 1975)

11. RADIATIVE DEEXCITATION OF THE 7.655-MeV STATE OF ^{12}C
Cary N. Davids, Richard C. Pardo, and Andrew W. Obst
Phys. Rev. C 11, 2063-2068 (June 1975)

12. MASS-EXCESS PREDICTIONS FOR NEUTRON-RICH ISOTOPES NEAR IRON
Cary N. Davids
Phys. Rev. C 13, 887-889 (February 1976)

13. BACK-ANGLE ELASTIC ALPHA SCATTERING FROM ^{89}Y AND $^{90,91,94}Zr$
M. Wit,‡ J. Schiele,‡ K. A. Eberhard,‡ and J. P. Schiffer
Phys. Rev. C 12, 1447-1451 (November 1975)

14. STUDY OF THE ($^{6}Li, ^{6}He$) REACTIONS
W. R. Wharton and P. T. Debevec
Phys. Rev. C 11, 1963-1975 (June 1975)

15. $^{41}K(^{3}He,t)$ REACTION AT 25 MeV
M. Stautberg Greenwood, M. Pluta, L. R. Greenwood, and N. Anantaraman
Phys. Rev. C 11, 1983-1994 (June 1975)

16. $^{89}Y(^{3}He,t)$ REACTION AT 25 MeV
M. Stautberg Greenwood, M. Pluta, N. Anantaraman, and L. R. Greenwood
Phys. Rev. C 11, 1995-2000 (June 1975)

17. THE g-FACTOR OF THE 6^+ STATE OF ^{90}Nb
R. E. Holland, F. J. Lynch, R. J. Mitchell,§ T. V. Ragland,§ and R. P. Scharenberg§
Phys. Lett. 58B, 43-45 (18 August 1975)

---

*Massachusetts Institute of Technology, Cambridge, Massachusetts.

†Niels Bohr Institute, Copenhagen, Denmark.

‡Universität München, München, Germany.

§Purdue University, Lafayette, Indiana.

18. ISOMERISM IN ^{194}Au
S. W. Yates* and F. J. Lynch
Phys. Rev. C 12, 1080-1082 (September 1975)

19. EVIDENCE FOR AN ALIGNMENT EFFECT IN THE MOTION OF SWIFT ION CLUSTERS THROUGH SOLIDS
Donald S. Gemmell,† J. Remillieux,‡ J.-C. Poizat,‡ M. J. Gaillard,‡ Robert E. Holland, and Zeev Vager§
Phys. Rev. Lett. 34, 1420-1424 (9 June 1975)

20. NUCLEAR DATA FOR A=96 ISOBARS
L. R. Medsker
Nucl. Data Sheets B8, 599 (1972)

21. NUCLEAR DATA SHEETS FOR A = 97
L. R. Medsker
Nucl. Data Sheets 10, 1 (1973)

22. NUCLEAR DATA SHEETS FOR A = 98
L. R. Medsker
Nucl. Data Sheets 11, 157 (1974)

23. NUCLEAR DATA SHEETS FOR A = 99
L. R. Medsker
Nucl. Data Sheets 12, 431 (1974)

24. NUCLEAR RAMAN SCATTERING OF 11.387-MeV PHOTONS BY DEFORMED HEAVY NUCLEI
H. E. Jackson, G. E. Thomas, and K. J. Wetzel‖
Phys. Rev. C 11, 1664-1668 (May 1975)

25. THERMAL NEUTRON CAPTURE GAMMA RAYS FROM NEUTRON CAPTURE IN ^{59}Ni AND ^{63}Ni
W. M. Wilson, G. E. Thomas, and H. E. Jackson
Phys. Rev. C 11, 1477-1481 (April 1975)

---

*Chemistry Division, ANL.

†Universität München, München, Germany.

‡Université Claude Bernard, Lyon, France.

§Weizmann Institute of Science, Rehovot, Israel.

‖University of Portland, Portland, Oregon.

26. STATES IN ^{184}W VIA NEUTRON CAPTURE AND BETA-DECAY EXCITATIONS
D. L. Bushnell,* J. Hawkins,* R. Goebbert,* and R. K. Smither
Phys. Rev. C 11, 1401-1421 (April 1975)

27. SEARCH FOR STABLE, ABNORMAL (COLLAPSED) NUCLEI IN NATURE
R. J. Holt, J. P. Schiffer, J. Specht, L. M. Bollinger, G. E. Thomas, S. M. Fried,† J. J. Hines,† and A. M. Friedman†
Phys. Rev. Lett. 36, 183-186 (26 January 1976)
Erratum: Phys. Rev. Lett. 36, 689 (22 March 1976)

28. EVIDENCE FOR AN M1 GIANT RESONANCE IN ^{138}Ba
R. J. Holt and H. E. Jackson
Phys. Rev. C 12, 56-62 (July 1975)

29. VERY LOW ENERGY PHOTOFISSION OF ^{238}U
C. D. Bowman,‡ I. G. Schröder,‡ C. E. Dick,‡ and H. E. Jackson
Phys. Rev. C 12, 863-870 (September 1975)

30. PHOTONEUTRON POLARIZATION STUDIES OF THE GIANT M1 RESONANCE IN ^{208}Pb
R. J. Holt and H. E. Jackson
Phys. Rev. Lett. 36, 244-248 (2 February 1976)

31. AN INTEGRATING SCINTILLATION DETECTOR AS A BEAM MONITOR FOR HIGH RATES
Thomas P. Wangler and Steven E. Vigdor
Nucl. Instrum. Methods 129, 437-440 (15 November 1975)

32. SHELL-MODEL SYSTEMATICS OF THE ZIRCONIUM AND NIOBIUM ISOTOPES
D. H. Gloeckner
Nucl. Phys. A253, 301-323 (24 November 1975)

33. E6 TRANSITION IN ^{53}Fe
D. H. Gloeckner and R. D. Lawson
Phys. Rev. C 11, 1832-1835 (May 1975)

---

*Northern Illinois University, DeKalb, Illinois.

†Chemistry Division, ANL.

‡National Bureau of Standards, Washington, D.C.

34. THE ISOSPIN FORBIDDEN $1^- \rightarrow 0^+$ TRANSITION IN ^{40}Ca
D. H. Gloeckner* and R. D. Lawson
Phys. Lett. 56B, 301-304 (12 May 1975)

35. ASYMMETRY OF MIRROR γ DECAYS IN ^{13}C AND ^{13}N
D. Kurath
Phys. Rev. Lett. 35, 1546-1547 (1 December 1975)

36. THE PARTICLE-HOLE INTERACTION AND THE BETA DECAY OF ^{14}B
D. J. Millener† and D. Kurath
Nucl. Phys. A255, 315-338 (22 December 1975)

37. SHELL-MODEL STUDY OF THE N=49 ISOTONES
F. J. D. Serduke, R. D. Lawson, and D. H. Gloeckner
Nucl. Phys. A256, 45-86 (5 January 1976)

38. COLLECTIVE NUCLEAR STATES AS REPRESENTATIONS OF A SU(6) GROUP
A. Arima‡ and F. Iachello
Phys. Rev. Lett. 35, 1069-1072 (20 October 1975)

39. ELASTIC ELECTRON-DEUTERON SCATTERING AS A PROBE OF THE DEUTERON WAVE FUNCTION
F. Coester and A. Ostebee
Phys. Rev. C 11, 1836-1848 (May 1975)

40. SPIN SATURATION AND THE SKYRME INTERACTION
B. D. Chang
Phys. Lett. 56B, 205-208 (28 April 1975)
Ph. D. Thesis, University of Chicago, 1974

41. CALCULATION OF ODD AND DOUBLY-ODD NUCLEI WITH SKYRME-TYPE FORCES
K.-H. Passler
Nucl. Phys. A257, 253-263 (2 February 1976)

42. MICROSCOPIC DESCRIPTION OF THE REAL ALPHA-NUCLEUS POTENTIAL AT LARGE DISTANCES
Y. Eisen, B. Day, and E. Friedman§
Phys. Lett. 56B, 313-317 (12 May 1975)

---

*Rutgers University, New Brunswick, New Jersey.

†Oxford University, Oxford, England.

‡University of Tokyo, Tokyo, Japan.

§Hebrew University, Jerusalem, Israel.

43. DO LOWEST-ORDER APPROXIMATIONS ADEQUATELY DESCRIBE NUCLEAR MATTER?
V. R. Pandharipande,* R. B. Wiringa,* and B. D. Day
Phys. Lett. 57B, 205-209 (7 July 1975)

44. EFFECTS OF FINAL-STATE CHARGE EXCHANGE IN THE $(\pi, \pi N)$ REACTION ON NICKEL TARGETS
J. E. Monahan and F. J. D. Serduke
Phys. Rev. Lett. 36, 224-225 (26 January 1976)

45. COMMENTS ON "BOSE CONDENSATION IN SUPERCRITICAL EXTERNAL FIELDS"
Abraham Klein† and Johann Rafelski
Phys. Rev. D 12, 1194-1195 (1975)

46. EXPERIMENTAL TESTS AND IMPLICATIONS OF THE ZWEIG-IIZUKA RULE
H. J. Lipkin
Phys. Lett. 60B, 371-374 (2 February 1976)

47. NEW SYSTEMATICS IN HADRON TOTAL CROSS SECTION
Harry J. Lipkin
Phys. Rev. D 11, 1827-1831 (1 April 1975)

48. $^{48}Ti(^{3}He,t)^{48}V$ REACTION
J. C. Manthuruthil,‡ C. P. Poirier,‡ and L. Meyer-Schützmeister
Phys. Rev. C 11, 1141-1151 (April 1975)

49. MAGNETIC SPLITTING OF QUASIMOLECULAR ELECTRONIC STATES IN STRONG FIELDS
Johann Rafelski and Berndt Müller
Phys. Rev. Lett. 36, 517-520 (8 March 1976)

50. POSSIBLE EVIDENCE FOR THE EXISTENCE OF STRANGENESS ANALOG STATES
J. P. Schiffer and H. J. Lipkin
Phys. Rev. Lett. 35, 708-710 (15 September 1975)

51. GRAPHEASY—A GRAPHICAL EXTENSION TO SPEAKEASY
Stanley Cohen
Computer Graphics 9, 43-51 (Fall 1975)

---

*University of Illinois, Urbana, Illinois.

†University of Pennsylvania, Philadelphia, Pennsylvania.

‡Aerospace Research Laboratory, Wright-Patterson Air Force Base, Dayton, Ohio.

52. 'SPEAKEASY' PROVIDES ESCAPE FROM COMPLEX LANGUAGES
David C. Briery
Computerworld IX(25), 19 (18 June 1975)

53. THE STRUCTURE OF Tl_2F_2 FROM PHOTOELECTRON SPECTROSCOPY
D. G. Streets and J. Berkowitz
Chem. Phys. Lett. 38, 475-478 (15 March 1976)

54. PHOTOIONIZATION MASS SPECTROMETRIC STUDY OF FORMALDEHYDE H_2CO, HDCO AND D_2CO
Paul Marie Guyon, William A. Chupka, and Joseph Berkowitz
J. Chem. Phys. 64, 1419-1436 (15 February 1976)

55. HIGH RESOLUTION STUDY OF PHOTOIONIZATION PROCESSES IN O_2
P. M. Dehmer and W. A. Chupka
J. Chem. Phys. 62, 4525-4534 (1 June 1975)

56. WAVELENGTH DEPENDENCE OF THE PHOTOELECTRON ANGULAR DISTRIBUTIONS OF THE RARE GASES
J. L. Dehmer,* W. A. Chupka, J. Berkowitz, and W. T. Jivery
Phys. Rev. A 12, 1966-1973 (November 1975)

57. HIGH RESOLUTION PHOTOIONIZATION STUDY OF ION-PAIR FORMATION IN H_2, HD, AND D_2
W. A. Chupka, P. M. Dehmer, and W. T. Jivery
J. Chem. Phys. 63, 3929-3944 (1 November 1975)

58. PES OF HIGH TEMPERATURE VAPORS. VII. S_2 AND Te_2
J. Berkowitz
J. Chem. Phys. 62, 4074-4079 (15 May 1975)

59. MÖSSBAUER SPECTRA OF SOME ALKYLTELLURIUM(IV) COMPOUNDS
Kenneth V. Smith,† John S. Thayer,† and B. J. Zabransky
Inorg. Nucl. Chem. Lett. 11, 441-446 (1975)

60. Erratum: MÖSSBAUER STUDY OF ^{83}Kr IN THE COMPOUND KrF_2 [Phys. Rev. 147, 348 (1966)]
S. L. Ruby and H. Selig‡
Phys. Rev. B 12, 1991 (1 September 1975)

---

*Radiological and Environmental Research Division, ANL.

†University of Cincinnati, Cincinnati, Ohio.

‡Chemistry Division, ANL.

1. DIFFUSION OF IRON IONS IN A COLD LIQUID: EVIDENCE AGAINST A "JUMP" MODEL
   S. L. Ruby, J. C. Love, P. A. Flinn, and B. J. Zabransky
   Appl. Phys. Lett. 27, 320-322 (15 September 1975)

62. USE OF ^{57}Mn IN MÖSSBAUER RADIATION DAMAGE STUDIES
   R. S. Preston* and B. J. Zabransky
   Phys. Lett. 55A, 179-180 (1 December 1975)

63. ION SOURCE OF HIGH BRIGHTNESS USING LIQUID METAL
   V. E. Krohn and G. R. Ringo
   Appl. Phys. Lett. 27, 479-481 (1 November 1975)

64. MICROSCOPIC TRACING OF DEUTERIUM
   Walter Kisieleski† and Roy Ringo
   J. Microscopy (Oxford) 104, 199-204 (July 1975)

65. HYPERFINE QUANTUM BEATS IN ORIENTED ^{14}N IV
   H. G. Berry, L. J. Curtis,‡ D. G. Ellis,‡ and R. M. Schectman‡
   Phys. Rev. Lett. 35, 274-277 (4 August 1975)

66. MULTIPLY-EXCITED STATES IN BEAM-FOIL SPECTROSCOPY
   H. G. Berry
   Physica Scripta 12(1-2), 5-20 (1975)

67. EXPERIMENTAL LIFETIMES IN VANADIUM V
   H. G. Berry
   Physica Scripta 13, 36-38 (1976)

68. CORRELATION BETWEEN BLISTER SKIN THICKNESS, THE MAXIMUM IN THE DAMAGE-ENERGY DISTRIBUTION, AND PROJECTED RANGES OF He^+ IONS IN METALS: V
   M. Kaminsky, S. K. Das, and G. Fenske
   J. Nucl. Mater. 59, 86-89 (1976)

69. CORRELATION BETWEEN BLISTER SKIN THICKNESS, THE MAXIMUM IN THE DAMAGE-ENERGY DISTRIBUTION, AND PROJECTED RANGES OF He^+ IONS IN METALS: Nb
   M. Kaminsky, S. K. Das, and G. Fenske
   Appl. Phys. Lett. 27, 521-523 (15 November 1975)

---

*Northern Illinois University, DeKalb, Illinois.

†Biological and Medical Research Division, ANL.

‡University of Toledo, Toledo, Ohio.

70. 14.1-MeV NEUTRON SPUTTERING OF POLYCRYSTALLINE AND MONOCRYSTALLINE NIOBIUM WITH DIFFERENT SURFACE MICROSTRUCTURES
M. Kaminsky and S. K. Das
J. Nucl. Mater. 60, 111-116 (1976)

71. REDUCTION OF SURFACE EROSION CAUSED BY HELIUM BLISTERING: MICROSTRUCTURAL EFFECTS
S. K. Das, M. Kaminsky, and T. D. Rossing*
Appl. Phys. Lett. 27, 197-199 (15 August 1975)

B. PUBLISHED LECTURE SERIES

International School of Physics "Enrico Fermi," Varenna, Italy, 22 July-3 August 1974

1. NUCLEAR-STRUCTURE EFFECTS IN CLUSTER TRANSFER
D. Kurath
Nuclear Spectroscopy and Nuclear Reactions with Heavy Ions, Course LXII, edited by H. Faraggi and R. A. Ricci (Italian Physical Society, Bologna, 1976), pp. 58-81

---

*Northern Illinois University, DeKalb, Illinois.

C. PUBLISHED REPORTS AT MEETINGS

Fifth International Congress of Radiation Research, Seattle, Washington, 14-20 July 1974

1. PHOTOIONIZATION
   J. Berkowitz
   Radiation Research—Biomedical, Chemical, and Physical Perspectives (Proceedings of the Congress), edited by O. F. Nygaard, H. I. Adler, and W. K. Sinclair (Academic Press, New York, 1975), pp. 188-204
   + Abstracts of Papers, edited by O. F. Nygaard (Academic Press, New York, 1974), p. 89

IV International Conference on Vacuum Ultraviolet Radiation Physics, Hamburg, 22-26 July 1974

2. PHOTOELECTRON AND PHOTOION SPECTROSCOPY OF MOLECULES
   J. Berkowitz
   Vacuum Ultraviolet Radiation Physics (Proceedings of the Conference), edited by E. E. Koch, R. Haensel, and C. Kunz (Pergamon-Vieweg, 1974), pp. 107-136

3. EFFECT OF SPIN-ORBIT COUPLING ON THE WAVELENGTH DEPENDENCE OF ATOMIC BRANCHING RATIOS
   J. Berkowitz and J. L. Dehmer*
   Vacuum Ultraviolet Radiation Physics, pp. 160-162
   + Extended Abstract No. 10

Topical Conference on Problems of Vibrational Nuclei, Zagreb, Yugoslavia, 24-27 September 1974

4. SIMILARITIES BETWEEN THE Sm AND Cd, EVEN-Z, EVEN-N NUCLEI AND THE SYSTEMATICS OF THE LEVEL SCHEMES OF THE INTERVENING NUCLEI
   Robert K. Smither
   Fizika 7, Suppl. 2, 227-235 (1975) (Proceedings of the Conference, Vol. II, Contributed Papers)

---

*Radiological and Environmental Research Division, ANL.

Plasma Physics and Controlled Nuclear Fusion Research 1974 (Proceedin of the Fifth International Conference, Tokyo, 11-15 November 1974) (IAEA, Vienna, 1975)

5. PLASMA CONTAMINATION AND WALL EROSION IN CONTROLLED THERMONUCLEAR FUSION DEVICES AND REACTORS
   M. S. Kaminsky
   Vol. II, pp. 287-299

Report of the Workshop on BeV/Nucleon Collisions of Heavy Ions—How and Why, Bear Mountain, New York, 29 November-1 December 1974, organized by A. Kerman et al. (Brookhaven National Laboratory Associated Universities, Inc., 1975), BNL 50445

6. SEARCH FOR STABLE STRANGE NUCLEI
   John P. Schiffer
   pp. 61-66

Conference on Nuclear Cross Sections and Technology, Washington, D.C., 3-7 March 1975

7. ABSOLUTE CROSS SECTIONS FOR NEUTRONS FROM ^{6}Li+d REACTIONS AT ENERGIES BETWEEN 0.2 AND 0.9 MeV
   A. J. Elwyn, R. E. Holland, F. J. Lynch, J. E. Monahan, and F. P. Mooring
   Nuclear Cross Sections and Technology (Proceedings of the Conference), edited by R. A. Schrack and C. D. Bowman (National Bureau of Standards Special Publication 425, 1975), Vol. II, pp. 692-696
   + Bull. Am. Phys. Soc. 20, 163 (1975)

8. THRESHOLD PHOTONEUTRON SPECTROSCOPY OF NUCLEI NEAR A = 140
   R. J. Holt and H. E. Jackson
   Nuclear Cross Sections and Technology, Vol. II, pp. 784-787
   + Bull. Am. Phys. Soc. 20, 167 (1975)

9. OBSERVATION AND ANALYSIS OF ELASTIC NEUTRON SCATTERING FROM ^{12}C
   R. J. Holt, A. B. Smith,* and J. F. Whalen*
   Nuclear Cross Sections and Technology, Vol. I, pp. 246-249
   + Bull. Am. Phys. Soc. 20, 145 (1975)

---

*Applied Physics Division, ANL.

)75 Particle Accelerator Conference—Accelerator Engineering and echnology, Washington, D.C., 12-14 March 1975

10. HEAVY-ION ACCELERATION WITH A 5 $\lambda/2$ SUPERCONDUCTING-HELIX RESONATOR
J. Aron,* R. Benaroya,* L. M. Bollinger, B. E. Clifft,* A. H. Jaffey,* K. W. Johnson,* T. K. Khoe,† J. J. Livingood, P. J. Markovich,* J. M. Nixon,* G. W. Parker,* and W. A. Wesolowski*
Bull. Am. Phys. Soc. 20, 186 (1975)

11. ULTRA-SHORT PULSES OF HEAVY IONS
L. M. Bollinger, T. K. Khoe,† F. J. Lynch, B. Zeidman, R. Benaroya,* J. J. Bicek, Jr., B. E. Clifft,* A. H. Jaffey,* K. W. Johnson,* J. M. Nixon,* and W. A. Wesolowski*
IEEE Trans. Nucl. Sci. NS-22(3), 1148-1152 (June 1975)

12. UPGRADING THE ARGONNE 4-MV DYNAMITRON
F. P. Mooring, A. Langsdorf, Jr., and R. L. Amrein
IEEE Trans. Nucl. Sci. NS-22(3), 1726-1729 (June 1975)
+ Bull. Am. Phys. Soc. 20, 204 (1975)

13. MODIFICATION OF THE ARGONNE FN TANDEM
J. L. Yntema and P. J. Billquist
IEEE Trans. Nucl. Sci. NS-22(3), 1659-1661 (June 1975)
+ Bull. Am. Phys. Soc. 20, 202 (1975)

Clustering Phenomena in Nuclei: II (Proceedings of the Second International Conference, College Park, Maryland, 21-25 April 1975), edited by D. A. Goldberg, J. B. Marion, and S. J. Wallace (National Technical Information Service, Springfield, Virginia, 1975), ORO-4856-26

14. EVIDENCE FOR A $^{12}C+^{12}C$ COLLECTIVE BAND IN ^{24}Mg
E. R. Cosman,‡ T. M. Cormier,‡ K. Van Bibber,‡ A. Sperduto,‡ G. Young,‡ J. Erskine, L. Greenwood, and O. Hansen§
pp. 528-529

---

*Chemistry Division, ANL.

†Accelerator Research Facilities Division, ANL.

‡Massachusetts Institute of Technology, Cambridge, Massachusetts.

Niels Bohr Institute, Copenhagen, Denmark.

Clustering Phenomena in Nuclei, College Park, 21-25 April 1975 (Cont'c

15. CLUSTER SPECTROSCOPIC FACTORS—CONCEPT AND PRACTICE
    D. Kurath
    pp. 439-449 + discussion on pp. 450-452

16. CLUSTERS AND EXOTIC PROCESSES
    J. P. Schiffer
    pp. 329-342 + discussion on pp. 343-344

American Physical Society, Washington, D.C., 28 April-1 May 1975

17. PERFORMANCE CAPABILITIES OF THE TANDEM-LINAC HEAVY-ION ACCELERATOR CONCEPT
    Lowell M. Bollinger
    Bull. Am. Phys. Soc. 20, 686 (April 1975)

18. ULTRA-SHORT PULSES OF HEAVY IONS
    L. M. Bollinger, F. J. Lynch, B. Zeidman, R. Benaroya,* J. J. Bicek, B. E. Clifft,* K. W. Johnson,* and W. A. Wesolowski*
    Bull. Am. Phys. Soc. 20, 562 (April 1975)

19. FAST ANALOGUE COMPUTATION FOR PARTICLE IDENTIFICATION IN A MAGNETIC SPECTROGRAPH
    T. H. Braid and J. Bobis†
    Bull. Am. Phys. Soc. 20, 601 (April 1975)

20. STATEFIT: A COMPUTER PROGRAM TO FACILITATE THE INTERPRETATION OF SPECTROSCOPIC DATA
    S. B. Burson, G. T. Wood, and C. H. Batson
    Bull. Am. Phys. Soc. 20, 734 (April 1975)

21. EVIDENCE FOR A $^{12}C+^{12}C$ QUASI-MOLECULAR ROTATIONAL BAND IN ^{24}Mg
    E. R. Cosman,‡ T. M. Cormier,‡ K. Van Bibber,‡ A. Sperduto,‡ G. Young,‡ J. Erskine, L. R. Greenwood, and O. Hansen§
    Bull. Am. Phys. Soc. 20, 664 (April 1975)

---

*Chemistry Division, ANL.

†Electronics Division, ANL.

‡Massachusetts Institute of Technology, Cambridge, Massachusetts.

§Niels Bohr Institute, Copenhagen, Denmark.

APS, Washington, D. C., 28 April-1 May 1975 (Cont'd.)

22. HIGH-RESOLUTION PHOTOIONIZATION STUDY OF ION-PAIR FORMATION IN H_2, HD, AND D_2
P. M. Dehmer and W. A. Chupka
Bull. Am. Phys. Soc. 20, 729 (April 1975)

23. BACK-ANGLE EXCITATION FUNCTIONS OF $\alpha + {}^{39}K$ AND $\alpha + {}^{40,44}Ca$ SCATTERING BETWEEN 20 AND 27 MeV
K. A. Eberhard,* T. H. Braid, T. Renner, J. P. Schiffer, and S. Vigdor
Bull. Am. Phys. Soc. 20, 627 (April 1975)

24. ANGULAR DISTRIBUTIONS OF THE ${}^{48}Ca({}^{16}O, {}^{18}O){}^{46}Ca$ AND THE ${}^{42}Ca({}^{16}O, {}^{18}O){}^{40}Ca$ REACTIONS
Y. Eisen, H. T. Fortune, W. Henning, D. G. Kovar, T. R. Ophel, P. Sperr, S. Vigdor, and B. Zeidman
Bull. Am. Phys. Soc. 20, 574 (April 1975)

25. A COMBINED IONIZATION CHAMBER AND POSITION-SENSITIVE PROPORTIONAL COUNTER FOR THE DETECTION OF HEAVY IONS IN A MAGNETIC SPECTROGRAPH
J. R. Erskine, T. H. Braid, and J. C. Stoltzfus†
Bull. Am. Phys. Soc. 20, 602 (April 1975)

26. LEVELS IN ${}^{98}Nb$ FROM TWO-NUCLEON PICKUP
H. T. Fortune, L. R. Medsker,‡ and T. H. Braid
Bull. Am. Phys. Soc. 20, 719-720 (April 1975)

27. SOUTHWEST OF ${}^{88}Sr$
D. H. Gloeckner§ and F. J. D. Serduke
Bull. Am. Phys. Soc. 20, 599 (April 1975)

28. TOTAL AND PARTIAL DIRECT REACTION CROSS SECTIONS IN HEAVY-ION INDUCED REACTIONS
W. Henning
Bull. Am. Phys. Soc. 20, 621-622 (April 1975)

---

*University of Washington, Seattle, Washington.

†Beloit College, Beloit, Wisconsin.

‡University of Pennsylvania, Philadelphia, Pennsylvania.

§Rutgers University, New Brunswick, New Jersey.

APS, Washington, D. C., 28 April-1 May 1975 (Cont'd.)

29. ^{16}O AND ^{18}O INDUCED REACTIONS ON ^{118}Sn AT THE COULOMB BARRIER
H. J. Körner, Y. Eisen, W. Henning, D. G. Kovar, J. P. Schiffer, S. Vigdor, and B. Zeidman
Bull. Am. Phys. Soc. 20, 575 (April 1975)

30. FAST PION INDUCED PROCESSES IN COMPLEX NUCLEI: PROJECTILE SYSTEMATICS
D. G. Kovar, V. G. Lind,* E. N. Hatch,* O. H. Otteson,* R. E. McAdams,* H. E. Jackson, L. Meyer-Schützmeister, J. P. Schiffer, R. E. Segel, S. Vigdor, T. P. Wangler, R. L. Burman,† P. A. M. Gram,† D. M. Drake,† R. B. Clark,‡ and B. C. Cook§
Bull. Am. Phys. Soc. 20, 662 (April 1975)

31. FAST PION INDUCED PROCESSES IN COMPLEX NUCLEI: CROSS SECTION AND ALPHA REMOVAL
V. G. Lind,* E. N. Hatch,* O. H. Otteson,* R. E. McAdams,* H. E. Jackson, D. G. Kovar, L. Meyer-Schützmeister, J. P. Schiffer, R. E. Segel, S. Vigdor, T. P. Wangler, R. L. Burman,† P. A. M. Gram,† D. M. Drake,† R. B. Clark,‡ and B. C. Cook§
Bull. Am. Phys. Soc. 20, 662 (April 1975)

32. PARTIAL-WAVE STRUCTURE OF HEAVY-ION TRANSFER AMPLITUDES
M. H. Macfarlane
Bull. Am. Phys. Soc. 20, 555 (April 1975)

33. THE $^{50}Ti(^{3}He,t)^{50}V$ REACTION
J. C. Manthuruthil,‖ C. P. Poirier,‖ and L. Meyer-Schützmeister
Bull. Am. Phys. Soc. 20, 564 (April 1975)

---

*Utah State University, Logan, Utah.

†Los Alamos Scientific Laboratory, Los Alamos, New Mexico.

‡Texas A & M University, College Station, Texas.

§Iowa State University, Ames, Iowa.

‖Aerospace Research Laboratories, Wright-Patterson Air Force Base, Dayton, Ohio.

APS, Washington, D. C., 28 April-1 May 1975 (Cont'd.)

34. STUDY OF THE $^{54}Fe(\alpha,\gamma)^{58}Ni$ REACTION
L. Meyer-Schützmeister, W. Wharton, P. Debevec, R. E. Segel, and K. Raghunathan
Bull. Am. Phys. Soc. 20, 565 (April 1975)

35. MEASUREMENT OF THE g FACTOR OF THE 6^+, 88-μsec ISOMERIC STATE OF ^{90}Nb
R. J. Mitchell,* T. V. Ragland,* R. P. Scharenberg,* R. E. Holland, and F. J. Lynch
Bull. Am. Phys. Soc. 20, 566 (April 1975)

36. DECAY OF THE NEW NEUTRON-RICH ISOTOPE ^{53}Ti
Lewis A. Parks, Cary N. Davids, and Richard C. Pardo
Bull. Am. Phys. Soc. 20, 564 (April 1975)

37. NEUTRON "B(E2)" FROM INELASTIC PION SCATTERING
J. P. Schiffer, H. E. Jackson, D. G. Kovar, R. D. Lawson, L. Meyer-Schützmeister, R. E. Segel, S. Vigdor, and T. Wangler
Bull. Am. Phys. Soc. 20, 662-663 (April 1975)

38. FAST PION INDUCED PROCESSES IN COMPLEX NUCLEI: SYSTEMATICS IN PRODUCT NUCLEI
R. E. Segel, V. G. Lind,† E. N. Hatch,† O. H. Otteson,† R. E. McAdams,† H. E. Jackson, D. G. Kovar, L. Meyer-Schützmeister, J. P. Schiffer, S. Vigdor, T. P. Wangler, R. L. Burman,‡ P. A. M. Gram,‡ D. M. Drake,‡ R. B. Clark,§ and B. C. Cook‖
Bull. Am. Phys. Soc. 20, 662 (April 1975)

39. STUDY OF THE (^{16}O, ^{20}Ne) REACTION ON CALCIUM ISOTOPES AT E = 56 MeV
S. E. Vigdor, Y. Eisen, W. Henning, D. G. Kovar, T. Ophel, P. Sperr, and B. Zeidman
Bull. Am. Phys. Soc. 20, 574 (April 1975)

---

*Purdue University, Lafayette, Indiana.

†Utah State University, Logan, Utah.

‡Los Alamos Scientific Laboratory, Los Alamos, New Mexico.

§Texas A & M University, College Station, Texas.

‖Iowa State University, Ames, Iowa.

APS, Washington, D. C., 28 April-1 May 1975 (Cont'd.)

40. PERFORMANCE OF A SCINTILLATOR BEAM MONITOR SYSTEM FOR HIGH INTENSITY SECONDARY CHARGED-PARTICLE BEAMS
T. P. Wangler and S. E. Vigdor
Bull. Am. Phys. Soc. 20, 601 (April 1975)

41. A COMPARISON OF THE γ-RAY SPECTRA RESULTING FROM THERMAL NEUTRON CAPTURE AND 2.8-keV NEUTRON CAPTURE IN ^{23}Na
W. M. Wilson, G. E. Thomas, and H. E. Jackson
Bull. Am. Phys. Soc. 20, 572 (April 1975)

The Twenty-Third Annual Conference on Mass Spectrometry and Allied Topics, Houston, Texas, 25-30 May 1975 (American Society for Mass Spectrometry, 1975)

42. ION-PAIR FORMATION IN H_2, HD, AND D_2
J. Berkowitz and P. L. Kronebusch
pp. 117-118

43. PHOTOIONIZATION MASS SPECTROMETRIC STUDY OF CO_2 AND H_2O IN THE EXTREME ULTRAVIOLET
P. L. Kronebusch and J. Berkowitz
pp. 114-116

Effective Interactions and Operators in Nuclei (Proceedings of the Tucson International Topical Conference on Nuclear Physics, University of Arizona, Tucson, 2-6 June 1975), edited by B. R. Barrett (Springer-Verlag Berlin, 1975) (Lecture Notes in Physics 40)

44. IS THERE A UNIVERSAL RELATIONSHIP CONNECTING ALL TWO-BODY EFFECTIVE INTERACTIONS?
J. P. Schiffer
pp. 168-190

ixth International Conference on High Energy Physics and Nuclear tructure, Santa Fe and Los Alamos, 9-14 June 1975, edited by R. Mischke, C. Hargrove, and C. Hoffman (International Union of Pure and Applied Physics, 1975), Abstracts of Contributed Papers

45. ALPHA AND MULTINUCLEON REMOVAL FROM ^{58}Ni AND ^{60}Ni BY FAST PIONS
H. E. Jackson, D. G. Kovar, L. Meyer-Schützmeister, J. P. Schiffer, S. Vigdor, T. P. Wangler, R. E. Segel, R. L. Burman,* P. A. M. Gram,* D. M. Drake,* R. B. Clark,† B. C. Cook,‡ V. G. Lind,§ E. N. Hatch,§ O. H. Otteson,§ and R. E. McAdams§
p. 102

46. SYSTEMATICS OF FAST PION INDUCED PROCESSES IN COMPLEX NUCLEI
R. E. Segel, H. E. Jackson, D. G. Kovar, L. Meyer-Schützmeister, S. Vigdor, T. P. Wangler, J. P. Schiffer, V. G. Lind,§ E. N. Hatch,§ O. H. Otteson,§ R. E. McAdams,§ R. L. Burman,* P. A. M. Gram,* D. M. Drake,* and B. C. Cook‡
p. 103

American Physical Society, Knoxville, Tennessee, 16-18 June 1975

47. METHODS FOR THE REDUCTION OF SURFACE EROSION CAUSED BY HELIUM BLISTERING
S. K. Das, M. Kaminsky, and T. Rossing‖
Bull. Am. Phys. Soc. 20, 810 (June 1975)

48. INTERACTION OF FAST PIONS WITH COMPLEX NUCLEI
L. Meyer-Schützmeister
Bull. Am. Phys. Soc. 20, 821 (June 1975)

49. CORRELATION BETWEEN BLISTER SKIN THICKNESS AND PROJECTED RANGES OF He^+ IONS IN METALS: Nb AND V
M. Kaminsky, S. K. Das, and G. Fenske¶
Bull. Am. Phys. Soc. 20, 810 (June 1975)

---

*Los Alamos Scientific Laboratory, Los Alamos, New Mexico.

†Texas A & M University, College Station, Texas.

‡Iowa State University, Ames, Iowa.

§Utah State University, Logan, Utah.

‖Northern Illinois University, DeKalb, Illinois.

¶University of Illinois, Urbana, Illinois.

New Directions in Hadron Spectroscopy (Proceedings of the Summer Symposium, ANL, 7-10 July 1975), edited by S. L. Kramer and E. L. Berger, Argonne National Laboratory Report ANL-HEP-CP-75-58

50. SPECTROSCOPY AFTER THE NEW PARTICLES
Harry J. Lipkin
pp. 96-114

Proceedings of the International Conference on Radiation Test Facilities for the CTR Surface and Materials Program, Argonne National Laboratory, 15-18 July 1975, organized by P. J. Persiani, M. M. Cohen, and K. M. Zwilsky, Argonne National Laboratory Report ANL/CTR-75-4

51. CONSIDERATIONS OF TEST FACILITY REQUIREMENTS FOR CTR SURFACE SCIENCE EXPERIMENTS
M. Kaminsky
pp. 16-45

Electronic and Atomic Collisions (Abstracts of Papers of the IXth International Conference on the Physics of Electronic and Atomic Collisions, Seattle, 24-30 July 1975), edited by J. S. Risley and R. Geballe (University of Washington Press, Seattle, 1975)

52. PHOTOIONIZATION MASS SPECTROMETRIC STUDY OF SEVERAL MOLECULES IN THE EXTREME ULTRAVIOLET
J. Berkowitz, P. L. Kronebusch, and P. M. Larson
Vol. 1, pp. 12-13

53. HIGH-RESOLUTION STUDY OF PHOTOIONIZATION PROCESSES IN H_2, HD, AND D_2
W. A. Chupka, P. M. Dehmer, and W. T. Jivery
Vol. 2, pp. 1130-1131

54. WAVELENGTH DEPENDENCE OF PHOTOELECTRON ANGULAR DISTRIBUTIONS. Kr, Xe, AND N_2
J. L. Dehmer,* W. A. Chupka, and J. Berkowitz
Vol. 1, pp. 565-566

55. PHOTOELECTRON SPECTROSCOPY OF VERY HIGH TEMPERATURE VAPORS PRODUCED BY LASER-INDUCED VAPORIZATION
D. G. Streets, K. Radler, and J. Berkowitz
Vol. 2, pp. 705-706

---

*Radiological and Environmental Research Division, ANL.

pplications of Ion Beams to Materials, 1975 (Proceedings of the nternational Conference, University of Warwick, 8-12 September 1975), edited by G. Carter, J. S. Colligon, and W. A. Grant (Institute of Physics, Conference Series Number 28, London, 1976)

56. CORRELATION BETWEEN BLISTER SKIN THICKNESS, THE MAXIMUM IN THE DAMAGE-ENERGY DISTRIBUTION, AND THE PROJECTED RANGES OF He^+ IONS IN METALS: A COMPARISON FOR Al, V, AND Nb
S. K. Das, M. Kaminsky, and G. Fenske
Chap. 7, pp. 293-298

Beam-Foil Spectroscopy (Proceedings of the Fourth International Conference, Gatlinburg, Tennessee, 15-19 September 1975), edited by I. A. Sellin and D. J. Pegg (Plenum, N.Y., 1976)

57. SPECTROSCOPY OF HEAVY IONS USING THE BEAM-FOIL TECHNIQUE
H. G. Berry and C. H. Batson
Vol. 1, pp. 367-375

58. THE SURFACE INTERACTION IN BEAM FOIL SPECTROSCOPY
H. G. Berry, L. J. Curtis,* D. G. Ellis,* R. D. Hight,* and R. M. Schectman*
Vol. 2, pp. 755-771

59. PROBLEMS OF QUANTUM ELECTRODYNAMICS IN HEAVY-ION COLLISIONS
Berndt Müller
Vol. 2, pp. 483-495

60. DOUBLY-EXCITED STATES IN B III
K. X. To,† E. J. Knystautas,† R. Drouin,† and H. G. Berry
Vol. 1, pp. 385-391

Ion Beam Surface Layer Analysis, Vol. 2 (Proceedings of the International Conference, Karlsruhe, Germany, 15-19 September 1975), edited by O. Meyer, G. Linker, and F. Käppeler (Plenum, N.Y., 1976)

61. HELIUM TRAPPING IN ALUMINUM AND SINTERED ALUMINUM POWDERS
S. K. Das, M. Kaminsky, and T. Rossing
pp. 567-574

---

*University of Toledo, Toledo, Ohio.

†Université Laval, Quebec, Canada.

Proceedings of the VIth International Conference on Atomic Collisions in Solids, Amsterdam, 22-26 September 1975

62. SOME NEW EFFECTS SEEN IN THE PASSAGE OF SWIFT ION CLUSTERS THROUGH SOLIDS
Donald S. Gemmell, J. Remillieux,* J.-C. Poizat,* M. J. Gaillard,* Robert E. Holland, and Zeev Vager
Nucl. Instrum. Methods 132, 61-67 (1976)

Atomic Spectroscopy Symposium, National Bureau of Standards, Gaithersburg, Maryland, 23-26 September 1975, organized by John G. Conway et al. (National Bureau of Standards, 1975), Program and Abstracts

63. THE CONFIGURATIONS $5f^N 7s^2 7p$ IN THE NEUTRAL ACTINIDES
Mark Fred,† William J. Childs, Hannah M. Crosswhite,† and Jean E. Blaise‡
p. 128

Fourth Annual International Conference of the Nuclear Target Development Society, Argonne National Laboratory, Argonne, Illinois, 30 September-2 October 1975

64. THIN FOILS FOR BEAM-FOIL SPECTROSCOPY
H. G. Berry
Proceedings of the Conference, edited by G. E. Thomas and F. J. Karasek, Physics Division Informal Report ANL/PHY/MSD-76-1 (1976), pp. 193-204
+ Program of the Conference, Abstract C-4

65. BEAM HEATING OF TARGET FOILS
W. C. Corwin
Proceedings, pp. 221-230

66. TARGETS FOR HIGH-RESOLUTION STUDIES WITH HEAVY-ION REACTIONS
John R. Erskine
Proceedings, pp. 141-166
+ Program of the Conference, Abstract C-1

---

*Université Claude Bernard, Lyon, France.

†Chemistry Division, ANL.

‡Laboratoire Aimé Cotton, Orsay, France.

onference of the Nuclear Target Development Society, ANL,
0 September-2 October 1975 (Cont'd.)

67. PREPARATION OF CALCIUM-SEPARATED ISOTOPE TARGETS USING SMALL SAMPLES
G. E. Thomas
Proceedings, pp. 255-267
+ Program of the Conference, Abstract D-6

68. TARGET VACUUM STORAGE FACILITY
J. N. Worthington, R. J. Jedlowski, and G. E. Thomas
Proceedings, pp. 68-74
+ Program of the Conference, Abstract A-6

69. CARBON FOILS AS HEAVY ION STRIPPERS
J. L. Yntema
Proceedings, pp. 188-192
+ Program of the Conference, Abstract C-3

1975 Annual Meeting, Optical Society of America, Boston, Massachusetts,
21-24 October 1975

70. HYPERFINE STRUCTURE, NUCLEAR MOMENTS, AND CONFIGURATION INTERACTION IN NEUTRAL ^{237}Np
M. Fred,* W. J. Childs, J. E. Blaise,† and P. Camus†
J. Opt. Soc. Am. 65, 1188 (October 1975)

Division of Nuclear Physics, American Physical Society, Austin, Texas,
30 October-1 November 1975

71. A NEW NEUTRON-RICH MANGANESE ISOTOPE: ^{59}Mn
C. N. Davids, E. B. Norman, R. C. Pardo, and L. A. Parks
Bull. Am. Phys. Soc. 20, 1164 (September 1975)

72. ELASTIC ALPHA SCATTERING AND THE N-N FORCE
Y. Eisen and B. Day
Bull. Am. Phys. Soc. 20, 1159 (September 1975)

73. LOW-ENERGY CROSS SECTIONS OF POTENTIAL INTEREST IN THERMONUCLEAR APPLICATIONS: ^{6}Li + d
A. J. Elwyn
Bull. Am. Phys. Soc. 20, 1153 (September 1975)

---

*Chemistry Division, ANL.

†Laboratoire Aimé Cotton, Orsay, France.

APS, Austin, Texas, 30 October-1 November 1975 (Cont'd.)

74. THRESHOLD PHOTONEUTRON STUDIES OF THE GIANT M1 RESONANCE REGION OF ^{138}Ba AND ^{208}Pb
R. J. Holt
Bull. Am. Phys. Soc. 20, 1186 (September 1975)

75. CROSS SECTION SYSTEMATICS FOR TRANSFER REACTIONS INDUCED BY ^{16}O ON $^{40,42,44,48}Ca$ AT 56 MeV
D. Kovar, S. Vigdor, Y. Eisen, P. Sperr, W. Henning, T. Ophel, and B. Zeidman
Bull. Am. Phys. Soc. 20, 1191 (September 1975)

76. AN "EXACT" CALCULATION OF THE LOWEST ORDER π-NUCLEUS OPTICAL POTENTIAL
T.-S. H. Lee
Bull. Am. Phys. Soc. 20, 1192 (September 1975)

77. MEASUREMENT OF THE g FACTOR OF THE $\frac{3}{2}^+$, 630-μsec ISOMERIC STATE IN ^{43}Sc
R. J. Mitchell,* T. V. Ragland,* R. P. Scharenberg,* R. E. Holland, and F. J. Lynch
Bull. Am. Phys. Soc. 20, 1163 (September 1975)

78. POSSIBLE EVIDENCE FOR THE EXISTENCE OF STRANGENESS ANALOG STATES
J. P. Schiffer and H. J. Lipkin
Bull. Am. Phys. Soc. 20, 1159-1160 (September 1975)

79. FLUCTUATIONS IN THE EXCITATION FUNCTION FOR COMPLETE FUSION OF $^{16}O + ^{12}C$
P. Sperr, Y. Eisen, W. Henning, D. G. Kovar, T. Ophel, S. Vigdor, and B. Zeidman
Bull. Am. Phys. Soc. 20, 1174 (September 1975)

80. TOTAL REACTION CROSS SECTIONS FOR $^{16}O + ^{40,42,44,48}Ca$ AT $E_L(^{16}O) = 56$ MeV
S. Vigdor, D. G. Kovar, Y. Eisen, W. Henning, T. Ophel, P. Sperr, and B. Zeidman
Bull. Am. Phys. Soc. 20, 1191 (September 1975)

---

*Purdue University, Lafayette, Indiana.

roceedings of the Sixth Symposium on Engineering Problems of Fusion Research, San Diego, California, 18-21 November 1975 (IEEE Service Center, Piscataway, New Jersey, 1976), IEEE Pub. No. 75CH1097-5-NPS

81. X-RAY IMPACT INDUCED DESORPTION OF GASES FROM STAINLESS STEEL SURFACES
S. Brumbach and M. Kaminsky
pp. 1135-1140

82. REDUCTION OF SURFACE EROSION CAUSED BY HELIUM BLISTERING: COMPARISON BETWEEN VACUUM-CAST AND SINTERED-BERYLLIUM
S. K. Das and M. Kaminsky
pp. 1151-1153

83. IRRADIATION OF GRAPHITE CLOTH AT VARIOUS TEMPERATURES WITH DEUTERONS AND HELIUM IONS
R. Ekern, S. K. Das, and M. Kaminsky
pp. 1146-1150

84. PARTICLE EMISSION FROM POLYCRYSTALLINE AND MONOCRYSTALLINE NIOBIUM UNDER 14.1 MeV NEUTRON IMPACT
M. Kaminsky and S. K. Das
pp. 1141-1145

Division of Electron and Atomic Physics, American Physical Society, Tucson, Arizona, 3-6 December 1975

85. FORMATION AND REACTIONS OF METASTABLE H AND D ATOMS IN H_2, HD, AND D_2
W. A. Chupka* and P. M. Dehmer
Bull. Am. Phys. Soc. 20, 1454 (November 1975)

86. DECAY OF RYDBERG STATES OF H_2
P. M. Dehmer and W. A. Chupka*
Bull. Am. Phys. Soc. 20, 1457 (November 1975)

87. HIGH-RESOLUTION PHOTOIONIZATION STUDY OF AUTOIONIZING STATES OF ATOMIC OXYGEN
P. M. Dehmer, W. A. Chupka,* and W. Luken*
Bull. Am. Phys. Soc. 20, 1460 (November 1975)

---

*Yale University, New Haven, Connecticut.

American Physical Society, New York, 2-5 February 1976

88. MOLECULAR-DYNAMICS APPROACH TO HIGH-ENERGY COLLISIONS OF NUCLEI
A. R. Bodmer and C. N. Panos
Bull. Am. Phys. Soc. 21, 13 (January 1976)

89. RELATIVISTIC HARTREE CALCULATIONS OF THE NUCLEAR SURFACE
J. Boguta and A. R. Bodmer
Bull. Am. Phys. Soc. 21, 49 (January 1976)

90. DIFFUSION OF IONS IN A SUPERCOOLED LIQUID
J. C. Love,* S. L. Ruby, and B. J. Zabransky
Bull. Am. Phys. Soc. 21, 21 (January 1976)

91. MÖSSBAUER SCATTERING FROM PAIRS OF NUCLEI
S. L. Ruby
Bull. Am. Phys. Soc. 21, 22 (January 1976)

92. THE $^{37}Cl(\alpha,d)^{39}Ar$ REACTION AT 27 MeV
R. E. Segel, J. F. Tonn, W. C. Corwin, and L. L. Rutledge†
Bull. Am. Phys. Soc. 21, 82 (January 1976)

93. THE $^{40}Ar(p,d)^{39}Ar$ REACTION AT 35 MeV
J. F. Tonn, R. E. Segel, P. T. Debevec, W. S. Chien,‡ and J. A. Nolen‡
Bull. Am. Phys. Soc. 21, 82 (January 1976)

Proceedings of SHARE XLVI, San Francisco, 22-27 February 1976 (SHARE Inc., 1976)

94. A SPEAKEASY SAMPLER: LEVEL LAMBDA
Stan Cohen
Vol. III, pp. 1730-1739

95. SPEAKEASY AND STATISTICS
S. Cohen and M. L. Hopper§
Vol. III, pp. 1631-1633

---

*Florida Institute of Technology, Melbourne, Florida.

†Northwestern University, Evanston, Illinois.

‡Michigan State University, East Lansing, Michigan.

§Applied Mathematics Division, ANL.

D. TOPICAL REPORTS

1. A GUIDE TO TSO SPEAKEASY
   S. Cohen, J. Fink, F. J. D. Serduke, and H. Z. Kriloff*
   Argonne National Laboratory Topical Report ANL-75-44
   (October 1975)

2. PTOLEMY—A PROGRAM FOR HEAVY-ION DIRECT-REACTION CALCULATIONS
   D. H. Gloeckner, M. H. Macfarlane, and Steven C. Pieper
   Argonne National Laboratory Topical Report ANL-76-11
   (March 1976)

E. PHYSICS DIVISION INFORMAL REPORTS

1. STATEFIT: A COMPUTER PROGRAM TO FACILITATE THE INTERPRETATION OF SPECTROSCOPIC DATA
   S. B. Burson, G. T. Wood, and C. H. Batson
   Physics Division Informal Report ANL-PHY-75-1
   (May 1975)

2. PROCEEDINGS OF THE FOURTH ANNUAL INTERNATIONAL CONFERENCE OF THE NUCLEAR TARGET DEVELOPMENT SOCIETY, Argonne National Laboratory, Argonne, Illinois, 30 September-2 October 1975
   edited by G. E. Thomas and F. J. Karasek†
   Physics Division Informal Report ANL/PHY/MSD-76-1
   (1976)

---

*University of Illinois, Chicago Circle Campus, Chicago, Illinois.

†Materials Science Division, ANL.

THIS PAGE

WAS INTENTIONALLY

LEFT BLANK

STAFF MEMBERS OF THE PHYSICS DIVISION

The Physics Division staff for the year ending 31 March 1976 is listed below. Although the members are classified by programs, it must be understood that many of them work in two or more of the areas. In such cases, the classification indicates only the current primary interest.

In the period from 1 April 1975 through 31 March 1976, there were 45 temporary staff members and visitors (including 9 postdoctoral fellows), 18 graduate students, and 16 undergraduates. In these lists, the Temporary Scientific Staff are those with appointments for ≥9 months, while Visitors are on shorter appointments. Research Participants come to Argonne part-time for research while continuing their work at their own institutions.

EXPERIMENTAL NUCLEAR PHYSICS

Permanent Scientific Staff

[†] Lowell M. Bollinger, Ph.D., Cornell University, 1951

[‡] Thomas H. Braid, Ph.D., Edinburgh University, 1950

[*] S. Bradley Burson, Ph.D., University of Illinois, 1946

[§] Cary N. Davids, Ph.D., California Institute of Technology, 1967

Alexander J. Elwyn, Ph.D., Washington University, 1956

John R. Erskine, Ph.D., University of Notre Dame, 1960

---

[*] No longer at Argonne as of 31 March 1976.

[†] Director of the Physics Division until November 1975; in charge of Superconducting Linac Project.

[‡] Joint appointment as Associate Editor of Applied Physics Letters; Acting Editor October 1974—June 1975. Transferred to Reactor Analysis and Safety Division March 1976.

[§] Full time at Argonne. Also Visiting Scholar at the Enrico Fermi nstitute, University of Chicago.

†Gerald T. Garvey, Ph. D., Yale University, 1962

‡Donald S. Gemmell, Ph. D., Australian National University, 1960

Robert E. Holland, Ph. D., University of Iowa, 1950

Roy J. Holt, Ph. D., Yale University, 1972

§Harold E. Jackson, Jr., Ph. D., Cornell University, 1959

Dennis G. Kovar, Ph. D., Yale University, 1970

Alexander Langsdorf, Jr., Ph. D., Massachusetts Institute of Technology, 1937

‖John J. Livingood, Ph. D., Princeton University, 1929

Frank J. Lynch, B. S., University of Chicago, 1944

Luise Meyer-Schützmeister, Ph. D., Technical University of Berlin, 1943

¶F. P. Mooring, Ph. D., University of Wisconsin, 1951

††John P. Schiffer, Ph. D., Yale University, 1954

‡‡Ralph E. Segel, Ph. D., Johns Hopkins University, 1955

Kenneth W. Shepard, Ph. D., Stanford University, 1970

Robert K. Smither, Ph. D., Yale University, 1956

Thomas P. Wangler, Ph. D., University of Wisconsin, 1964

§§J. L. Yntema, Ph. D., Free University of Amsterdam, 1952

‖‖Benjamin Zeidman, Ph. D., Washington University, 1957

---

†Director of the Physics Division as of March 1976.

‡In charge of Dynamitron accelerator operations as of February 1976. Temporarily at University of Munich (September 1974—September 1975).

§Temporarily at Centre d'Etudes Nucleaires, Saclay, France (August 1975—August 1976).

‖Emeritus.

¶In charge of Dynamitron accelerator operations until February 1976.

††Associate Director of the Physics Division. Joint appointment with the University of Chicago.

‡‡Joint appointment with Northwestern University.

§§In charge of Tandem accelerator operations.

‖‖Temporarily at Max-Planck Institut für Kernphysik, Heidelberg, Germany (August 1975—August 1976).

Temporary Scientific Staff

Yossi Eisen, Ph. D., Weizmann Institute of Science, 1974

*Walter Henning, Ph. D., Technical University, Munich, 1968
(From Technical University, Munich, Germany)

Ronald Laszewski, Ph. D., University of Illinois, 1975

Mogens C. Olesen, M. S., Technical University of Denmark, 1955
(From Niels Bohr Institute, Copenhagen, Denmark)

*Trevor R. Ophel, Ph. D., Australian National University, 1959
(From Australian National University)

Peter Sperr, Dr. rer. nat., Technical University, Munich, 1973
(From Technical University, Munich, Germany)

Samuel L. Tabor, Ph. D., Stanford University, 1972

Zeev Vager, Ph. D., Weizmann Institute of Science, 1960
(From Weizmann Institute of Science)

Steven E. Vigdor, Ph. D., University of Wisconsin, 1973

*William M. Wilson, Ph. D., Duke University, 1973

Visitors

*David L. Bushnell, Ph. D., Virginia Polytechnic Institute, 1961
(From Northern Illinois University)

Duane J. Buss, Ph. D., University of Notre Dame, 1966
(Research participant from Illinois Benedictine College)

*Klaus A. Eberhard, Ph. D., University of Heidelberg, 1968
(From Technical University, Munich, Germany)

*Bernard Hamermesh, Ph. D., New York University, 1944
(From Cleveland State University)

Francis W. Prosser, Ph. D., University of Kansas, 1955
(Research participant from University of Kansas)

Loyd L. Rutledge, Ph. D., Texas A & M University, 1974
(Research participant from Northwestern University)

*Esther L. Segel, Ph. D., University of Rochester, 1960
(Research participant from Illinois Institute of Technology)

---

*No longer at Argonne as of 31 March 1976.

Supporting Staff

Charles H. Batson

John J. Bicek

William F. Evans

*Linda R. Gritter

Joseph E. Kulaga

James R. Specht

Robert V. Straz

George E. Thomas, Jr.

James N. Worthington

Bruce J. Zabransky

Graduate Students

*Richard L. Boudrie (University of Kansas)

Tsewei Chen (Northwestern University)

*William C. Corwin (Illinois Institute of Technology)

Kasra Daneshvar (University of Illinois, Chicago Circle Campus)

*Michael A. Lee (Northwestern University)

Martin J. Murphy (University of Chicago)

Eric B. Norman (University of Chicago)

Richard C. Pardo (University of Texas)

Lewis A. Parks (University of Texas)

Krishnaswamy Raghunathan (Northwestern University)

Timothy R. Renner (University of Chicago)

*Jeffrey F. Tonn (Northwestern University)

---

*No longer at Argonne as of 31 March 1976.

THEORETICAL PHYSICS

Permanent Scientific Staff

Yehuda B. Band, Ph. D., University of Chicago, 1973

†Arnold R. Bodmer, Ph. D., Manchester University, 1953

Fritz Coester, Ph. D., University of Zurich, 1944

Stanley Cohen, Ph. D., Cornell University, 1955

Benjamin Day, Ph. D., Cornell University, 1963

Dieter Kurath, Ph. D., University of Chicago, 1951

Robert D. Lawson, Ph. D., Stanford University, 1953

‡Malcolm H. Macfarlane, Ph. D., University of Rochester, 1959

James E. Monahan, Ph. D., St. Louis University, 1953

§Murray Peshkin, Ph. D., Cornell University, 1951

Steven C. Pieper, Ph. D., University of Illinois, 1970

Johann Rafelski, Ph. D., Johann Wolfgang Goethe University, 1973

Franklin J. D. Serduke, Ph. D., University of California, Davis, 1970

Temporary Scientific Staff

*Bei-dwo Chang, Ph. D., University of Chicago, 1975

Tsung-Shung Harry Lee, Ph. D., University of Pittsburgh, 1973

Visitors

*John Boguta, Ph. D., University of Illinois, 1968

*John W. Clark, Ph. D., Washington University, 1959
(Research participant from Washington University)

*Morton Hamermesh, Ph. D., New York University, 1940
(From University of Minnesota)

*Tetsutaro Hirano, B. S., University of Tokyo, 1950
(From Hosei University)

---

*No longer at Argonne as of 31 March 1976.

†Joint appointment with the University of Illinois, Chicago Circle Campus.

‡Joint appointment with the University of Chicago.

§Associate Director of the Physics Division; Acting Director November 1975—May 1976.

*Francesco Iachello, Ph. D., Massachusetts Institute of Technology, 19(
(From Kernfysisch Versneller Instituut, Groningen, Netherlands)

*Hermann G. Kuemmel, Ph. D., Free University of Berlin, 1952
(From Ruhr Universität, Bochum, Germany)

*†Harry J. Lipkin, Ph. D., Princeton University, 1950
(From Weizmann Institute of Science, Rehovot, Israel)

*Ulrich B. Mosel, Dr. Phil. Nat., University of Frankfurt, 1968
(From University of Giessen, Germany)

*Berndt Müller, Ph. D., University of Frankfurt, 1973

Arnold Müller-Arnke, Ph. D., Technische Hochschule Darmstadt, 1967
(From Technische Hochschule, Darmstadt, Germany)

*Karl-Heinz Passler, Ph. D., University of Giessen, 1975
(From University of Giessen, Germany)

William D. Teeters, Ph. D., University of Iowa, 1968
(Research participant from Chicago State University)

Graduate Students

Soumya Chakravarti (University of Chicago)

*James A. Paget (Oberlin College)

Constantine N. Panos (University of Illinois, Chicago Circle Campus)

*Michael J. Stob (University of Chicago)

EXPERIMENTAL ATOMIC AND MOLECULAR PHYSICS

Permanent Scientific Staff

Joseph Berkowitz, Ph. D., Harvard University, 1955

‡H. Gordon Berry, Ph. D., University of Wisconsin, 1967

§Stephen B. Brumbach, Ph. D., Pennsylvania State University, 1971

---

*No longer at Argonne as of 31 March 1976.

†Joint appointment with the Fermi National Accelerator Laboratory.

‡Joint appointment with the University of Chicago.

§Transferred to Special Materials and Services Division February 1976

William J. Childs, Ph. D., University of Michigan, 1956

Santosh K. Das, Ph. D., University of California, Berkeley, 1971

†Leonard S. Goodman, Ph. D., University of Chicago, 1952

‡David C. Hess, Ph. D., University of Chicago, 1949

Manfred S. Kaminsky, Ph. D., University of Marburg, 1957

Victor E. Krohn, Ph. D., Case Western Reserve University, 1952

§Gilbert J. Perlow, Ph. D., University of Chicago, 1940

G. R. Ringo, Ph. D., University of Chicago, 1940

Stanley L. Ruby, B. A., Columbia University, 1947

*Henry E. Stanton, Ph. D., University of Chicago, 1944

Temporary Scientific Staff

‖Patricia M. Dehmer, Ph. D., University of Chicago, 1972

Ronald J. Ekern, Ph. D., Clarkson College of Technology, 1975

*Karl Radler, Ph. D., University of Hamburg, 1974

Thomas D. Rossing, Ph. D., Iowa State University, 1954
(From Northern Illinois University)

Richard M. Schectman, Ph. D., Cornell University, 1962
(From University of Toledo)

*David G. Streets, Ph. D., University of London, 1971

Morris J. Weiss, Ph. D., University of Florida, 1963
(From The Hebrew University, Jerusalem)

Visitors

*William A. Chupka, Ph. D., University of Chicago, 1951
(From Yale University)

---

*No longer at Argonne as of 31 March 1976.

†Assistant Director of the Physics Division.

‡Joint appointment as Associate Editor of the Journal of Applied Physics and Applied Physics Letters.

§Joint appointment as Editor of the Applied Physics Letters. Temporarily at Technical University of Munich, Germany (October 1974—June 1975).

‖Transferred to Radiological and Environmental Research Division November 1975.

Jean M. G. Desesquelles, Ph. D., Université Claude Bernard, 1970
(From C.N.R.S., France)

*Bailey L. Donnally, Ph. D., University of Minnesota, 1961
(Research participant from Lake Forest College)

Ben Greenebaum, Ph. D., Harvard University, 1965
(Research participant from University of Wisconsin—Parkside)

*John C. Love, Ph. D., Ohio State University, 1969
(Research participant from Florida Institute of Technology)

Walter Potzel, Ph. D., Technical University, Munich, 1971
(From Technical University, Munich, Germany)

*A. Burke Ritchie, Ph. D., University of Virginia, 1968
(Research participant from University of Alabama)

Supporting Staff

John A. Dalman

Peter J. Dusza

*Warren T. Jivery

*Marvin J. Kral

*Peter D. Schnur

Graduate Students

George R. Fenske (University of Illinois)

*Albert A. Forster (Technical University, Munich, Germany)

ADMINISTRATIVE STAFF

†Albert J. Hatch, M.S., University of Illinois, 1947

---

*No longer at Argonne as of 31 March 1976.

†Assistant Director of the Physics Division.

Distribution of ANL-76-96

Internal

R. G. Sachs
M. V. Nevitt
R. V. Laney
R. M. Adams
R. Avery
N. Beyer
L. Burris
S. A. Davis
P. M. Dehmer
P. R. Fields
T. H. Fields
M. S. Freedman
A. Friedman
B. R. T. Frost
M. Gordon
M. Inokuti
M. A. Kanter
A. B. Krisciunas (15)
J. J. Livingood
M. S. Matheson
S. A. Miller
M. Novick
T. E. O'Connor
E. G. Pewitt
D. C. Price
R. J. Royston
W. K. Sinclair
R. G. Staker
A. F. Stehney
F. W. Thalgott
J. F. Thomson
C. E. Till
S. Wexler
Y. Band
J. Berkowitz
H. G. Berry
A. R. Bodmer
L. M. Bollinger
W. J. Childs
F. Coester
S. Cohen
J. A. Dalman
S. Das
C. N. Davids
B. Day
J. H. D. Eland
A. J. Elwyn
J. R. Erskine
G. T. Garvey (75)
D. S. Gemmell
L. S. Goodman
A. J. Hatch
W. Henning
D. C. Hess
R. E. Holland
R. J. Holt
H. E. Jackson
M. S. Kaminsky
D. G. Kovar
V. E. Krohn
D. Kurath
A. Langsdorf
R. D. Lawson
M. H. Macfarlane
L. Meyer
J. E. Monahan
F. P. Mooring
K. M. Pemble
G. J. Perlow
M. Peshkin
S. C. Pieper
J. Rafelski
G. R. Ringo
S. L. Ruby
J. P. Schiffer
R. E. Segel
K. W. Shepard
R. K. Smither
G. E. Thomas
J. L. Yntema
B. Zabransky
B. Zeidman
T. J. Bowles
D. F. Geesaman
B. Greenebaum
S-K. Lam
R. Laszewski
T. S. H. Lee
A. E. Livingston
A. D. MacKellar
A. J. Ratkowski
K. E. Rehm
W. Pietsch
L. Rutledge
S. L. Tabor
W. D. Teeters
M. Wehrenberg
ANL Contract File
ANL Libraries (5)
TIS Files (6)

External

ERDA-TIC, for distribution per UC-34 (136)
Manager, Chicago Operations Officer
Chief, Chicago Patent Group
President, Argonne Universities Association
Physics Division Review Committee:
D. A. Bromley, Yale Univ.
W. L. Brown, Bell Telephone Labs.
H. Feshbach, Massachusetts Institute of Technology
R. Middleton, Univ. of Pennsylvania
D. E. Nagle, Los Alamos Scientific Laboratory
D. A. Shirley, Univ. of California, Berkeley
J. Weneser, Brookhaven National Lab.
ronutronic Div. of Philco Corp., Newport Beach, Calif.

R. G. Allas, U. S. Naval Research Lab.
N. Anantaraman, U. Rochester
Antioch College, Olive Kettering Library
E. N. Argyres, State Univ. College of Arts and Science, Plattsburgh, N.Y.
P. Axel, U. Illinois
H. H. Barschall, U. Wisconsin
B. Bayman, U. Minnesota
G. B. Beard, Wayne State U.
R. C. Bearse, U. Kansas
G. L. Bennett, Space Nuclear Systems Div., USERDA
A. Bernabei, Manhattan College, Bronx
A. M. Bincer, U. Wisconsin
C. H. Blanchard, U. Wisconsin
E. Bleuler, Pennsylvania State U.
D. Borlin, Washington U., St. Louis
Boston College, Preprint Library
R. L. Boudrie, U. Colorado
G. Breit, SUNY at Buffalo
Brooklyn College, Dept. of Physics
S. B. Burson, Office of Nuclear Regulatory Res., USNRC
D. L. Bushnell, Northern Illinois U.
D. J. Buss, Illinois Benedictine College
California Inst. of Technology, Synchrotron Lab.
L. E. Campbell, Hobart & William Smith Colleges
Catholic University of America, Keane Physics Research Center
J. Cerny III, Lawrence Berkeley Lab.
B.-d. Chang, U. Rochester
G. F. Chew, Lawrence Berkeley Lab.
W. A. Chupka, Yale U.
Univ. of Cincinnati, Physics-Mathematics Library
C. M. Class, Rice U.
E. Clothiaux, Duquesne U.
H. Cohen, California State College, Los Angeles
V. W. Cohen, Battelle Northwest Labs.
J. R. Comfort, Princeton U.
C. F. Dam, Cornell College, Mount Vernon, Ia.
S. E. Darden, U. of Notre Dame
P. T. Debevec, Indiana U.
D. Dehnhard, U. Minnesota
Univ. of Denver, Physics Dept.
J. J. Devaney, Los Alamos Scientific Lab.
B. Donnally, Lake Forest College, Lake Forest, Ill.
T. Ehlert, Marquette U.
U. Fano, U. Chicago
G. R. Fenske, U. Illinois
H. J. Fischbeck, U. Oklahoma
H. T. Fortune, U. Pennsylvania
J. L. Fowler, Oak Ridge National Lab.
H. Q. Fuller, U. Missouri at Rolla
P. Gilles, U. Kansas
T. B. Glegg, U. North Carolina
D. H. Gloeckner, Rutgers U.
H. Goldstein, Columbia U.
A. A. Gordus, U. Michigan

E. Gove, U. Rochester
Haeberli, U. Wisconsin
M. Hamermesh, U. Minnesota
S. S. Hanna, Stanford U.
xA. O. Hanson, U. Illinois
W. Harper, Iowa State U.
R. R. Hart, Boston, Mass.
M. Hasan, Northern Illinois U.
H. G. Heard, Woodside, Calif.
D. W. Heikkinen, Lawrence Livermore Lab.
R. G. Helmer, Aerojet Nuclear Co.
E. M. Henley, U. Washington
R. G. Herb, U. Wisconsin
R. E. Honig, RCA Labs.
V. W. Hughes, Yale U.
J. R. Huizenga, U. Rochester
IIT Research Institute, Physics Library
Univ. of Illinois, Chicago Circle, Physical Science Dept.
Indiana University, Cyclotron Project
M. Inghram, U. Chicago
D. R. Inglis, U. Massachusetts
Institute for Advanced Study, Physics Preprint Library, Princeton
W. T. Jivery, Ironwood, Mich.
P. B. Kahn, SUNY at Stony Brook
A. K. Kerman, Massachusetts Inst. of Technology
C. W. Kimball, Northern Illinois U.
B. B. Kinsey, U. of Texas at Austin
E. D. Klema, College of Engineering, Tufts U.
N. Koller, Rutgers U.
E. J. Konopinski, Indiana U.
F. T. Kuchnir, Elmhurst, Ill.
R. O. Lane, Ohio U.
L. L. Lee, Jr., SUNY at Stony Brook
C. Leu, Central College, Pella, Ia.
L. F. Long, U. Notre Dame
G. D. Loper, Wichita State U.
Louisiana State University, Dept. of Physics and Astronomy, Librarian
J. J. MacKenzie, Massachusetts Inst. of Technology
A. P. Magruder, EG&G, Las Vegas, Nev.
J. V. Maher, U. Pittsburgh
J. Margrave, Rice U.
J. P. Marion, Chicago
Marquette Univ., Physics Department
R. Marshall, Pasadena
Massachusetts Institute of Technology, Nuclear Res. Publns. Office
D. A. McClure, Georgia Inst. of Technology
G. W. Meisner, U. North Carolina
Michigan State University, Cyclotron Lab., Librarian
R. C. Mikkelson, Macalester College
H. G. Miller, Defiance College
University of Mississippi, Library
Moinester, U. Rochester
F. Moore, Univ. of Texas at Austin
N. C. Mukhopadhyay, U. Maryland

A. I. Namenson, Naval Research Lab.
H. Newson, Duke U.
New York University Medical Center, Environmental Medicine Lib.
J. A. Nolen, Jr., Michigan State U.
Univ. of North Dakota, Physics Dept., c/o M. Muraskin
Northeastern University, Physics Research Lib. Committee
L. Olsen, U. S. Naval Postgraduate School
D. N. Olson, St. Olaf College
W. K. H. Panofsky, Stanford Linear Accelerator Center
L. A. Parks, Florida State U.
R. S. Preston, Northern Illinois U.
F. W. Prosser, U. Kansas
S. Raboy, Harpur College, SUNY, Binghamton
J. L. Rainwater, Columbia U., Irvington
A. R. Rana, West Virginia Inst. of Technology
H. R. Reiss, U. S. Naval Ordnance Lab.
G. Reynolds, Palmer Physics Lab., Princeton U.
H. D. Richardson, Nuclear Science Center, Louisiana State U.
M. T. Rodine, Gustavus Adolphus College
M. E. Rose, U. Virginia
N. Rosenzweig, SUNY at Albany
S. G. Sanders, Southern Illinois U.
R. P. Scharenberg, Purdue U.
R. M. Schectman, U. Toledo
L. Schmid, HEDL
P. D. Schnur, Charles B. Chrystal Co., New York City
J. J. Schwartz, U. Rochester
F. J. D. Serduke, Lawrence Livermore Lab.
K. K. Seth, Northwestern U.
S. M. Shafroth, U. North Carolina
R. Sherr, Palmer Physics Lab., Princeton U.
H. Shugart, U. California, Berkeley
C. G. Shull, Massachusetts Inst. of Technology
H. Shwe, East Stroudsburg State College
C. E. Skov, Monmouth College
C. P. Slichter, U. Illinois
A. H. Snell, Oak Ridge National Laboratory
H. E. Stanton, Oak Lawn, Ill.
State University of New York at Stony Brook, Preprint Lib., Dept. of Physics
N. Stein, Yale U.
M. B. Sterns, Ford Scientific Lab.
xJ. Stoltzfus, Beloit College
W. G. Stoppenhagen, Ohio U., Lancaster
M. Svonavec, Purdue U., Calumet Campus
S. Tabor, U. Pennsylvania
R. F. Taschek, Los Alamos Scientific Lab.
A. H. Taub, U. California, Berkeley
J. S. Toll, U. Maryland
C. C. Trail, Brooklyn College
J. J. Turin, U. Toledo
L. A. Turner, Palmer Physical Lab., Princeton U.
U. S. Naval Research Laboratory, Nucleonics Div., Librarian
R. Vandenbosch, U. Washington
S. E. Vigdor, Indiana U.

C. M. Vincent, U. Pittsburgh
I. Vincent, U. Michigan
. Wangler, Los Alamos Scientific Lab.
B. A. Watson, Stanford U.
L. Weaver, Kansas State U.
G. H. Wedberg, U. Pittsburgh
M. J. Weiss, Adrenzl Lab., V.A. Hospital, Bronx
V. Weisskopf, Massachusetts Inst. of Technology
K. J. Wetzel, U. Portland
W. R. Wharton, Carnegie-Mellon U.
J. A. Wheeler, Palmer Physical Lab., Princeton U.
H. B. White, Jr., Michigan State U.
M. G. White, Princeton U.
E. P. Wigner, Princeton U.
H. B. Willard, Case Western Reserve U.
W. M. Wilson, Jr., U. Florida
Univ. of Wisconsin, Physics Library
G. T. Wood, Cleveland State U.
C. S. Wu, Columbia U.
O. B. Young, Southern Illinois U.
F. J. Zehr, Westminster College
A. J. F. Boyle, U. Western Australia, Australia
J. E. Moyal, Macquarie U., Australia
J. O. Newton, Australian National U., Australia
T. R. Ophel, Australian National U., Australia
C. Osborne, Monash U., Australia
L. J. Tassie, Australian National U., Australia
E. W. Titterton, Australian National U., Australia
J. W. G. Wignall, U. Melbourne, Australia
J. Baier, Osterr. Studiengesellschaft f. Atomenergie Reaktorzentrum, Seibersdorf, Austria
W. Schneider, Zentralbibliothek d. Physik Inst., Vienna, Austria
Atomic Energy Centre, Library, Dacca, Bangladesh
Katholieka Universiteit Leuven, Inst. voor Theoretische Fysica, Belgium
Universite Catholique de Louvain, Inst. de Physique Theorique, Belgium
J. Spaepen, Euratom, Geel, Belgium
J. Vervier, Institut de Physique Corpusculaire, Louvain-la-Neuve, Belgium
M. D. A. Anastacio, Comissao Nacional de Energia Nuclear, Rio de Janeiro, Brazil
C. Brasileiro, de Pesquisas Fisicas, Rio de Janeiro, Brazil
Universidade de Brasilia, Inst. Central de Fisica, Brazil
O. Sala, Universidade de Sao Paulo, Brazil
Universidade de Sao Paulo, Inst. de Fisica e Quimica de Sao Carlos, Brazil
Univ. of Alberta, Nuclear Research Centre, Dept. of Physics, Canada
G. A. Bartholomew, Atomic Energy Canada Ltd., Canada
T. J. Kennett, McMaster U., Canada
J. D. Kurbatov, Victoria, B.C., Canada
McGill Univ., Theoretical Physics Group, Physical Sciences Centre, Canada
J. Montague, Queens U., Kingston, Canada
G. C. Nielson, U. Alberta, Edmonton, Canada
W. V. Prestwich, McMaster U., Canada
W. J. Romo, Carleton U., Canada
J. Roy, U. Alberta, Canada
J-s. Maa, National Tsing-Hua U., China
Tseng, National Taiwan U., China
Yang, National Tsing-Hua U., China

A. Bohr, Inst. for Theoretical Physics, Copenhagen, Denmark
C. J. Christensen, Danish AEC, Risø, Denmark
J. Koch, U. Copenhagen, Denmark
B. R. Mottelson, Inst. for Theoretical Physics, Copenhagen, Denmark
Niels Bohr Inst., The Library, Copenhagen, Denmark
W. D. Allen, Rutherford High Energy Lab., England
Berkeley Nuclear Labs., Central Electricity Generating Bd., Librarian, England
J. B. Birks, The University, Manchester, England
D. R. Chick, Surrey, England
Culham Lab., UKAEA, Librarian, England
N. Daly, UKAWRE, Aldermaston, England
A. T. G. Ferguson, AERE, Harwell, England
M. Grace, Nuclear Physics Dept., Oxford, England
C. E. Johnson, AERE, Harwell, England
G. Moorhouse, Rutherford Lab., Harwell, England
G. C. Morrison, U. Birmingham, England
R. S. Nelson, AERE, Harwell, England
P. Rice-Evans, Bedford College, London, England
J. M. Soper, AERE, Harwell, England
D. G. Streets, Lincoln, England
Sussex, Univ. of Library, Brighton, England
M. W. Thompson, U. Sussex, England
J. C. Willmott, The University, Manchester, England
S. Zienau, University College, London, England
K. V. Laurikainen, U. Helsinki, Finland
K.-E. Nysten, Helsinki, Finland
A. Abragam, CEN Saclay, France
G. Bassani, CEN Saclay, France
Centre de Recherches Nucleaires, Strasbourg, France
C.N.R.S., Centre de Physique Theorique, Marseille, France
J. Delaunay, CEN Saclay, France
Ecole Polytechnique, Centre de Physique, Theorique, Library, Paris, France
H. Ekstein, C.N.R.S., Marseille, France
Institut des Sciences Nucleaires, Librarian, Grenoble, France
A. Michaudon, C.E.A., Centre d'Etudes de Bruyeres le Chatel
University of Paris, Bibliotheque du Lab. de Physique Theorique, France
A. M. Peers, Laboratoire Curie, Paris, France
J. C. Poizat, Univ. Claude Bernard, Villeurbanne, France
J. M. Remillieux, Univ. Claude Bernard, Villeurbanne, France
C. Samour, CEN Saclay, France
R. Seltz, Univ. de Strasbourg, France
J. C. Sens, Centre de Recherches Nucleaires, Strasbourg, France
Service de Physique Theorique, Bibliotheque, Saclay, France
M. Wery, Centre de Recherches Nucleaires, Strasbourg, France
K. Bethge, Universitat Heidelberg, Germany
R. Bock, Max-Planck-Institut, Germany
Deutsches Elektronen-Synchrotron, Librarian, Hamburg, Germany
K. A. Eberhard, Univ. of Munich, Germany
H. Ehrhardt, Universitat Freiburg, Germany
R. Fleischmann, Erlangen, Germany
S. Flugge, Universitat Freiburg, Germany
A. A. Forster, Techn. Univ. Munchen, Germany
I. W. Fuchs, Physikalischen Inst., Aachen, Germany
Gesellschaft fur Schwerionen-forschung mbH, Bibliothek, Darmstadt, Germany

K-O. Groeneveld, Universitat Frankfurt, Germany
Hinterberger, Max-Planck-Inst. f. Chemie, Mainz, Germany
K. Ilgen, Inst. f. Strahlenphysik, Stuttgart, Germany
P. Kienle, Technische Hochschule Munchen, Germany
H-J. Korner, Technische Universitat Munchen, Germany
L. Lassen, Universitat Heidelberg, Germany
N. Marquardt, Inst. fur Experimentalphysik III, Ruhr-Universitat Bochum, Germany
C. Mayer-Boricke, Kernforschungsanlage Julich, Germany
T. Mayer-Kuckuk, Universitat Bonn, Germany
U. B. Mosel, Universitat Giessen, Germany
A. Muller-Arnke, Technischen Hochschule, Darmstadt, Germany
O. Osberghaus, Universitat Freiburg, Germany
W. Potzel, Technical University Munich, Germany
K. Radler, Hamburg, Germany
A. Richter, Universitat Bochum, Germany
G. Roepstorff, Univ. Hamburg, Germany
R. Santo, Univ. Munchen, Germany
R. E. Schlier, Univ. Freiburg, Germany
O. B. Schult, Technischen Hochschule Munchen, Germany
K. D. Schuy, Max-Planck-Institut fur Chemie, Mainz, Germany
P. Sperr, Technische Universitat Munchen, Germany
J. Speth, Inst. fur Kernphysik der KFA, Julich, Germany
H. Stettmeier, Technische Universitat Munchen, Germany
U. Strohbusch, Inst. fur Experimentalphysik Zyklotron, Hamburg, Germany
R. Taubert, Physikalisch-Technische Bundesanstalt, Braunschweig, Germany
Technischen Universitat Munchen, Library, Physik Dept., Germany
D. von Ehrenstein, Univ. Bremen, Germany
W. Walcher, Univ. Marburg, Germany
F. G. Weller, Karlsruhe, Germany
N. K. Ailawadi, Tata Inst. of Fundamental Research, India
M. R. Bhiday, G.S. Technological Inst., Indore, India
R. Chand, Himachal Pradesh University, India
K. V. K. Iyengar, Tata Inst. of Fundamental Research, India
A. B. Kulkarni, Kurukshetra Univ., India
N. Nath, Kurukshetra Univ., India
S. P. Pandya, Physical Research Lab., Ahmedabad, India
N. G. Puttaswamy, Bangalore Univ., India
N. N. Raina, Univ. Kashmir, India
Saha Inst. of Nuclear Physics, The Director, India
A. P. Shukla, Indian Inst. of Technology, Kanpur, India
P. C. Sood, Banaras Hindu Univ., India
Physics Library, Univ. of Technology, Tehran, Iran
A. A. Azooz, Univ. Mosul, Iraq
A. E. Blaugrund, Weizmann Inst. of Science, Israel
A. deShalit, Weizmann Inst. of Science, Israel
Y. Eisen, Weizmann Institute of Science, Israel
P. Federman, Weizmann Inst. of Science, Israel
P. Hillman, Weizmann Inst. of Science, Israel
A. Katz, Weizmann Inst. of Science, Israel
A. Marinov, Hebrew Univ. in Jerusalem, Israel
Univ. of Negev, Physics Preprint Library, Israel
B. Rosner, Technion – Israel Inst. of Tech., Israel
Aviv Univ., Dept. of Physics and Astronomy, Israel
/ager, Weizmann Inst. of Science, Israel

A. Weinreb, Hebrew Univ., Israel
N. Zeldes, Hebrew Univ., Israel
M. Ageno, Istituto Superiore di Sanita, Rome, Italy
C. Coceva, C.N.E.N., Ispra, Italy
L. Fano, Istituto di Fisica "A. Righi," Bologna, Italy
I. Filosofo, Istituto Nazionale di Fisica Nucleare, Padova, Italy
Istituto di Fisica, Preprint Librarian, Torino, Italy
Istituto di Fisica del Politecnico, c/o Dr. Mario Rasetti, Torino, Italy
Istituto Nazionale di Fisica Nucleare, Sezione di Pisa, Italy
M. Mando, Phys. Inst. of the University, Firenze, Italy
C. Signorini, Istituto di Fisica, Padova, Italy
K. Hiida, Inst. for Nuclear Study, U. Tokyo, Japan
T. Hirano, Hosep Univ., Tokyo, Japan
K. Katori, U. of Tsukuba, Japan
Nagoya University, Dept. of Physics, Preprint Center, Japan
G. Narumi, U. Hiroshima, Japan
H. Ohnuma, U. Tokyo, Japan
M. Seki, Hiroshima Univ., Japan
K. Sugiyama, Tohoku Univ., Japan
Univ. of Tokyo, Particle Physics Lab., Dept. of Physics, Japan
G. Takeda, Dir., Inst. for Nuclear Study, U. Tokyo, Japan
K. Tsukada, Japan Atomic Energy Research Inst., Japan
Y. S. Kim, Atomic Energy Research Institute, Seoul, Korea
Instituto de Fisica, Theoretical Physics Grp., Preprint Lib., Mexico City, Mexico
Instituto Politecnico Nacional, Physics Dept. Lib., Mexico City, Mexico
Univ. de. Sonora, Lib., Escuela de Altos Estudios, Mexico
H. de Waard, Univ. Groningen, The Netherlands
P. F. A. Goudsmit, Inst. for Nuclear Physics Research, Amsterdam, The Netherlands
C. C. Jonker, Nat. Lab. Free University, Amsterdam, The Netherlands
R. H. Siemssen, Univ. Groningen, The Netherlands
R. van Wageningen, Inst. for Theoretical Physics, Groningen, The Netherlands
A. Poletti, Univ. Auckland, New Zealand
R. E. White, Univ. Auckland, New Zealand
M. S. Bokhari, P.A.E.C., Karachi, Pakistan
M. J. Khan, Univ. Peshawar, Pakistan
Q. O. Navarro, Philippine Atomic Research Center, Quezon City, Philippine Islands
J. Kuzminski, Inst. of Physics, Katowice, Poland
W. Zych, Inst. of Nuclear Research, Warsaw, Poland
A. M. Baptista, Inst. Portugues de Oncologia, Lisbon, Portugal
F. da Silva, Lab. de Fisica e Engenharia Nucleares, Sacavem, Portugal
T. Ponta, Inst. for Atomic Physics, Bucharest, Romania
Univ. of Timisoara, Library, Romania
D. Branford, Univ. Edinburgh, Scotland
R. W. Pringle, Edinburgh, Scotland
F. D. Brooks, Univ. of Cape Town, South Africa
C. A. Engelbrecht, Atomic Energy Board, Pretoria, South Africa
W. R. McMurray, Southern Universities Nuclear Inst., Faure, South Africa
D. Mingay, Univ. of the Witwatersrand, South Africa
D. Reitmann, Atomic Energy Board, Pretoria, South Africa
J. P. F. Sellschop, Univ. of the Witwatersrand, South Africa
O. Almen, Chalmers Univ. of Technology, Sweden
I. Bergstrom, Nobelinstitut for Fysik, Stockholm
B. Domeij, Nobelinstitut for Fysik, Stockholm, Sweden
N. Ryde, Chalmers Univ. of Technology, Sweden

Tandem Accelerator Lab., Uppsala, Sweden
. Spohr, Balzers Aktiengesellschaft fur Hochvakuum und Dunne Schichten, Furstentum Liechtenstein, Switzerland
S. Ketudat, Chulalongkorn Univ., Thailand
A. Saplakoglu, Middle East Technical Univ., Ankara, Turkey
F. ElBedewi, Atomic Energy Establishment, Cairo, United Arab Republic
M. ElNadi, Cairo Univ., United Arab Republic
I. Hamouda, Atomic Energy Establishment, Cairo, United Arab Republic
A. Osman, Cairo Univ., United Arab Republic
K. M. A. Refaey, Atomic Energy Establishment, Cairo, United Arab Republic
A. S. Yousef, Cairo University, United Arab Republic
A. J. Kalnay, IVIC, Physics Section, Caracas, Venezuela
Universidad Central de Venezuela, Physics Dept., Caracas, Venezuela
R. Popic, Inst. of Nuclear Sciences "B. Kidric," Belgrade, Yugoslavia
F. Tkebuchava, Dept. of Physics, Tbilisi State University, U.S.S.R.

☆U.S. GOVERNMENT PRINTING OFFICE: 1977—0-750-565